frontiers | Research Topics

Women in psychiatry neuroimaging and stimulation 2021

Edited by
Martine Hoogman and Neeltje E. M. Van Haren

Published in
Frontiers in Psychiatry

ISSN 1664-8714
ISBN 978-2-8325-4117-3
DOI 10.3389/978-2-8325-4117-3

About Frontiers

Frontiers is more than just an open access publisher of scholarly articles: it is a pioneering approach to the world of academia, radically improving the way scholarly research is managed. The grand vision of Frontiers is a world where all people have an equal opportunity to seek, share and generate knowledge. Frontiers provides immediate and permanent online open access to all its publications, but this alone is not enough to realize our grand goals.

Frontiers journal series

The Frontiers journal series is a multi-tier and interdisciplinary set of open-access, online journals, promising a paradigm shift from the current review, selection and dissemination processes in academic publishing. All Frontiers journals are driven by researchers for researchers; therefore, they constitute a service to the scholarly community. At the same time, the *Frontiers journal series* operates on a revolutionary invention, the tiered publishing system, initially addressing specific communities of scholars, and gradually climbing up to broader public understanding, thus serving the interests of the lay society, too.

Dedication to quality

Each Frontiers article is a landmark of the highest quality, thanks to genuinely collaborative interactions between authors and review editors, who include some of the world's best academicians. Research must be certified by peers before entering a stream of knowledge that may eventually reach the public - and shape society; therefore, Frontiers only applies the most rigorous and unbiased reviews. Frontiers revolutionizes research publishing by freely delivering the most outstanding research, evaluated with no bias from both the academic and social point of view. By applying the most advanced information technologies, Frontiers is catapulting scholarly publishing into a new generation.

What are Frontiers Research Topics?

Frontiers Research Topics are very popular trademarks of the *Frontiers journals series*: they are collections of at least ten articles, all centered on a particular subject. With their unique mix of varied contributions from Original Research to Review Articles, Frontiers Research Topics unify the most influential researchers, the latest key findings and historical advances in a hot research area.

Find out more on how to host your own Frontiers Research Topic or contribute to one as an author by contacting the Frontiers editorial office: frontiersin.org/about/contact

Women in psychiatry 2021: Neuroimaging and stimulation

Topic editors

Martine Hoogman — Radboud University Medical Centre, Netherlands

Neeltje E. M. Van Haren — Department of Child and Adolescent Psychiatry, Sophia Children's Hospital, Erasmus Medical Center, Netherlands

Citation

Hoogman, M., Van Haren, N. E. M., eds. (2023). *Women in psychiatry 2021: Neuroimaging and stimulation*. Lausanne: Frontiers Media SA.

doi: 10.3389/978-2-8325-4117-3

Table of contents

frontiers | Frontiers in Psychiatry

TYPE Editorial
PUBLISHED 18 October 2022
DOI 10.3389/fpsyt.2022.1057330

OPEN ACCESS

EDITED AND REVIEWED BY
Kathrin Koch,
Technical University of Munich, Germany

*CORRESPONDENCE
Neeltje E. M. van Haren
n.vanharen@erasmusmc.nl

SPECIALTY SECTION
This article was submitted to Neuroimaging and Stimulation, a section of the journal Frontiers in Psychiatry

RECEIVED 29 September 2022
ACCEPTED 04 October 2022
PUBLISHED 18 October 2022

CITATION
van Haren NEM and Hoogman M (2022) Editorial: Women in psychiatry 2021: Neuroimaging and stimulation. *Front. Psychiatry* 13:1057330. doi: 10.3389/fpsyt.2022.1057330

Editorial: Women in psychiatry 2021: Neuroimaging and stimulation

Neeltje E. M. van Haren[1]* and Martine Hoogman[2,3,4]

[1]Department of Child and Adolescent Psychiatry/Psychology, Erasmus Medical Centre – Sophia Children's Hospital, Rotterdam, Netherlands, [2]Department of Psychiatry, Radboud University Medical Center, Nijmegen, Netherlands, [3]Department of Human Genetics, Radboud University Medical Center, Nijmegen, Netherlands, [4]Donders Institute for Brain, Cognition and Behavior, Radboud University, Nijmegen, Netherlands

KEYWORDS

neuroimaging, psychiatric disorders, women scientists, brain stimulation, talents

Editorial on the Research Topic
Women in psychiatry 2021: Neuroimaging and stimulation

With the Research Topic series *Women in Psychiatry*, Frontiers in Psychiatry offers a unique platform to promote the work of female scientists across all fields of Psychiatry. It thereby increases visibility of female scientists by showcasing the depth of talent and the excellence and innovativeness of their work. We are proud to showcase in this Research Topic *Women in Psychiatry – Neuroimaging and Stimulation nine* excellent contributions to the field, all first and/or last-authored by our female colleagues.

Studies were performed across a wide variety of populations, ranging from healthy individuals to individuals with psychiatric disorders, and across different neuroimaging and brain stimulation methods.

Two papers contribute to understanding healthy brain development. van Aalst et al. conducted a yoga intervention in healthy young adult females and showed effect on behavioral but not on multimodal imaging biomarkers. Blok et al. applied normative modeling in a large longitudinal dataset of T1-weighted images from the Generation R population study to establish typical development curves for (sub-)cortical volume and cortical thickness and showed how trajectories deviate in the presence of psychopathological symptoms.

Several papers contribute to advancing our understanding of the effect of treatment on outcome and symptoms of psychiatric disorders. Kahn et al. describe the effect of deep brain stimulation in patients with obsessive-compulsive disorder and psychiatric comorbidity while Baumann et al. report the findings of the effect of Transcranial Direct Current Stimulation in anorexia nervosa. Moreover, the effects of lithium response were investigated on amygdala and hippocampal shape using 7T MRI in bipolar disorder by Athey et al.

Two contributions aimed to understand the underlying biological mechanisms of psychiatric disorders. Jakobi et al. studied the neural correlates of

observing dynamic facial expressions with levels of reactive aggression in adult attention-deficit/hyperactivity disorder using fMRI. Proteau-Lemieux et al. set out to investigate whether EEG markers of brain maturation are affected in fragile X syndrome.

Finally, in addition to empirical studies, the Research Topic contains a perspective and a review. Conelea et al. wrote a perspective article on the need to combine cognitive behavioral therapies (CBT) and non-invasive brain stimulation (NIBS) with the aim of improving the treatment of psychiatric disorders while Cubillo integrated the literature on the neurobiological correlates of the social and emotional impact of peer victimization.

This Research Topic celebrates the breadth of scientific ideas, techniques, approaches, and findings that female scientists contribute to the field of psychiatric neuroimaging and stimulation. It is a demonstration of creativity, vision, and perseverance. We hope it serves as an inspiration for neuroscientists of all ages, genders, cultures, or socioeconomic backgrounds.

Author contributions

NH wrote the manuscript. MH critically reviewed the manuscript. All authors approved the final version.

Conflict of interest

The authors declare that the research was conducted in the absence of any commercial or financial relationships that could be construed as a potential conflict of interest.

Publisher's note

frontiers in Psychiatry

ORIGINAL RESEARCH
published: 16 February 2021
doi: 10.3389/fpsyt.2021.614010

A 7 Tesla Amygdalar-Hippocampal Shape Analysis of Lithium Response in Bipolar Disorder

Thomas L. Athey[1,2,3], *Can Ceritoglu*[1], *Daniel J. Tward*[1,2,3], *Kwame S. Kutten*[1], *J. Raymond DePaulo*[4], *Kara Glazer*[5], *Fernando S. Goes*[4], *John R. Kelsoe*[6,7], *Francis Mondimore*[4], *Caroline M. Nievergelt*[7], *Kelly Rootes-Murdy*[8], *Peter P. Zandi*[4,9], *J. Tilak Ratnanather*[1,2,3] *and Pamela B. Mahon*[4,10,11]*

[1] Center for Imaging Science, Johns Hopkins University, Baltimore, MD, United States, [2] Institute for Computational Medicine, Johns Hopkins University, Baltimore, MD, United States, [3] Department of Biomedical Engineering, Johns Hopkins University, Baltimore, MD, United States, [4] Department of Psychiatry and Behavioral Science, Johns Hopkins School of Medicine, Baltimore, MD, United States, [5] Department of Occupational Therapy, Boston University, Boston, MA, United States, [6] Department of Psychiatry, VA San Diego Healthcare System, La Jolla, CA, United States, [7] Department of Psychiatry, University of California, San Diego, La Jolla, CA, United States, [8] Department of Psychology, Georgia State University, Atlanta, GA, United States, [9] Department of Mental Health, Johns Hopkins Bloomberg School of Public Health, Baltimore, MD, United States, [10] Department of Psychiatry, Brigham & Women's Hospital, Boston, MA, United States, [11] Department of Psychiatry, Harvard School of Medicine, Boston, MA, United States

OPEN ACCESS

Edited by:
Neeltje E. M. Van Haren, Sophia Children's Hospital, Netherlands

Reviewed by:
Delfina Janiri, Sapienza University of Rome, Italy
Gabriele Sani, Università Cattolica del Sacro Cuore, Italy

***Correspondence:**
Pamela B. Mahon
pmahon@bwh.harvard.edu

Specialty section:
This article was submitted to Neuroimaging and Stimulation, a section of the journal Frontiers in Psychiatry

Received: 20 October 2020
Accepted: 19 January 2021
Published: 16 February 2021

Citation:
Athey TL, Ceritoglu C, Tward DJ, Kutten KS, DePaulo JR, Glazer K, Goes FS, Kelsoe JR, Mondimore F, Nievergelt CM, Rootes-Murdy K, Zandi PP, Ratnanather JT and Mahon PB (2021) A 7 Tesla Amygdalar-Hippocampal Shape Analysis of Lithium Response in Bipolar Disorder. Front. Psychiatry 12:614010. doi: 10.3389/fpsyt.2021.614010

Research to discover clinically useful predictors of lithium response in patients with bipolar disorder has largely found them to be elusive. We demonstrate here that detailed neuroimaging may have the potential to fill this important gap in mood disorder therapeutics. Lithium treatment and bipolar disorder have both been shown to affect anatomy of the hippocampi and amygdalae but there is no consensus on the nature of their effects. We aimed to investigate structural surface anatomy changes in amygdala and hippocampus correlated with treatment response in bipolar disorder. Patients with bipolar disorder ($N = 14$) underwent lithium treatment, were classified by response status at acute and long-term time points, and scanned with 7 Tesla structural MRI. Large Deformation Diffeomorphic Metric Mapping was applied to detect local differences in hippocampal and amygdalar anatomy between lithium responders and non-responders. Anatomy was also compared to 21 healthy comparison participants. A patch of the ventral surface of the left hippocampus was found to be significantly atrophied in non-responders as compared to responders at the acute time point and was associated at a trend-level with long-term response status. We did not detect an association between response status and surface anatomy of the right hippocampus or amygdala. To the best of our knowledge, this is the first shape analysis of hippocampus and amygdala in bipolar disorder using 7 Tesla MRI. These results can inform future work investigating possible neuroimaging predictors of lithium response in bipolar disorder.

Keywords: lithium, 7T MRI, shape analysis, amygdala, hippocampus, bipolar disorder

1. INTRODUCTION

Bipolar I disorder (BD) is characterized by a relapsing and remitting course and is common, affecting an estimated 1% of the population (1). Treatment of BD is complex, often involves polypharmacy, and it can take months or even years to find an effective treatment for an individual patient (2). Lithium is a common mood-stabilizing treatment that has been shown to significantly reduce risk of depressive or manic relapse (3, 4). However, only about 50% of patients with BD respond to lithium (5). Identification of reliable predictors of treatment response could greatly reduce illness burden and improve the lives of patients with BD (6–8).

A limited number of predictors of lithium response in BD have been identified, including clinical and genetic features (6–9). Clinical predictors of positive response include an illness pattern of manic episodes before depressive episodes and later age of onset of the disorder. However, no single clinical feature has been found to strongly predict lithium response (8). In terms of genetics, Genome Wide Association Studies (GWAS) have now identified genetic variation associated with lithium response, including single nucleotide polymorphisms (SNPs) located in a region containing genes for long non-coding RNAs that regulate gene expression and in the genes SESTD1 and in GADL1 (10–12). Additional suggestive associations of lithium response have been reported with SNPs located in the gene GRIA2 and with microRNAs (13, 14).

Another data modality that may predict treatment response is neuroimaging (7). Decreased bilateral volumes of hippocampi, amygdalae, and thalamus, and increased lateral ventricle volume have been shown in BD, along with altered function and connectivity in related cortico-limbic circuits (15–20). Lithium treatment in BD has been associated with larger volumes of structures such as the hippocampus and amygdala, although not consistently, as well as hypoactivation in subcortical structures typically found to be hyperactivated in BD (18, 21–24). Only a few previous studies have used neuroimaging to examine response to lithium treatment, with some identifying patterns of structure and function in cortico-limbic regions and circuits consistent with a normalizing effect of lithium (25–29). Most studies examining lithium effects on structural MRI have examined brain volumes, cortical thickness or surface area, reducing all morphological information to a single statistic (17, 21, 22, 30). Exploring more local effects may provide additional information and potentially help further elucidate lithium's neurobiological action. While a few studies have examined subcortical structure at a more detailed level, with some reporting localized differences in hippocampus including in CA1, CA2/3 and subiculum, such studies assessed structural changes related to lithium use and did not take into account differences in individual responses to lithium treatment (23, 31–34).

In this study, we combined a focus on response to lithium treatment with an examination of local structural effects, utilizing Large Deformation Diffeomorphic Metric Mapping (LDDMM) methods to identify local morphological differences between patients with BD who responded to lithium monotherapy treatment, those who did not respond, and healthy comparison participants (HC). LDDMM methods can quantify local morphological differences in brain structures and have been used previously to study patterns of atrophy in diseases such as Alzheimer's and Huntington's (35, 36). Our goal was to identify amygdalar and hippocampal shape correlates of lithium response in BD. This preliminary study could help identify brain features to be examined in future neuroimaging studies to identify predictors of lithium response in BD.

2. MATERIALS AND METHODS

2.1. Participants

Participants with BD were recruited at the Johns Hopkins site of the Pharmacogenomics of Bipolar Disorder Study (PGBD), an eleven site prospective trial of lithium monotherapy in adult patients with BD (37). Diagnostic and Statistical Manual of Mental Disorders (DSM-IV) research diagnosis was made by a psychiatrist using the Diagnostic Interview for Genetic Studies (DIGS) (38). Participants with BD were included if they (i) met DSM-IV criteria for bipolar I disorder, (ii) were currently euthymic with Beck Depression Inventory (BDI)$<$19 and Clinician-Administered Rating Scale for Mania (CARS-M)$<$8 (39, 40) and (iii) were enrolled in the PGBD study [for inclusion and exclusion criteria of that study see (37)]. HC were recruited from the community using flyers, or from participants in previous research studies at Johns Hopkins who had given written permission to be re-contacted for future research, and were included if they had (i) no self-reported psychiatric history based on the Mini-International Neuropsychiatric Interview (MINI) (41), (ii) no self-reported family history of psychiatric disorder in any first-degree family member. All participants met the inclusion criteria of (i) 18–65 years old, (ii) right handed and were excluded by (i) alcohol or substance abuse or dependence during the past 6 months, (ii) dementia or mild cognitive impairment, (iii) contraindication to an MRI scan.

As part of the PGBD study, participants with BD were followed through a 16-week stabilization phase to stabilize mood and titrate off psychotropic medications other than lithium, followed by a 4-week observation phase. During the 4-week observation phase, subjects with a Clinical Global Impression-Severity (CGI-S) score of 3 or less (mildly ill) for at least 4 weeks were advanced to a maintenance phase. During maintenance participants were assessed every 2 months for up to 24 months. Determination of lithium response was according to the PGBD study (37). Non-response was defined by failure to remit over the stabilization phase and/or observation phase, or relapse during the maintenance phase. Relapse was defined by either (i) meeting criteria for mania and having a CGI-S score of 4 or greater (markedly ill), (ii) meeting criteria for a major depressive episode with a 4-week duration, (iii) meeting criteria for a mixed episode with a CGI-S score of 4 or greater, (iv) psychiatric hospitalization for a mood episode, or (v) if in the physician's judgment, the patient could not be managed on monotherapy and required a change in medication. Response was defined at two time points: "acute response" considering whether the patient remained well enough to advance to the maintenance phase, and "long-term

response" considering up to 24 months of follow-up during the maintenance phase.

Participants with BD were consented and enrolled into the MRI study after beginning the PGBD study. Of the 25 participants (17 female, 8 male) who consented to participate in the MRI study, two were later excluded due a change in mood disorder diagnosis, one due to treatment non-compliance, and one was unable to complete the MRI scan. Participants were scheduled for MRI scanning after a clinical determination of acute response was made. A total of 7 participants were lost to follow-up prior to the MRI scan. Thus, a clinical determination of lithium response and a completed MRI scan were available for 14 participants with BD (9 acute responders, 5 acute non-responders). Two acute responders were determined to be long-term non-responders. Twenty-one HC were enrolled into the study and scanned.

2.2. Clinical Assessment

On the day of the MRI scan, all participants completed the Hopkins Adult Reading Test (42) as an indicator of Full Scale IQ, as well as the BDI and CARS-M to assess current dessive and manic symptoms, respectively. Possible dementia and mild cognitive impairment were assessed using the Mini Mental Status Exam (43) and Montreal Cognitive Assessment (44).

As some participants with BD had initiated treatment with lithium prior to entering the study, duration of lithium monotherapy at the time of the scan ranged from 2 months to 12 years. The mean dose of lithium in the participants was $1,000 \pm 300$ MG. At the time of the MRI, four participants who had exited the PGBD study had recently added an antipsychotic or antidepressant medication.

2.3. Image Acquisition and Segmentation

T1-weighted MP-RAGE brain scans (TR = 4.3 ms, TE = 1.92 ms, axial orientation, matrix = 225 × 288 × 288, resolution = 0.8 × 0.764 × 0.764 mm) were acquired on a Phillips 7.0-Tesla scanner (32 channel head coil) at Kennedy Krieger Institute (Baltimore, MD).

Binary segmentations in the population were obtained using the multi-atlas random orbit model (45). First, multi-atlases of segmented hippocampi, amygdalae and coarse regions were created from a subset of the population and then used to generate segmentations in the entire population. The initial segmentation and editing were manually performed using Seg3D (46), summarized here.

1. A contributor who was unblinded to the subjects' clinical features selected 5 subjects who were representative of the larger cohort with respect to sex, age, education, and diagnosis. These subjects are henceforth referred to as the atlas subjects. All following steps were performed by a contributor who was blinded to the subjects' clinical features.
2. Skull strip masks were constructed manually for the atlas subjects. This segmentation followed the dura mater around the cerebrum and cerebellum. The inferior most slice was inferior border of the cerebellum (47).
3. The atlas subjects were segmented for left and right hippocampus, and left and right amygdala according to the Mai atlas (48).

   The amygdalae were segmented primarily in the coronal plane, similar to (49). In anterior slices of the amygdalae, white matter defined the ventrolateral and ventromedial borders. The dorsomedial border was defined by the semilunar gyrus. The lateral border was defined by the striations between the amygdala and claustrum. In more posterior slices, the lateral ventricle composed the ventrolateral border and the hippocampus/alveus composed the ventromedial border. The region of white matter that includes the optic tract composed the dorsal border of the amygdala.

   The hippocampi were segmented primarily in the coronal and sagittal planes, similar to (50). In the sagittal plane, the lateral most slice was identified as where gray matter appeared in the temporal horn of the lateral ventricle. In the lateral slices, white matter defined the ventral border, and cerebrospinal fluid (CSF) defined the anterior and posterior borders. The dorsal border of the hippocampus was defined by two white matter structures, the alveus and fimbria. The alveus sits above the anterior portion of the hippocampus and was included in the segmentation. The fimbria is posterior to the alveus and was not included in the segmentation. In the medial slices, the curvature of the hippocampus causes it to appear in two sections, one anterior to the other. In both sections, white matter defined the ventral border. Also, a combination of white matter and CSF from the lateral ventricle defined the dorsal border. In the anterior section, the medial most slice was where the alveus converged with the white matter inferior to the hippocampus. In the posterior section, the medial-most slice is where the splenium of the corpus callosum appears.

   These guidelines include CA1, CA2, and CA3 regions of the hippocampus but exclude the subiculum.
4. The 5 atlas subjects were downsampled to $1 \times 1 \times 1\ mm^3$ voxel size and then passed to MRICloud for *single-atlas* segmentation of coarse regions ("7 Label" Segmentation) such as gray matter, white matter, ventricles, CSF, skull, and background (51). The MRICloud atlas used was Adult22_50yrs_283Labels_26atlases_M2_V9B.
5. The automatic labels from Step 4 were upsampled to the original resolution then combined with the manual labels of hippocampi and amygdalae from Step 3.
6. Using the labeled atlas images from step 5, the LDDMM algorithm from MRICloud was used to perform automatic *multi-atlas* segmentation in the remaining 30 subjects to segment the hippocampi and amygdalae (45, 52, 53). Atlas information was based on segmentations of the atlas subjects from steps 3 and 4.
7. The 30 amygdala and hippocampus segmentations from Step 6 were reviewed and manually revised when necessary.

2.4. Shape Analysis via Surface-Based Morphometry

Earlier works have described this method in more detail (35, 36, 54). Briefly,

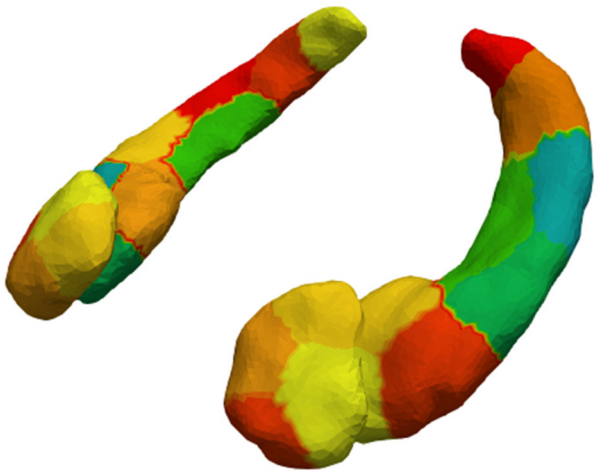

FIGURE 1 | Amygdalar and hippocampal surface discretization from spectral clustering. After clustering, left and right amygdala are divided into 4 patches each and left and right hippocampus into 9 patches each.

1. Segmentations of the four structures (left/right amygdala and hippocampus) were converted to triangulated surfaces with Restricted Delaunay Triangulation (55).
2. The triangulated surfaces were passed to MRICloud to create population surface templates for both amygdalae and hippocampi (56). These templates serve as a common coordinate system for each subcortical structure.
3. The surface templates from step 2, and the triangulated surfaces from step 1 were passed to MRICloud to calculate deformations from each patient to the surface templates. The features on which this paper focuses are the surface Jacobians of the deformation at each vertex of the surface. The surface Jacobian measures the local expansion/atrophy around a particular vertex (56).
4. We downsampled the vertices into surface patches for computational efficiency. The surface patches were constructed with a spectral clustering method, which only relies on surface geometry (36). This method computes the first k eigenvectors of the Laplace-Beltrami operator associated with the surface. Then, each vertex is transformed into a k dimensional vector according to the corresponding elements in the eigenvectors. Finally, we cluster the vertices using the k-means algorithm. We downsampled the structures so the patches would have an average surface area of 150 mm^2 (57). **Figure 1** shows the 4 patches on the amygdalae, and the 9 patches on the hippocampi. The surface Jacobians of all vertices in a patch were averaged to obtain the local expansion/atrophy for that patch.

2.5. Statistical Analysis

Differences in demographic and clinical characteristics and volumes between the HC, responder, and non-responder groups were examined using chi-squared tests, one-way ANOVAs and two-sample *t*-tests implemented in MATLAB. We used general linear models to test for associations between groups (e.g., responder vs. non-responder) and brain shape. The method has been described in detail elsewhere (36). The same method was applied to each of the four structures being investigated, left and right amygdalae, and left and right hippocampi. After surface mapping described above, each participant had an expansion factor for each surface patch in the triangulated surfaces. The expansion factors associated with a brain structure were concatenated into a vector indexed by participant i: y_i (e.g., 4 dimensional vector for the left amygdala). These vectors describe how the brain structure of each participant differs from the template, or "average," brain structure.

To determine whether clinical response status had a significant association with brain shape, we constructed a null linear model and alternative linear model. The alternative model included response status and the null model did not. Both models included covariates for sex, age, and intracranial volume (ICV). The model coefficients β were fit to minimize the sum of squared errors (across all subjects) between the predicted expansion factors and the actual expansion factors.

$$Y = \begin{bmatrix} | & | & \dots & | \\ y_1 & y_2 & \dots & y_n \\ | & | & \dots & | \end{bmatrix}, X = \begin{bmatrix} 1 & 1 & \dots & 1 \\ x_{1,age} & x_{2,age} & \dots & x_{n,age} \\ x_{1,sex} & x_{2,sex} & \dots & x_{n,sex} \\ x_{1,icv} & x_{2,icv} & \dots & x_{n,icv} \\ x_{1,response} & x_{2,response} & \dots & x_{n,response} \end{bmatrix}$$

$$Y_{null} = \begin{bmatrix} | & | & | & | & | \\ \beta_{intercept} & \beta_{age} & \beta_{sex} & \beta_{icv} & 0 \\ | & | & | & | & | \end{bmatrix} X$$

$$Y_{alt} = \begin{bmatrix} | & | & | & | & | \\ \beta_{intercept} & \beta_{age} & \beta_{sex} & \beta_{icv} & \beta_{response} \\ | & | & | & | & | \end{bmatrix} X$$

In words, $Y(a, b)$ corresponded to the expansion factor of the ath patch in participant b and $X(c, d)$ corresponded to the cth covariate in participant d.

For each patch, the sum of squared errors across all subjects was computed for both models and the test statistic considered for patch p was $s_p = \frac{\sum_{i=1}^{n}(Y(p,i)-Y_{null}(p,i))^2}{\sum_{i=1}^{n}(Y(p,i)-Y_{alt}(p,i))^2}$. If the error at a patch was significantly lower in the alternative model, then the test statistic was large. A large test statistic implied that the feature was informative at that patch, i.e., the feature was associated with expansion or atrophy at that location. We used permutation testing to control the familywise error rate to 5% (58). A permutation test rearranged the features among the subjects and at each rearrangement, the maximum test statistic (across all surface patches) was used to form a permutation distribution. Then, the test statistics from the original, true feature arrangement, were compared to this permutation distribution. Any test statistic above the 95th percentile of the permutation distribution was considered significant.

TABLE 1 | Demographic and clinical characteristics and brain volumes, by group.

	Healthy comparison (*N* = 21)	Acute responder (*N* = 9)	Acute non-responder (*N* = 5)	*p*-value
Demographic characteristics				
Age (yrs)	36.3 (13.0)	37.7 (15.2)	31.0 (9.8)	0.65
Sex (% female)	71%	78%	100%	0.39
Education (yrs)	15.4 (2.9)	15.0 (2.5)	17.2 (1.8)	0.32
Clinical characteristics				
BDI	1.4 (1.9)	6.4 (6.5)	11.6 (7.3)	**<0.01***
CARS-M	0.5 (1.3)	1.3 (2.4)	1.0 (2.2)	0.51
HART-FSIQ	110.4 (8.7)	124.9 (8.3)	123.9 (7.8)	**<0.01***
Volumes (cm^3)				
Intracranial (ICV)	1,503 (132)	1,472 (134)	1,406 (34)	0.30
Volumes, normalized by ICV				
Amygdala, left	0.65 (0.13)	0.69 (0.15)	0.66 (0.23)	0.80
Amygdala, right	0.69 (0.13)	0.71 (0.12)	0.70 (0.19)	0.93
Hippocampus, left	1.81 (0.22)	1.85 (0.20)	1.71 (0.25)	0.52
Hippocampus, right	1.61 (0.21)	1.68 (0.28)	1.61 (0.21)	0.73

Shown are mean (standard deviation) unless otherwise indicated. Group differences tested using chi-square tests for dichotomous variables and F*-tests for continuous variables. Post-hoc pairwise* t*-tests performed when evidence of a significant (*p *< 0.05) group difference. *For BDI and HART-FSIQ,* p *< 0.01 for post-hoc groupwise comparisons of responders vs. healthy comparison and non-responders vs. healthy comparison.*

3. RESULTS

3.1. Demographic and Clinical Characteristics

Table 1 describes the distributions of demographic and clinical variables in each acute response group and in HC. As expected, participants with BD had higher levels of depressive symptoms than HC, with non-responders displaying the highest levels of depressive symptoms. Also expected, duration of treatment with lithium was longer for participants responding to lithium than those not responding. We did not detect significant between group differences for the other demographic or clinical variables tested.

3.2. Volume Results

Average ICV and ICV-normalized region of interest (ROI) volumes, are presented in **Table 1**. We did not detect significant between-group differences of ICV or normalized ROI volumes.

3.3. Shape Analysis

Minimum p-values across all patches are presented in **Table 2**. We observed a significant association between expansion factor and response status in the left hippocampus at the acute time point. **Figure 2** shows that the patch significantly associated with response status is on the ventral surface, near the CA1, subiculum junction. This patch was atrophied by about 15% in non-responders when compared to the other groups. The association between expansion factor for this patch and response status maintained trend-level significance at the longer-term treatment time point for the comparison of non-responders vs. responders. We did not detect a significant association between expansion factor and response status in any other structure or patch.

TABLE 2 | Associations between response status and expansion factor, minimum *p*-values.

		Minimum patch *p*-value	
		Acute	Long
Non-responders vs. Responders	Right amygdala	0.20	0.09
	Left Amygdala	0.61	0.90
	Right hippocampus	0.11	0.28
	Left hippocampus	**0.03***	0.10
Non-responders vs. Healthy Comparison ∪ Responders	Right amygdala	0.11	0.13
	Left amygdala	0.51	0.76
	Right hippocampus	0.27	0.82
	Left hippocampus	**0.03***	0.49

Shown are the minimum p*-value in each structure (minimum of 4 patches in amygdala or 9 patches in hippocampus). The first comparison is between non-responders and responders, the second comparison is between non-responders, and the combined group of healthy subjects and responders. *For left hippocampus, minimum patch p < 0.05.*

4. DISCUSSION

Results of this study provide evidence of lateralized morphometric differences in hippocampus in a group of patients with BD who did and did not respond to lithium treatment. We observed a significant difference in a region of the ventral left hippocampus, near the CA1/subiculum junction, which was relatively atrophied in non-responders as compared to responders. We did not find a significant difference in volumes of amygdalae or hippocampi between the lithium responders, non-responders, and HC groups. In this study, we examined individuals' responses to lithium treatment and localized differences in structure, factors that could help explain

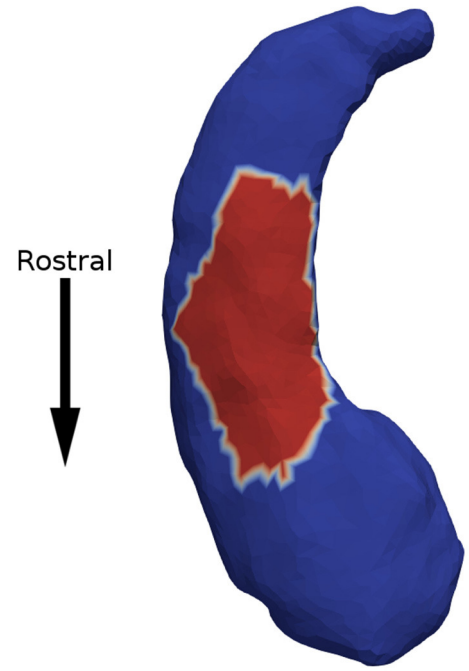

FIGURE 2 | Non-responders were found to have 15% atrophy in a surface patch on the ventral side of the left hippocampus (in red), when compared to responders.

disparate findings related to effects of lithium use on structure of amygdala and hippocampus in the literature (17, 21, 31, 59, 60). In our sample, all participants with BD were treated with lithium monotherapy and were prospectively assessed for their response. Our surface mapping tools allowed for analysis of more localized shape changes that might not be detected by less detailed metrics like volume.

While identification of neuroimaging markers holds potential to predict treatment response, only a few previous studies have used neuroimaging to examine response to lithium treatment in BD. Task-based brain activation changes have been reported in lithium responders as compared to non-responders using functional MRI. One study found greater activation to an emotional faces task in prefrontal cortex and lesser activation in limbic regions in lithium responders as compared to non-responders (25). Another study comparing patients with first episode mania responding vs. not responding to either lithium or quetiapine observed differential changes in activation in subcortical regions in response to a continuous performance task with emotional distractors (29). Studies using functional MRI methods have also identified correlations between lithium response and amygdala-ventromedial prefrontal cortex functional connectivity and a normalizing effect of lithium on resting state connectivity measures (27, 28). Emerging research suggests these normalizing changes could come from neuroprotective effects of lithium against glutamatergic excitotoxicity or its association with higher levels of brain-derived neurotrophic factor (61). One study using structural MRI found a correlation between overall gray matter hypertrophy and clinical response to lithium in BD, but this study did not examine localized brain changes (26).

Most studies examining effects of lithium use on structural MRI have examined brain volumes, cortical thickness or surface area, reducing all morphological information to a single statistic (17, 21, 22, 30, 62). These studies have identified larger volumes of amygdalae and hippocampi in lithium-treated patients compared to patients not treated with lithium, although not consistently. In a large meta-analysis conducted by the ENIGMA consortium of 1,710 subjects with BD and 2,594 HC, though smaller hippocampi and amygdalae were observed in subjects with BD than in HC subjects, an effect of lithium use on these volumes was not found (17). Exploring more local effects in subcortical structure may provide additional information and potentially help further elucidate lithium's neurobiological action. A few studies have examined such structure at a more detailed level, testing volumes of hippocampal subfields, hippocampal thickness and subcortical shape (23, 31–34). These studies reported more localized differences in hippocampus including in CA1, CA2/3 and subiculum, although not consistently. However, these studies assessed structural changes related to lithium use and did not take into account differences in individual responses to lithium treatment.

We combined an examination of local effects in subcortical structure with a focus on individual differences in response to lithium treatment and observed a significant difference in a region of the ventral left hippocampus, near the CA1/subiculum junction, which was relatively atrophied in non-responders as compared to responders. CA1 is the primary output of the hippocampus and is integral in encoding memory related to space (63), novel objects (64), and fear (65). While there is limited literature on morphological differences between patients with BD taking and not taking lithium, our results are consistent with one previous study that identified smaller left CA1 and CA2/3 volumes in patients with BD not using lithium treatment than in a group using lithium, but only among participants with numerous affective episodes (33). Alterations in right hippocampus have also been reported, including a deficit in right CA1 in unmedicated patients with BD as compared to lithium treated patients and reduced volume of right CA2/3 and CA4/DG in patients with psychotic BD not taking vs. taking lithium (31, 32). Other studies have not detected a difference between lithium treated vs. not-treated patients with BD when examining measures of hippocampal shape (23, 34). We note that these inconsistencies in the literature could be at least partially explained by the focus on lithium treatment, not taking into account individual differences in response.

Our observation of a morphological difference in left hippocampus in lithium non-responders as compared to responders builds upon previous work describing lithium's effects in the brain. Using ^{7}Li magnetic resonance imaging, euthymic patients with BD who were treated with lithium for 2 or more years were found to have the highest brain lithium content within a defined cluster in the left hippocampus (66). Additional support for a laterality effect in lithium response comes from a longitudinal study showing a decrease in left

hippocampus volume over the course of treatment in patients with BD who were non-responders (67). Hippocampal laterality effects have also been shown with respect to patients with BD taking vs. not taking lithium, where left hippocampal volume or subfield volume has been shown to be smaller in those not taking lithium compared to those taking lithium or HC (33, 68, 69). Taken together, these findings suggest that left hippocampus may play a key role in lithium's mood stabilizing effects, and coupled with existing evidence of neurogenesis within the hippocampus lend support for the hypothesis of a neurogenic mechanism of action for lithium (70).

Interpretation of this study is limited by the small sample size. There are no males in our non-responder group, which may impact on the generalizability of our findings. There may exist potential confounding by clinical variables such as duration of illness (71), duration of treatment (21), depressive predominant polarity (72), or stressful life events (73) and these variables should be examined in a larger sample powered to do so. It is also important to note that the images in this study were collected after treatment was initiated so these results indicate correlations between brain shape and response, not predictors of response. Although we utilized a manual segmentation process, it was primarily performed by a single trained person blinded to clinical features and so should not differ systematically between groups. Subregions in this study were split along the surfaces and thus any changes occurring within the amygdalae or hippocampi would not have been detected. However, these methods could support deeper subregion analysis in future studies by segmenting images for each subregion, rather than for the whole amygdalae and hippocampi.

This study, to our knowledge, is the first *in-vivo* shape analysis of human brain structures in BD using 7T MRI. Previous morphological studies in humans used MRI field strengths of 3T or less (17, 21–23). Higher field strengths produce images with a higher signal to noise ratio (74) and might detect more subtle differences in neuroanatomy. MRICloud's implementation of LDDMM allowed for both a fast segmentation process and detection of localized shape changes in brain structures.

In order to answer the important question of how to predict lithium response in BD, larger and longitudinal neuroimaging studies are needed to establish whether there are any appreciable differences between responders and non-responders and whether those differences can predict response prior to treatment initiation or at an early stage of treatment. In this paper, we describe a possible approach to studying lithium response via neuroanatomy and report on a specific sub-region of the hippocampus, CA1, which may be associated with lithium response.

DATA AVAILABILITY STATEMENT

The datasets presented in this article are not readily available because they require specialized training to interpret. Requests to access the datasets should be directed to mood@bwh.harvard.edu.

ETHICS STATEMENT

The studies involving human participants were reviewed and approved by Johns Hopkins Institutional Review Board. The patients/participants provided their written informed consent to participate in this study.

AUTHOR CONTRIBUTIONS

PBM, PPZ, JTR, JRD, JRK, and CMN contributed to the study design and implementation. TLA, CC, DJT, KSK, and PBM performed the data analysis. FSG, FM, KR-M, KG, and PBM acquired participant data. All authors contributed to the manuscript preparation.

FUNDING

This work was supported by grants from the National Institutes of Health K01MH093870 (PBM), R01MH110797 (PBM), U01MH092758 (JRK), P41EB015909 (JTR), and R01EB020062 (JTR).

ACKNOWLEDGMENTS

We are appreciative of the PGBD study as this work utilizes clinical information obtained at the Johns Hopkins site as part of that study (PI: JRK; Site PI: PPZ).

REFERENCES

1. Merikangas KR, Akiskal HS, Angst J, Greenberg PE, Hirschfeld RMA, Petukhova M, et al. Lifetime and 12-month prevalence of bipolar spectrum disorder in the National Comorbidity Survey replication. *Arch Gen Psychiatry*. (2007) 64:543–52. doi: 10.1001/archpsyc.64.5.543
2. Kendall T, Morriss R, Mayo-Wilson E, Marcus E. Assessment and management of bipolar disorder: summary of updated NICE guidance. *Brit Med J*. (2014) 349:g5673. doi: 10.1136/bmj.g5673
3. Wyatt RJ, Henter ID, Jamison JC. Lithium revisited: savings brought about by the use of lithium, 1970-1991. *Psychiatr Q*. (2001) 72:149–66. doi: 10.1023/A:1010319610021
4. Geddes JR, Burgess S, Hawton K, Jamison K, Goodwin GM. Long-term lithium therapy for bipolar disorder: systematic review and meta-analysis of randomized controlled trials. *Am J Psychiatry*. (2004) 161:217–22. doi: 10.1176/appi.ajp.161.2.217
5. Yildiz A, Vieta E, Leucht S, Baldessarini RJ. Efficacy of antimanic treatments: meta-analysis of randomized, controlled trials. *Neuropsychopharmacology*. (2011) 36:375. doi: 10.1038/npp.2010.192
6. Rybakowski JK. Response to lithium in bipolar disorder: clinical and genetic findings. *ACS Chem Neurosci*. (2014) 5:413–21. doi: 10.1021/cn5000277
7. Tighe SK, Mahon PB, Potash JB. Predictors of lithium response in bipolar disorder. *Therapeut Adv Chronic Dis*. (2011) 2:209–26. doi: 10.1177/2040622311399173

8. Kleindienst N, Engel RR, Greil W. Which clinical factors predict response to prophylactic lithium? A systematic review for bipolar disorders. *Bipolar Disord*. (2005) 7:404–17. doi: 10.1111/j.1399-5618.2005.00244.x
9. Etain B, Lajnef M, Brichant-Petitjean C, Geoffroy P, Henry C, Gard S, et al. Childhood trauma and mixed episodes are associated with poor response to lithium in bipolar disorders. *Acta Psychiatr Scand*. (2017) 135:319–27. doi: 10.1111/acps.12684
10. Chen CH, Lee CS, Lee MTM, Ouyang WC, Chen CC, Chong MY, et al. Variant GADL1 and response to lithium therapy in bipolar I disorder. *N Engl J Med*. (2014) 370:119–28. doi: 10.1056/NEJMoa1212444
11. Hou L, Heilbronner U, Degenhardt F, Adli M, Akiyama K, Akula N, et al. Genetic variants associated with response to lithium treatment in bipolar disorder: a genome-wide association study. *Lancet*. (2016) 387:1085–93. doi: 10.1016/S0140-6736(16)00143-4
12. Song J, Bergen SE, Di Florio A, Karlsson R, Charney A, Ruderfer DM, et al. Genome-wide association study identifies SESTD1 as a novel risk gene for lithium-responsive bipolar disorder. *Mol Psychiatry*. (2016) 21:1290–7. doi: 10.1038/mp.2015.165
13. Perlis RH, Smoller JW, Ferreira MAR, McQuillin A, Bass N, Lawrence J, et al. A genomewide association study of response to lithium for prevention of recurrence in bipolar disorder. *Am J Psychiatry*. (2009) 166:718–25. doi: 10.1176/appi.ajp.2009.08111633
14. Reinbold CS, Forstner AJ, Hecker J, Fullerton JM, Hoffmann P, Hou L, et al. Analysis of the influence of microRNAs in lithium response in bipolar disorder. *Front Psychiatry*. (2018) 9:207. doi: 10.3389/fpsyt.2018.00207
15. Arnone D, Cavanagh J, Gerber D, Lawrie SM, Ebmeier KP, McIntosh AM. Magnetic resonance imaging studies in bipolar disorder and schizophrenia: meta-analysis. *Brit J Psychiatry*. (2009) 195:194–201. doi: 10.1192/bjp.bp.108.059717
16. McDonald C, Zanelli J, Rabe-Hesketh S, Ellison-Wright I, Sham P, Kalidindi S, et al. Meta-analysis of magnetic resonance imaging brain morphometry studies in bipolar disorder. *Biol Psychiatry*. (2004) 56:411–7. doi: 10.1016/j.biopsych.2004.06.021
17. Hibar DP, Westlye LT, van Erp TGM, Rasmussen J, Leonardo CD, Faskowitz J, et al. Subcortical volumetric abnormalities in bipolar disorder. *Mol Psychiatry*. (2016) 21:1710–6. doi: 10.1038/mp.2015.227
18. Phillips M, Ladouceur C, Drevets W. Neural systems underlying voluntary and automatic emotion regulation: toward a neural model of bipolar disorder. *Mol Psychiatry*. (2008) 13:829. doi: 10.1038/mp.2008.82
19. Phillips ML, Swartz HA. A critical appraisal of neuroimaging studies of bipolar disorder: toward a new conceptualization of underlying neural circuitry and a road map for future research. *Am J Psychiatry*. (2014) 171:829–43. doi: 10.1176/appi.ajp.2014.13081008
20. Langan C, McDonald C. Neurobiological trait abnormalities in bipolar disorder. *Mol Psychiatry*. (2009) 14:833–46. doi: 10.1038/mp.2009.39
21. Sani G, Simonetti A, Janiri D, Banaj N, Ambrosi E, De Rossi P, et al. Association between duration of lithium exposure and hippocampus/amygdala volumes in type I bipolar disorder. *J Affect Disord*. (2018) 232:341–8. doi: 10.1016/j.jad.2018.02.042
22. Savitz J, Nugent AC, Bogers W, Liu A, Sills R, Luckenbaugh DA, et al. Amygdala volume in depressed patients with bipolar disorder assessed using high resolution 3T MRI: the impact of medication. *Neuroimage*. (2010) 49:2966–76. doi: 10.1016/j.neuroimage.2009.11.025
23. van Erp TGM, Thompson PM, Kieseppä T, Bearden CE, Marino AC, Hoftman GD, et al. Hippocampal morphology in lithium and non-lithium-treated bipolar I disorder patients, non-bipolar co-twins, and control twins. *Hum Brain Mapp*. (2012) 33:501–10. doi: 10.1002/hbm.21239
24. Anand A, Nakamura K, Spielberg JM, Cha J, Karne H, Hu B. Integrative analysis of lithium treatment associated effects on brain structure and peripheral gene expression reveals novel molecular insights into mechanism of action. *Transl Psychiatry*. (2020) 10:1–10. doi: 10.1038/s41398-020-0784-z
25. Rootes-Murdy K, Glazer K, Mondimore FM, Goes FS, Zandi PP, Bakker A, et al. A pilot fMRI study of lithium response in bipolar disorder. *Psychiatry Res Neuroimaging*. (2019) 286:1. doi: 10.1016/j.pscychresns.2019.02.003
26. Lyoo IK, Dager SR, Kim JE, Yoon SJ, Friedman SD, Dunner DL, et al. Lithium-induced gray matter volume increase as a neural correlate of treatment response in bipolar disorder: a longitudinal brain imaging study. *Neuropsychopharmacology*. (2010) 35:1743–50. doi: 10.1038/npp.2010.41
27. Altinay M, Karne H, Anand A. Lithium monotherapy associated clinical improvement effects on amygdala-ventromedial prefrontal cortex resting state connectivity in bipolar disorder. *J Affect Disord*. (2018) 225:4–12. doi: 10.1016/j.jad.2017.06.047
28. Spielberg JM, Matyi MA, Karne H, Anand A. Lithium monotherapy associated longitudinal effects on resting state brain networks in clinical treatment of bipolar disorder. *Bipolar Disord*. (2019) 21:361–71. doi: 10.1111/bdi.12718
29. Strakowski SM, Fleck DE, Welge J, Eliassen JC, Norris M, Durling M, et al. fMRI brain activation changes following treatment of a first bipolar manic episode. *Bipolar Disord*. (2016) 18:490–501. doi: 10.1111/bdi.12426
30. Hibar DP, Westlye LT, Doan NT, Jahanshad N, Cheung JW, Ching CRK, et al. Cortical abnormalities in bipolar disorder: an MRI analysis of 6503 individuals from the ENIGMA bipolar disorder working group. *Mol Psychiatry*. (2018) 23:932–42. doi: 10.1038/mp.2017.73
31. Bearden CE, Thompson PM, Dutton RA, Frey BN, Peluso MA, Nicoletti M, et al. Three-dimensional mapping of hippocampal anatomy in unmedicated and lithium-treated patients with bipolar disorder. *Neuropsychopharmacology*. (2008) 33:1229–38. doi: 10.1038/sj.npp.1301507
32. Giakoumatos CI, Nanda P, Mathew IT, Tandon N, Shah J, Bishop JR, et al. Effects of lithium on cortical thickness and hippocampal subfield volumes in psychotic bipolar disorder. *J Psychiatr Res*. (2015) 61:180–7. doi: 10.1016/j.jpsychires.2014.12.008
33. Hartberg CB, JÃ8rgensen KN, Haukvik UN, Westlye LT, Melle I, Andreassen OA, et al. Lithium treatment and hippocampal subfields and amygdala volumes in bipolar disorder. *Bipolar Disord*. (2015) 17:496–506. doi: 10.1111/bdi.12295
34. Vecchio D, Piras F, Piras F, Banaj N, Janiri D, Simonetti A, et al. Lithium treatment impacts nucleus accumbens shape in bipolar disorder. *Neuroimage Clin*. (2020) 25:102167. doi: 10.1016/j.nicl.2020.102167
35. Miller MI, Younes L, Ratnanather JT, Brown T, Trinh H, Lee DS, et al. Amygdalar atrophy in symptomatic Alzheimer's disease based on diffeomorphometry: the BIOCARD cohort. *Neurobiol Aging*. (2015) 36:S3–10. doi: 10.1016/j.neurobiolaging.2014.06.032
36. Younes L, Ratnanather JT, Brown T, Aylward E, Nopoulos P, Johnson H, et al. Regionally selective atrophy of subcortical structures in prodromal HD as revealed by statistical shape analysis. *Hum Brain Mapp*. (2014) 35:792–809. doi: 10.1002/hbm.22214
37. Oedegaard KJ, Alda M, Anand A, Andreassen OA, Balaraman Y, Berrettini WH, et al. The Pharmacogenomics of Bipolar Disorder study (PGBD): identification of genes for lithium response in a prospective sample. *BMC Psychiatry*. (2016) 16:129. doi: 10.1186/s12888-016-0732-x
38. Nurnberger JI, Blehar MC, Kaufmann CA, York-Cooler C, Simpson SG, Harkavy-Friedman J, et al. Diagnostic interview for genetic studies: rationale, unique features, and training. *Arch Gen Psychiatry*. (1994) 51:849–59. doi: 10.1001/archpsyc.1994.03950110009002
39. Beck AT, Ward CH, Mendelson M, Mock J, Erbaugh J. An inventory for measuring depression. *Arch Gen Psychiatry*. (1961) 4:561–71. doi: 10.1001/archpsyc.1961.01710120031004
40. Altman EG, Hedeker DR, Janicak PG, Peterson JL, Davis JM. The clinician-administered rating scale for mania (CARS-M): development, reliability, and validity. *Biol Psychiatry*. (1994) 36:124–34. doi: 10.1016/0006-3223(94)91193-2
41. Sheehan DV, Lecrubier Y, Sheehan KH, Amorim P, Janavs J, Weiller E, et al. The Mini-International Neuropsychiatric Interview (MINI): the development and validation of a structured diagnostic psychiatric interview for DSM-IV and ICD-10. *J Clin Psychiatry*. (1998) 59:22–33. doi: 10.1037/t18597-000
42. Schretlen DJ, Winicki JM, Meyer SM, Testa SM, Pearlson GD, Gordon B. Development, psychometric properties, and validity of the Hopkins Adult Reading Test (HART). *Clin Neuropsychol*. (2009) 23:926–43. doi: 10.1080/13854040802603684
43. Folstein MF, Folstein SE, McHugh PR. "Mini-mental state": a practical method for grading the cognitive state of patients for the clinician. *J Psychiatr Res*. (1975) 12:189–98. doi: 10.1016/0022-3956(75)90026-6
44. Nasreddine ZS, Phillips NA, Bédirian V, Charbonneau S, Whitehead V, Collin I, et al. The Montreal Cognitive Assessment, MoCA: a brief screening tool for mild cognitive impairment. *J Am Geriatr Soc*. (2005) 53:695–9. doi: 10.1111/j.1532-5415.2005.53221.x

45. Tang X, Oishi K, Faria AV, Hillis AE, Albert MS, Mori S, et al. Bayesian parameter estimation and segmentation in the multi-atlas random orbit model. *PLoS ONE*. (2013) 8:e65591. doi: 10.1371/journal.pone.0065591
46. CIBC. *Seg3D: Volumetric Image Segmentation and Visualization*. Scientific Computing and Imaging Institute (SCI) (2016). Available online at: http://www.seg3d.org
47. Malone IB, Leung KK, Clegg S, Barnes J, Whitwell JL, Ashburner J, et al. Accurate automatic estimation of total intracranial volume: a nuisance variable with less nuisance. *Neuroimage*. (2015) 104:366–72. doi: 10.1016/j.neuroimage.2014.09.034
48. Mai JK, Majtanik M, Paxinos G. *Atlas of the Human Brain*. Academic Press (2015).
49. Entis JJ, Doerga P, Barrett LF, Dickerson BC. A reliable protocol for the manual segmentation of the human amygdala and its subregions using ultra-high resolution MRI. *Neuroimage*. (2012) 60:1226–35. doi: 10.1016/j.neuroimage.2011.12.073
50. Berron D, Vieweg P, Hochkeppler A, Pluta JB, Ding SL, Maass A, et al. A protocol for manual segmentation of medial temporal lobe subregions in 7 Tesla MRI. *Neuroimage Clin*. (2017) 15:466–82. doi: 10.1016/j.nicl.2017.05.022
51. Ye C, Ma T, Wu D, Ceritoglu C, Miller MI, Mori S. Atlas preselection strategies to enhance the efficiency and accuracy of multi-atlas brain segmentation tools. *PLoS ONE*. (2018) 13:e0200294. doi: 10.1371/journal.pone.0200294
52. Mori S, Wu D, Ceritoglu C, Li Y, Kolasny A, Vaillant MA, et al. MRICloud: delivering high-throughput MRI neuroinformatics as cloud-based software as a service. *Comput Sci Eng*. (2016) 18:21–35. doi: 10.1109/MCSE.2016.93
53. Wang H, Pouch A, Takabe M, Jackson B, Gorman J, Gorman R, et al. Multi-atlas segmentation with robust label transfer and label fusion. In: *International Conference on Information Processing in Medical Imaging*. Springer (2013) p. 548–59. doi: 10.1007/978-3-642-38868-2_46
54. Mahon PB, Lee DS, Trinh H, Tward D, Miller MI, Younes L, et al. Morphometry of the amygdala in schizophrenia and psychotic bipolar disorder. *Schizophrenia Res*. (2015) 164:199–202. doi: 10.1016/j.schres.2015.02.011
55. Chew LP. Constrained Delauney tirangulations. *Algorithmica*. (1989) 4:97–108. doi: 10.1007/BF01553881
56. Ma J, Miller MI, Younes L. A Bayesian generative model for surface template estimation. *Int J Biomed Imaging*. (2010) 2010:1–14. doi: 10.1155/2010/974957
57. Faria AV, Ratnanather JT, Tward DJ, Lee DS, van den Noort F, Wu D, et al. Linking white matter and deep gray matter alterations in premanifest Huntington disease. *Neuroimage Clin*. (2016) 11:450–60. doi: 10.1016/j.nicl.2016.02.014
58. Nichols T, Hayasaka S. Controlling the familywise error rate in functional neuroimaging: a comparative review. *Stat Methods Med Res*. (2003) 12:419–46. doi: 10.1191/0962280203sm341ra
59. Lopez-Jaramillo C, Vargas C, Diaz-Zuluaga AM, Palacio JD, Castrillon G, Bearden C, et al. Increased hippocampal, thalamus and amygdala volume in long—term lithium—treated bipolar I disorder patients compared with unmedicated patients and healthy subjects. *Bipolar Disord*. (2017) 19:41–9. doi: 10.1111/bdi.12467
60. Hajek T, Kopecek M, Hoschl C, Alda M. Smaller hippocampal volumes in patients with bipolar disorder are masked by exposure to lithium: a meta-analysis. *J Psychiatry Neurosci*. (2012) 37:333. doi: 10.1503/jpn.110143
61. Machado-Vieira R. Lithium, stress, and resilience in bipolar disorder: deciphering this key homeostatic synaptic plasticity regulator. *J Affect Disord*. (2018) 233:92–9. doi: 10.1016/j.jad.2017.12.026
62. Blumberg HP, Kaufman J, Martin A, Whiteman R, Zhang JH, Gore JC, et al. Amygdala and hippocampal volumes in adolescents and adults with bipolar disorder. *Arch Gen Psychiatry*. (2003) 60.12:1201–08. doi: 10.1001/archpsyc.60.12.1201
63. Hartley T, Lever C, Burgess N, O'Keefe J. Space in the brain: how the hippocampal formation supports spatial cognition. *Philos Trans R Soc B Biol Sci*. (2014) 369:20120510. doi: 10.1098/rstb.2012.0510
64. Cohen SJ, Stackman RW Jr. Assessing rodent hippocampal involvement in the novel object recognition task. A review. *Behav Brain Res*. (2015) 285:105–17. doi: 10.1016/j.bbr.2014.08.002
65. Izquierdo I, Furini CR, Myskiw JC. Fear memory. *Physiol Rev*. (2016) 96:695–750. doi: 10.1152/physrev.00018.2015
66. Stout J, Hozer F, Coste A, Mauconduit F, Djebrani-Oussedik N, Sarrazin S, et al. Accumulation of lithium in the hippocampus of patients with bipolar disorder: a lithium-7 magnetic resonance imaging study at 7 Tesla. *Biol Psychiatry*. (2020) 88:426–33. doi: 10.1016/j.biopsych.2020.02.1181
67. Selek S, Nicoletti M, Zunta-Soares GB, Hatch JP, Nery FG, Matsuo K, et al. A longitudinal study of fronto-limbic brain structures in patients with bipolar I disorder during lithium treatment. *J Affect Disord*. (2013) 150:629–33. doi: 10.1016/j.jad.2013.04.020
68. Hajek T, Cullis J, Novak T, Kopecek M, Höschl C, Blagdon R, et al. Hippocampal volumes in bipolar disorders: opposing effects of illness burden and lithium treatment. *Bipolar Disord*. (2012) 14:261–70. doi: 10.1111/j.1399-5618.2012.01013.x
69. Zung S, Souza-Duran F, Soeiro-de Souza M, Uchida R, Bottino C, Busatto G, et al. The influence of lithium on hippocampal volume in elderly bipolar patients: a study using voxel-based morphometry. *Transl Psychiatry*. (2016) 6:e846. doi: 10.1038/tp.2016.97
70. Toda T, Gage FH. Adult neurogenesis contributes to hippocampal plasticity. *Cell Tissue Res*. (2018) 373:693–709. doi: 10.1007/s00441-017-2735-4
71. Javadapour A, Malhi GS, Ivanovski B, Chen X, Wen W, Sachdev P. Hippocampal volumes in adults with bipolar disorder. *J Neuropsychiatry Clin Neurosci*. (2010) 22:55–62. doi: 10.1176/jnp.2010.22.1.55
72. Janiri D, Simonetti A, Piras F, Ciullo V, Spalletta G, Sani G. Predominant polarity and hippocampal subfield volumes in Bipolar disorders. *Bipolar Disord*. (2020) 22:490–7. doi: 10.1111/bdi.12857
73. Janiri D, Sani G, De Rossi P, Piras F, Banaj N, Ciullo V, et al. Hippocampal subfield volumes and childhood trauma in bipolar disorders. *J Affect Disord*. (2019) 253:35–43. doi: 10.1016/j.jad.2019.04.071
74. Vaughan JT, Garwood M, Collins CM, Liu W, DelaBarre L, Adriany G, et al. 7T vs. 4T: RF power, homogeneity, and signal-to-noise comparison in head images. *Magnet Reson Med*. (2001) 46:24–30. doi: 10.1002/mrm.1156

Conflict of Interest: JRD reports that he is Chairperson of the Board of Directors of the National Network of Depression Centers and receives reimbursement for official travel (amounting to less than $1500 annually). He has been an unpaid consultant for Myriad Neuroscience (formerly Assurex Health, Inc.) on behalf of the NNDC for meetings in 2017 and 2019. The NNDC was compensated for his effort. JRD owns stock in CVS-Health (275 shares valued today at just over $20,000).

The remaining authors declare that the research was conducted in the absence of any commercial or financial relationships that could be construed as a potential conflict of interest.

frontiers in Psychiatry

ORIGINAL RESEARCH
published: 24 March 2021
doi: 10.3389/fpsyt.2021.568932

Deep Brain Stimulation for Obsessive-Compulsive Disorder: Real World Experience Post-FDA-Humanitarian Use Device Approval

Lora Kahn[1], Brianne Sutton[2], Helena R. Winston[2], Aviva Abosch[3], John A. Thompson[4,5†] and Rachel A. Davis[2†]*

[1] Department of Neurosurgery, Ochsner Health, Tulane University-Ochsner Health Neurosurgery Program, New Orleans, LA, United States, [2] Department of Psychiatry, University of Colorado, Anschutz Medical Campus, Aurora, CO, United States, [3] Department of Neurosurgery, University of Nebraska Medical Center, Omaha, NE, United States, [4] Department of Neurosurgery, University of Colorado, Anschutz Medical Campus, Aurora, CO, United States, [5] Department of Neurology, University of Colorado, Anschutz Medical Campus, Aurora, CO, United States

OPEN ACCESS

Edited by:
Bartosz Zurowski, University Medical Center Schleswig-Holstein, Germany

Reviewed by:
Kelly Douglas Foote, University of Florida, United States
Osama Ali Abulseoud, National Institute on Drug Abuse (NIDA), United States

***Correspondence:**
Rachel A. Davis
rachel.davis@cuanschutz.edu

† These authors have contributed equally to this work and share senior authorship

Specialty section:
This article was submitted to Neuroimaging and Stimulation, a section of the journal Frontiers in Psychiatry

Received: *02 June 2020*
Accepted: *10 February 2021*
Published: *24 March 2021*

Citation:
Kahn L, Sutton B, Winston HR, Abosch A, Thompson JA and Davis RA (2021) Deep Brain Stimulation for Obsessive-Compulsive Disorder: Real World Experience Post-FDA-Humanitarian Use Device Approval. Front. Psychiatry 12:568932. doi: 10.3389/fpsyt.2021.568932

Background: While case series have established the efficacy of deep brain stimulation (DBS) in treating obsessive-compulsive disorder (OCD), it has been our experience that few OCD patients present without comorbidities that affect outcomes associated with DBS treatment. Here we present our experience with DBS therapy for OCD in patients who all have comorbid disease, together with the results of our programming strategies.

Methods: For this case series, we assessed five patients who underwent ventral capsule/ventral striatum (VC/VS) DBS for OCD between 2015 and 2019 at the University of Colorado Hospital. Every patient in this cohort exhibited comorbidities, including substance use disorders, eating disorder, tic disorder, and autism spectrum disorder. We conducted an IRB-approved, retrospective study of programming modifications and treatment response over the course of DBS therapy.

Results: In addition to patients' subjective reports of improvement, we observed significant improvement in the Yale-Brown Obsessive-Compulsive Scale (44%), the Montgomery-Asberg Depression Rating Scale (53%), the Quality of Life Enjoyment and Satisfaction Questionnaire (27%), and the Hamilton Anxiety Rating scales (34.9%) following DBS. With respect to co-morbid disease, there was a significant improvement in a patient with tic disorder's Total Tic Severity Score (TTSS) ($p = 0.005$).

Conclusions: DBS remains an efficacious tool for the treatment of OCD, even in patients with significant comorbidities in whom DBS has not previously been investigated. Efficacious treatment results not only from the accurate placement of the electrodes by the surgeon but also from programming by the psychiatrist.

Keywords: psychiatric DBS, co-morbidity, deep brain stimulation, obsessive-compulsive disorder, DBS programming

INTRODUCTION

Obsessive-compulsive disorder (OCD) is a debilitating disorder characterized by obsessions and compulsions that afflicts ∼1.2% of people in the United States and between 1.1 and 1.8% worldwide (1). Obsessions are unwanted thoughts, urges, or images that cause distress. Compulsions are repetitive behaviors or mental "acts" (such as counting) that are performed to assuage distress or to prevent a feared event from happening. Many but not all compulsions make sense cognitively but consume far more time than they would for someone without OCD. For example, fear of contamination might lead to excessive handwashing or fear of burning down the house might lead to excessive checking of the stove. While there are different severities of OCD, some people suffer extreme impairment to the degree that they are unable to maintain regular employment or enjoy everyday activities (2). There are five general subsets of symptoms within OCD, including contamination obsessions with washing/cleaning compulsions; harm obsessions with checking compulsions, obsessions without visible compulsions; symmetry obsessions with ordering, arranging, and counting compulsions, and hoarding (3).

Treatment generally includes cognitive-behavior therapy (CBT) with exposure and response prevention (EX/RP) alone or a combination of EX/RP and medications such as selective serotonin reuptake inhibitors (SSRIs), the tricyclic antidepressant clomipramine, and/or antipsychotics (4, 5). Despite maximal treatment, usually combining EX/RP with serotonergic and other augmenting agents, it is seldom that patients with OCD are able to achieve full remission, which is defined as a subclinical score of $\leq$7 on the Yale-Brown Obsessive Compulsive Score (Y-BOCS). Approximately 10% remain severely incapacitated despite receiving EX/RP coupled with therapeutic medication regimens (6). For these refractory patients, treatment options are extremely limited.

Deep brain stimulation (DBS) involves a technique by which stimulating electrodes are placed in the deep nuclei of the brain, usually the ventral capsule/ventral striatum. The mechanism of DBS in OCD has not been fully elucidated but is thought to modify aberrant circuitry, including the cortico-striato-thalamic-cortical (CSTC) circuit. Applied initially to intractable pain, DBS is most commonly employed in movement disorders such as Parkinson's disease but has been used for the treatment of OCD predicated on the understanding of the CSTC circuit's involvement in this disorder (7). The idea of applying DBS to OCD grew out of observations that lesional procedures such as anterior capsulotomy, utilized for the treatment of OCD since the 1950s, are about 50–60% effective in treating refractory patients with the disorder (8–10). However, whereas lesional procedures create enduring changes in the brain by permanently destroying tissue and irreversibly interrupting circuits, DBS is a reversible and titratable form of neuromodulation.

The first case of DBS for refractory OCD was performed in 1999 in the anterior limb of the internal capsule (ALIC; the same target as in anterior capsulotomy) before being further refined to the ventral capsule/ventral striatum (VC/VS). Both the AC and VC/VS participate in the same CSTC circuit (10, 11). In fact, stimulating different targets within the CSTC circuit has been shown to have similar efficacy (12). VC/VS is the most commonly reported target in the literature, followed by the nucleus accumbens (NAc) and then others (13). Bilateral targeting is performed in DBS surgery as the 2014 evidenced-based guidelines reported that there are insufficient data to support unilateral targeting (14). DBS received a Humanitarian Use Device (HUD) designation in 2009 under a Humanitarian Device Exemption (HDE), meaning that it can be used to treat "severe to extreme" refractory cases of OCD. An HDE is granted for Humanitarian Use Devices (HUDs) that have been found to be safe, have probable benefit, and are intended to be used in <8,000 patients per year. HDEs are designed to bring hope to those suffering severely who cannot wait for extensive large-scale trials that would be required to demonstrate the effectiveness and may never be feasible (15).

While previous studies have established that DBS for OCD is likely to be a beneficial treatment for refractory severely impaired patients, these studies have largely ignored how DBS impacts (or does not affect) the other psychiatric diseases that are so frequently comorbid with OCD (12). OCD rarely occurs in isolation. For example, according to the DSM5, 76% of patients with OCD also have a lifetime diagnosis of an anxiety disorder such as panic disorder, generalized anxiety disorder, or social anxiety disorder; 41% have a lifetime diagnosis of major depressive disorder (MDD); 22% have a lifetime diagnosis of a bipolar spectrum or depressive disorder other than MDD; and 30% have a lifetime tic disorder. The DSM5 also states that rates of OCD are elevated in those with eating disorders and schizophrenia-spectrum disorders. Here we discuss our DBS treatment of refractory OCD patients who have such comorbid disease and our experiences with programming for OCD while managing multiple symptoms of these other illnesses and minimizing side effects.

METHODS

Between 2015 and 2019, five patients were implanted bilaterally with 4-contact electrodes (Model 3391, Medtronic, Minneapolis, MN) targeting the VC/VS at our institution by a single surgeon (AA) after approval by an interdisciplinary ethics conference as advised in the literature (16). Three cases were done awake with microelectrode recording and intraoperative testing by a single psychiatrist (RD), and the remaining two patients elected for an asleep protocol using an MRI-guided direct targeting technique. Consensus coordinates were utilized for initial targeting; however, the targets were ultimately refined directly based on each patient's individual images. The indirect targeting anatomic coordinates used were 7–10 mm lateral to the midline on the X axis, 0–5 mm anterior to the anterior commissure (AC) in the Y axis, and 1–5 mm inferior to the inferior border of the AC in the Z axis. In all cases, the target was advanced by 3 mm (the depth of one contact) after the identification of the direct target to allow for the space between contacts 0 and 1 to rest at the junction of the anterior limb of the internal capsule (ALIC) with the anterior limb of the AC. All

patients returned at least 1 week after cranial lead implantation for placement of bilateral extension cables and pulse generators. There were no associated surgical complications. Rating scales were performed by a single psychiatrist (RD) who was also the primary programmer; when multiple scales were available from pre-operative assessment, they were averaged for the sake of our analysis. We have from 1 to 4 years of follow-up for each patient. Patients provided informed, written consent for this retrospective case report and reviewed the material described in this report; in addition, all efforts have been made to preserve anonymity.

Calculation of Charge Density

For monopolar configurations, charge density was calculated with the standard approach:

Charge density = (current * PW)/surface area. For bipolar configuration, charge density was calculated by dividing the current at the cathode and anode.

Measurement of Distance Between the Active Contact(s) and the Anterior Commissure (AC) – Anterior Limb of the Internal Capsule (ALIC) Junction

For each patient, using pre-operative MRI, expert identification of the AC-ALIC junction was localized to the axial plane at the optimal level for the AC. Following co-registration of the pre-operative MRI with the post-operative CT (in cases 2–5) or post-operative MRI (case 1), the ventral-most point of the lead artifact was localized. Next, for each patient, the final follow-up active contacts were used to estimate the location along the lead artifact for localizing the active contact in the CT space. For a monopolar setting, the midpoint of the contact was used; for bipolar or double monopolar settings, the midpoint between the contacts was used as the active contact location. Finally, the distance in mm between the active contact location along the electrode artifact and the AC-ALIC junction was measured.

Methodology for Programming

A single psychiatrist (RD) performed initial and ongoing programming for all 5 patients. Initial programming took place over three consecutive days, then weekly for several weeks, followed by every other week for about 6 weeks, then monthly with spacing to every 3 months once ideal settings were selected. The programming algorithm described by Widge et al. (17) was followed on the first 3 days, with adjustments to the algorithm as needed based on patient response (e.g., titrating in smaller increments for patient comfort or fine-tuning, not increasing to 6 V if the response was obvious at 4 V). Selection of parameters was based on a reduction in anxiety, an increase in energy, improvement in mood, the patients' subjective experience, and the programmer's observations of the patient's engagement and affect (18). On day one, the psychiatrist performed a monopolar survey at contacts 0, 1, 2, and 3 at amplitudes of 2, 4, and 6 V with frequency of 135 and pulse width of 90 microseconds. This was repeated at a pulse width of 150 microseconds and was done separately for each hemisphere. On day two, the psychiatrist performed a bipolar survey (with contact 3 as the anode) at each contact using a frequency of 135 and the pulse width value that yielded the best response during the monopolar survey. Widge et al., suggest using (0–, 1–, 3+) and (1–, 2–, 3+) (17). The psychiatrist in this report used (0–, 3+), (1–, 3+), (2–, 3+) or the combination of 2 cathodes as suggested by Widge et al. depending on patients' response during the monopolar survey (17). On day three, the psychiatrist selected the settings at which the patient had the best response and made minor adjustments as needed, such as increasing or decreasing amplitude, decreasing frequency (e.g., to target increased anxiety), or decreasing or increasing pulse width (e.g., if a patient had more improvement at 150 microseconds but also more adverse effects, an intermediate pulse width could be selected).

Statistical Analysis for Diagnostic Rating Scales

For all five patients, the following scales were assessed before DBS surgery and at every programming session after implantation: the Yale-Brown Obsessive Compulsive Scale (Y-BOCs), the Montgomery-Asberg Depression Rating Scale (MADRS), the Hamilton Anxiety Rating Scale (HAM-A), and the Quality of Life Enjoyment and Satisfaction questionnaire (Q-LES-Q-SF), and the Young Mania Rating Scale (YMRS). Individual cases exhibited comorbidities that were assessed with relevant scales: Case 1, with a history of anorexia nervosa, assessed with Eating Disorder Examination 16.0 (19); Case 2, with a history of tic disorder, assessed with Yale Global Tic Severity Scale (YGTSS) (20); Case 4, had comorbid substance use which was assessed substance craving scales for cigarettes, marijuana and alcohol (21). Rating scale scores collected following DBS were compared to the pre-surgical baseline by computing the percent change. For each case, on each scale, the change from baseline was statistically assessed by a univariate paired *t*-test between the average pre-surgery and post-surgical assessment data. A Bonferroni correction was for multiple comparisons (per scale, the number of comparisons was equal to the number of cases).

Case Vignettes

Case 1

A 32-year-old woman with a 24-year history of OCD and comorbid severe and enduring anorexia nervosa and severe major depressive disorder (MDD) presented with a Yale-Brown Obsessive-Compulsive Scale (YBOCS) rating of 36. Her obsessions included fear of bad things happening (of which one potential bad thing was weight gain), and her compulsions included repeating things a certain number of times, organizing and arranging, and reassurance seeking. Though she had previously worked briefly as a registered nurse, she had been institutionalized for much of her child and adult life. She had one previous suicide attempt in 2013, and she continued to experience persistent, passive suicidal thoughts. She had episodes of self-harm, including an incident where she fractured her hand 18 months prior to evaluation. She continued to engage in self-harm when distressed, including scratching and excoriating herself. She had failed numerous medications [8 adequate trials of serotonergic medications, 7 atypical antipsychotics, 2 first generation antipsychotics, 2 monoamine oxidase inhibitors

(MAO-Is), 4 benzodiazepines, intranasal ketamine, and multiple augmenting agents] and electroconvulsive shock therapy. She elected to proceed with awake placement of bilateral VC/VS electrodes, and intraoperative exposure included the soft drink Coca-Cola, the candy Tootsie Pop, and the color red, to all of which she had an aversion.

Case 2

A 46-year-old man with a 25-year history of OCD together with autism-spectrum disorder, tic disorder, and MDD had failed 5 serotonergic medications including clomipramine at adequate dose and duration with appropriate augmenting strategies prior to presenting with a YBOCS of 39. His main obsession was that he was not seeing things correctly, and his compulsions included staring and checking. Despite doing well in advanced classes in high school, he was not able to finish higher education or maintain a job and thus elected to proceed with asleep direct targeting protocol placement of bilateral VC/VS electrodes. Details regarding Case 2 were previously published (22).

Case 3

The third patient was a 28-year-old man with a 19-year history of OCD together with attention deficit/hyperactivity disorder (ADHD), MDD, and a previous history of cannabis use disorder who failed multiple medications and augmenting strategies, including three trials of serotonergic medications at adequate dose and duration (one of which was clomipramine) and subsequently presented for treatment with a YBOCS of 32. His obsessions included disgust related to fast food, people who ate fast food, American cars, and anything/anyone from the East or the South. His compulsions including cleaning and washing. He had to withdraw from his graduate program but remained highly motivated to "be better." He underwent staged, awake placement of bilateral VC/VS electrodes.

Case 4

A 48-year-old male had been diagnosed with OCD at age 24 by a priest because he presented compulsively to confession. At the time of presentation, he had a YBOCS of 32 after having failed 3 serotonergic medications at adequate dosage and duration and 2 antipsychotics. His obsessions included a fear of displeasing God, a fear of going to Hell, and a fear of his mother being in Hell. His compulsions included praying and moving in certain ways. He had comorbid MDD, insomnia, and issues with substance use [nicotine use disorder, daily cannabis use, and heavy alcohol use – as defined by the NIAAA (23)]. He was working in construction at the time of surgery. He underwent staged, awake placement of bilateral VC/VS electrodes.

Case 5

The most recently operated patient is a 42-year-old man with a 23-year history of OCD with comorbid MDD and social anxiety disorder who presented with a YBOCS of 36. His obsessions included a fear that inanimate objects were watching him play video games and that if he saw people moving or speaking, this would mean he wouldn't be able to move or speak in the future. He recognized the illogical nature of these thoughts and referred to them as "psychotic." Though patient's obsessions were bizarre and irrational, he had good insight into this and did not meet criteria for a primary psychotic disorder. He had tried five different classes of medications, including 3 serotonergic medications including clomipramine at adequate dose and duration, benzodiazepines, antipsychotics, stimulants, and mood stabilizers. He had intravenous ketamine and underwent 40 sessions of deep transcranial magnetic stimulation (TMS) for OCD with limited effect. He had previously undergone a parathyroidectomy (pathology: normal) in attempt to ameliorate his symptoms; however, this did not result in the desired functional improvement. He subsequently elected to proceed with asleep-protocol bilateral placement of VC/VS electrodes.

Programming

Patient 1

This patient agreed to remain in whatever level of care was necessary to maintain ideal body weight during the first year of DBS programming, which was ultimately residential treatment. Positive effect on mood and energy was partially maintained by turning down amplitude bilaterally at night. Currently, stimulation amplitude is set higher relative to the other patients in this cohort, and the authors postulate this is due to two factors: (1) severe, profound depression at baseline [highest score on MADRS of the 5 patients – 41.67 mean pre-operative score vs. 29.67 (#2), 28.5 (#3), 30 (#4), and 35.5 (#5)] and (2) less obvious response to stimulation led to continued titration.

Patient 2

Programming was complicated by this patient's autism spectrum disorder leading to difficulty describing his internal mood and anxiety states. He disliked any obvious changes so amplitude was increased very gradually, and frequency was lowered to 100 Hz.

Patient 3

The left electrode was pulled back post-operatively due to imaging showing it was abutting the internal carotid artery. There was still noted benefit during initial programming, but the patient felt the effect was less noticeable than the right. This patient experienced dramatic reduction in YBOCS and improvement in mood in the first week (YBOCS: 9 = 72% reduction; MADRS: 12 = 58% reduction; YMRS = 1) with R hemisphere: case +/0–/1–; 3.5 V; 135 Hz; 150 μs and L hemisphere: case +/0–; 4 V; 135 Hz; 150 μs. To this patient's dismay, these effects did not last, and his Y-BOCS increased back to 24 (27% reduction from baseline) and MADRS to 32 (12% increase from baseline) by the second week. He was quite disappointed for several months, hoping the psychiatrist would do something to bring back those feelings. His MADRS peaked at 37 (30% increase from baseline) with a Y-BOCS of 18 at 7 weeks post-stimulation. At this point, low-dose olanzapine (2.5 g) was added, leading to marked improvement in OCD and depression symptoms. MADRS declined to 11 at 14 weeks post-stimulation with a Y-BOCS of 16, then increased again to MADRS of 31 and Y-BOCS of 22 at 32 weeks post-stimulation after a month's trial of reduction in pulse width from 150 to 120 μs (reduced due to patient feeling jittery and agitated at amplitudes higher than 2 V on the right). Mood and OCD symptoms improved with increase back to 150 μs bilaterally,

and he limited amplitude on the right to 2.6 V or less when in monopolar configuration. He has been on stable settings for the past 7 months and switches the right settings between monopolar (case+/1–; 2.4-2.6 V; 150 μs; 135 Hz) for sleep to bipolar (0+/1–; 5 V; 150 μs; 135 Hz) for work, school, or driving. He keeps the left at C+/2–; 4.0 V, 150 μs, 135 Hz.

Patient 4

This patient experienced transient improvement in OCD symptoms (29% reduction in Y-BOCS at 16 weeks) with relapse to 1 point higher than baseline at 3 weeks. He experienced marked dysphoria and irritability when pulse width was increased to 210 at 28 weeks post-stimulation. This resolved with temporary addition of olanzapine 5 mg (at 32 weeks) and decrease back to a pulse width of 150. At 71 weeks, patient's Y-BOCS had decreased to 25, and he described his remaining compulsions as reflexive and habit-like. The psychiatrist conceptualized his residual movement-related compulsions as "tourettic" (24), so haloperidol was added and titrated to 5 mg at bedtime. The patient experienced a marked reduction in Y-BOCS to 16 over the next 8 weeks without further change to DBS parameters.

Patient 5

This patient experienced early, marked improvement at low amplitude and pulse width. He began to experience hypomania with marked irritability at (R: case +/1–; 2.7 V; 90 μs; 135 Hz and L: C+/0–; 2.7 V; 90 μs; 135 Hz). Attempts to taper paroxetine (decrease from 80 to 60 mg/day) led to increase in intrusive thoughts. Patient did not tolerate trials of valproic acid and lithium. Irritability and hypomania remitted with change to bipolar settings at 21 weeks post-stimulation (R: 0–/3+; 4.5 V; 90 μs; 135 Hz and L: 0–/3+; 4.2 V; 90 μs; 135 Hz), but patient did not find this as effective for his OCD. Ultimately, he remains on monopolar settings without hypomania and manages building irritability by switching to bipolar settings (usually once or twice a day). He specifically changes to bipolar before driving because he recognizes this is a time where he is more prone to irritability, and he also switches to bipolar for sleep.

RESULTS

Anecdotal Evidence

Patient 1

Despite persistent low BMI of 14, she has remained out of the hospital for 29 months, the longest time period since onset of OCD and anorexia. She is working part time as a research assistant, is active in her church, and, though she wishes for further reduction in symptoms, she notes her quality of life and mood is better than prior to DBS. In addition, she no longer engages in self-injurious behaviors and no longer experiences suicidal ideation.

Patient 2

Patient has been volunteering regularly and is happy to find that others enjoy working with him. He has returned to school and learned computer and basic life skills (e.g., doing online banking), which pleases his mother who is worried about his ability to be independent once she dies.

Patient 3

He began a healthcare management graduate programming and did very well but decided that was not the career path for him. He is currently thriving in a new graduate program for architectural design.

Patient 4

Sustained improvement has only been recent, and he is struggling to determine how to fill his day, given that much of his time was previously occupied by compulsions. He recently started working as a history teacher and is finding this very challenging to do virtually (due to the pandemic and in-person learning restrictions).

Patient 5

He is thrilled at his ability to play video games without intrusion from OCD, he took a drawing class, and he has resumed playing in a racquet-ball league. He is considering whether he would like to find a volunteer position vs. apply for a job as a staff accountant.

Diagnostic Scale Analysis

Five diagnostic scales were applied to all cases: Y-BOCs, MADRS, and the Q-LES-Q-SF, HAM-A, and YMRS. The median post-stimulation change as a percent of baseline, across all cases for Y-BOCs, was −44% (IQR = 44%) and at final follow-up the mean percent change was −49.1%; MADRS, the median change was −53% (IQR = 49%) and at final follow-up the mean percent change was −54.1%; Q-LES-Q, DBS resulted in a median increase of 27% (IQR = 68%) in perceived quality of life and satisfaction and at final follow-up the mean percent change was 37.6%; YMRS, DBS induced a median increase of 100% and at final follow-up the mean percent change was 32.4%; HAM-A, DBS induced a median reduction of −51% and at final follow-up the mean percent change was −35.0% (**Figure 1A**). For individual cases, a varying number of post-stimulation parameter adjustments were required to achieve optimal response. **Figure 1B** shows that most patients showed significant improvement in MADRS, HAM-A and YMRS, by around 100 days post-stimulation, whereas both Q-LES-Q-SF and Y-BOCS required more than 250 days for at least 3 of the cases to achieve peak change from baseline. Variation in response to programming was also evident as a function of time. For Y-BOCS, most cases exhibited a significant improvement in obsessive compulsive behaviors that persisted for the duration of their documented therapy. **Figure 2A** depicts that 3 of the 5 cases exhibit over 50% improvement in YBOCs; however, there are slight fluctuations between 40 and 60% improvement likely modulated by changes in programming parameters. Despite fluctuations, all 5 cases show a trajectory toward improvement as therapy progresses. **Figure 2B** highlights the change over time in Q-LES-Q-SF response. For this quality-of-life measurement, 4 out of 5 cases (P2–P5), show marked improvement either at the outset of stimulation (P4 and P5) or as function of changes

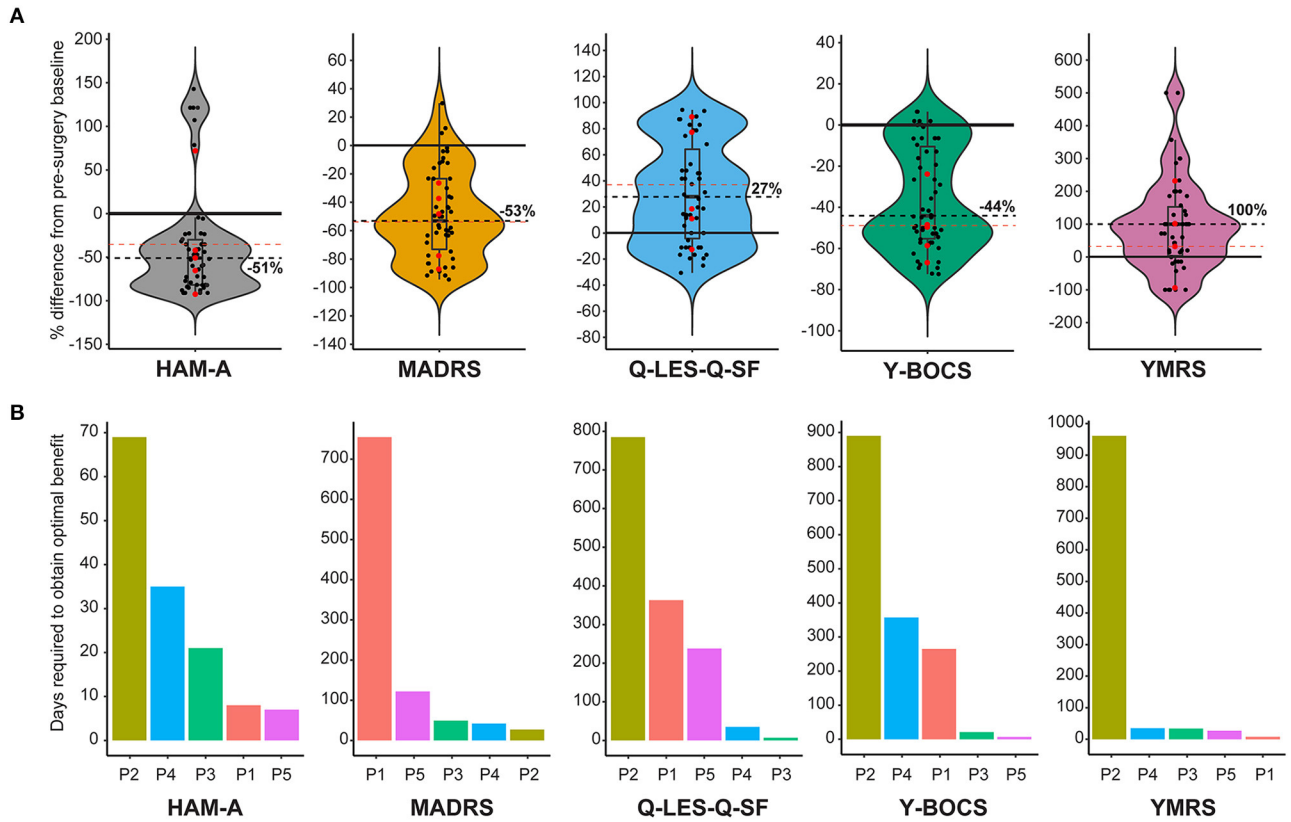

FIGURE 1 | (A) Violin plots showing group level representation of the percent change from pre-DBS surgery baseline across the five mood disorder scale metrics used for our cohort: Hamilton Anxiety Rating Scale (HAM-A), Montgomery-Åsberg Depression Rating Scale (MADRS), Quality of Life Enjoyment and Satisfaction Questionnaire (Q-LES-Q-SF), Yale-Brown Obsessive-Compulsive Scale (Y-BOCS), Young Mania Rating Scale (YMRS). Dots represent post-surgery DBS programming sessions. Each scale plot represents all subjects and all post-surgery DBS programming sessions for the first year of follow-up. The solid line demarcates no change (0%) on the y-axis, and the dotted line indicates the median percent change. Red points indicate percent change in scale metrics for each individual patient from the final follow-up and the red dotted line represents the mean for all patients for the final follow up. **(B)** Individual and scale differences in the number of programming sessions necessary to achieve optimal therapeutic stimulation. Each scale plot denotes the number of days required to achieve optimal stimulation for each patient highlighted by a different color.

in programming parameters (P2 and P3). Finally, **Figure 2C** shows that improvement in MADRS is immediate and invariant over time in 3 out of 5 cases. P1 shows no change and no fluctuations, and P3 shows an immediate improvement that gradually increases over time.

Comorbid Scale Analysis

Specific cases in this OCD cohort exhibited comorbid symptoms that in other OCD-DBS reports have responded to DBS. Case 2 had a history of tic disorder manifestations and was assessed pre- and post-surgical using the YGTSS and sub-scale Total Tic Severity Score (TTSS). **Figures 3A,B** show that TTSS did not significantly change from pre-surgical baseline ($p = 0.22$); however, YGTSS did show a significant reduction that was more marked following initial programming ($p = 0.005$). Case 4 was diagnosed with nicotine use disorder, at risk alcohol use, and daily cannabis use. To assess whether DBS affected the patient's craving for these substances, we measured craving pre- and post-surgery. **Figures 3C–E** depict Case 4's craving response following DBS. Alcohol craving in **Figure 3C** shows a marked response during the initial 200 days of stimulation; however, it rebounds back to the pre-stimulation baseline during the latter half of therapy. There is no effect of DBS on marijuana craving overall; however, during many sessions, DBS appears to increase craving. Finally, in **Figure 3E**, tobacco craving (measured using a cigarette craving rating scale) shows the most lasting response to DBS, with both an immediate and sustained drop in craving by 30%.

Charge Density Calculated for the Final Follow-up

All patients in this cohort experienced improvement in their OCD symptoms as measured by change in Y-BOCS, however the stimulation parameters and selected therapeutic contacts at final follow-up varied across patients. To determine whether an association between anatomical location of therapeutic contacts and tissue activation as measured by charge density, we analyzed the relationship between charge density and distance between the AC-ALIC junction and the mid-point of the active contact(s). We found that the lower the charge density was negatively

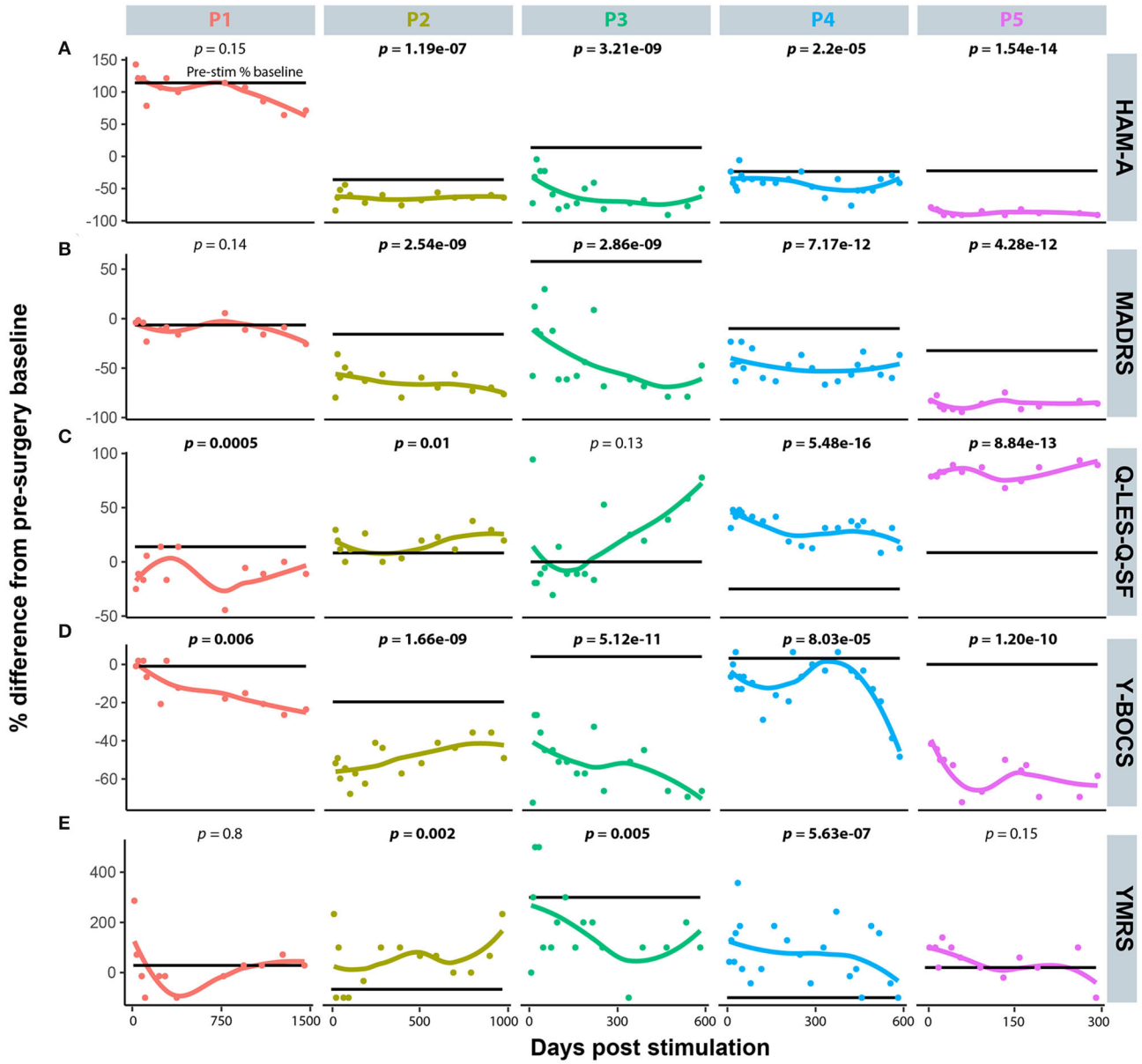

FIGURE 2 | The individual time course representation for patient response to DBS programming modifications across the five mood disorder scale metrics. **(A)** Hamilton Anxiety Rating Scale (HAM-A). **(B)** Montgomery-Åsberg Depression Rating Scale (MADRS). **(C)** Quality of Life Enjoyment and Satisfaction Questionnaire (Q-LES-Q-SF). **(D)** Yale-Brown Obsessive-Compulsive Scale (Y-BOCS). **(E)** Young Mania Rating Scale (YMRS).

correlated with the distance between the AC-ALIC junction and the active contact(s); $r = -0.58$, $p = 0.037$ (see **Figure 4** and **Table 1**).

Adverse Events

Some adverse events were encountered during programming, but these were all temporary. Hypomania was the most encountered adverse effect. Patient 1 had jaw tightening and pulling and tongue tingling. Patient 2 experienced transient hypomania and insomnia after an increase in amplitude, and this resolved without intervention within 1–2 days. Patient 3 had hypomania and sympathomimetic effects including flushing, tachycardia, and hypertension. Patient 4 had dysphoria and irritability at a pulse width of 210. Patient 5 experienced hypomania with irritability and aggression.

DISCUSSION

While the efficacy of DBS for OCD has been well-established, there are few reports of success in patients with comorbidities,

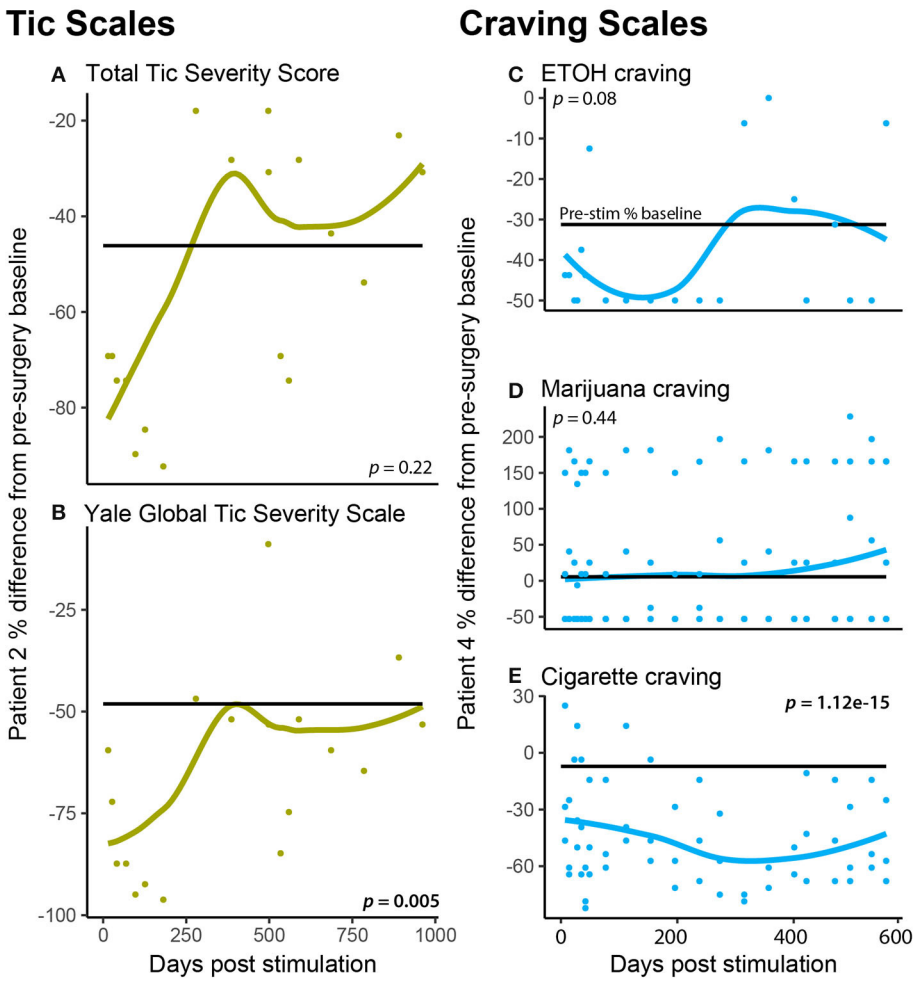

FIGURE 3 | Patient specific comorbidities. **(A,B)** A patient (P2) had a comorbid autism-spectrum disorder, tic disorder, which was measured at each DBS programming session using the **(A)** Total Tic Severity Score and the **(B)** Yale Global Tic Severity Scale **(C–E)**. A patient (P4) had comorbid substance use (nicotine use disorder, daily cannabis use, and at-risk alcohol use), which was measured at each DBS programming session using craving scales for ETOH **(C)**, marijuana **(D)**, and cigarettes **(E)**.

despite the reality that most patients have comorbid psychiatric diagnoses in addition to OCD (25). Here we report the results of VC/VS DBS in five patients whose comorbidities include substance use disorders, MDD, autism spectrum disorder, psychosis, anorexia nervosa, and tic disorder. A recent study of quality of life QOL in OCD demonstrated that QOL in OCD is often as dependent on the comorbid psychiatric disease as the OCD itself (26). This underscores the fact that "success" from DBS in these patients is heavily dependent on their comorbidities in addition to their OCD.

Anorexia

DBS has been performed for anorexia since 2010, when Israel et al. targeted the subgenual cingulate cortex (27). Other targets include the NAc and the bed nucleus of the stria terminalis (28, 29). These studies have been case reports and case series, so high quality recommendations are not available, though 1-year results of an open label trial at University of Toronto for subcallosal cingulate stimulation demonstrate improvement in body mass index and affective symptoms (30). Comorbid anorexia and OCD have previously been treated by both anterior capsulotomy or VC/VS DBS with improvement in both disorders (31, 32).

Autism

Case reports have demonstrated improvement in both YBOCS and autism spectrum disorder (ASD) in a patient with co-morbid OCD and autism who underwent stimulation of the NAc (33) and of another patient whose NAc was targeted for isolated self-injurious behavior (SIB) in the setting of ASD (34). Other targets reported for SIB in ASD include the basolateral amygdala (35), globus pallidus interna (GPi), and GPi together with ALIC (36),

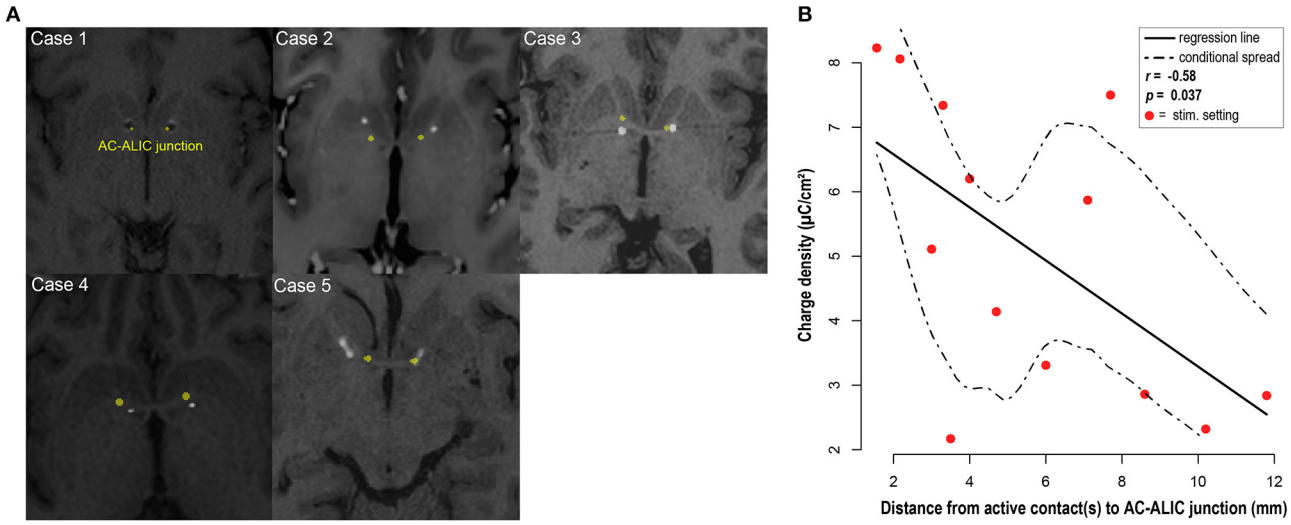

FIGURE 4 | DBS electrode placement. **(A)** For each patient, localization of the bilateral DBS leads is visualized in the axial plane at the level of the anterior commissure (AC) – anterior limb of the internal capsule (ALIC) junction; marked in yellow. Axial slices depict co-registered pre-operative MRI and post-operative CT for cases 2–5 and co-registered pre- and post-operative MRI for case 1. Hyperintense circular artifacts in cases 2–5 represent the DBS lead from the post-operative CT; the hypointense circular artifacts in case 1 represent the DBS lead. Note that the axial images depicting lead location at the junction between AC and ALIC, do not necessarily depict the location of the active contact. **(B)** Visualization and analysis of the association between the distance from the active contact(s) at final follow-up to the AC-ALIC junction and charge density. A significant negative correlation was observed for the relationship between distance between the active contact(s) and the AC-ALIC junction and charge density ($p = 0.037$, $r = -0.58$).

with improvement in the first two cases but only temporary improvement in the third.

Tourette's

DBS has been studied in Tourette syndrome more robustly. About 200 cases have been reported in the literature, and five randomized controlled trials comprising a total of 43 patients have been reported (37). However, the optimal target for Tourette's is still the subject of ongoing debate, as 10 different regions have been suggested in the aforementioned studies, including the GPi (anteromedial and posteroventrolateral portions), the globus pallidus externus, the NAc, the ALIC, the subthalamic nucleus (STN), and four regions within the centromedial thalamus. A recent multi-institutional retrospective study aimed to determine whether one target is superior to others in resolving tics. The study did not find that one target was superior to others for resolution of tics, but it did find that regions superior, medial, or within the GPi were associated with greater improvement in co-morbid OCD symptoms than those inferior (38).

Depression

DBS for treatment-resistant depression (TRD) has been the subject of significant controversy. While open label studies of VC/VS demonstrated promising results (39), a previous randomized-controlled RECLAIM study on the subject was halted early due to lack of significant difference between the two arms after 30 patients had been enrolled (40). Interestingly, in a RCT of 25 patients with bilateral VC/VS DBS in the Netherlands, discontinuation of therapy during the crossover phase resulted in reemergence of symptoms (41). Fifty percent response and 30% remission was noted in open-label long-term follow-up of 28 patients receiving subcallosal cingulate stimulation (42). Other targets being investigated for TRD include superolateral branch of medial forebrain bundle and lateral habenula.

ADHD

No trials of DBS for ADHD have been performed.

Substance Use Disorder

Most work regarding DBS for addiction remains in translational stages. While NAc is the most commonly considered target, the lateral hypothalamus, medial prefrontal (PFC) cortex, STN, lateral habenula, and insula have also been targeted with promising results in animal models (43).

Psychosis

The ventral portion of the CA1 region of the hippocampus, PFC, ventral striatum, NAc, substantia nigra, and ventral tegmental area have been posited as potential targets in schizophrenia (44, 45).

DBS of the VC/VS and NAc has been found to be slightly less effective than lesional anterior capsulotomy for OCD in a literature review, though the groups compared were not exactly analogous since those treated with DBS were more likely to have more severe disease and for a longer time, but it seems that the modulatory nature of DBS makes it more socially acceptable in the fraught world of psychiatric surgery than creation of a

TABLE 1 | DBS programming parameters.

Mean Y- BOCS score pre-surgery		6 months	Y-BOCS reduction at 6 months		Most recent		Y-BOCS reduction at last follow-up
Patient 1: **35.33**	R PG	(C+, 1–) 6.2 V/150 μs/100 Hz	21% (28) (7 mos)	R	(C+, 0–, 1–) 8 V/120 μs/135 Hz **15.5mA**	1,434 d	26% (27)
	L	(C+, 1–) 7.2/150 μs/100 Hz		L	(C+,0-,1-) 6.7V/150μsec/135Hz **12.8mA**		
Patient 2: **37.33**	R	(0+, 1–) 7 V/60 μs/100 Hz	62% (14)	R	(0+, 1–) 6.5 V/100 μs/100 Hz **6.5mA**	961 d	49% (19)
	L	(0+, 1–) 7 V/60 μs/100 Hz		L	(0+, 1–) 5.0 V/100 μs/100 Hz **5.0mA**		
Patient 3: **32.67** (switches R side between group A and B)	R	(C+, 1–) 3.2 V/120 μs/135 Hz	57% (14)	R A	(C+, 1–) 2.6 V/150 μs/135 Hz **4.9mA**	601 d	66% (11)
				R B	(0+, 1–) 5 V/150 μs/135 Hz **5.9mA**		
	L	(C+, 2–) 4.4 V/120 μs/135 Hz		L	(C+, 2–) 4 V, 150 μs/135 Hz **6.0mA**		
Patient 4: **31**	R	(C+, 1–) 5.5 V/210 μs/135 Hz	19% (25)	R	(C+, 0–, 1–) 4 V/150 μs/135 Hz **8.9mA**	562 d	48% (16)
	L	(C+, 0–) 5.5 V/210 μs/135 Hz		L	(C+, 0–, 1–) 3.5 V/150 μs/135Hz **8.0mA**		
Patient 5: **36** (switches between group Aand group B)	R A	(0–, 3+) 4.5 V/90 μs/135 Hz	69% (11)	R A	(0–, 3+) 4.5 V/90 μs/135Hz **3.8mA**	266 d	58% (15)
	L A	(0–, 3+) 4.2 V/90 μs/135 Hz		L A	(0–, 3+) 4.2 V/90 μs/135 Hz **3.3mA**		
	R B	(C+, 1–) 2.7 V/90 μs/135 Hz		R B	(C+, 1–) 2.7 V/90 μs/135 Hz **3.8mA**		
	L B	(C+, 0–) 2.7 V/90 μs/135 Hz		L B	(C+, 0–) 2.7 V/90 μs/135 Hz **2.9mA**		

R/L, Right/Left pulsegenerator. Bold values indicate therapeutic current.

permanent lesion (10). Side-effect profiles were similar in both groups. However, as our ability to identify connectivity pathways improves, so too may we be able to predict which patients are the most likely to respond positively to DBS: recent hypotheses focus on the medial and lateral PFC and frontothalamic radiation (46). Another recent study has demonstrated that PFC-related cognitive control, including theta oscillations, improves after DBS of VC/VS (47).

In previous meta-analysis, obsessions and compulsions with sexual and/or religious content are more likely to respond to DBS than other types of compulsions (12). It has also been posited that CBT post-operatively may augment the efficacy of DBS; however, this has only been demonstrated preliminarily in an open-phase trial (48).

Challenges of Programming

This case series highlights many challenges that psychiatrists may face during programming. Patients may feel markedly improved with initial programming (particularly with regards to mood), and, unfortunately, this degree of improvement does not always persist. This may lead patients to feel disappointed and "chase" the good feeling. To limit the chance of this, the primary programmer has learned to increase amplitude very gradually and only to test higher amplitude during initial programming if response is not evident at lower amplitudes. Programming is more difficult in patients who do not have a good awareness of their internal states or emotions. The programmer may need to rely on more objective observations: for example, increased talkativeness, changes in affect, and

degree of indecision. It is useful to have friends and/or family members in the room during programming as this allows for more natural conversation and observation of interactions. It can be helpful to discuss a topic of interest to the patient in order to observe his or her level of interest, engagement, and spontaneity. Additionally, patients with OCD often have trouble making decisions, and providing self-ratings during programming is no exception. Some patients have tended to rate their symptoms (on a scale of 0–10) in increments of 0.25, not wanting to mistakenly over-report changes. Again, the programmer can rely on more objective observations in these cases.

Another challenging aspect of programming is that sometimes patients experience adverse effects at the settings associated with most clinical improvement, such as feeling physically anxious, being more irritable, experiencing insomnia, or having sympathomimetic effects. As described above, one patient manages increased irritability by changing settings depending on context. Another patient changes settings for sleep. Psychiatrists may need to add medication for insomnia. Adjustments to pulse width and frequency may mitigate adverse effects in some patients. The programmer must allow adequate time between changes in settings so that effects from a previous setting do not carry over to the next setting. Sometimes a change is very clear, and the programmer can make changes within 30–60 s. Other times, it is less clear, and the programmer may have the patient take a break for 10–20 min or so on one setting then do the same on another to better compare.

As described above, some patients were able to change from one setting to another in order to mitigate side effects or allow for sustained benefit. Other patients were not able to do this effectively. For example, Patient 2 has not been able to turn down DBS (or turn one hemisphere off) at night due to a fear that he will do it incorrectly and "mess up" his DBS. Patient 4 did not tolerate turning amplitude down at night due to feeling significantly more depressed and anxious. One patient (not included in this case series due to having surgery after this manuscript was drafted) developed compulsions related to her DBS, feeling the urge to repeatedly turn DBS on and off in response to obsessions. Some patients may be unable to manage changes appropriately using the patient programmer initially but may be better able to do so farther along the path of DBS programming as their OCD begins to improve.

It is also important to keep in mind that DBS may not mitigate all of a patient's symptoms, but a patient may have a better response to medication with DBS on. As described, patient #4 had residual tic-like compulsions that did not respond to DBS but did respond to addition of an antipsychotic (when a previous trial of an antipsychotic had not been effective). In summary, though an initial algorithm may be followed, DBS programming must be individualized to each patient, and the programmer must be flexible and creative in order to maximize clinical response while minimizing adverse effects.

Finally, while every effort was made to maintain objectivity, we recognize that our un-blinded status and the lack of a control arm are major limitations to our study. Nonetheless, we feel our case series data are worth sharing given the dearth of co-morbid psychiatric disease in more formal studies of DBS for OCD.

Conclusions

DBS has proven to be an efficacious treatment with an acceptable side effect profile for treatment of refractory OCD. Here, we have reported our institutional experience with five patients, all with significant co-morbidities. Furthermore, we report programming parameters, which have been seldom discussed in the literature. While these represent only retrospective data, they aid in our corpus of knowledge regarding bilateral VC/VS DBS for OCD and underscore the need for more high-quality Level I evidence regarding surgical management of OCD.

DATA AVAILABILITY STATEMENT

The raw data supporting the conclusions of this article will be made available by the authors, without undue reservation.

ETHICS STATEMENT

The studies involving human participants were reviewed and approved by Colorado Multiple Institutional Review Board. The patients/participants provided their written informed consent to participate in this study. Written informed consent was obtained from the individual(s) for the publication of any potentially identifiable images or data included in this article.

AUTHOR CONTRIBUTIONS

LK, AA, and RD conceived of the manuscript. JT and BS performed statistical analyses. LK, AA, and RD provided direct care for the patients. JT created the figures. JT, AA, LK, RD, BS, and HW contributed directly to the writing and editing of the manuscript. All authors contributed to the article and approved the submitted version.

REFERENCES

1. Association American Psychiatric. *Diagnostic and Statistical Manual of Mental Disorders.* 5th ed. (2013). Available online at: https://www.psychiatry.org/psychiatrists/practice/dsm (accessed April 16, 2020).
2. Kessler RC, Wai TC, Demler O, Walters EE. Prevalence, severity, and comorbidity of 12-month DSM-IV disorders in the National Comorbidity Survey Replication. *Arch Gen Psychiatry.* (2005) 62:617–27. doi: 10.1001/archpsyc.62.6.617
3. Robbins TW, Vaghi MM, Banca P. Obsessive-compulsive disorder: puzzles and prospects. *Neuron.* (2019) 102:27–47. doi: 10.1016/j.neuron.2019.01.046
4. Franklin ME, Abramowitz JS, Kozak MJ, Levitt JT, Foa EB. Effectiveness of exposure and ritual prevention for obsessive-compulsive

disorder: randomized compared with nonrandomized samples. *J Consult Clin Psychol.* (2000) 68:594–602. doi: 10.1037/0022-006X.68.4.594
5. Hezel D, Simpson H. Exposure and response prevention for obsessive-compulsive disorder: a review and new directions. *Indian J Psychiatry*. (2019) 61:S85–92. doi: 10.4103/psychiatry.IndianJPsychiatry_516_18
6. Kohl S, Schönherr DM, Luigjes J, Denys D, Mueller UJ, Lenartz D, et al. Deep brain stimulation for treatment-refractory obsessive compulsive disorder: a systematic review. *BMC Psychiatry*. (2014) 14:214. doi: 10.1186/s12888-014-0214-y
7. Mian MK, Campos M, Sheth SA, Eskandar EN. Deep brain stimulation for obsessive-compulsive disorder: past, present, and future. *Neurosurg Focus.* (2010) 29:1–9. doi: 10.3171/2010.4.FOCUS10107
8. Jenike MA. Neurosurgical treatment of obsessive-compulsive disorder. *Br J Psychiatry*. (1998) 173:79–90. doi: 10.1192/S0007125000297936
9. Greenberg BD, Price LH, Rauch SL, Friehs G, Noren G, Malone D, et al. Neurosurgery for intractable obsessive-compulsive disorder and depression: critical issues. *Neurosurg Clin N Am.* (2003) 14:199–212. doi: 10.1016/S1042-3680(03)00005-6
10. Pepper J, Hariz M, Zrinzo L. Deep brain stimulation vs. anterior capsulotomy for obsessive-compulsive disorder: a review of the literature. *J Neurosurg.* (2015) 122:1028–37. doi: 10.3171/2014.11.JNS132618
11. Nuttin B, Cosyns P, Demeulemeester H, Gybels J, Meyerson B. Electrical stimulation in anterior limbs of internal capsules in patients with obsessive-compulsive disorder. *Lancet.* (1999) 354:1526. doi: 10.1016/S0140-6736(99)02376-4
12. Alonso P, Cuadras D, Gabriëls L, Denys D, Goodman W, Greenberg BD, et al. Deep brain stimulation for obsessive-compulsive disorder: a meta-analysis of treatment outcome and predictors of response. *PLoS ONE.* (2015) 10:e0133591. doi: 10.1371/journal.pone.0133591
13. Borders C, Hsu F, Sweidan AJ, Matei ES, Bota RG. Deep brain stimulation for obsessive compulsive disorder: a review of results by anatomical target. *Ment Illn.* (2018) 10:40–4. doi: 10.1108/mi.2018.7900
14. Hamani C, Pilitsis J, Rughani AI, Rosenow JM, Patil PG, Slavin KS, et al. Deep brain stimulation for obsessive-compulsive disorder: systematic review and evidence-based guideline sponsored by the American society for stereotactic and functional neurosurgery and the congress of neurological surgeons (CNS) and endorsed by the CNS and American association of neurological surgeons. *Neurosurgery.* (2014) 75:327–33. doi: 10.1227/NEU.0000000000000499
15. Stahl D, Cabrera L, Gibb T. Should DBS for psychiatric disorders be considered a form of psychosurgery? Ethical and legal considerations. *Sci Eng Ethics.* (2018) 24:1119–42. doi: 10.1007/s11948-017-9934-y
16. Bell E, Leger P, Sankar T, Racine E. Deep brain stimulation as clinical innovation: an ethical and organizational framework to sustain deliberations about psychiatric deep brain stimulation. *Neurosurgery.* (2016) 79:3–9. doi: 10.1227/NEU.0000000000001207
17. Widge AS, Dougherty DD. Managing patients with psychiatric conditions treated with deep brain stimulation. In: *Deep Brain Stimulation Management*. Cambridge University Press (2015). p. 124–37. Available online at: https://www.cambridge.org/core/books/deep-brain-stimulation-management/managing-patients-with-psychiatric-conditions-treated-with-deep-brain-stimulation/6D5D3F0540E8C4BDF9B88302ADD96CF5 (accessed December 7, 2020).
18. Widge AS, Dougherty DD. Deep brain stimulation for treatment-refractory mood and obsessive-compulsive disorders. *Curr Behav Neurosci Rep.* (2015) 2:187–97. doi: 10.1007/s40473-015-0049-y
19. Jennings KM, Phillips KE. Eating disorder examination–questionnaire (EDE–Q): norms for a clinical sample of males. *Arch Psychiatr Nurs.* (2017) 31:73–6. doi: 10.1016/j.apnu.2016.08.004
20. Leckman JF, Riddle MA, Hardin MT, Ort SI, Swartz KL, Stevenson J, et al. The yale global tic severity scale: initial testing of a clinician-rated scale of tic severity. *J Am Acad Child Adolesc Psychiatry.* (1989) 28:566–73. doi: 10.1097/00004583-198907000-00015
21. Rojewski AM, Morean ME, Toll BA, McKee SA, Krishnan-Sarin S, Green BG, et al. The yale craving scale: development and psychometric properties. *Drug Alcohol Depend.* (2015) 154:158–66. doi: 10.1016/j.drugalcdep.2015.06.040
22. Davis RA, Winston H, Gault JM, Kern DS, Mikulich-Gilbertson SK, Abosch A. Deep brain stimulation for OCD in a patient with comorbidities: epilepsy, tics, autism, and major depressive disorder. *J Neuropsychiatry Clin Neurosci.* (2021). doi: 10.1176/appi.neuropsych.20060153. [Epub ahead of print].
23. U.S. Department of Health and Human Services and U.S. Department of Agriculture. *Dietary Guidelines for Americans*. 8th Edition. (2015–2020). Available online at: https://health.gov/our-work/food-nutrition/previous-dietary-guidelines/2015
24. Mansueto CS, Keuler DJ. Tic or compulsion? *Behav Modif.* (2005) 29:784–99. doi: 10.1177/0145445505279261
25. Pinto A, Mancebo MC, Eisen JL, Pagano ME, Rasmussen SA. The brown longitudinal obsessive compulsive study: clinical features and symptoms of the sample at intake. *J Clin Psychiatry.* (2006) 67:703–11. doi: 10.4088/JCP.v67n0503
26. Remmerswaal KCP, Batelaan NM, Hoogendoorn AW, van der Wee NJA, van Oppen P, van Balkom AJLM. Four-year course of quality of life and obsessive–compulsive disorder. *Soc Psychiatry Psychiatr Epidemiol.* (2019) 55:989–1000. doi: 10.1007/s00127-019-01779-7
27. Israël M, Steiger H, Kolivakis T, McGregor L, Sadikot AF. Deep brain stimulation in the subgenual cingulate cortex for an intractable eating disorder. *Biol Psychiatry.* (2010) 67:e53–4. doi: 10.1016/j.biopsych.2009.11.016
28. Wu H, Van Dyck-Lippens PJ, Santegoeds R, Van Kuyck K, Gabriëls L, Lin G, et al. Deep-Brain stimulation for anorexia nervosa. *World Neurosurg.* (2013) 80:S29.e1-S29.e10. doi: 10.1016/j.wneu.2012.06.039
29. Manuelli M, Franzini A, Galentino R, Bidone R, Dell'Osso B, Porta M, et al. Changes in eating behavior after deep brain stimulation for anorexia nervosa. A case study. *Eat Weight Disord.* (2019) 25:1481–6. doi: 10.1007/s40519-019-00742-4
30. Lipsman N, Lam E, Volpini M, Sutandar K, Twose R, Giacobbe P, et al. Deep brain stimulation of the subcallosal cingulate for treatment-refractory anorexia nervosa: 1 year follow-up of an open-label trial. *Lancet Psychiatry.* (2017) 4:285–94. doi: 10.1016/S2215-0366(17)30076-7
31. Barbier J, Gabriëls L, Van Laere K, Nuttin B. Successful anterior capsulotomy in comorbid anorexia nervosa and obsessive-compulsive disorder: case report. *Neurosurgery.* (2011) 69:E745–51. doi: 10.1227/NEU.0b013e31821964d2
32. McLaughlin NCR, Didie ER, MacHado AG, Haber SN, Eskandar EN, Greenberg BD. Improvements in anorexia symptoms after deep brain stimulation for intractable obsessive-compulsive disorder. *Biol Psychiatry.* (2013) 73:e29–31. doi: 10.1016/j.biopsych.2012.09.015
33. Doshi PK, Hegde A, Desai A. Nucleus accumbens deep brain stimulation for obsessive-compulsive disorder and aggression in an autistic patient: a case report and hypothesis of the role of nucleus accumbens in autism and comorbid symptoms. *World Neurosurg.* (2019) 125:387–91. doi: 10.1016/j.wneu.2019.02.021
34. Park HR, Kim IH, Kang H, Lee DS, Kim BN, Kim DG, et al. Nucleus accumbens deep brain stimulation for a patient with self-injurious behavior and autism spectrum disorder: functional and structural changes of the brain: report of a case and review of literature. *Acta Neurochir.* (2017) 159:137–43. doi: 10.1007/s00701-016-3002-2
35. Sturm V, Fricke O, Bührle CP, Lenartz D, Maarouf M, Treuer H, et al. DBS in the baso-lateral amygdala improves symptoms of autism and related self-injurious behavior: a case report and hypothesis on the pathogenesis of the disorder. *Front Hum Neurosci.* (2012) 6:341. doi: 10.3389/fnhum.2012.00341
36. Stocco A, Baizabal-Carvallo JF. Deep brain stimulation for severe secondary stereotypies. *Park Relat Disord.* (2014) 20:1035–6. doi: 10.1016/j.parkreldis.2014.06.019
37. Muller-Vahl KR. Deep brain stimulation in Tourette syndrome: the known and the unknown. *J Neurol Neurosurg Psychiatry.* (2019) 90:1076–7. doi: 10.1136/jnnp-2019-321008

38. Johnson KA, Fletcher PT, Servello D, Bona A, Porta M, Ostrem JL, et al. Image-based analysis and long-term clinical outcomes of deep brain stimulation for Tourette syndrome: a multisite study. *J Neurol Neurosurg Psychiatry*. (2019) 90:1078–90. doi: 10.1136/jnnp-2019-320379
39. Malone DA, Dougherty DD, Rezai AR, Carpenter LL, Friehs GM, Eskandar EN, et al. Deep brain stimulation of the ventral capsule/ventral striatum for treatment-resistant depression. *Biol Psychiatry*. (2009) 65:267–75. doi: 10.1016/j.biopsych.2008.08.029
40. Dougherty DD, Rezai AR, Carpenter LL, Howland RH, Bhati MT, O'Reardon JP, et al. A randomized sham-controlled trial of deep brain stimulation of the ventral capsule/ventral striatum for chronic treatment-resistant depression. *Biol Psychiatry*. (2015) 78:240–8. doi: 10.1016/j.biopsych.2014.11.023
41. Bergfeld IO, Mantione M, Hoogendoorn MLC, Ruhé HG, Notten P, van Laarhoven J, et al. Deep brain stimulation of the ventral anterior limb of the internal capsule for treatment-resistant depression. *JAMA Psychiatry*. (2016) 73:456. doi: 10.1001/jamapsychiatry.2016.0152
42. Crowell AL, Riva-Posse P, Holtzheimer PE, Garlow SJ, Kelley ME, Gross RE, et al. Long-term outcomes of subcallosal cingulate deep brain stimulation for treatment-resistant depression. *Am J Psychiatry*. (2019) 176:949–56. doi: 10.1176/appi.ajp.2019.18121427
43. Wang TR, Moosa S, Dallapiazza RF, Elias WJ, Lynch WJ. Deep brain stimulation for the treatment of drug addiction. *Neurosurg Focus*. (2018) 45:E11. doi: 10.3171/2018.5.FOCUS18163
44. Ewing SG, Winter C. The ventral portion of the CA1 region of the hippocampus and the prefrontal cortex as candidate regions for neuromodulation in schizophrenia. *Med Hypotheses*. (2013) 80:827–32. doi: 10.1016/j.mehy.2013.03.026
45. Gault JM, Davis R, Cascella NG, Saks ER, Corripio-Collado I, Anderson WS, et al. Approaches to neuromodulation for schizophrenia. *J Neurol Neurosurg Psychiatry*. (2018) 89:777–87. doi: 10.1136/jnnp-2017-316946
46. Baldermann JC, Melzer C, Zapf A, Kohl S, Timmermann L, Tittgemeyer M, et al. Connectivity profile predictive of effective deep brain stimulation in obsessive-compulsive disorder. *Biol Psychiatry*. (2019) 85:735–43. doi: 10.1016/j.biopsych.2018.12.019
47. Widge AS, Zorowitz S, Basu I, Paulk AC, Cash SS, Eskandar EN, et al. Deep brain stimulation of the internal capsule enhances human cognitive control and prefrontal cortex function. *Nat Commun*. (2019) 10:1536. doi: 10.1038/s41467-019-09557-4
48. Mantione M, Nieman DH, Figee M, Denys D. Cognitive-behavioural therapy augments the effects of deep brain stimulation in obsessive-compulsive disorder. *Psychol Med*. (2014) 44:3515–22. doi: 10.1017/S0033291714000956

Conflict of Interest: LK has received grant funding from Medtronic in the past. RD provides *ad hoc* paid consulting for Medtronic. RD participated in a BrainsWay TMS for OCD Advisory Board in 2019.

The remaining authors declare that the research was conducted in the absence of any commercial or financial relationships that could be construed as a potential conflict of interest.

frontiers in Psychiatry

PERSPECTIVE
published: 12 April 2021
doi: 10.3389/fpsyt.2021.660180

Considerations for Pairing Cognitive Behavioral Therapies and Non-invasive Brain Stimulation: Ignore at Your Own Risk

Christine A. Conelea[1]*, *Suma Jacob*[1], *A. David Redish*[2] and *Ian S. Ramsay*[1]

[1] Department of Psychiatry and Behavioral Sciences, University of Minnesota, Minneapolis, MN, United States, [2] Department of Neuroscience, University of Minnesota, Minneapolis, MN, United States

Multimodal approaches combining cognitive behavioral therapies (CBT) with non-invasive brain stimulation (NIBS) hold promise for improving the treatment of neuropsychiatric disorders. As this is a relatively new approach, it is a critical time to identify guiding principles and methodological considerations to enhance research rigor. In the current paper, we argue for a principled approach to CBT and NIBS pairings based on synergistic activation of neural circuits and identify key considerations about CBT that may influence pairing with NIBS. Careful consideration of brain-state interactions and CBT-related nuances will increase the potential for these combinations to be positively synergistic.

Keywords: neuromodulation, cognitive behavioral therapy, intervention, brain stimulation, neuroscience

OPEN ACCESS

Edited by:
Paul Croarkin,
Mayo Clinic, United States

Reviewed by:
Chris Baeken,
Ghent University, Belgium
Frank P. MacMaster,
University of Calgary, Canada

***Correspondence:**
Christine A. Conelea
cconelea@umn.edu

Specialty section:
This article was submitted to Neuroimaging and Stimulation, a section of the journal Frontiers in Psychiatry

Received: *28 January 2021*
Accepted: *15 March 2021*
Published: *12 April 2021*

Citation:
Conelea CA, Jacob S, Redish AD and Ramsay IS (2021) Considerations for Pairing Cognitive Behavioral Therapies and Non-invasive Brain Stimulation: Ignore at Your Own Risk. Front. Psychiatry 12:660180. doi: 10.3389/fpsyt.2021.660180

INTRODUCTION

A paradigm shift in research focused on neuropsychiatric applications of non-invasive brain stimulation (NIBS) is underway. The traditional focus on non-invasive brain stimulation (NIBS) monotherapy has shifted to calls for research coupling NIBS with cognitive and behavioral interventions (1, 2), reflecting findings of the past two decades demonstrating NIBS effects are "state dependent": stimulation outcomes depend upon the state of neural activity in the targeted cortical region (3). Recognition of this interaction has sparked interest in improving NIBS efficacy via "functional targeting" that combines NIBS with cognitive tasks that modulate the same circuit being stimulated (4).

One functional targeting approach for psychiatric applications has been to combine NIBS with cognitive-behavioral therapies (CBT). "CBT" encompasses therapy procedures that target maladaptive behaviors and cognitions that underlie psychopathology. CBT is a logical choice for NIBS augmentation. Broadly speaking, CBT has both a strong evidence base and room to be enhanced in terms of efficacy, efficiency, durability, and impact on symptom improvement. CBT enables some degree of control over brain state, and research on the neural mechanisms of CBT is increasingly informing our understanding of its effects on the brain. Early research in this area suggests that combined CBT+NIBS protocols may enhance patient outcomes (5, 6).

We contend that launching this research necessitates we (1) follow principled approaches to inform decisions about *how* to combine CBT and NIBS, (2) identify key CBT considerations that may influence the rigor of future research, and (3) leverage insights about these assumptions into novel methodologies. In the current paper, we highlight several key considerations related to combining therapist-delivered CBT with NIBS techniques that can be feasibly administered

simultaneously or nearly-simultaneously with CBT (i.e., transcranial magnetic stimulation, TMS; transcranial electrical stimulation, tES).

SUCCESSFUL CBT+NIBS INTERVENTIONS DEPEND UPON NEURAL CIRCUIT MATCHMAKING

Functional targeting requires that NIBS and the behavior elicited by a CBT procedure synergistically engage neurocircuitry. It is well-established that different, clinically relevant behaviors targeted in CBT arise from information processing within different neural circuits (7–9). For example, fear conditioning accesses amygdala circuits (10), and override processes that allow behaviors to proceed in spite of fear access ventromedial prefrontal regions [IL in rats (11, 12) and subgenual ACC in humans (13)]. Planning processes depend on prefrontal-hippocampal circuits (14), overtrained habit processes depend on circuits between motor cortical regions and dorsolateral striatum (15), and motivation and reward processes depend on orbitofrontal, ventral tegmental, and nucleus accumbens circuits (16). Current theories suggest that psychiatric conditions can arise from multiple dysfunctions within these neural circuits, and that treatment will need to be focused on repairing damaged circuits or enhancing compensating circuits (17).

CBT+NIBS interventions should activate common or complementary circuitry (2), or otherwise engage compensatory circuits to enhance CBT outcomes. Eliciting specific thoughts, memories, and action-selection processes subserved by the aforementioned circuits through behavioral techniques (such as CBT) makes them labile and manipulable (18–20). This privileges those thoughts and actions to modification, suggesting that the sensitivity of neural circuits will depend on their activation. This suggests a way forward whereby specific CBT-elicited behavioral interactions activate certain circuits, making them amenable to targeted manipulation by neuromodulation techniques. This also implies that NIBS protocols should be designed to bias a circuit engaged by a CBT-evoked behavior toward the desired outcome (e.g., by increasing or decreasing circuit activity). Empirical testing is needed to clarify optimal CBT+NIBS pairings—the key is to begin testing pairings based on hypothesized synergistic co-activation of neural circuits.

CONSIDERATIONS FOR FUTURE RESEARCH

Consideration 1: CBT Is a Collection of Heterogeneous, Dynamic Interventions, and Does Not Uniformly Engage Single Neural Circuits

CBT interventions have shared characteristics (21) but are organized into specific protocols that target particular diagnoses or transdiagnostic processes, developmental stages, patient groups, and/or practice settings. CBT protocols are, by design, multi-component interventions. Components include procedures that target specific symptomatology and those that enhance therapy uptake or durability. Content is intentionally dynamic to support learning and often individualized to address idiographic symptom presentation. Multiple components are also typically delivered within a single therapy session. Notably, there is ongoing debate about which components are necessary and sufficient within particular CBT protocols (22, 23), and the precise learning processes and neural circuits that individual CBT elements impact are not entirely known (24).

Because CBT is a heterogeneous, dynamic intervention, it does not uniformly engage single neural circuits. Optimal CBT+NIBS pairing depends on understanding "*which circuits are engaged when*." Future research must develop dynamic functional targeting approaches that enable optimal NIBS delivery and timing depending on the specific CBT elements engaged per session. We must identify the neural circuitry driving a behavioral output before NIBS can be used to modulate the circuitry supporting the targeted behavior. Methodological details that enhance our fine-grained understanding of CBT+NIBS pairings and enhance replicability should be included in published protocols. Though common practice, identifying an intervention only as "CBT" is like calling a specific pharmaceutical a "medication." CBT+NIBS trials should specify the exact protocol used and detail timing and duration of procedural elements within CBT sessions and in relation to stimulation.

Consideration 2: CBT+NIBS Synergy May Not Necessarily Result From Stimulating a Circuit Shown to Change Pre-post CBT

Due to CBT's dynamic nature, the ways that specific CBT+NIBS procedures interact may be inconsistent over time. For example, circuits are not necessarily engaged consistently within and across CBT sessions and can differ depending on learning stage (25). There may also be individual differences in the circuits patients engage to arrive at the same clinical outcomes, as well as a combination of restorative and compensatory mechanisms associated with treatment response. Animal models may provide insights into how circuit engagement is influenced by biological therapeutics (e.g., stimulation, medication), behavioral training, and potential moderators (e.g., genetics, learning history, development, sex/hormonal status), as well as highlight individual differences to leverage and personalize CBT+NIBS. We should also consider strategies to time-lock circuit-based measurement with methods that quantify human behavior or targeted neural activation during CBT procedures in an effort to inform closed-loop neuromodulation (26). One emerging technique that may be useful in this regard is brain oscillation-synchronized TMS, which uses real-time electroencephalography (EEG) to trigger TMS pulses depending on the oscillatory phase of the EEG signal (27).

Consideration 3: Delivering a Procedural Element of CBT Is Not Equivalent to Delivering a Full CBT Protocol

Some approaches to combining CBT and NIBS have delivered a procedure from within a CBT protocol alongside stimulation, such as presenting anxiety cues as a proxy for exposure therapy

(28, 29). This approach may be useful, in that it may more selectively engage a behavior/circuit. However, this approach becomes problematic when critical elements of the procedure are discarded. For example, in trials presenting anxiety cues for OCD (28) and PTSD (29), elements necessary for corrective learning from exposure were not included [e.g., activation of anxiety, restriction of avoidance/escape behaviors (30, 31)]. This example highlights the problem of plucking a procedure out of CBT without attending to specific procedural details that render it therapeutic. A CBT procedure labeled as "therapy" should contain all procedural elements known to be critical for therapeutic change. Methodological decisions about which CBT components to keep or discard alongside NIBS must consider the broader theory and evidence base underpinning the CBT intervention. If a NIBS study uses a CBT component outside of a full CBT package, the element selected should be described precisely (e.g., "anxiogenic stimulus presentation" instead of "exposure therapy"), and a rationale for this choice and implementation should be provided. If participants are given choices about how to engage in the procedure, engagement should be explored as a moderator of outcomes.

Consideration 4: CBT Efficacy Varies Across Individuals and Practitioners

Though CBT is a class of effective interventions with solid empirical support, effects are generally in the "medium" range and vary by disorder (32, 33). Individual differences in personality, motivation, psychosocial environment, cognitive ability, genetics, and neural processes influence CBT gains (34–37). Specific CBT interventions can have unique mediators and moderators of response that may limit or enhance efficacy. Therapist factors can also impact outcomes, such as clinician competence, training, theoretical orientation, protocol adherence, and personal characteristics. Failure to impact clinical outcomes in CBT+NIBS trials may not be a shortcoming of NIBS, but instead reflect CBT's variable efficacy. Efficacy of the standalone CBT protocol should be demonstrated prior to NIBS augmentation. CBT+NIBS trials should also incorporate established treatment fidelity methods to ensure that the CBT is delivered, received, and enacted as intended (38, 39). Quantification of process elements [e.g., patient/therapist behaviors (40)] and measurement of relevant moderators and mediators should also be considered, as these methods may reveal causes of variable outcomes, information that can in turn be used to further refine, personalize, or optimize the intervention.

Consideration 5: The Change Agent of CBT Often Occurs Outside the CBT Session

A core feature of CBT protocols is the completion of "homework" outside of the formal therapy session. Homework typically entails skills practice for learning and generalization, and it engages therapeutic mechanisms necessary for clinical change (41). While some in-session CBT components, such as *in vivo* exposure, do activate therapeutic mechanisms, homework to repeatedly engage these mechanisms is seen as crucial for solidifying learning and ensuring that gains are not specific to the clinic context (42). Furthermore, in some CBT protocols, the majority or entire therapeutic change process is presumed to occur outside of session, such that the session itself is used to plan and prepare for homework (43). Homework completion is an important predictor of treatment response (44, 45), underscoring that some essential aspects of CBT occur outside of the clinic. This poses challenges for CBT+NIBS, such that neuromodulation may not be delivered in conjunction with mechanisms driving therapeutic change.

To impact homework (or the mechanisms engaged by homework), NIBS likely needs to be deployed in close temporal proximity to skills practice or delivered in naturalistic circumstances. One approach could be to adapt CBT sessions to emphasize active skills implementation or rehearsal concurrently or sequentially to stimulation. Optimal timing of specific CBT and NIBS procedures should be tested; although concurrent administration seems preferable for tES (2), timing is more of an open question for TMS and may differ depending on the outcome being targeted. Another approach could be to test use of NIBS to target circuitry that underlies skill acquisition (learning) during a CBT session. Finally, making NIBS more accessible in a patient's natural environment could enable pairing of homework with stimulation, as well as potentially offer the added benefit of enhancing skills generalization across contexts. Home-based tES delivery holds promise in this regard. Existing research demonstrates home-based tES is acceptable and safe, and guidelines for facilitating compliance and safety monitoring have been established (46, 47).

Additional NIBS Considerations

It is beyond the scope of this paper to review the progress and challenges of NIBS to date, but here we highlight a few NIBS-specific considerations relevant to pairing it with CBT. First, individual patients can respond differently to the same NIBS procedures, with variable response attributable to many factors, including brain anatomy and physiology, medications, and hormonal status. Efforts to control, measure, and ultimately tailor NIBS protocols [e.g., to subgroups or biotypes (48)] should also be considered in CBT augmentation research.

Second, NIBS outcomes reflect an interaction between brain state and the modulated circuit. Cognitive processing, concurrent behavior, emotional state, priming, and wakefulness can moderate NIBS effects (49). Unfortunately, research often overlooks the importance of brain state in favor of focusing on technical aspects of NIBS delivery (e.g., biomechanics of device). Protocols often specify only stimulation parameters and the cortical region being targeted. While these factors are critical to study, doing so without considering brain state attends to only "half of the equation." Our understanding of CBT+NIBS would be greatly improved by research that systematically measures and manipulates brain states alongside circuit modulation.

Third, more research is needed to determine how different NIBS methods impact specific circuits acutely and longitudinally. Pre-clinical and translational research that systematically and parametrically tests how particular NIBS methods impact disease- or CBT-relevant circuits is a useful prerequisite to informing CBT+NIBS pairings. For example, systematic

translational studies can be used to optimize stimulation parameters prior to deploying the NIBS as a treatment [e.g., see (50) for an example in TMS for cocaine use disorder]. Research focused on testing how to best time NIBS delivery in relation to CBT protocols is also critically needed. Timing parameters that could be explored include simultaneous delivery, near-simultaneous delivery (e.g., one immediately following the other, where the first primes the targeted circuit), or sequential delivery (e.g., fully completing one intervention before the other).

Fourth, we should not assume that the circuit that is dysfunctional in a given disorder is the right one to stimulate alongside CBT. As noted above, optimal pairing likely depends on stimulating circuits that promote CBT-evoked behaviors. It is reasonable to suspect that these may in some situations be different circuits than those driving pathology. Researchers should also consider targeting circuits that engage compensatory processes or enhance cognitive strengths. If we over-focus on targeting deficits in an attempt to "normalize" functioning, we will miss opportunities to leverage patient strengths that can improve clinical functioning.

DISCUSSION

The convergence of CBT and NIBS research presents promising opportunities to improve the well-being of those living with psychiatric illness, though we must proceed thoughtfully. If the goal of combining NIBS and CBT is to improve patient outcomes, we have to carefully consider brain state-circuit interactions, circuit activity during specific CBT components, timing of stimulation, and the influences of individual differences, providers, and delivery format. Quantifying what actually happens in and out of CBT sessions will help identify optimal ways to arrange positive synergy between both modalities. We can use NIBS to either target the neural processes that benefit from that CBT component *or* boost compensatory processes to enhance benefit from that component.

We should also consider innovative ways to modify CBT to better work alongside NIBS. CBT could be modified to more precisely and effectively target neurocognitive processes that are most likely to drive clinical change, for example by dropping unnecessary CBT components or changing the process of how the CBT component is delivered. CBT approaches that target specific symptomatology or cognitive endophenotypes with known underlying circuitry may also be better candidates for NIBS augmentation than CBT approaches that target DSM diagnoses or general cognitive or emotional processes.

These considerations generalize to other multimodal intervention approaches. New technologies that directly manipulate neural circuits are continually emerging. Combining new technologies with CBT will require cognizance of which neural circuits are impacted by CBT so that these two paradigms will be synergistic rather than passing by each other, or worse, interfering with each other.

DATA AVAILABILITY STATEMENT

The original contributions presented in the study are included in the article/supplementary material, further inquiries can be directed to the corresponding author/s.

AUTHOR CONTRIBUTIONS

CC developed the paper concept and contributed to writing and editing. SJ, AR, and IR contributed to refining the paper concept and contributed to writing and editing. All authors contributed to the article and approved the submitted version.

FUNDING

We acknowledge funding support from the National Institute of Mental Health [P50MH119569 (AR and IR), R61MH123754 (CC), K01MH117451 (IR)].

ACKNOWLEDGMENTS

We thank the University of Minnesota NeuroPlasticity Research in Support of Mental Health (NeuroPRSMH) group for discussions leading to insights that are infused throughout this paper. We thank Song Burkhart for administrative support.

REFERENCES

1. Sathappan AV, Luber BM, Lisanby SH. The dynamic duo: combining noninvasive brain stimulation with cognitive interventions. *Prog Neuropsychopharmacol Biol Psychiatry.* (2019) 89:347–60. doi: 10.1016/j.pnpbp.2018.10.006
2. Dedoncker J, Baeken C, De Raedt R, Vanderhasselt MA. Combined transcranial direct current stimulation and psychological interventions: state of the art and promising perspectives for clinical psychology. *Biol Psychol.* (2021) 158:107991. doi: 10.1016/j.biopsycho.2020.107991
3. Silvanto J, Muggleton N, Walsh V. State-dependency in brain stimulation studies of perception and cognition. *Trends Cogn Sci.* (2008) 12:447–54. doi: 10.1016/j.tics.2008.09.004
4. Bikson M, Rahman A. Origins of specificity during tDCS: anatomical, activity-selective, and input-bias mechanisms. *Front Hum Neurosci.* (2013) 7:688. doi: 10.3389/fnhum.2013.00688
5. Donse L, Padberg F, Sack AT, Rush AJ, Arns M. Simultaneous rTMS and psychotherapy in major depressive disorder: clinical outcomes and predictors from a large naturalistic study. *Brain Stimul.* (2018) 11:337–45. doi: 10.1016/j.brs.2017.11.004
6. Nasiri F, Mashhadi A, Bigdeli I, Chamanabad AG, Ellard KK. Augmenting the unified protocol for transdiagnostic treatment of emotional disorders with transcranial direct current stimulation in individuals with generalized anxiety disorder and comorbid depression: a randomized controlled trial. *J Affect Disord.* (2020) 262:405–13. doi: 10.1016/j.jad.2019.11.064
7. O'keefe J, Nadel L. *The Hippocampus as a Cognitive Map*. Oxford: Clarendon Press. (1978).
8. Doya K. What are the computations of the cerebellum, the basal ganglia and the cerebral cortex? *Neural Netw.* (1999) 12:961–74. doi: 10.1016/S0893-6080(99)00046-5
9. David Redish A. *The Mind Within the Brain: How We Make Decisions and How Those Decisions Go Wrong*. New York, NY: OUP USA (2013).

10. LeDoux JE. Emotion circuits in the brain. *Annu Rev Neurosci.* (2000) 23:155–84. doi: 10.1146/annurev.neuro.23.1.155
11. Milad MR, Quirk GJ. Neurons in medial prefrontal cortex signal memory for fear extinction. *Nature.* (2002) 420:70–4. doi: 10.1038/nature01138
12. Lebrón K, Milad MR, Quirk GJ. Delayed recall of fear extinction in rats with lesions of ventral medial prefrontal cortex. *Learn Mem.* (2004) 11:544–8. doi: 10.1101/lm.78604
13. Nili U, Goldberg H, Weizman A, Dudai Y. Fear thou not: activity of frontal and temporal circuits in moments of real-life courage. *Neuron.* (2010) 66:949–62. doi: 10.1016/j.neuron.2010.06.009
14. Redish AD. Vicarious trial and error. *Nat Rev Neurosci.* (2016) 17:147–59. doi: 10.1038/nrn.2015.30
15. Graybiel A, Aosaki T, Flaherty A, Kimura M. The basal ganglia and adaptive motor control. *Science.* (1994) 265:1826–31. doi: 10.1126/science.8091209
16. Haber SN, Knutson B. The reward circuit: linking primate anatomy and human imaging. *Neuropsychopharmacology.* (2010) 35:4–26. doi: 10.1038/npp.2009.129
17. David Redish A, Gordon JA. *Computational Psychiatry: New Perspectives on Mental Illness*. Cambridge, MA: MIT Press. (2016). doi: 10.7551/mitpress/9780262035422.001.0001
18. Nader K, Schafe GE, Le Doux JE. Fear memories require protein synthesis in the amygdala for reconsolidation after retrieval. *Nature.* (2000) 406:722–6. doi: 10.1038/35021052
19. Levitan D, Fortis-Santiago Y, Figueroa JA, Reid EE, Yoshida T, Barry NC, et al. Memory retrieval has a dynamic influence on the maintenance mechanisms that are sensitive to ζ-inhibitory peptide (ZIP). *J Neurosci.* (2016) 36:10654–62. doi: 10.1523/JNEUROSCI.1568-16.2016
20. Alberini CM. The role of reconsolidation and the dynamic process of long-term memory formation and storage. *Front Behav Neurosci.* (2011) 5:12. doi: 10.3389/fnbeh.2011.00012
21. Hofmann SG, Asmundson GJG. *The Science of Cognitive Behavioral Therapy*. London: Elsevier (2017).
22. Gaudiano BA. Cognitive-behavioural therapies: achievements and challenges. *Evid Based Ment Health.* (2008) 11:5–7. doi: 10.1136/ebmh.11.1.5
23. Pompoli A, Furukawa TA, Efthimiou O, Imai H, Tajika A, Salanti G. Dismantling cognitive-behaviour therapy for panic disorder: a systematic review and component network meta-analysis. *Psychol Med.* (2018) 48:1945–53. doi: 10.1017/S0033291717003919
24. Chalah MA, Ayache SS. Disentangling the neural basis of cognitive behavioral therapy in psychiatric disorders: a focus on depression. *Brain Sci.* (2018) 8:150. doi: 10.3390/brainsci8080150
25. Barth AL, Ray A. Progressive circuit changes during learning and disease. *Neuron.* (2019) 104:37–46. doi: 10.1016/j.neuron.2019.09.032
26. Mansouri F, Fettes P, Schulze L, Giacobbe P, Zariffa J, Downar J. A real-time phase-locking system for non-invasive brain stimulation. *Front Neurosci.* (2018) 12:877. doi: 10.3389/fnins.2018.00877
27. Zrenner B, Zrenner C, Gordon PC, Belardinelli P, McDermott EJ, Soekadar SR, et al. Brain oscillation-synchronized stimulation of the left dorsolateral prefrontal cortex in depression using real-time EEG-triggered TMS. *Brain Stimul.* (2020) 13:197–205. doi: 10.1016/j.brs.2019.10.007
28. Carmi L, Tendler A, Bystritsky A, Hollander E, Blumberger DM, Daskalakis J, et al. Efficacy and safety of deep transcranial magnetic stimulation for obsessive-compulsive disorder: a prospective multicenter randomized double-blind placebo-controlled trial. *Am J Psychiatry.* (2019) 176:931–8. doi: 10.1176/appi.ajp.2019.18101180
29. Osuch EA, Benson BE, Luckenbaugh DA, Geraci M, Post RM, McCann U. Repetitive TMS combined with exposure therapy for PTSD: a preliminary study. *J Anxiety Disord.* (2009) 23:54–9. doi: 10.1016/j.janxdis.2008.03.015
30. Foa EB, Kozak MJ. Emotional processing of fear: exposure to corrective information. *Psychol Bull.* (1986) 99:20–35. doi: 10.1037/0033-2909.99.1.20
31. Craske MG, Kircanski K, Zelikowsky M, Mystkowski J, Chowdhury N, Baker A. Optimizing inhibitory learning during exposure therapy. *Behav Res Ther.* (2008) 46:5–27. doi: 10.1016/j.brat.2007.10.003
32. Hofmann SG, Smits JAJ. Cognitive-behavioral therapy for adult anxiety disorders: a meta-analysis of randomized placebo-controlled trials. *J Clin Psychiatry.* (2008) 69:621–32. doi: 10.4088/JCP.v69n0415
33. Hofmann SG, Asnaani A, Vonk IJJ, Sawyer AT, Fang A. The efficacy of cognitive behavioral therapy: a review of meta-analyses. *Cognit Ther Res.* (2012) 36:427–40. doi: 10.1007/s10608-012-9476-1
34. Lueken U, Zierhut KC, Hahn T, Straube B, Kircher T, Reif A, et al. Neurobiological markers predicting treatment response in anxiety disorders: a systematic review and implications for clinical application. *Neurosci Biobehav Rev.* (2016) 66:143–62. doi: 10.1016/j.neubiorev.2016.04.005
35. Lester KJ, Eley TC. Therapygenetics: using genetic markers to predict response to psychological treatment for mood and anxiety disorders. *Biol Mood Anxiety Disord.* (2013) 3:4. doi: 10.1186/2045-5380-3-4
36. Aharonovich E, Hasin DS, Brooks AC, Liu X, Bisaga A, Nunes EV. Cognitive deficits predict low treatment retention in cocaine dependent patients. *Drug Alcohol Depend.* (2006) 81:313–22. doi: 10.1016/j.drugalcdep.2005.08.003
37. Schindler A, Hiller W, Witthöft M. What predicts outcome, response, and drop-out in CBT of depressive adults? A naturalistic study. *Behav Cogn Psychother.* (2013) 41:365–70. doi: 10.1017/S1352465812001063
38. Bellg AJ, Borrelli B, Resnick B, Hecht J, Minicucci DS, Ory M, et al. Enhancing treatment fidelity in health behavior change studies: best practices and recommendations from the NIH behavior change consortium. *Health Psychol.* (2004) 23:443–51. doi: 10.1037/0278-6133.23.5.443
39. Waltman SH, Sokol L, Beck AT. Cognitive behavior therapy treatment fidelity in clinical trials: review of recommendations. *Curr Psychiatry Rev.* (2017) 13:311–5. doi: 10.2174/1573400514666180109150208
40. Benito KG, Machan J, Freeman JB, Garcia AM, Walther M, Frank H, et al. Measuring fear change within exposures: functionally-defined habituation predicts outcome in three randomized controlled trials for pediatric OCD. *J Consult Clin Psychol.* (2018) 86:615–30. doi: 10.1037/ccp0000315
41. Addis ME, Jacobson NS. A closer look at the treatment rationale and homework compliance in cognitive-behavioral therapy for depression. *Cognit Ther Res.* (2000) 24:313–26. doi: 10.1023/A:1005563304265
42. Craske MG, Treanor M, Conway CC, Zbozinek T, Vervliet B. Maximizing exposure therapy: an inhibitory learning approach. *Behav Res Ther.* (2014) 58:10–23. doi: 10.1016/j.brat.2014.04.006
43. Carroll KM, Nich C, Ball SA. Practice makes progress? Homework assignments and outcome in treatment of cocaine dependence. *J Consult Clin Psychol.* (2005) 73:749–55. doi: 10.1037/0022-006X.73.4.749
44. Cammin-Nowak S, Helbig-Lang S, Lang T, Gloster AT, Fehm L, Gerlach AL, et al. Specificity of homework compliance effects on treatment outcome in CBT: evidence from a controlled trial on panic disorder and agoraphobia: homework effects in CBT for panic disorder. *J Clin Psychol.* (2013) 69:616–29. doi: 10.1002/jclp.21975
45. LeBeau RT, Davies CD, Culver NC, Craske MG. Homework compliance counts in cognitive-behavioral therapy. *Cogn Behav Ther.* (2013) 42:171–9. doi: 10.1080/16506073.2013.763286
46. Sandran N, Hillier S, Hordacre B. Strategies to implement and monitor in-home transcranial electrical stimulation in neurological and psychiatric patient populations: a systematic review. *J Neuroeng Rehabil.* (2019) 16:58. doi: 10.1186/s12984-019-0529-5
47. Charvet LE, Shaw MT, Bikson M, Woods AJ, Knotkova H. Supervised transcranial direct current stimulation (tDCS) at home: a guide for clinical research and practice. *Brain Stimul.* (2020) 13:686–93. doi: 10.1016/j.brs.2020.02.011
48. Cocchi L, Zalesky A. Personalized transcranial magnetic stimulation in psychiatry. *Biol Psychiatry Cogn Neurosci Neuroimaging.* (2018) 3:731–41. doi: 10.1016/j.bpsc.2018.01.008
49. Boes AD, Kelly MS, Trapp NT, Stern AP, Press DZ, Pascual-Leone A. Noninvasive brain stimulation: challenges and opportunities for a new clinical specialty. *J Neuropsychiatry Clin Neurosci.* (2018) 30:173–9. doi: 10.1176/appi.neuropsych.17110262

50. Hanlon CA, Kearney-Ramos T, Dowdle LT, Hamilton S, DeVries W, Mithoefer O, et al. Developing repetitive transcranial magnetic stimulation (rTMS) as a treatment tool for cocaine use disorder: a series of six translational studies. *Curr Behav Neurosci Rep.* (2017) 4:341–52. doi: 10.1007/s40473-017-0135-4

Conflict of Interest: CC and SJ are investigators on National Institute of Mental Health-funded SBIR grants awarded to Posit Science [R43MH121209 (CC), R43MH124542 (CC and SJ)]. SJ has been an investigator in multisite autism treatment trials by Roche and on an autism advisory board for Roche.

The remaining authors declare that the research was conducted in the absence of any commercial or financial relationships that could be construed as a potential conflict of interest.

frontiers in Psychiatry

ORIGINAL RESEARCH
published: 06 October 2021
doi: 10.3389/fpsyt.2021.717255

Effects of Transcranial Direct Current Stimulation Treatment for Anorexia Nervosa

Silvie Baumann[1,2], Tadeáš Mareš[2,3], Jakub Albrecht[2,3], Martin Anders[2,3], Kristýna Vochosková[1,4], Martin Hill[5], Josef Bulant[3,5,6], Anna Yamamotová[7], Ota Štastný[4], Tomáš Novák[1,4], Petra Holanová[2,3], Alena Lambertová[2,3] and Hana Papežová[2,3]*

[1] Department of Psychotherapy, National Institute of Mental Health, Klecany, Czechia, [2] First Faculty of Medicine, Charles University, Prague, Czechia, [3] Department of Psychiatry, First Faculty of Medicine, Charles University in Prague and General University Hospital in Prague, Prague, Czechia, [4] Third Faculty of Medicine, Charles University, Prague, Czechia, [5] Department of Steroid Hormones and Proteohormones, Institute of Endocrinology, Prague, Czechia, [6] Department of Pediatrics and Inherited Metabolic Disorders, First Faculty of Medicine, Charles University and General University Hospital in Prague, Prague, Czechia, [7] Department of Physiology, Third Faculty of Medicine, Charles University, Prague, Czechia

OPEN ACCESS

Edited by:
Wenbin Guo,
Central South University, China

Reviewed by:
Maximilian Achim Friehs,
University College Dublin, Ireland
Gianluca Serafini,
San Martino Hospital (IRCCS), Italy
Guido K. W. Frank,
University of California, San Diego, United States

***Correspondence:**
Silvie Baumann
silvie.baumann@nudz.cz

Specialty section:
This article was submitted to Neuroimaging and Stimulation, a section of the journal Frontiers in Psychiatry

Received: *30 May 2021*
Accepted: *27 August 2021*
Published: *06 October 2021*

Citation:
Baumann S, Mareš T, Albrecht J, Anders M, Vochosková K, Hill M, Bulant J, Yamamotová A, Štastný O, Novák T, Holanová P, Lambertová A and Papežová H (2021) Effects of Transcranial Direct Current Stimulation Treatment for Anorexia Nervosa. Front. Psychiatry 12:717255. doi: 10.3389/fpsyt.2021.717255

Background: Anorexia nervosa (AN) is a life-threatening illness with poor treatment outcomes. Although transcranial direct current stimulation (tDCS) is a promising non-invasive brain stimulation method, its effect in patients with AN remains unclear.

Objective: This study investigated changes in maladaptive eating behavior, body mass index (BMI), and depression after 10 sessions of anodal tDCS over the left dorsolateral prefrontal cortex (DLPFC).

Methods: In this double-blind, randomized controlled trial, 43 inpatients with AN were divided to receive either active ($n = 22$) or sham ($n = 21$) tDCS over the left DLPFC (anode F3/cathode Fp2, 2 mA for 30 min). All patients filled the Eating Disorder Examination Questionnaire (EDE-Q) and Zung Self-Rating Depression Scale (ZUNG), and their BMI was measured. These values were obtained repeatedly in four stages: (1) before tDCS treatment, (2) after tDCS treatment, (3) in the follow-up after 2 weeks, and (4) in the follow-up after 4 weeks.

Results: Primary outcomes (EDE-Q) based on the ANOVA results do not show any between-group differences either after the active part of the study or in the follow-up. Secondary analysis reveals a reduction in some items of EDE-Q. Compared with sham tDCS, active tDCS significantly improved self-evaluation based on body shape ($p < 0.05$) and significantly decreased the need of excessive control over calorie intake ($p < 0.05$) in the 4-week follow-up. However, the results do not survive multiple comparison correction. In both sham and active groups, the BMI values improved, albeit not significantly.

Conclusion: We did not observe a significant effect of tDCS over the left DLPFC on complex psychopathology and weight recovery in patients with AN. tDCS reduced the

need to follow specific dietary rules and improved body image evaluation in patients with AN. Tests with a larger sample and different positions of electrodes are needed.

Clinical Trial Registration: www.ClinicalTrials.gov, identifier: NCT03273205.

Keywords: self-perception, anorexia nervosa, brain stimulation, tDCS, transcranial direct current stimulation, EDE-Q, Zung scale of depression

INTRODUCTION

Anorexia nervosa (AN) is a serious life-threatening illness, which is found throughout all countries and all socioeconomic layers. AN is estimated to occur in 0.3–1.0% females and 0.1–0.3% males (1, 2). It is associated with the highest mortality rate among all mental disorders (5.1 deaths per 1,000 person/years), and the suicide rate for AN is 1.3 per 1,000 person/years (3). AN is a severe eating disorder characterized by deliberate weight loss induced and maintained purposefully by the patient. This disorder is associated with specific psychopathology, in which the intense fear of weight gain persists as an intrusive thought. Food restriction, excessive physical activity, and self-induced vomiting or diarrhea are usually present, resulting in malnutrition with secondary endocrine and metabolic changes. A distortion of self-perceived body image is present in many patients suffering from this condition (4). Standard treatment consists of regimen therapy (restriction of exercise and regular food intake), as well as psychotherapy and psychopharmacological support (antidepressants, anxiolytics, and antipsychotics). Despite medical progress and therapeutic advances, the efficiency of current treatment is only around 40% (5, 6). Therefore, further treatment options should be investigated.

Neurostimulation is a biological approach in psychiatry that includes intentional modulation of basic neuronal activity through targeted delivery of a stimulus (by a magnetic field, by an electric current, or both) (7). Transcranial direct current stimulation (tDCS) is a modern, well-tolerated method, which can be easily applied by trained personnel. It is assumed to be a safe technique (8–10), and the adverse effects are overall mild. The advantages of this method are low purchase costs and great therapeutic potential. In contrast to repetitive transcranial magnetic stimulation (TMS), the current delivered by tDCS is not considered strong enough to evoke an action potential in neurons. tDCS is commonly referred to as both a "subthreshold" and "neuromodulatory" stimulation technique. tDCS acts to modulate the rate of naturally occurring firing of neurons within the stimulated tissue (11). The stimulation shifts cortical excitability to a state of excitation or inhibition (12), depending on the position of electrodes. Anodal tDCS is associated with excitation of the stimulated brain area by depolarizing neurons and increasing the propensity for neuronal firing, whereas cathodal tDCS is associated with hyperpolarization (13, 14). Hundreds of trials in many areas (e.g., schizophrenia, post-stroke aphasia, and tinnitus) are ongoing due to advantages and potential of tDCS. Level B recommendation (probable efficacy) has been proved for treating of craving, major depressive disorder (MDD), and fibromyalgia (15). tDCS treatment of AN has not been consolidated and varies.

Unlike some other mental and neurological disorders, the exact neurobiological correlates of AN have not been fully elucidated. It is assumed that there is a dysfunction in brain reward and emotional circuits, and impaired balance between interoceptive and reward processing. It is known that patients with AN have increased cognitive control and ability to suppress hunger (16–18). There are several targets for invasive neuromodulation (deep brain stimulation) in AN: the nucleus accumbens, which is active on mood and reward pathways; the subcallosal cingulate gyrus as part of mood and anxiety pathways; and the ventral capsule/ventral striatum or anterior limb of internal capsule, which is included in anxiety and emotion pathways (19). Techniques of non-invasive brain stimulation (NIBS; TMS and tDCS) mainly focus on dorsolateral prefrontal cortex (DLPFC). The insula, which modulates reward processing, decision making, interoception, and mentalization (19), was used as a target of neuromodulation in one study only, with the authors using H-coil deep TMS (20). In another study, the dorsomedial prefrontal cortex (DMPFC), which is involved in self-regulation, cognitive and impulse control, decision making, and inhibition, was modulated (21).

DLPFC is involved in cognitive control, executive functioning, working memory, craving, and also control and regulation of the valence of emotional experiences (22–24). Extreme caloric restriction in AN can be a manifestation of a maladaptive mechanism for coping with anxiety, mood disorders, and other negative emotions (16). In the evidence-based guidelines on the therapeutic use of tDCS, anodal tDCS over the left DLPFC (with right orbitofrontal cathode) is promoted in the treatment of major depressive episodes without drug resistance (15). Similarly, tDCS over DLPFC (anodal left and cathodal right DLPFC) improves cognitive control over negative emotions in borderline personality disorder (25). Consequently, stimulation of DLPFC, important in emotion regulation, could reduce the need for dietary behavior. On the other hand, AN is known for excessive cognitive control (16), and DLPFC is considered to be one of the main areas of the cognitive control system (26, 27). Even recovered patients with AN have elevated cognitive control over reward processing (18). Based on these findings, the inhibition of DLPFC has potential to reduce excessive cognitive control in AN.

For AN, Hecht suggested placing the anode over the left prefrontal cortex and the cathode, either on the right homotopic region for non-selective serotonin reuptake inhibitor (non-SSRI)-medicated anorexics or on a non-cephalic site for SSRI-medicated anorexics (28). Khedr et al. (29) applied 10 sessions of anodal stimulation over the left DLPFC (anode F3, cathode

extracephalic—over the contralateral arm) in an open-label study to seven treatment-resistant patients with AN. Five of the patients improved, as shown in results from questionnaires on eating pathology and depressive symptoms directly after the stimulations. Three of them were shown to have maintained the improvement at their 1-month follow-up assessments. Recently, Costanzo et al. (30) compared tDCS and family-based therapy (FBT) in patients with AN. They placed the anode on the left DLPFC and the cathode on the right DLPFC in study of 11 participants (three sessions a week, for 6 weeks). The second group of 12 patients received FBT in an open-label study. Body mass index (BMI) significantly increased in the tDCS group compared with the FBT group. No group differences were reported regarding eating disorder symptoms. Strumila et al. (31) stimulated nine patients with AN for 10 days, twice a day with the same placement (anode F3/cathode F4). They noticed reduced eating disorder and depressive symptoms after 20 stimulations and in 1-month follow-up.

We aimed to explore the effect of anodal tDCS over the left DLPFC and with the cathode over the right orbitofrontal region in the first randomized, double-blind, sham-controlled trial of 43 patients with AN. The primary objective of the study was to observe its effect on the eating psychopathology evaluated by Eating Disorder Examination Questionnaire (EDE-Q). The secondary objective was to collect clinical outcomes from stage 1 to 4, including BMI, Zung Self-Rating Depression Scale (ZUNG), tolerability, and safety of tDCS. As the anodal tDCS can influence the emotional regulation (25), we hypothesized that in the group of patients with active tDCS, there will be a greater weight gain and an improvement in eating behavior (e.g., less restriction and reduction of vomiting). Second, because the same protocol is used to treat MDD (15), we expected the rate of depression to decrease more significantly in the stimulated group.

MATERIALS AND METHODS

Participants

All enrolled participants received standard treatment, as they were hospitalized in the Center for Diagnosis and Treatment of Eating Disorders in the Psychiatric Clinic of the First Medical Faculty, Charles University, Prague. The patients followed an intensive, comprehensive in-patient program with individual and group psychotherapy. The refeeding program was individually driven and depended on each patient's current BMI value. They used medication, if needed, over the study period. All participants obtained the tDCS treatment on top of the standard care.

Inclusion criteria consisted of subjects between the ages of 18 and 65 with the diagnosis of AN according to the International Classification of Diseases 10th revision. Exclusion criteria included pregnancy or breastfeeding, a history of strong and frequent headaches, epileptic paroxysm and other severe neurological disorders, history of brain injury, and metallic objects within the neurocranium. Due to COVID-19 and certain technical and organizational challenges, we could not evaluate all consecutively hospitalized patients. All participants signed an informed consent and a General Data Protection Regulation processing agreement (approved by Ethical Committee No. 1955/16 S-IV). The recruitment period was from May 2017 to May 2020. Forty-three patients were selected for the study during this period. Thirty-nine patients were diagnosed with AN (90.7%), and four of them with atypical AN (9.3%). Eight of them were diagnosed with a personality disorder, seven with unipolar depression, and 10 with anxiety disorders, and five had a history of substance abuse (all of them sober for at least 3 months). The demographic data are shown in **Table 1**. The dataset had to be reduced due to a high dropout rate brought about by various reasons. Two patients (both from sham) kept breaking the rules of the Department (e.g., intentional vomiting and excessive exercising) and consequently were dismissed from the hospital, resulting in the termination in the study. Furthermore, two participants (one from sham and one from active) decided to leave the hospital against medical advice. Two females (sham group) requested to leave the study without disclosing the reason. Side effects represented the last reason (all four patients were from the active group): two patients left due to headache, another one was excluded following mood changes (toward hypomania), and one patient had troubles with blood sugar and an onset of diabetes (32). As a result, the data of 17 patients in the stimulated group and 16 in the sham (placebo) group remained eligible for the statistical analysis at the time of stage 2. Seven patients were lost to follow-up. One patient (active group) suffered from influenza during the third stage, and four participants (three from active and one from sham) finished the therapeutic program and left the Department before the termination of the study. Two patients (sham) withdrew from the study at stage 3. In the end, data of only 13 patients in each group were relevant for the statistical analysis (**Figure 1**).

Study Protocol

The study protocol was approved by the Independent Ethics Committee on January 19, 2017, and is registered under number 1955/16 S-IV. The study was also registered in the ClinicalTrials.gov under the identifier NCT03273205. The design adhered to the latest version of the Declaration of Helsinki and International Council for Harmonisation (ICH)/Good Clinical Practice guidelines. It was a two-arm, double-blind, randomized controlled trial. We did not assess the blindness in our study. Participants were randomly assigned to active or sham groups by blocked randomization, and a block size of 4 was given.

We measured BMI, ZUNG, and EDE-Q in four stages: (1) before tDCS treatment, (2) after tDCS treatment, (3) in the follow-up after 2 weeks, and (4) in the follow-up after 4 weeks (**Table 2**). EDE-Q as a primary measurement for symptoms of AN consists of the four subscales demonstrating acceptable internal consistency with Cronbach's alphas ranging from 0.70 to 0.93 (33). Internal consistency (reliability) of ZUNG is reported in several studies with values around 0.8 (34, 35). The participants as well as the research team on-site remained unaware of the stimulation conditions until the last control.

The active protocol consisted of ten 30-min sessions of 2-mA anodal stimulation over the left DLPFC (F3 in 10–20 electroencephalography (EEG) system) with the cathode over

TABLE 1 | Baseline demographic and clinical characteristics of the study participants.

	Active tDCS ($n = 17$)		Sham ($n = 16$)		Test
Characteristics	**Median (quartiles)**	**Mean (SD)**	**Median (quartiles)**	**Mean (SD)**	**Statistics**
BMI	15.7 (14.7, 16.8)	16 (1.69)	17.3 (15.1, 18.3)	16.8 (2.47)	0.257[a]
EDE-Q total	96 (57, 131)	94.8 (40.2)	69 (33.3, 112)	75.9 (47.1)	0.183[a]
ZUNG	74 (70, 76)	71.6 (8.57)	72 (65.8, 79.5)	72.3 (11.4)	0.971[a]
Length of the illness (months)	48 (24, 84)	59.4 (46)	72 (46.5, 144)	98.6 (79.9)	0.176[a]
Number of psychiatric hospitalizations	2 (1, 3)	2.47 (2.1)	2 (1, 4)	4.19 (6.34)	0.583[a]
Number of psych. hospitalizations due to ED	1 (1, 3)	2.41 (2.12)	2 (1, 4)	4.06 (6.3)	0.480[a]
Age (years)	21 (20, 26)	23.7 (6.38)	26 (23.5, 33)	28.1 (7.95)	0.058[a]
Characteristics		***n* (%)**			
Depression	3 (17.6%)		4 (25%)		1.000[b]
Anxiety	3 (17.6%)		6 (37.5%)		0.259[b]
History of substance abuse	0 (0%)		5 (31.3%)		0.018[b]
Personality disorder	2 (11.8%)		3 (18.8%)		0.656[b]

EDE-Q, Eating Disorder Examination Questionnaire; ZUNG, Zung Self-Rating Depression Scale; BMI, body mass index; ED, eating disorder.
[a]*Mann–Whitney test.*
[b]*Fisher's exact test.*

the right orbitofrontal region (Fp2). The HDCstim portable programmable direct current stimulator made by Newronika s.r.l. (Milan, Italy) was used together with electrodes (anode 5 × 5 cm, cathode 6 × 8.5 cm) covered by hydratable holding bags soaked in saline (0.9%) to lower resistance. The current density was calculated at 0.571 A/m^2. Modeling of electric fields was performed through SimNIBS software package (36) (**Supplementary Figure 1**).

For sham tDCS, the same protocol was used, but the device was automatically turned off after 30 s to mimic the typical initial sensation of tDCS and turned on for the last 30 s before the end of the session (so-called ramp-up and ramp-down, respectively). All other factors were the same for both groups (nutritional, pharmacological, and psychoeducational complex treatment "as usual").

Concomitant Treatment

The patients were enrolled in the study with their current pharmacotherapy. Due to the severity of their conditions, we did not build a washout period into our protocol. The medication is shown in **Table 3**.

Statistical Analysis

The relationship between metric variables on the one side and the stage of the treatment and stimulation on the other side was assessed by ANOVA models. These models included the Subject factor explaining inter-individual variability, between-subject factor Stimulation (Stimulation vs. placebo), within-subject factor Stage (Stages 1, 2, 3, and 4), Stimulation × Stage interaction, and further factors such as comorbidities (MDD, anxiety, and personality disorders) and medication (antidepressants and antipsychotics) as covariates.

Before statistical testing, the parametric data were transformed utilizing power transformations toward normal distribution and homoscedasticity of data and residuals as described elsewhere (37, 38). The symmetry of the data distribution and the presence of outliers in the transformed data were evaluated using methods described in the literature (38–40). After analyses were performed, the obtained results were re-transformed by the recurrence formula to the original scale for their presentation.

Relationships between relevant variables in the first stage of the trial and their changes in the second stage of the trial on the one hand and the effect of stimulation on the other hand were evaluated by multivariate regression with a reduction of dimensionality known as orthogonal projection to latent structure (OPLS) (41–44). OPLS is capable of coping with the problem of severe multicollinearity in the matrix of explaining variables, while ordinary multiple regression fails to evaluate such data. In our OPLS models, the logarithm of the ratio of the probability that the subject underwent the stimulation to the probability that the subject was on placebo [logarithm of the likelihood ratio (LLR)] was chosen as a single dependent variable.

The variability in relevant explaining variables was separated into two groups of mutually independent components. The first one contained the variability of relevant explaining variables, which was shared with the effect of stimulation (the predictive component), while the orthogonal components explained the variability shared within the explaining variables.

The OPLS identified the relevant explaining variables and their combinations to estimate the effect of stimulation (**Supplementary Figure 2**). The relevant explaining variables were chosen using variable importance of projection (VIP) statistics. The statistical software SIMCA-P v.12.0 from Umetrics AB (Umeå, Sweden), which was used for OPLS analysis, detected multivariate non-homogeneities and tested the multivariate normal distribution and homoscedasticity (constant variance). The analysis was adjusted for multiple comparisons using Bonferroni's method. The respective algorithm is in **Supplementary Figure 3**.

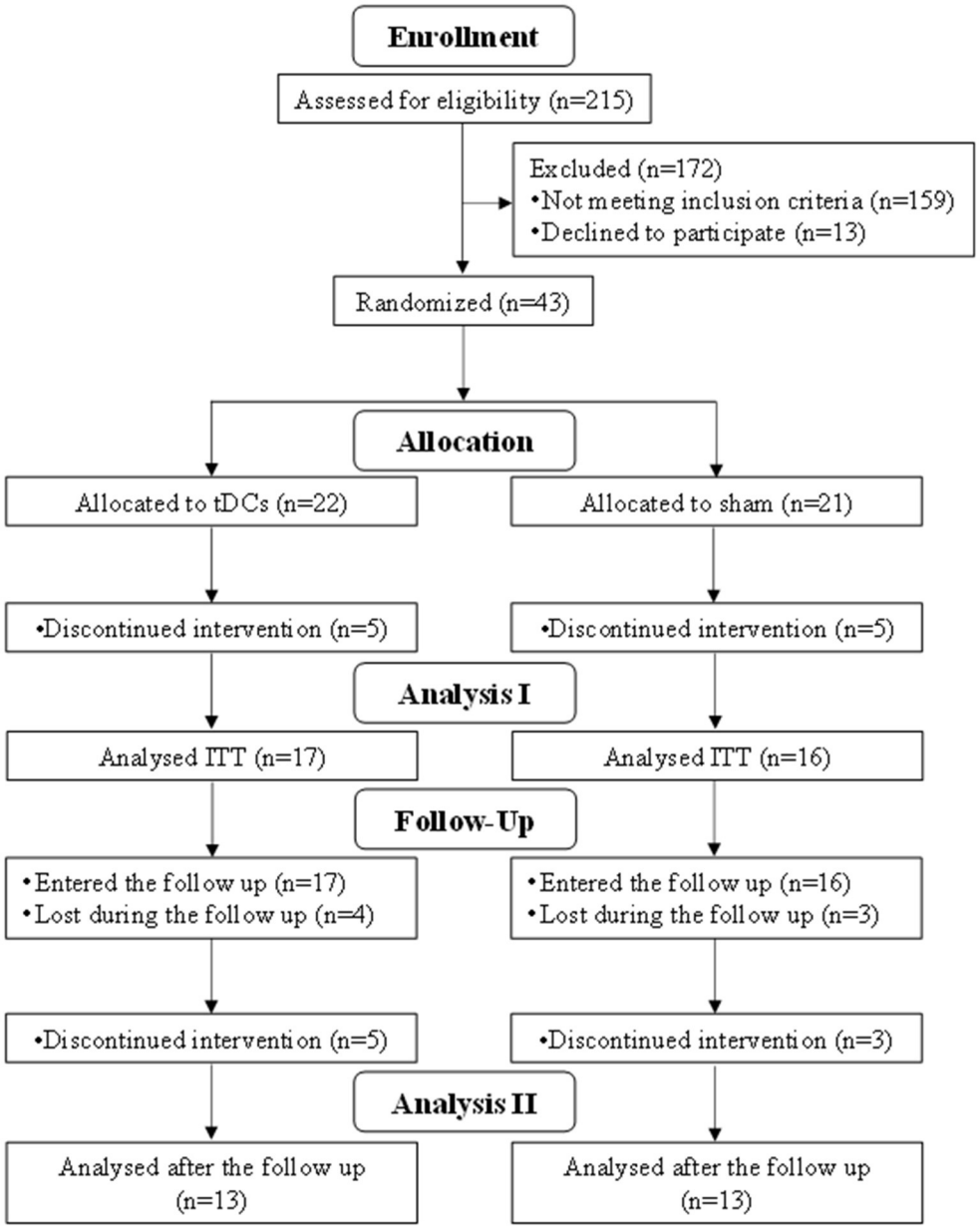

FIGURE 1 | Enrollment to the study.

RESULTS

Primary outcomes based on the ANOVA results do not show any differences between groups either after the active part of the study or in the follow-up. Secondary analysis (OPLS) reveals a reduction in certain items of EDE-Q in the 4-week follow-up. However, the results do not survive multiple comparison correction. In sham tDCS, several mood symptoms improved significantly ($p < 0.01$). In both sham and active groups, the BMI values improved, albeit not significantly.

Table 4 shows the OPLS model that analyzes the relationships between the effect of stimulation and monitored parameters at the beginning of the study as well as the differences between the values at the second and first stages of the study (Δ = *Stage 2 – Stage 1*). There is a significant positive relationship between the stimulation and the changes in the overall score ($p < 0.01$) as well as in some individual questions of the ZUNG 5, 11, 12, and 20 ($p < 0.01$) and question 21 in EDE-Q ($p < 0.05$). This indicates that the sham group experienced a more pronounced decline in the aforementioned parameters. **Table 4** also shows that more patients in the sham group took mirtazapine, smoked more cigarettes, and were older than patients in the active group. After Bonferroni's correction, only the following variables have $p < 0.05$: age, amount

TABLE 2 | The timeline of the study.

Stage	Timing	BMI	EDE-Q	ZUNG
1	Before tDCS	X	X	X
2	After tDCS	X	X	X
3	2 weeks after	X	X	X
4	4 weeks after	X	X	X

TABLE 3 | The concomitant treatment.

Medication	Active tDCS (*n*)	Sham tDCS (*n*)
Antidepressants	12	16
Antipsychotics	11	6
Benzodiazepines	4	3
Mood stabilizer (lamotrigine)	0	1
Pregabaline	0	1

of cigarettes, single questions in ZUNG, and the total score in ZUNG.

Table 5 shows the OPLS model that analyzes the relationships between the effect of stimulation and parameters at the beginning of the study. In addition, it analyzes the differences between the situation at the final stage of the study and at the beginning of the study (Δ = *Stage 4 – Stage 1*). **Table 5** shows significant positive relationships between the changes in two questions in ZUNG (10, 16) and negative associations with two questions of EDE-Q (4, 23). Compared with sham tDCS, active tDCS significantly improved self-evaluation based on one's body shape (EDE-Q 23) and significantly decreased the need of excessive control over calorie intake (EDE-Q 4) in a follow-up after 4 weeks ($p < 0.05$). In sham tDCS, questions 10 (concerning fatigue) and 16 (ability to make decisions) improved significantly ($p < 0.01$). This shows that the active group experienced a more pronounced decline in the aforementioned EDE-Q changes but a less pronounced reduction in the ZUNG ones. In addition, more patients took mirtazapine and generally some antidepressants in the sham group. After Bonferroni's correction, the $p < 0.05$ holds true only for the question 10 in the ZUNG.

Table 6 shows the side effects of tDCS in our study. They are very similar to the side effects mentioned in literature (45, 46). The most common side effects were burning sensation under the electrodes and headache. Interestingly, one of the patients indicated an improvement of toothache; one mentioned remission of headache; and another patient noticed a decline in night sweating. On the contrary, there was an onset of type I diabetes mellitus in one patient with active tDCS (32).

DISCUSSION

In this study, we aimed to explore the effects of 10 sessions over the left DLPFC in patients with AN. The main analysis did not prove any significant effect on complex psychopathology and weight recovery in patients with AN. The secondary analysis indicates possible positive impact of tDCS treatment on questions 4 and 23 in EDE-Q. These findings indicate that active tDCS might reduce the urge to follow specific dietary rules and improves self-evaluation based on body shape. These factors are crucial for the long-term outcome of eating disorders.

Depression is often present in patients with AN as one of the comorbidities. According to the literature, tDCS is effective in the treatment of MDD (15, 47), which is why we expected some improvement of the active group in the ZUNG. However, just after the last stimulation (stage 2), the sham group had better results in the total score and in questions 5, 11, 12, and 20 in the ZUNG ($p < 0.01$). When we compared the first and last stages, there was a significant decrease in the sham group in questions 10 and 16 ($p < 0.01$ and $p < 0.05$). This may be explained by higher levels of MDD and higher doses of antidepressants, especially mirtazapine, in the sham group (**Tables 1**, **3**, **4**, **5**). These could be important factors influencing our results. Another possible explanation is that in AN, affective difficulties are more likely to be secondary to primary eating pathology and increase with age (sham group is older). Thus, if the patients' core difficulties did not sufficiently change, neither did their moods.

The BMI values increased from the first stage to the last stage in both groups. It could be explained by regular food intake and strict control of the medical staff over the patients' eating habits. These might be confounding variables. For more accurate results, we would need a control group of inpatients receiving only the usual treatment.

The results of our study did not confirm promising studies that explored the effect of tDCS in AN. Two open-label trials were applied tDCS in seven and 10 patients (29, 31). Both of them showed an improvement in most of the patients. Costanzo et al. (30) tried to compare active tDCS and family psychotherapy and found that active tDCS was more effective. If we had not compared the active tDCS with the sham, our findings would have shown positive effects of active tDCS. However, in comparison with those of the sham group, most of our findings were not statistically significant.

The present study faces several limitations. First, the results could be influenced by different medications taken by the patients and higher antidepressant doses (mirtazapine in particular) taken by the sham group participants. The second limitation perhaps would be the small number of patients. We analyzed only 33 out of 43 patients enrolled in this trial, which is a borderline number for this kind of study. Third, the number of stimulations was rather small. Unfortunately, low compliance is typical for the diagnosis of AN, and the dropout rate equals to ∼20–40% (48). In our study, the dropout rate was 23% up to stage 2, and 40% including the follow-up. To secure participation, we used only 10 stimulations, but it appears that the effects of tDCS can be cumulative (49, 50). Some studies demonstrate a long-term effect of tDCS in months or even years (51–54). We might not have reached the full potential of our protocol due to the small number of sessions in our study. Another important shortcoming of our study was a large number of variables (different ages, comorbidities, durations of the illness, and numbers of hospitalizations). Typically, the more chronic the illness, the lower the probability to recover.

TABLE 4 | Relationships between the effect of stimulation (stimulated vs. non-stimulated patients, logarithm of the likelihood ratio, and LLR) and other parameters for the predictive component as evaluated by the OPLS model (for details, see *Statistical Analysis*).

		OPLS model Predictive component				Ordinary multiple regression		
	Variable	**Component loading**	**t-statistics**	**R[a]**		**Regression coefficient**	**t-statistics**	
Relevant predictors (matrix **X**)	Trittico	−0.129	−1.68	−0.257		−0.071	−2.26	*
	Mirtazapine	−0.246	−2.65	−0.489	*	−0.134	−1.93	*
	Cigarettes	−0.178	−5.09	−0.354	** †	−0.091	−2.49	*
	Age	−0.256	−3.18	−0.508	** †	−0.105	−3.59	**
	EDE-Q, 4	0.161	1.53	0.320		0.095	1.82	
	EDE-Q, 15	0.248	1.65	0.492		0.116	1.83	
	ZUNG, 12	−0.227	−2.30	−0.451	*	−0.077	−2.69	*
	ΔEDE-Q, 21	0.123	2.33	0.245	*	0.078	2.26	*
	ΔEDE-Q, 28	0.255	1.72	0.506		0.094	3.36	**
	ΔZUNG, total	0.398	9.56	0.792	** †	0.148	5.94	**
	ΔZUNG, 5	0.287	3.76	0.571	** †	0.120	3.70	**
	ΔZUNG, 11	0.381	4.89	0.758	** †	0.136	3.76	**
	ΔZUNG, 12	0.355	5.78	0.706	** †	0.133	5.06	**
	ΔZUNG, 20	0.350	8.25	0.696	** †	0.149	5.91	**
(matrix **Y**)	Stimulation (LLR)	1.000	9.12	0.844	**			
Explained variability				71.2% (63.6% after cross-validation)				

OPLS, orthogonal projection to latent structure; EDE-Q, Eating Disorder Examination Questionnaire; ZUNG, Zung Self-Rating Depression Scale.

EDE-Q, 4 = the need of excessive control over calorie intake; EDE-Q, 15 = number of episodes of overeating; EDE-Q, 21 = concerned when others see you eating; EDE-Q, 28 = uncomfortable feelings when others see your shape or figure (changing rooms, swimming, etc.); ZUNG, 5 = food intake as previously; ZUNG, 11 = clear mind; ZUNG, 12 = ability to do the things as before; ZUNG, 20 = hedonism.

aR = Component loadings expressed as correlation coefficients with predictive component, $^{*}p < 0.05$, $^{**}p < 0.01$; $^{\dagger}p < 0.05$ after correction using Bonferroni's method; Δ symbolizes post-intervention change (Stage 2 – Stage 1).

Sensitivity (95% CI) = 0.938 (0.717; 0.989); Specificity (95% CI) = 1.000 (0.772; 1.000). Cut-off probability = 0.5.

To ensure appropriate application of tDCS, it is necessary to consider several factors, with the first being the target area, which should be selected based on neuroimaging studies and recent neuroscientific knowledge. Most of NIBS studies in AN targeted left DLPFC (19). Phillipou et al. published a systematic review of the neurobiology of AN and reported structural and functional brain imaging in AN. Nevertheless, the results are not definite due to many inconsistencies across study procedures, and the mechanism of this illness is still poorly understood (55). We can only presume that anodal modulation over the left DLPFC can bring some changes in patients with AN. There are several brain structures, which could be potentially suitable for the NIBS in AN. Phillipou et al. found distinctive eye movement abnormalities in patients with AN (56) and suggested neuromodulation of the inferior parietal lobe (57). As already mentioned at the beginning, also DMPFC (21) and insula (20) might be possible targets. The right DLPFC seems to be one of the fundamental regions for response inhibition (58, 59), which is one of the main cognitive processes. Based on the analyzed tDCS studies, it is mainly anodal tDCS over the right DLPFC, which improves the performance in healthy volunteers (60). As the patients with AN have an increased cognitive control, it would be worth trying cathodal tDCS over the right prefrontal cortex with anode extracephalic.

The electrode placement and their size are also important factors. The tDCS montage should be designed based on a current flow simulation executed beforehand. The reference electrode should be big enough, so that the current density under the electrode is insignificant, or another possibility is the use of several small return electrodes, which is even more efficient (61). That is why high-definition tDCS (four to eight electrodes), with more precise targeting, could be one of the possible future directions. One of the protocols for AN is already suggested by Phillipou et al. (57). Friehs et al. presented a simulation of current flow (performed with SimNIBS) when targeting the right DLPFC through two distinct setups. The first option encompassed a small anodal electrode (9 cm^2) over the F4 position and cathode (9 cm^2) extracephalic. The second option included 35 cm^2 anode over F4 and 35 cm^2 over the left supraorbital area. The presented difference is striking (60). Even if two studies target the same region, the different stimulation setups bring different effects. Also, our electrode placement may not have been optimal for maximum left DLPFC stimulation. The cathodal placement (Fp2) did not allow us to distinguish specific effect of left DLPFC excitation and decreased the stimulation focality (**Supplementary Figure 1**). It would have been more appropriate to place anodal electrode over the left DLPFC and cathodal electrode extracephalic as suggested by Hecht (28). An innovative placement was used by Frings et al. as they tried to influence cognition in healthy volunteers by a single session of tDCS. Instead of frequently used F3–F4 setup, a small electrode of 9 cm^2 was placed over the left DLPFC and an electrode of 35 cm^2 was placed over the parieto-occipital cortex. This alternative approach contrasting anodal vs. cathodal

TABLE 5 | Relationships between the effect of Stimulation (stimulated vs. non-stimulated patients, logarithm of the likelihood ratio, and LLR) and other parameters as evaluated by the OPLS model and ordinary multiple regression (for details, see *Statistical Analysis*).

		OPLS model Predictive component				Ordinary multiple regression		
	Variable	**Component loading**	**t-statistics**	**R[a]**		**Regression coefficient**	**t-statistics**	
Relevant predictors (matrix **X**)	Mirtazapine	−0.266	−2.36	−0.588	*	−0.319	−4.99	**
	Antidepressants	−0.205	−2.00	−0.455	*	−0.176	−2.87	*
	EDE-Q, 1	0.179	2.04	0.395	*	0.103	1.49	
	EDE-Q, 2	0.288	4.64	0.638	**	0.147	1.26	
	EDE-Q, 3	0.212	4.26	0.469	**	0.012	0.19	
	EDE-Q, 4	0.300	4.78	0.664	**	0.130	1.61	
	EDE-Q, 5	0.172	4.98	0.380	**	−0.033	−0.54	
	EDE-Q, 8	0.165	2.09	0.365	*	0.023	0.30	
	EDE-Q, 10	0.195	3.24	0.431	**	0.012	0.25	
	EDE-Q, 11	0.174	2.27	0.384	*	0.008	0.18	
	EDE-Q, 12	0.154	3.51	0.341	**	−0.014	−0.30	
	EDE-Q, 18	0.202	2.72	0.448	*	0.040	0.40	
	EDE-Q, 20	0.142	1.97	0.314	*	−0.049	−0.78	
	EDE-Q, 22	0.234	2.88	0.517	*	0.124	1.80	
	EDE-Q, 23	0.234	3.89	0.517	**	0.103	1.68	
	EDE-Q, total	0.184	3.07	0.408	**	−0.068	−1.50	
	EDE-Q, restraint	0.264	4.99	0.584	**	0.066	1.66	
	EDE-Q, weight	0.149	2.50	0.330	*	−0.039	−1.54	
	ZUNG, 5	−0.207	−2.63	−0.459	*	−0.333	−3.54	**
	ΔEDE-Q, 4	−0.194	−2.73	−0.429	*	0.014	0.21	
	ΔEDE-Q, 23	−0.156	−2.00	−0.346	*	−0.024	−0.50	
	ΔZUNG, 10	0.160	3.78	0.354	** †	0.105	1.80	
	ΔZUNG, 16	0.266	2.11	0.589	*	0.198	2.29	*
(matrix **Y**)	Stimulation (LLR)	1.000	13.51	0.921	**			
Explained variability				84.7% (65.7% after cross-validation)				

OPLS, orthogonal projection to latent structure; EDE-Q, Eating Disorder Examination Questionnaire; ZUNG, Zung Self-Rating Depression Scale.
EDE-Q, 1 = limitation of the amount of food intake; EDE-Q, 2 = periods without eating; EDE-Q, 3 = exclusion of favorite food; EDE-Q, 4 = the need of excessive control over calorie intake; EDE-Q, 5 = a desire to have an empty stomach; EDE-Q, 8 = overthinking about body shape and weight influences your concentration; EDE-Q, 10 = a fear of gaining weight; EDE-Q, 11 = feeling fat; EDE-Q, 12 = a desire to lose weight; EDE-Q, 18 = compulsive exercising; EDE-Q, 20 = feeling guilty for eating; EDE-Q, 22 = influence of the weight on self-estimation; EDE-Q, 23 = influence of the shape on self-estimation; ZUNG, 5 = food intake as previously; ZUNG, 10 = fatigue; ZUNG, 16 = ability to make decisions.
aR = Component loadings expressed as correlation coefficients with predictive component, $^{*}p < 0.05$, $^{**}p < 0.01$; $^{\dagger}p < 0.05$ after correction using Bonferroni's method; Δ symbolizes post-intervention change (Stage 4 – Stage 1).
Sensitivity (95% CI) = 1.000 (0.758; 1.000); Specificity (95% CI) = 1.000 (0.758; 1.000). Cut-off probability = 0.5.

stimulation can help to distinguish inhibition vs. stimulation of the DLPFC (62).

Moreover, the current strength and current density should be taken into account. The smaller electrode, the lower the strength of the current necessary to achieve a constant value of the current density (61). For more practice guidelines in tDCS procedures, see Friehs et al. (60).

The psychiatric comorbidities are very common in people with eating disorders (>70%) (63). They usually share some similar characteristics; e.g., patients with AN have often obsessive compulsive disorder and MDD symptoms. Future tDCS studies in patients with AN could leverage more personalized protocols according to the predominant symptoms (19). A similar practice was used in electroconvulsive therapy (ECT) for treating AN [e.g., (64, 65)] or in deep brain stimulation studies (66). In the future, also individual placement guided by MRI (67) and a combination of tDCS and cognitive remediation or psychotherapy are another potential options for clinical research in AN. Although research in the identification of responders to repetitive TMS (rTMS) using EEG has yielded results (68), there may be underlying yet unidentified physiological factors that limit the response to tDCS. Research in this area also seems to be essential in order to personalize the treatment.

CONCLUSION

Compared with sham, active treatment was not effective enough to cure complex psychopathology of AN. Our study suggests that tDCS may be beneficial for those with persisting body image disturbances or obsessive-compulsive calorie control, important factors for the remission achievement. More studies are necessary to confirm our results and specify clinical implementation additional to therapy as usual. Further research

TABLE 6 | Summary of side effects.

Total number of patients *n* = 43
Sham *n* = 21
Active tDCS *n* = 22

Side effects	Sham (*n*)	Sham	Active tDCS (*n*)	Active tDCS	p-value Fisher's exact test
Tingling	3	14.3%	3	13.6%	1.000
Itching	1	4.8%	3	13.6%	0.607
Burning sensation	3	14.3%	6	27.3%	0.457
Headache	4	19.0%	4	18.2%	1.000
Fatigue	2	9.5%	2	9.1%	1.000
Stitching	1	4.8%	1	4.5%	1.000
Pressure in the head	0	0.0%	1	4.5%	1.000
Acute mood changes	1	4.8%	2	9.1%	1.000
Pinching	3	14.3%	2	9.1%	0.664
Warm feelings under the electrodes	1	4.8%	0	0.0%	0.488
Metallic taste in the mouth	1	4.8%	0	0.0%	0.488
Phosphenes	2	9.5%	0	0.0%	0.233
Blurred vision	1	4.8%	1	4.5%	1.000
Scalp pain	0	0.0%	1	4.5%	1.000
Hyperglycemia with an onset of diabetes mellitus I	0	0.0%	1	4.5%	1.000
Dizziness	1	4.8%	0	0.0%	0.488
Burning in the eyes	0	0.0%	1	4.5%	1.000
Hand shaking	1	4.8%	0	0.0%	0.488
Neck stiffness	1	4.8%	0	0.0%	0.488
Tinnitus	1	4.8%	0	0.0%	0.488
Twitching of the eye	0	0.0%	1	4.5%	1.000
Remission of headache	1	4.8%	0	0.0%	0.488
Positive mood	2	9.5%	1	4.5%	0.607
Declined night sweating	1	4.8%	0	0.0%	0.488
Remission of toothache	1	4.8%	0	0.0%	0.488

of efficacy of tDCS needs to concentrate on more specific and personalized indications.

DATA AVAILABILITY STATEMENT

The raw data supporting the conclusions of this article will be made available by the authors, without undue reservation.

ETHICS STATEMENT

The studies involving human participants were reviewed and approved by Ethics Committee of the General University Hospital in Prague, No 1955/16 S-IV. The patients/participants provided their written informed consent to participate in this study.

AUTHOR CONTRIBUTIONS

SB, TM, OŠ, and KV: data acquisition. SB, TM, JA, MA, and HP: study design. TN, MH, JB, and SB: data analysis and interpretation. HP, PH, AL, and AY: project supervision. MH: contribution to the manuscript. SB: wrote the manuscript. TN, HP, TM, and JA: commented on the manuscript. All authors contributed to the article and approved the submitted version.

FUNDING

This study was supported by Charles University Project GA UK No. 104121; MH CZ—DRO VFN64165; Q27/LF1; AZV 17-28905; and Progres Q35.

ACKNOWLEDGMENTS

We thank all the patients who were willing to take part in the study. A big thank-you also to the nurses and doctors from the Center for Diagnosis and Treatment of Eating Disorders who enabled us to complete this project.

SUPPLEMENTARY MATERIAL

The Supplementary Material for this article can be found online at: https://www.frontiersin.org/articles/10.3389/fpsyt.2021.717255/full#supplementary-material

REFERENCES

1. Smink FR, van Hoeken D, Hoek HW. Epidemiology of eating disorders: incidence, prevalence and mortality rates. *Curr Psychiatry Rep.* (2012) 14:406–14. doi: 10.1007/s11920-012-0282-y
2. Treasure J, Claudino AM, Zucker N. Eating disorders. *Lancet.* (2010) 375:583–93. doi: 10.1016/S0140-6736(09)61748-7
3. Smink FR, van Hoeken D, Hoek HW. Epidemiology, course, and outcome of eating disorders. *Curr Opin Psychiatry.* (2013) 26:543–8. doi: 10.1097/YCO.0b013e328365a24f
4. World Health Organization. *The ICD-10 Classification of Mental and Behavioural Disorders: Clinical Descriptions and Diagnostic Guidelines*. Geneva (1992). Available online at: http://www.who.int/classifications/icd/en/bluebook.pdf
5. Herpertz-Dahlmann B, Dempfle A, Egberts KM, Kappel V, Konrad K, Vloet JA et al. Outcome of childhood anorexia nervosa-The results of a five- to ten-year follow-up study. *Int J Eat Disord.* (2018) 51:295–304. doi: 10.1002/eat.22840
6. Fichter MM, Quadflieg N, Crosby RD, Koch S. Long-term outcome of anorexia nervosa: results from a large clinical longitudinal study. *Int J Eat Disord.* (2017) 50:1018–30. doi: 10.1002/eat.22736
7. Philip NS, Nelson BG, Frohlich F, Lim KO, Widge AS, Carpenter LL. Low-intensity transcranial current stimulation in psychiatry. *Am J Psychiatry.* (2017) 174:628–39. doi: 10.1176/appi.ajp.2017.16090996
8. Bikson M, Grossman P, Thomas C, Zannou AL, Jiang J, Adnan T et al. Safety of transcranial direct current stimulation: evidence based update 2016. *Brain Stimul.* (2016) 9:641–61. doi: 10.1016/j.brs.2016.06.004
9. Aparício LVM, Guarienti F, Razza LB, Carvalho AF, Fregni F, Brunoni AR. A systematic review on the acceptability and tolerability of transcranial direct current stimulation treatment in neuropsychiatry trials. *Brain Stimul.* (2016) 9:671–81. doi: 10.1016/j.brs.2016.05.004
10. Buchanan DM, Bogdanowicz T, Khanna N, Lockman-Dufour G, Robaey P, D'Angiulli A. Systematic review on the safety and tolerability of transcranial direct current stimulation in children and adolescents. *Brain Sci.* (2021) 11:212. doi: 10.3390/brainsci11020212
11. Stagg CJ, Nitsche MA. Physiological basis of transcranial direct current stimulation. *Neuroscientist.* (2011) 17:37–53. doi: 10.1177/1073858410386614
12. Ciechanski P, Kirton A. Transcranial Direct-Current Stimulation (tDCS): principles and emerging applications in children. In: Kirton A, Gilbert DL, editors *Pediatric Brain Stimulation.* London; San Diego, CA; Oxford; Cambridge: Academic Press (2016). p. 85–115.
13. Impey D, de la Salle S, Knott V. Assessment of anodal and cathodal transcranial direct current stimulation (tDCS) on MMN-indexed auditory sensory processing. *Brain Cogn.* (2016) 105:46–54. doi: 10.1016/j.bandc.2016.03.006
14. Lozano AM, Hallett M. *Brain Stimulation*. Amsterdam: Newnes (2013). p. 456.
15. Lefaucheur JP, Antal A, Ayache SS, Benninger DH, Brunelin J, Cogiamanian F et al. Evidence-based guidelines on the therapeutic use of transcranial direct current stimulation (tDCS). *Clin Neurophysiol.* (2017) 128:56–92. doi: 10.1016/j.clinph.2016.10.087
16. Kaye WH, Fudge JL, Paulus M. New insights into symptoms and neurocircuit function of anorexia nervosa. *Nat Rev Neurosci.* (2009) 10:573–84. doi: 10.1038/nrn2682
17. Silvers JA, Weber J, Wager TD, Ochsner KN. Bad and worse: neural systems underlying reappraisal of high-and low-intensity negative emotions. *Soc Cogn Affect Neurosci.* (2014) 10:172–9. doi: 10.1093/scan/nsu043
18. Ehrlich S, Geisler D, Ritschel F et al. Elevated cognitive control over reward processing in recovered female patients with anorexia nervosa. *J Psychiatry Neurosci.* (2015) 40:307. doi: 10.1503/jpn.140249
19. Duriez P, Bou Khalil R, Chamoun Y, Maatoug R, Strumila R, Seneque M, et al. Brain stimulation in eating disorders: state of the art and future perspectives. *J Clin Med.* (2020) 9:2358. doi: 10.3390/jcm9082358
20. Knyahnytska YO, Blumberger DM, Daskalakis ZJ, Zomorrodi R, Kaplan AS. Insula H-coil deep transcranial magnetic stimulation in severe and enduring anorexia nervosa (SE-AN): a pilot study. *Neuropsychiatr Dis Treat.* (2019) 15:2247–56. doi: 10.2147/NDT.S207630
21. Woodside DB, Colton P, Lam E, Dunlop K, Rzeszutek J, Downar J. Dorsomedial prefrontal cortex repetitive transcranial magnetic stimulation treatment of posttraumatic stress disorder in eating disorders: an open-label case series. *Int J Eat Disord.* (2017) 50:1231–4. doi: 10.1002/eat.22764
22. Kane MJ, Engle RW. The role of prefrontal cortex in working-memory capacity, executive attention, and general fluid intelligence: an individual-differences perspective. *Psychon Bull Rev.* (2002) 9:637–71. doi: 10.3758/BF03196323
23. Ghanavati E, Salehinejad MA, Nejati V, Nitsche MA. Differential role of prefrontal, temporal and parietal cortices in verbal and figural fluency: implications for the supramodal contribution of executive functions. *Sci Rep.* (2019) 9:3700. doi: 10.1038/s41598-019-40273-7
24. Nejati V, Majdi R, Salehinejad MA, Nitsche MA. The role of dorsolateral and ventromedial prefrontal cortex in the processing of emotional dimensions. *Sci Rep.* (2021) 11:1971. doi: 10.1038/s41598-021-81454-7
25. Molavi P, Aziziaram S, Basharpoor S, Atadokht A, Nitsche MA, Salehinejad MA. Repeated transcranial direct current stimulation of dorsolateral-prefrontal cortex improves executive functions, cognitive reappraisal emotion regulation, and control over emotional processing in borderline personality disorder: a randomized, sham-controlled, parallel-group study. *J Affect Disord.* (2020) 274:93–102. doi: 10.1016/j.jad.2020.05.007
26. Ridderinkhof KR, van den Wildenberg WP, Segalowitz SJ, Carter CS. Neurocognitive mechanisms of cognitive control: the role of prefrontal cortex in action selection, response inhibition, performance monitoring, and reward-based learning. *Brain Cogn.* (2004) 56:129–40. doi: 10.1016/j.bandc.2004.09.016
27. Miller EK, Cohen JD. An integrative theory of prefrontal cortex function. *Annu Rev Neurosci.* (2001) 24:167–202. doi: 10.1146/annurev.neuro.24.1.167
28. Hecht D. Transcranial direct current stimulation in the treatment of anorexia. *Med Hypotheses.* (2010) 74:1044–7. doi: 10.1016/j.mehy.2009.12.032
29. Khedr EM, Elfetoh NA, Ali AM, Noamany M. Anodal transcranial direct current stimulation over the dorsolateral prefrontal cortex improves anorexia nervosa: a pilot study. *Restor Neurol Neurosci.* (2014) 32:789–97. doi: 10.3233/RNN-140392
30. Costanzo F, Menghini D, Maritato A, Castiglioni MC, Mereu A, Varuzza C et al. New Treatment perspectives in adolescents with anorexia nervosa: the efficacy of non-invasive brain-directed treatment. *Front Behav Neurosci.* (2018) 12:133. doi: 10.3389/fnbeh.2018.00133
31. Strumila R, Thiebaut S, Jaussent I, Seneque M, Attal J, Courtet P et al. Safety and efficacy of transcranial direct current stimulation (tDCS) in the treatment of Anorexia Nervosa. The open-label STAR study. *Brain Stimul.* (2019) 12:1325–7. doi: 10.1016/j.brs.2019.06.017
32. Mares T, Ceresnakova S, Albrecht J, Buday J, Klasova J, Horackova K et al. The onset of diabetes during transcranial direct current stimulation treatment of anorexia nervosa - a case report. *Front Psychiatry.* (2020) 11:40. doi: 10.3389/fpsyt.2020.00040
33. Berg KC, Peterson CB, Frazier P, Crow SJ. Psychometric evaluation of the eating disorder examination and eating disorder examination-questionnaire: a systematic review of the literature. *Int J Eat Disord.* (2012) 45:428–38. doi: 10.1002/eat.20931
34. Gabrys JB, Peters K. Reliability, discriminant and predictive validity of the Zung Self-rating Depression Scale. *Psychol Rep.* (1985) 57(Pt 2):1091–6. doi: 10.2466/pr0.1985.57.3f.1091
35. de Jonghe JF, Baneke JJ. The Zung Self-rating depression scale: a replication study on reliability, validity and prediction. *Psychol Rep.* (1989) 64:833–34. doi: 10.2466/pr0.1989.64.3.833
36. Thielscher A, Antunes A, Saturnino GB. Field modeling for transcranial magnetic stimulation: a useful tool to understand the physiological effects of TMS? *Annu Int Conf IEEE Eng Med Biol Soc.* (2015) 2015:222–5. doi: 10.1109/EMBC.2015.7318340
37. Hill M, Bicíková M, Parízek A, Havlíková H, Klak J, Fajt T et al. Neuroactive steroids, their precursors and polar conjugates during parturition and postpartum in maternal blood: 2. Time profiles of pregnanolone isomers. *J Steroid Biochem Mol Biol.* (2001) 78:51–7. doi: 10.1016/S0960-0760(01)00073-5
38. Meloun M, Militký J. *Statistická Analýza Experimentálních Dat*. Prague: Academia (2004).
39. Meloun M, Militký J, Hill M, Brereton RG. Crucial problems in regression modelling and their solutions. *Analyst.* (2002) 127:433–50. doi: 10.1039/b110779h

40. Meloun M, Hill M, Militký J, Vrbíková J, Stanická S, Skrha J. New methodology of influential point detection in regression model building for the prediction of metabolic clearance rate of glucose. *Clin Chem Lab Med.* (2004) 42:311–22. doi: 10.1515/CCLM.2004.057
41. Trygg J, Holmes E, Lundstedt T. Chemometrics in metabonomics. *J Proteome Res.* (2007) 6:469–79. doi: 10.1021/pr060594q
42. Trygg J, Wold S. Orthogonal projections to latent structures (O-PLS). *J Chemometr J Chemometr Soc.* (2002) 16:119–28. doi: 10.1002/cem.695
43. Madsen R, Lundstedt T, Trygg J. Chemometrics in metabolomics–a review in human disease diagnosis. *Anal Chim Acta.* (2010) 659:23–33. doi: 10.1016/j.aca.2009.11.042
44. Czech C, Berndt P, Busch K, Schmitz O, Wiemer J, Most V, et al. Metabolite profiling of Alzheimer's disease cerebrospinal fluid. *PLoS One.* (2012) 7:e31501. doi: 10.1371/journal.pone.0031501
45. Eryilmaz G, Sayar GH, Ünsalver BÖ, Gül IG, ÖztenE, & Saglam E. Adverse effects of Transcranial Direct Current Stimulation (TDCS) in a group of psychiatric patients. *Scholars J Appl Med Sci.* (2014) 2:294–7. Available online at: https://www.researchgate.net/profile/Gokben-HizliSayar/publication/260554152_Adverse_Effects_of_Transcranial_Direct_Current_Stimulation_TDCS_in_a_Group_of_Psychiatric_Patients/links/00b7d5318e1660f599000000/Adverse-Effects-ofTranscranial-Direct-Current-Stimulation-TDCS-in-a-Group-of-Psychiatric-Patients.pdf
46. Kessler SK, Turkeltaub PE, Benson JG, Hamilton RH. Differences in the experience of active and sham transcranial direct current stimulation. *Brain Stimul.* (2012) 5:155–62. doi: 10.1016/j.brs.2011.02.007
47. Jog MV, Wang DJJ, Narr KL. A review of transcranial direct current stimulation (tDCS) for the individualized treatment of depressive symptoms. *Pers Med Psychiatry.* (2019) 17–18:17–22. doi: 10.1016/j.pmip.2019.03.001
48. Dejong H, Broadbent H, Schmidt U. A systematic review of dropout from treatment in outpatients with anorexia nervosa. *Int J Eat Disord.* (2012) 45:635–47. doi: 10.1002/eat.20956
49. Charvet LE, Shaw MT, Bikson M, Woods AJ, Knotkova H. Supervised transcranial direct current stimulation (tDCS) at home: a guide for clinical research and practice. *Brain Stimul.* (2020) 13:686–93. doi: 10.1016/j.brs.2020.02.011
50. Boggio PS, Nunes A, Rigonatti SP, Nitsche MA, Pascual-Leone A, Fregni F. Repeated sessions of noninvasive brain DC stimulation is associated with motor function improvement in stroke patients. *Restor Neurol Neurosci.* (2007) 25:123–9. Available online at: https://www.researchgate.net/publication/6114610_Repeated_sessions_of_noninvasive_brain_DC_stimulation_is_associated_with_motor_function_improvement_in_stoke_patients
51. Im JJ, Jeong H, Bikson M, Woods AJ, Unal G, Oh JK, et al. Effects of 6-month at-home transcranial direct current stimulation on cognition and cerebral glucose metabolism in Alzheimer's disease. *Brain Stimul.* (2019) 12:1222–8. doi: 10.1016/j.brs.2019.06.003
52. Clayton AM, Howard J, Dobbs B, Shaw MT, Charvet LE. Remotely supervised transcranial direct current stimulation after ECT improves mood and cognition in a patient with multiple sclerosis: a case study. *J ECT.* (2018) 34:e15. doi: 10.1097/YCT.0000000000000474
53. Pilloni G, Shaw M, Feinberg C, Clayton A, Palmeri M, Datta A et al. Long term at-home treatment with transcranial direct current stimulation (tDCS) improves symptoms of cerebellar ataxia: a case report. *J Neuroeng Rehabil.* (2019) 16:41. doi: 10.1186/s12984-019-0514-z
54. Andrade C. Once- to twice-daily, 3-year domiciliary maintenance transcranial direct current stimulation for severe, disabling, clozapine-refractory continuous auditory hallucinations in schizophrenia. *J ECT.* (2013) 29:239–42. doi: 10.1097/YCT.0b013e3182843866
55. Phillipou A, Rossell SL, Castle DJ. The neurobiology of anorexia nervosa: a systematic review. *Aust N Z J Psychiatry.* (2014) 48:128–52. doi: 10.1177/0004867413509693
56. Phillipou A, Rossell SL, Castle DJ, Gurvich C, Abel LA. Square wave jerks and anxiety as distinctive biomarkers for anorexia nervosa. *Invest Ophthalmol Vis Sci.* (2014) 55:8366–70. doi: 10.1167/iovs.14-15807
57. Phillipou A, Kirkovski M, Castle DJ, Gurvich C, Abel LA, Miles S, et al. High-definition transcranial direct current stimulation in anorexia nervosa: a pilot study. *Int J Eat Disord.* (2019) 52:1274–80. doi: 10.1002/eat.23146
58. Depue BE, Orr JM, Smolker HR, Naaz F, Banich MT. The organization of right prefrontal networks reveals common mechanisms of inhibitory regulation across cognitive, emotional, and motor processes. *Cereb Cortex.* (2016) 26:1634–46. doi: 10.1093/cercor/bhu324
59. Swann NC, Tandon N, Pieters TA, Aron AR. Intracranial electroencephalography reveals different temporal profiles for dorsal- and ventro-lateral prefrontal cortex in preparing to stop action. *Cereb Cortex.* (2013) 23:2479–88. doi: 10.1093/cercor/bhs245
60. Friehs MA, Frings C, Hartwigsen G. Effects of single-session transcranial direct current stimulation on reactive response inhibition. *Neurosci Biobehav Rev.* (2021) 128:749–65. doi: 10.1016/j.neubiorev.2021.07.013
61. Faria P, Hallett M, Miranda PC. A finite element analysis of the effect of electrode area and inter-electrode distance on the spatial distribution of the current density in tDCS. *J Neural Eng.* (2011) 8:066017. doi: 10.1088/1741-2560/8/6/066017
62. Frings C, Brinkmann T, Friehs MA, van Lipzig T. Single session tDCS over the left DLPFC disrupts interference processing. *Brain Cogn.* (2018) 120:1–7. doi: 10.1016/j.bandc.2017.11.005
63. Treasure J, Duarte TA, Schmidt U. Eating disorders. *Lancet.* (2020) 395:899–911. doi: 10.1016/S0140-6736(20)30059-3
64. Poutanen O, Huuhka K, Perko K. Severe anorexia nervosa, co-occurring major depressive disorder and electroconvulsive therapy as maintenance treatment: a case report. *Cases J.* (2009) 2:9362. doi: 10.1186/1757-1626-2-9362
65. Saglam T, Aksoy Poyraz C, Poyraz BÇ, Tosun M. Successful use of electroconvulsive therapy in a patient with anorexia nervosa and severe acute-onset obsessive-compulsive disorder. *Int J Eat Disord.* (2018) 51:1026–8. doi: 10.1002/eat.22923
66. Villalba Martínez G, Justicia A, Salgado P, Ginés JM, Guardiola R, Cedrón C, et al. A randomized trial of deep brain stimulation to the subcallosal cingulate and nucleus accumbens in patients with treatment-refractory, chronic, and severe anorexia nervosa: initial results at 6 months of follow up. *J Clin Med.* (2020) 9:1946. doi: 10.3390/jcm9061946
67. Cancelli A, Cottone C, Giordani A, Asta G, Lupoi D, Pizzella V et al. MRI-guided regional personalized electrical stimulation in multisession and home treatments. *Front Neurosci.* (2018) 12:284. doi: 10.3389/fnins.2018.00284
68. Hasanzadeh F, Mohebbi M, Rostami R. Prediction of rTMS treatment response in major depressive disorder using machine learning techniques and nonlinear features of EEG signal. *J Affect Disord.* (2019) 256:132–42. doi: 10.1016/j.jad.2019.05.070

Conflict of Interest: The authors declare that the research was conducted in the absence of any commercial or financial relationships that could be construed as a potential conflict of interest.

Publisher's Note: All claims expressed in this article are solely those of the authors and do not necessarily represent those of their affiliated organizations, or those of the publisher, the editors and the reviewers. Any product that may be evaluated in this article, or claim that may be made by its manufacturer, is not guaranteed or endorsed by the publisher.

frontiers in Psychiatry

ORIGINAL RESEARCH
published: 18 October 2021
doi: 10.3389/fpsyt.2021.739356

Twelve-Week Yoga vs. Aerobic Cycling Initiation in Sedentary Healthy Subjects: A Behavioral and Multiparametric Interventional PET/MR Study

June van Aalst[1], *Lise Jennen*[1], *Koen Demyttenaere*[2,3], *Stefan Sunaert*[4,5], *Michel Koole*[1], *Jenny Ceccarini*[1] *and Koen Van Laere*[1,6]*

[1] Nuclear Medicine and Molecular Imaging, Department of Imaging and Pathology, KU Leuven, Leuven, Belgium, [2] Research Group Psychiatry, Neurosciences, University Psychiatric Center KU Leuven, Leuven, Belgium, [3] Adult Psychiatry, University Hospitals Leuven, Leuven, Belgium, [4] Translational MRI, Department of Imaging and Pathology, KU Leuven, Leuven, Belgium, [5] Radiology, University Hospitals Leuven, Leuven, Belgium, [6] Division of Nuclear Medicine, University Hospitals Leuven, Leuven, Belgium

OPEN ACCESS

Edited by:
Anne M. Landau, Aarhus University, Denmark

Reviewed by:
Caroline Cristiano Real, Aarhus University, Denmark
Kiyotaka Nemoto, University of Tsukuba, Japan
David Matuskey, Yale University, United States

***Correspondence:**
Koen Van Laere
koen.vanlaere@uzleuven.be

Specialty section:
This article was submitted to Neuroimaging and Stimulation, a section of the journal Frontiers in Psychiatry

Received: *10 July 2021*
Accepted: *16 September 2021*
Published: *18 October 2021*

Citation:
van Aalst J, Jennen L, Demyttenaere K, Sunaert S, Koole M, Ceccarini J and Van Laere K (2021) Twelve-Week Yoga vs. Aerobic Cycling Initiation in Sedentary Healthy Subjects: A Behavioral and Multiparametric Interventional PET/MR Study. Front. Psychiatry 12:739356. doi: 10.3389/fpsyt.2021.739356

Interventional yoga studies with an active control group remain scarce and are important to clarify the underlying neurobiology. We conducted an interventional study in healthy controls using simultaneous positron emission tomography/magnetic resonance (PET/MR) imaging and psychometric scales. Thirty healthy, female volunteers (28.4 ± 8.4 years) participated and were randomly assigned to a 12-week yoga or indoor cycling intervention. Before and after the intervention, [^{18}F]FDG and [^{11}C]UCB-J PET was performed on a simultaneous GE Signa PET/MR with volumetric imaging. Psychometric scales were evaluated on affect, mindfulness, stress, worrying, self-compassion, and interoceptive awareness. Yoga subjects scored higher on interoceptive awareness compared to baseline ($p < 0.001$). Cognitive ($P = 0.009$) and overall cognitive functioning ($P = 0.01$) improved after the yoga intervention compared to the cycling group. We did not observe significant differences in glucose metabolism, synaptic density, or gray matter (GM) volume. The indoor cycling group did not show changes in psychometric variables, but significant increases in relative glucose metabolism were observed in the parahippocampal/fusiform gyrus and cerebellum ($P < 0.001$). In conclusion, 12 weeks of yoga practice has significant effects on interoceptive awareness and perceived cognitive function in starters. Longer interventions and/or higher frequency of yoga practice may be needed to detect cerebral metabolic and/or morphologic effects on the macroscopic level.

Keywords: yoga, longitudinal interventional study, PET/MR imaging, FDG, synaptic density, indoor cycling

INTRODUCTION

Yoga combines meditation (*dhyana*), physical postures (*asana*), and focused breathing (*pranayama*). It has become increasingly popular in the Western world as an approach to improve health and well-being (1) and has received more and more interest from a research perspective. Behavioral studies have shown that yoga can be an effective multi-component health intervention

to reduce stress, increase physical fitness, and improve general well-being and quality of life (2, 3). Psychological dimensions improved by yoga include self and body awareness, coping capacity, stress, mindfulness, and self-compassion (2, 3). Besides behavioral studies, a limited number of imaging studies have investigated the effects of yoga on objective biomarkers in the brain. Different advanced neuroimaging techniques such as positron emission tomography (PET) and magnetic resonance (MR) imaging allow to investigate the biochemical, functional, and structural effects of yoga in a non-invasive way (4). However, since most studies so far have focused specifically on the meditational dimension of yoga, evidence for the combined tripartite effects is scarce. Based on imaging and physiological data, a leading hypothesis of an underlying neurobiological mechanism of yoga is that breathing exercises, meditation, and baroreflex-promoting poses induce a shift in the parasympathetic nervous system through activation of gamma aminobutyric acid (GABA) release through the vagal nerve (5, 6).

In cross-sectional studies, structural effects on gray matter (GM) volume have been described by MR imaging, with increased GM volume in the insular cortex and hippocampus as most consistently reported findings in (experienced) yoga practitioners (7, 8). It has been postulated that changes in GM volume might be the result of neuroplasticity (9). Few functional or molecular PET studies have been conducted in yoga practitioners. [^{18}F]Fluorodeoxyglucose (FDG) PET imaging enables measurement of regional neuronal activity. In a recent [^{18}F]FDG PET study in experienced yoga practitioners, we found a significant decrease in the limbic system compared to physically active but yoga-naive subjects (10). Such downregulation in metabolic activity could be due to GABA-mediated inhibition, development of more efficient brain metabolism, or a pre-existing phenotype in yoga practitioners. Therefore, a longitudinal study is warranted to clarify possible underlying mechanisms. Glucose metabolism is majorly determined by glutamate neurotransmission and neuron-astrocyte interactions (11). Furthermore, recently imaging of synaptic density has become available by means of PET radiotracers such as [^{11}C]UCB-J. This ligand binds to the presynaptic vesicle protein 2A (SV2A) with high affinity and specificity, and is altered in several neuropsychiatric conditions (12–16). For the first time, this opens the possibility to investigate whether an intervention can induce neuroplasticity by axon sprouting and neurogenesis (9). Combined measurement of synaptic activity and synaptic density could therefore offer complimentary measures of brain function (17).

As the choice of an appropriate control group is critical to disentangle the impact of yoga practice on brain function without confounding factors (4, 18), we have chosen to use moderate-intensity indoor cycling as control intervention. Both interventions are practiced in group, can be guided by a skilled teacher, are of similar duration per exercise unit and can be metabolically matched. Also aerobic exercise induces beneficial psychological effects, such as increased self-esteem, self-satisfaction, confidence, and improved turmoil (19).

The aim of this study was to compare a 12-week yoga intervention vs. aerobic moderate intensity exercise with neuropsychological endpoints as well as longitudinal positron emission tomography/magnetic resonance (PET/MR) imaging of glucose metabolism, synaptic density and structural imaging. This was performed in yoga-naïve sedentary individuals to exclude effects of previous training.

MATERIALS AND METHODS

Subjects

In total, 30 right-handed healthy sedentary female volunteers [$n = 30$; age: 28.4 ± 8.4 (SD) years] participated in the study. Subjects were in good health according to their medical history, physical examination, general laboratory test (blood and urine) screening, and general neuropsychological evaluation [Symptoms Checklist (SCL90), Beck's depression inventory (BDI) (20), and mini-mental state examination (MMSE)]. The main exclusion criteria consisted of a history of major internal disease, previous severe head trauma, a psychiatric disorder, and use of centrally acting drugs. All subjects were required to have a sedentary lifestyle, defined as doing <1 h of exercise a week the year prior to study participation. The study was approved by the local University Ethics committee (study number S59792—Belgian Registration Number B32220173162) and was conducted in full accordance with the latest version of the Declaration of Helsinki. All participants provided written informed consent before inclusion in the study.

Study Design

The study design is reported in **Supplementary Figure 1**. All subjects underwent up to two PET/MR scans ([^{18}F]FDG in all and [^{11}C]UCB-J for most participants) at baseline and after 12 weeks of intervention. After the baseline scan, subjects were randomly assigned to either the yoga intervention group ($n = 15$) or an indoor cycling intervention group ($n = 15$) (physical blinded number picking by the subjects). The yoga group was planned to attend yoga classes for 12 weeks, twice a week with 60-min sessions. In addition, their regular exercise regimen (<1 h/per week) was allowed. All yoga sessions took place in the same studio in Leuven (Flowing Yoga, Mrs. K. Marent). Different yoga styles for beginners were allowed to the participant's choice, including easy flow, *prana vinyasa* easy flow, *ashtanga* basics, and *Yin* and *Yang* yoga. These yoga styles all included approximately the same time ratio of physical postures (±70%), breathing exercises (±25%, in between the different postures) and guided meditation (±5%).

Participants assigned to the cycling group had to attend 60 min of indoor cycling classes for 12 weeks, also twice a week (with regular exercise routine (<1 h of exercise/per week) allowed). At their first training, cycling group subjects had to perform an individual power level test, to determine their individual threshold power defined as 90% of their peak power. The cycling subjects then received the instruction to keep the mean power below 80% of their individually determined threshold during the cycling classes, in order to stay within aerobic conditions and to match the physical intensity level with the yoga intervention.

Both yoga and cycling sessions were registered by the yoga studio and sport center, respectively. Moreover, participants had

to keep a diary to track their lessons. For both groups a minimum of 20 lessons was required to complete the study.

Psychometric Evaluation

All participants completed a battery of psychometric questionnaires at baseline and post intervention. In line with the previously observed psychological effects of yoga (3), the following dimensions were sampled: affect (21), mindfulness (22–24), stress (2, 22), worrying (22), self-compassion (23), and interoceptive awareness (25). The specific scales sampled in this study included:

- *Multi-assessment interoceptive awareness* (MAIA) scale. The MAIA questionnaire measures interoceptive awareness, defined as the awareness of signals from the inside of the body and higher-order top down processes. In total eight subdimensions are measured: noticing, not-distracting, not-worrying, attention regulation, emotional awareness, self-regulation, body listening, and trust (26).
- *Leuven Affect and Pleasure Scale* (LAPS) (27). This scale offers a comprehensive assessment of negative and positive affect, hedonic tone, and independent variables on cognitive and overall functioning, evaluation of a meaningful live, and happiness.
- *Five-Facet Mindfulness Questionnaire* (FFMQ) (28). Mindfulness is defined as "paying attention in a particular way: on purpose, in the present moment, and non-judgmentally." This questionnaire includes five factors that represent elements of mindfulness, including observing, describing, acting with awareness, non-judging of inner experience, and non-reactivity to inner experience.
- *Perceived Stress Scale* (PSS) (29). This psychological instrument is used to measure perception of stress.
- *Penn State Worry Questionnaire* (PSWQ) (30) to measure the trait of worry.
- *Self-Compassion Scale* (SCS) (31). Self-compassion is described as "being open to and moved by one's own suffering, experiencing feelings of caring and kindness toward oneself, taking an understanding, non-judgmental attitude toward one's inadequacies and failures, and recognizing that one's own experience is part of the common human experience." This scale is a psychometrical measure of self-compassion and includes six subscales: self-kindness, self-judgment, common humanity, isolation, mindfulness, and over-identification.

Image Acquisition

All PET and MR data were acquired on a simultaneous Signa time-of-flight (TOF) PET/MR scanner with fast Silicon photomultiplier detectors inside a 3T MR magnet (GE Healthcare, Chicago, IL, USA). Subjects fasted at least 3 h prior to [^{18}F]FDG injection. Subjects received an intravenous bolus injection of [^{18}F]FDG (at baseline: 118 ± 12 MBq and post-intervention: 119 ± 9 MBq) in supine position with a 20-min accumulation period in a quiet and dimly lit environment. During the accumulation period, subjects were asked to close their eyes but remain awake. Subsequently, a static 30-min [^{18}F]FDG PET/MR scan was acquired. [^{18}F]FDG (Glucogast^{TM}, UZ Leuven, Belgium) was produced in-house according to an approved manufacturing authorization, with a radiochemical purity >95%. After the [^{18}F]FDG PET acquisition, a single venous blood sample was collected to measure blood glucose concentration and the remaining [^{18}F]FDG radioactivity to calculate a simplified measure of absolute glucose consumption (Hunter method) as validated previously against absolute arterial spin labeling (10, 32).

Additionally, a subset of participants (n = 20; 10 in each group) received an additional SV2A PET scan using [^{11}C]UCB-J. This subset was chosen randomly, and only based on the logistics (availability) of the [^{11}C]UCB-J tracer production. The precursor was obtained from UCB and labeled on site under GMP standards with a radiochemical purity >95%, as described previously (33). Subjects received a bolus injection of 270 ± 60 MBq (specific activity 239 ± 133 GBq/μmol) and of 262 ± 61 MBq (specific activity 187 ± 73 GBq/μmol) at baseline and post-intervention, respectively. This bolus was administered at least 100 min prior to the [^{18}F]FDG injection (with 20 min physical half-life the [^{11}C]UCB-J activity was mostly decayed before [^{18}F]FDG PET). Sixty minutes post-injection, a 30-min static [^{11}C]UCB-J scan was acquired to be quantified using a reference tissue approach (33).

PET data were rebinned in six frames of 5 min, corrected for dead time, randoms, scatter, and time-offset (34). An MR-based attenuation correction (MRAC), based on zero-echo time (ZTE) MR images (3D radial acquisition; Flip Angle: 0.8°; Bandwidth: 62.5 kHz), was used for attenuation correction (35). Positron emission tomography images were reconstructed using OSEM (ordered subset expectation maximization; 28 subsets; 4 iterations) algorithm, including time of flight (TOF) information, resolution modeling, and an in-plane Gaussian post-smoothing with a FWHM (full width at half maximum) of 4.5 mm.

Simultaneous with the PET data acquisition, the following MR sequences were acquired [using an eight-channel high-resolution receiver head coil (GE Healthcare)]: 3D volumetric T1-weighted BRAVO (plane: sagittal; TE: 3.2 ms; TR: 8.5 ms; TI: 450 ms; flip angle: 12°; receiver bandwidth: 31.25 kHz; voxel size: 1 × 1 × 1 mm) and fluid-attenuated inversion recovery (FLAIR) 3D CUBE (TR: 8,500 ms, TE 130 ms, voxel size: 1 × 1 × 1.4 mm).

Image Data Analysis

Both [^{18}F]FDG and [^{11}C]UCB-J PET data were analyzed on a voxelwise basis, using SPM12 (Statistical Parametric Mapping, Wellcome Department of Imaging Neuroscience, London, UK), and using a predefined volume-of-interest (VOI) approach (PMOD software v3.9, PMOD Inc., Zurich, Switzerland).

Reconstructed PET data were corrected for motion. Parametric standardized uptake value ratio (SUVR) images for [^{11}C]UCB-J were generated, using the centrum semiovale (CS) as validated reference region in healthy volunteers (33, 36). For [^{18}F]FDG PET regional cerebral metabolic rate of glucose (rCMRGlc) (mmol/l/min) maps, first blood glucose concentration was measured at the end of the scan and a venous blood sample was centrifuged for 5 min (4,000 rpm, 4°C) to measure the remaining tracer concentration in plasma (gamma counter; Perkin Elmer, 1480 WIZARD). A lumped

constant of 0.65 was applied for all regions to calculate rCMRGlc values (32, 37). For two subjects (both in the yoga group at post-intervention), these maps could not be generated due to technical errors in plasma analysis and blood sample withdrawal, respectively. These two subjects were therefore excluded from the rCMRGLc data analysis.

All post-intervention [^{18}F]FDG and [^{11}C]UCB-J parametric PET maps were first co-registered to their respective baseline images. Subsequently, all PET images were co-registered to the subject's own T1-weighted MR image and spatially normalized to the Montreal Neurological Institute (MNI) space using a non-linear normalization with a DARTEL algorithm (SPM12). To reduce noise at the voxel level and account for gyral variations, PET images were additionally smoothed using a Gaussian FWHM of 8 mm. To exclude extracerebral activity, a relative threshold of 80% of the mean and an implicit CSF and GM mask was used.

Voxel-based findings were corroborated with a predefined VOI analysis using the N30R83 Hammers probabilistic atlas and AAL-merged in PMOD (38, 39), as the AAL-atlas allows for a more detailed delineation of the entire brainstem (VOIs for the medulla, pons, and midbrain). To reduce dimensionality and avoid type II errors, the standard 83 VOIs were merged into 12 larger, bilateral VOIs: FCx, frontal cortex; ACCx, anterior cingulate cortex; PCCx, posterior cingulate cortex; LTL, lateral temporal lobe; MTL, medial temporal lobe; PCx, parietal cortex; OCx, occipital cortex; Str, striatum; Thal, thalamus; ICx, insular cortex; Cbl, cerebellum; Bs, brainstem.

For the voxel-based morphometry (VBM) analysis, the Computational Anatomy Toolbox (CAT12) (40) implemented in SPM12 was used. All individual T1-weighted MR images were segmented into GM, white matter (WM), and cerebrospinal fluid (CSF), spatially normalized using the DARTEL algorithm and modulated with the Jacobian warp parameters. After pre-processing, GM images were smoothed with a Gaussian kernel of 8 mm. An absolute threshold masking of 0.1 to avoid edge effects around borders between GM, WM, and CSF was used.

Statistical Analyses

Statistical analyses were conducted using Prism (v5, GraphPad, San Diego, USA) or SPSS (v26, IBM, Corporation, Chicago, Illinois). *P*-values were considered significant at an alpha level of 0.05. For the psychometric questionnaires, data were analyzed in a repeated ANOVA design (interaction effect group × time), followed by *post-hoc* between-group unpaired *t*-tests (yoga vs. indoor cycling, at baseline and post-intervention) and within-group paired *t*-tests (baseline vs. post-intervention, in the yoga and indoor cycling group). In SPM, both PET targets and the T1-weighted images (VBM) were explored in a flexible factorial design to investigate interaction effects and in a 2 × 2 design; *post-hoc* between-group unpaired *t*-tests (yoga vs. indoor cycling, at baseline and post-intervention) and within-group paired *t*-tests (baseline vs. post-intervention, in the yoga and indoor cycling group). Both absolute (parametric rCMRGlc images and SUVR [^{11}C]UCB-J images) and relative ([^{18}F]FDG uptake and [^{11}C]UCB-J, normalized to global [^{18}F]FDG uptake and global [^{11}C]UCB-J binding in GM, respectively) were analyzed. SPM data were analyzed at a voxel-level $P_{\text{height}} < 0.001$, cluster extent threshold $k_E = 237$ voxels (corresponding to a size of 0.8 cm^3; applied voxel size = 1.5 × 1.5 × 1.5 mm), and cluster-level $P_{\text{FWE}} < 0.05$. Total intracranial volume was used as covariate for the VBM SPM group analysis. Correlations between significant effects on brain regions and the psychometric scores were explored.

TABLE 1 | Subject demographics and study-related variables.

	Yoga group (*n* = 15)	Cycling group (*n* = 15)	*P*-value
Age	31.8 ± 9.8	24.9 ± 5.1	0.02
Sex (F/M)	15/0	15/0	
Activity level (hrs/wk)	0.5 ± 0.4	0.6 ± 0.5	0.98
Pre-PET scan sober glycaemia (mg/dl)	86.5 ± 6.1	85.5 ± 6.1	0.68
BMI (kg/m^2)	23.4 ± 2.3	22.5 ± 2.4	0.30
Educational level			0.66
High school	2 (13.3%)	4 (26.7%)	
Bachelor degree	8 (53.3%)	7 (46.7%)	
Master degree	5 (13.3%)	4 (26.7%)	
BDI	3 (0–8)	1 (0–8)	0.32
MMSE	30 (29,30)	29 (29,30)	0.07
Nr of attended classes (out of max 24)	21.1 ± 1.2	21.4 ± 1.4	0.49

BDI, beck depression inventory; BMI, body mass index; F, female; M, male; MMSE, mini-mental state examination. Data are presented as mean ± standard deviation for continuous variables, median (min-max) for integer variables and frequency (%).

RESULTS

Subject Characteristics

In total 33 subjects were initially included and scanned at baseline. Two subjects withdrew and one was excluded after the baseline scan due to significant WM lesions due to a delivery trauma at birth. After randomization (paper picking of numbers 1 or 2 by the subjects), a small but significant age difference [31.8 ± 9.8 years (yoga, range 22–51 years) vs. 24.9 ± 5.1 years (cycling, range 19–38 years), $P = 0.02$] was present between both groups. This difference was neglected as for FDG PET, SV2A PET density and structural MR imaging no significant age effect between 20 and 50 years is known (41–45). Also, although both female and male subjects were eligible in the study, only female subjects were included (**Table 1**). In the yoga group, the average number of lessons attended was 21.1 ± 1.2 (range 20–24); similar to the cycling group: 21.4 ± 1.4 (range 20–24), $P = 0.49$.

Psychometric Scales

For the psychometric scales, no significant interaction effect (group × timing) was found. However, a significant increase after yoga intervention was observed in the MAIA interoceptive awareness total score compared to baseline (26.2 ± 5.2 vs. 23.9 ± 4.7, $P = 0.001$ (uncorrected), remaining significant after Bonferroni correction for the number of scales) (**Figure 1**;

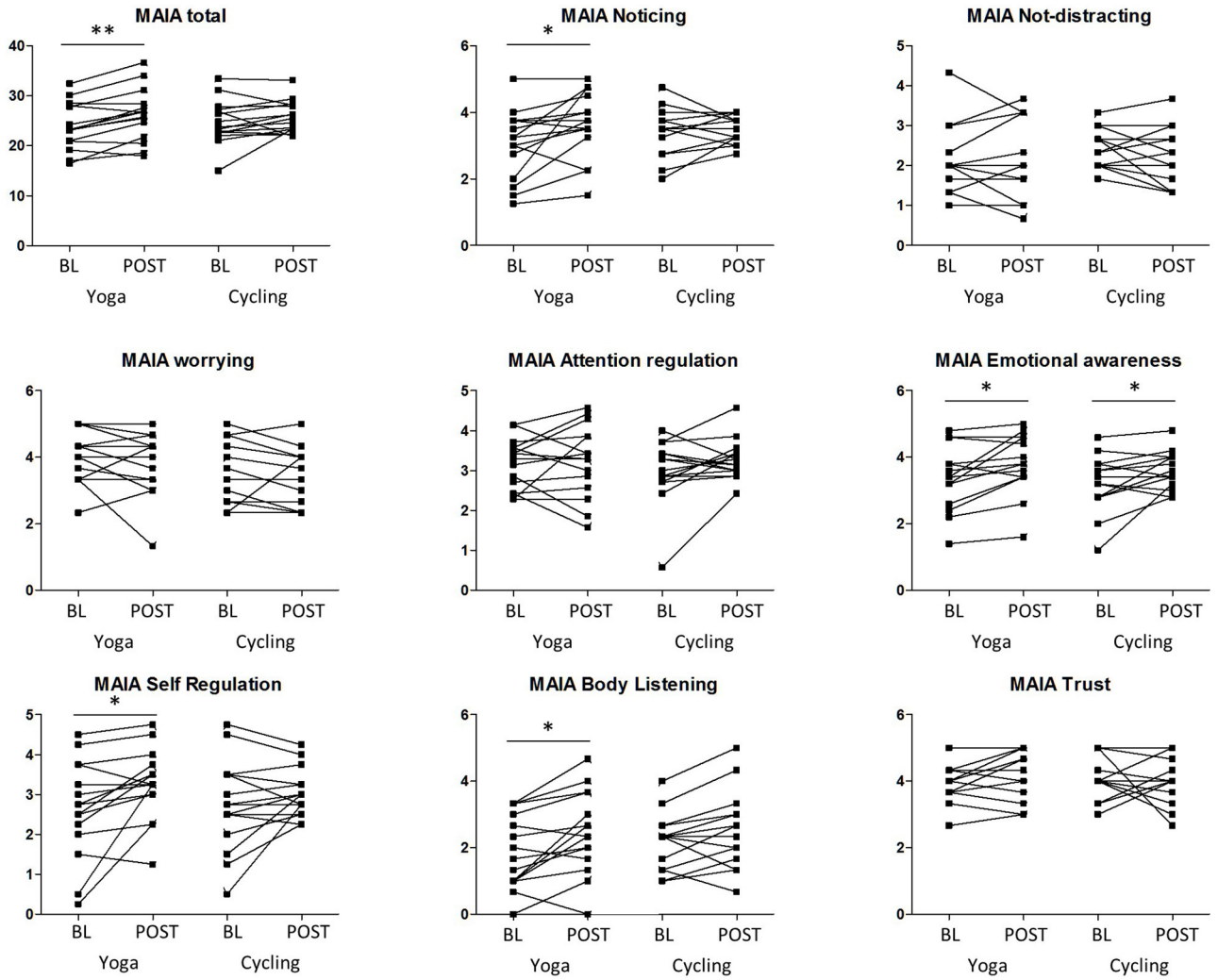

FIGURE 1 | Results of the multidimensional assessment of interoceptive awareness (MAIA) scale and subscales of both groups (yoga and cycling), at baseline (BL) and post-intervention (POST). Significant results of the paired tests are indicated with * ($P < 0.05$, uncorrected) and ** ($P < 0.005$, uncorrected).

Table 2). For the MAIA subscores, this increase was also reflected in the subdimensions "noticing" ($P = 0.02$ (uncorrected), Bonferroni uncorrected), "emotional awareness" ($P = 0.009$, uncorrected), "self-regulation" ($P = 0.015$, uncorrected), and "body listening" ($P = 0.007$, uncorrected). For the cycling group, a significant ($P = 0.04$, uncorrected) increase in the emotional awareness score was observed, but no overall effect on the global MAIA score.

Furthermore, in the yoga subjects, scores on the "observe items" of the mindfulness FFMQ questionnaire increased significantly ($P = 0.04$, uncorrected) compared to baseline (**Table 2**). No significant intervention differences were observed for the PSS, PSWQ, and SCS.

For the between group analysis at baseline, both groups did not score significantly different on the psychometric scales. A significant difference between groups was observed after the intervention however, showing higher scores on "cognitive functioning" ($P = 0.009$, uncorrected) and "overall functioning" ($P = 0.01$, uncorrected) subscales of the LAPS affect and pleasure scale in the yoga group compared to the cycling group.

Glucose Metabolism and Intervention Effects

No significant interaction effects were found. No significant differences in absolute glucose metabolism were found between both groups (at baseline and post-intervention), nor within groups (comparing the baseline vs. post-intervention condition). The mean absolute glucose metabolism values in the different composite VOIs are shown in **Figure 2A**. For relative glucose metabolism, normalized on total GM, no differences were found between groups **Figure 2B**. Within-group analyses showed no significant differences after the yoga intervention. However, for the indoor cycling group, the paired within-group showed significant increases in relative glucose metabolism in the

TABLE 2 | Psychometric results of the between and within group analyses.

	Yoga		Cycling		Repeated *ANOVA P*-value	Within groups (paired) (intervention effect)		Between groups (unpaired) (group effect)	
Scale	**Baseline**	**Post**	**Baseline**	**Post**	**Group × Time**	**Yoga**	**Cycling**	**Baseline**	**Post**
LAPS									
Positive affect	7.8(1.1)	7.9(1.3)	7.2(1.4)	7.3(1.2)	0.94	0.78	0.87	0.23	0.22
Negative affect	1.2(1.0)	2.0(1.6)	1.6(0.9)	2.2(1.5)	0.73	0.07	0.15	0.23	0.69
Hedonic tone	8.8(1.0)	8.6(1.1)	8.5(0.9)	8.1(1.1)	0.64	0.35	0.06	0.34	0.22
Independent variables:									
Cognitive functioning	8.1(1.7)	8.6(1.1)	7.9(1.5)	7.3(1.4)	0.06	0.20	0.18	0.66	0.009[a]
Overall functioning	8.7(1.3)	8.8(0.9)	8.2(1.3)	7.7(1.3)	0.26	0.84	0.19	0.28	0.01[a]
Meaningful life	8.5(1.0)	8.1(1.2)	7.4(2.2)	7.9(1.2)	0.30	0.21	0.52	0.10	0.56
Happiness	8.5(1.1)	8.3(1.2)	7.5(1.6)	7.7(1.5)	0.33	0.30	0.63	0.04	0.23
FFMQ	137.5(15.2)	138.9(18.9)	139.4(13.3)	140.9(13.9)	0.97	0.51	0.55	0.71	0.74
Observe items	24.5(5.4)	26.8(5.8)	25.9(4.4)	27.5(5.0)	0.54	0.04[a]	0.07	0.42	0.74
Describe items	28.67(5.4)	28.5(5.3)	30.1(5.5)	30.0(6.3)	0.96	0.81	0.90	0.47	0.48
Awareness items	29.7(5.4)	28.0(5.8)	29.3(4.7)	29.1(5.4)	0.35	0.09	0.87	0.86	0.59
Non-judge items	30.8(4.7)	30.9(4.9)	32.5(3.4)	32.4(4.0)	0.91	0.93	0.95	0.27	0.36
Non-react items	23.9(4.2)	24.7(3.5)	21.5(4.9)	21.9(4.5)	0.71	0.41	0.59	0.17	0.07
PSS	12.1(6.3)	12.6(5.4)	12.1(5.8)	12.9(5.4)	0.86	0.80	0.49	0.98	0.87
PSWQ	31.0(13.2)	30.1(14.9)	33.2(14.8)	36.6(15.2)	0.50	0.83	0.48	0.67	0.25
SCS	28.1(7.5)	27.2(6.0)	29.9(4.4)	28.0(4.3)	0.51	0.30	0.06	0.41	0.69
MAIA	23.9(4.7)	26.2(5.2)	24.8(4.4)	25.8(3.2)	0.18	0.001[b]	0.21	0.61	0.78
Noticing	3.0(1.0)	3.6(1.0)	3.5(0.8)	3.6(0.4)	0.07	0.02[a]	0.58	0.20	0.81
Not-distracting	2.1(0.8)	2.1(0.9)	2.4(0.5)	2.2(0.7)	0.39	0.88	0.17	0.25	0.72
Not-worrying	4.0(0.8)	3.8(0.9)	3.7(0.9)	3.6(0.9)	0.78	0.29	0.41	0.40	0.55
Attention regulation	3.2(0.6)	3.2(0.9)	3.0(0.8)	3.3(0.5)	0.45	0.68	0.14	0.52	0.94
Emotional awareness	3.4(0.9)	3.8(0.9)	3.3(0.9)	3.6(0.6)	0.90	0.009[a]	0.04[a]	0.69	0.56
Self-regulation	2.6(1.2)	3.3(0.9)	2.7(1.1)	3.0(0.6)	0.28	0.015[a]	0.40	0.82	0.40
Body listening	1.8(1.1)	2.5(1.2)	2.2(0.8)	2.5(1.1)	0.20	0.007[a]	0.10	0.33	0.96
Trusting	3.8(0.6)	4.0(0.8)	4.0(0.7)	4.0(0.7)	0.52	0.13	0.93	0.33	0.81

BL, baseline; FFMQ, five facet mindfulness questionnaire; LAPS, Leuven affect and pleasure scale; MAIA, multi-assessment interoceptive awareness; PSS, perceived stress scale; PSWQ, Penn state worrying questionnaire; SCS, self-compassion scale.

[a](significant) uncorrected, [b] remains significant after Bonferroni correction.

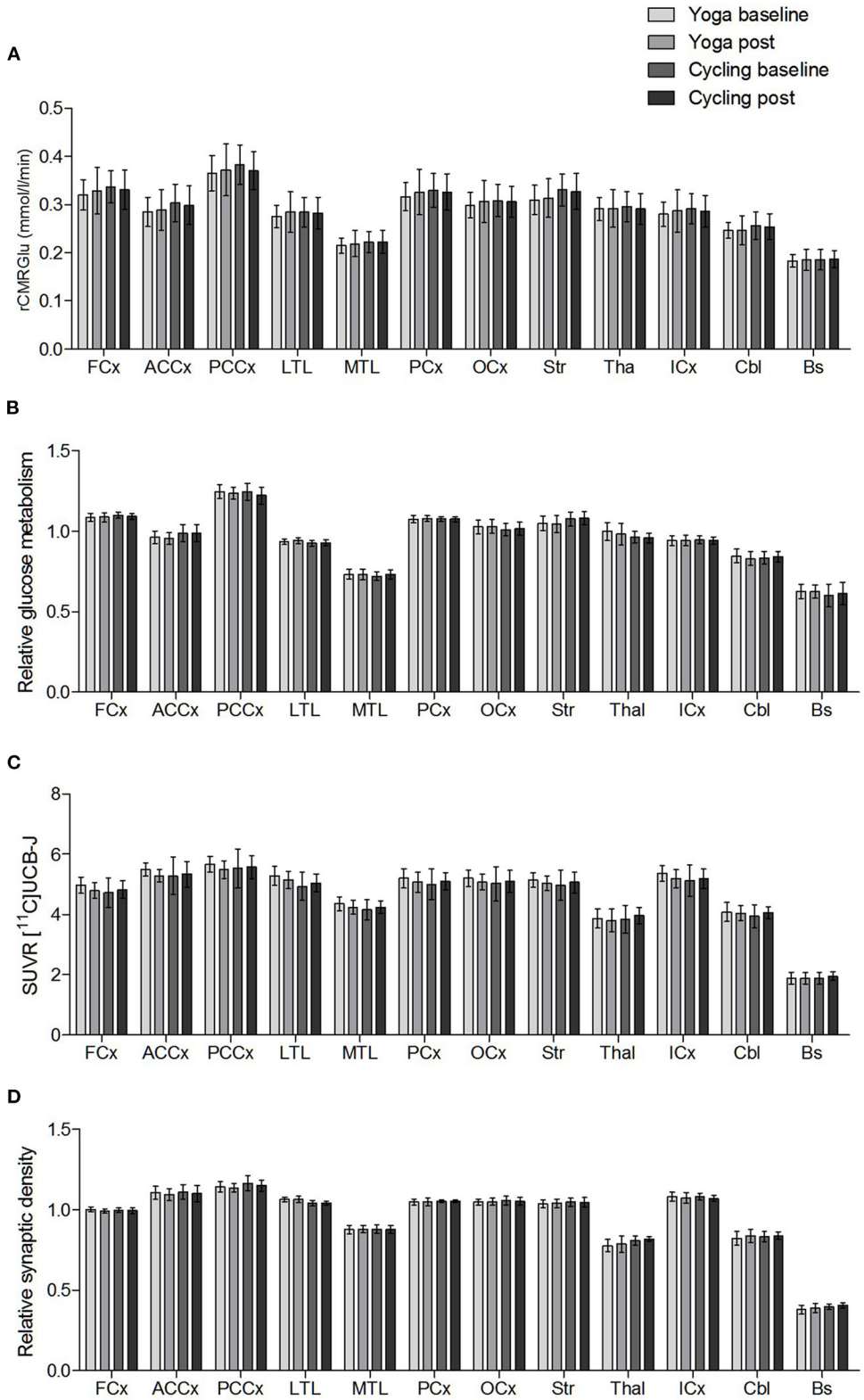

FIGURE 2 | Regional mean **(A)** absolute glucose metabolism (rCMRGlu), **(B)** relative glucose metabolism, **(C)** SUVR [^{11}C]UCB-J, and **(D)** relative synaptic density in the composite VOIs (FCx, frontal cortex; ACCx, anterior cingulate cortex; PCCx, posterior cingulate cortex; LTL, lateral temporal lobe; MTL, medial temporal lobe; PCx, parietal cortex; OCx, occipital cortex; Str, striatum; Thal, thalamus; ICx, insular cortex; Cbl, cerebellum; Bs, brainstem). Error bars represent one standard deviation.

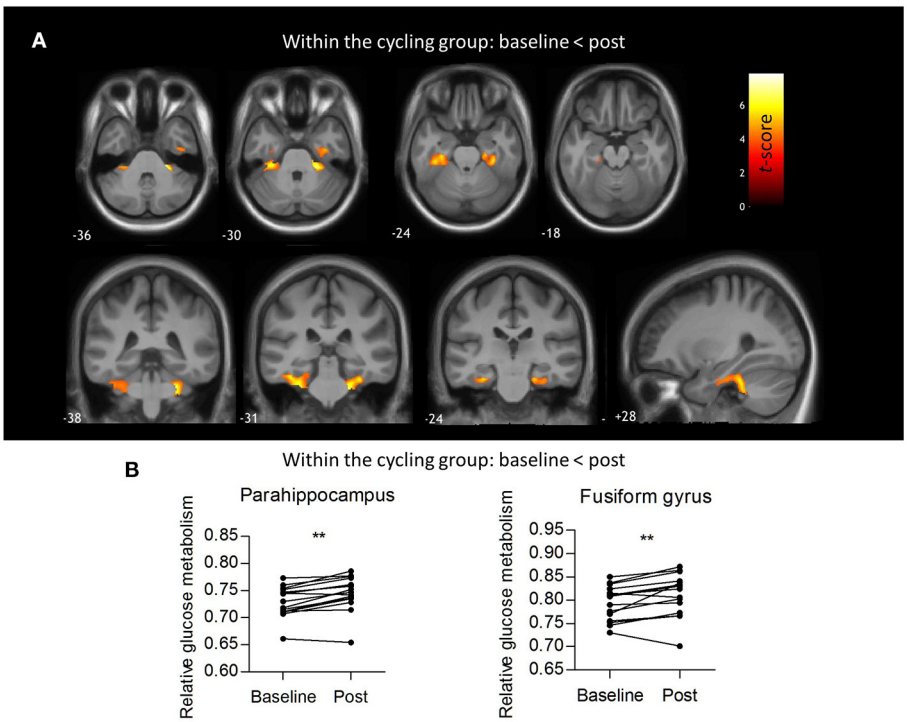

FIGURE 3 | Within-groups analysis of relative glucose metabolism. **(A)** Voxel-based paired *t*-statistical map for the cycling group showing increased relative glucose metabolism post intervention compared to baseline. Evaluation at $P_{FWE} < 0.05$ corrected at cluster level, $P_{height} < 0.001$ uncorrected at voxel level, $K_{ext} > 0.8$ cm^3. The results are projected on the group's average 3D T1-weighted MR. **(B)** Regional relative glucose metabolism in the parahippocampus (+2.2%; $P = 0.0002$) and fusiform gyrus (+2.2%; $P = 0.006$), paired *t*-tests. **: P < 0.005.

cerebellum (region 4, 5, 6, and 10), fusiform gyrus, and parahippocampus with a peak effect in the right and left upper cerebellar gyrus (region 4/5), of +4.3 and +5.7%, respectively (**Figure 3A**; **Supplementary Table 1**). The VOI-based analysis confirmed this significant relative increased glucose metabolism in the parahippocampus (+2.2%; $P = 0.0002$) and fusiform gyrus (+2.2%; $P = 0.006$) (**Figure 3B**). Regional average relative glucose metabolism values in the different composite VOIs are given in **Figure 2B**. No significant correlations were found between the psychometric scores and increased regional relative glucose metabolism in the indoor cycling group.

Synaptic Density and Intervention Effects

No significant interaction effects were found. The groups did not differ in synaptic density ($n = 10$ each), both in absolute (SUVR) as well as in relative terms. Neither intervention resulted in a demonstrable effect on regional synaptic density. The mean [^{11}C]UCB-J SUVR and relative synaptic density VOI-based values for the baseline and post intervention conditions are shown in **Figures 2C,D**.

Gray Matter Volume and Intervention Effects

No significant interaction effects were found. At baseline, no differences in GM volume values were found between both groups. Also, VBM did not show significant changes in GM volume after the 12-week yoga intervention nor after the cycling intervention.

DISCUSSION

Several cross-sectional imaging studies have shown that long-term yoga practice may lead to both structural and functional/metabolic alterations (7, 46). The objective of this (current) study was to determine in a longitudinal study whether behavioral and multimodal imaging biomarker change in sedentary healthy subjects starting either a yoga intervention vs. a physical matched intervention. Whereas, a clear effect on relevant behavioral changes was present, including interoceptive awareness and cognition scores, no significant imaging-based changes were found after this 12-week intervention.

For the psychometric scales, especially interoceptive awareness increased significantly after successful completion of a 12-week yoga intervention with more than 20 sessions. Previous studies have shown similar behavioral effects after mindfulness interventions, accompanied by increases in the MAIA subscales as well (26, 47). After a mindfulness intervention of 3 months, Bornemann et al. found significant overall increase in interoceptive awareness in healthy volunteers, with significant changes on self-regulation, attention regulation, emotional awareness, body listening, and trusting subscales. Also de Jong et al., investigating patients with chronic pain and comorbid

depression, reported significant effects of an 8-week mindfulness intervention, on self-regulation, emotional awareness, and not-distracting subscales (26, 47). Effects on the self-regulation and emotional awareness subscales, also found in our study, thus show an overlapping effect of mindfulness and yoga-based interventions. Of interest, in our study specific "formal" guided meditation components represent only a minor part of the whole yoga lesson. During yoga practice, interoceptive awareness is addressed by drawing attention, feeling emotions, and bodily sensations to the present moment. This indicates that adding the dimensions of breathing techniques and meditation are needed to alter interoceptive awareness, as only exercise as shown in the control arm with indoor cycling, was unable to change this. In contrast, the FFMQ, a particular scale oriented toward mindfulness did not change significantly in our study. This is in contrast to previous interventional studies that had a stronger focus on additional mindfulness or yoga philosophy components such as Kripalu yoga emphasizing the cultivation of "witness consciousness" and compassion, and a combination of yin yoga and mindfulness (22, 24), compared to the yoga styles practiced in this study. Specific mindfulness-based interventions may be needed to improve self-compassion (48). Also, a significant relationship between class frequency or practice experience with mindfulness scores and self-compassion levels has been found previously, suggesting that the frequency and length of a yoga intervention plays a crucial role in achieving optimal changes in mindfulness and self-compassion scores (23).

Mind-body interventions such as yoga are increasingly used for stress reduction, often investigated with the perceived stress scale (22, 24, 49). In a systematic review addressing the effects of yoga on stress in healthy individuals, yoga was beneficial on reducing stress levels in the majority of the included studies (50). However, here we did not observe a decrease in perceived stress. Some participants mentioned at the end of the study that introducing the intervention in their daily life schedule was even stressful at times. Other studies have found even increased stress levels at the end of a yoga intervention that could be related to a too overwhelming class schedule on top of daily activities and/or that the expectations were not in line with reality (49). As previous research has addressed a beneficial effect of yoga in mood disorder (depression and anxiety), we also explored the effects of yoga on affect in healthy subjects. In this study, we found increased scores on cognitive and overall functioning with the LAPS in the yoga group compared to the controls after the intervention. Although no differences were found on positive affect, increases in cognitive functioning may precede effects on positive affect, as a link between cognitive functioning and positive affect has been described previously (27).

Regarding the three neuroimaging markers (i.e., glucose metabolism, synaptic density, and GM volume), we did not observe significant differences in any of these markers after the yoga intervention compared to baseline. In our previous cross-sectional study, a strong and highly significant decrease in the medial temporal cortex, striatum, and brainstem was observed in experienced yoga subjects, with an average of 4.8 years of yoga experience and at least four practices per week, totaling at least 150 sessions per year (10). This is markedly different from the frequency and duration of the current study where yoga-naive participants practiced yoga only twice a week for 12 weeks with on average 21 sessions, which may have been too short or too infrequent to instigate measurable metabolic effects. The intervention duration for the current study was chosen as a practically achievable time scale, so new designs will have to take longer durations and/or more frequent sessions into consideration.

After the indoor cycling intervention, significant clusters of increased resting glucose metabolism were found in cognitive and motor brain areas: parahippocampal gyrus, fusiform gyrus, and upper cerebellum. The parahippocampal gyrus is associated with many cognitive processes, including visuospatial processing and episodic memory, but also emotion processing (51). Extensive involvement of the parahippocampal gyrus has been found in the majority of animal and human studies investigating neuronal activity in relation to physical activity (52), and was associated with positive effects on memory (53, 54). This is supported by evidence of increased levels of serum brain derived neurotrophic factor (BDNF) after exercise interventions (55–57). Brain derived neurotrophic factor is an important molecule for synaptic plasticity and known to play a crucial role in learning and memory (58). Increased levels of BDNF have been repeatedly reported in the hippocampal regions of rodents after physical activity (59, 60). Similarly, elderly healthy subjects that were more physically active showed higher glucose metabolism in the parahippocampus and fusiform gyrus (61). The link between physical activity and increased glucose metabolism in the fusiform gyrus remains speculative as the fusiform gyrus is mainly known for its involvement in functionally specialized computations of higher-order visual features such as object recognition and face perception (62, 63). In line with the observed increased glucose metabolism in the upper cerebellum, Talukdar et al. found that general aerobic fitness was significantly associated with increased brain activity in the upper cerebellum in addition to sensory, motor, and memory processing regions (64). The connections of the upper cerebellum with the primary motor cortex and a somatotopic organization of both lower and upper limbs, play a pivotal role in motor functioning, which is heavily interrogated during indoor cycling or aerobic activity (more than in slow, postural changes in yoga) and could therefore explain this association.

It can be hypothesized that alterations in glucose metabolism, a main determinant of synaptic activity, may after time lead to strengthening of synapses (65). Therefore, only after long enough metabolic activation, more synaptic connections (hence synaptic density) and ultimately microstructural increases in GM volume can be expected. Concerning effects of yoga on macroscopic structure, to the best of our knowledge only two studies have been published in a longitudinal interventional setting. Also here, despite daily practicing yoga (mindfulness based stress reduction including yoga postures and yogic meditation) over a period of 8–12 weeks, no increased GM volume was found (66, 67), (which is) in line with our data. In addition, interventional longitudinal imaging studies investigating physical activity in healthy subjects are limited as well. Erickson et al. found that in healthy elderly individuals hippocampal volumes increased after regular

aerobic exercise at moderate-intensity for 1 year (68). Another interventional study in healthy elderly individuals before and after 6 months of aerobic training found increased volumes in the anterior cingulate cortex, supplementary motor association cortex, inferior frontal gyrus, and left superior temporal gyrus (69). Thus, only in studies conducted over a longer time span and higher cumulated activity levels compared to our study, significant effects were found.

Additionally, no changes in synaptic density were found using [^{11}C]UCB-J PET imaging in the subcohort. Even a more liberal threshold up to 0.01 did not result in significant clusters. As the field of *in vivo* synaptic density imaging is still very young (12), no other studies investigating the effects of any behavioral/physical interventions on synaptic density in humans have been published so far. Therefore, it is difficult to speculate on the intensity of a behavioral intervention that would be needed for detection of a macroscopic difference combined to the test sensitivity (T-RT values about 5%) (70). In rodents, aerobic exercise (treadmill running), 5 days a week for 4 or 12 weeks resulted in increased hippocampal synaptic density (60.6–75.1% higher number of synapses per cubic micron of tissue in treadmill training vs. sedentary), using post-mortem immunofluorescent staining and electron microscopy (71, 72).

A few study limitations should be addressed. First, the group size in this academic interventional trial was relatively small and the duration and frequency of the intervention was limited, because the feasibility of the study for the subjects was considered. However, previous studies investigating effects of yoga on the brain used similar study designs in terms of study duration and frequency (4, 66, 67, 73–75). The study length and frequency were considered as an optimal balance between study feasibility, duration, cost, and potential drop-out rate. Secondly, as no significant differences in GM volume between both groups, nor between the baseline vs. the post- intervention condition, were found, we did not apply partial volume correction on the PET data. Thirdly, the participants were randomly assigned to either the yoga intervention or the indoor cycling intervention. As subjects may have showed preference toward one specific intervention, and preference of the participant may influence the outcome (76), a chance of underperforming in the control group may have occurred. However, based on the number of sessions followed and the detailed, consistent information in self-reporting logs of the participants in both groups, we expect no systematic bias from this aspect. Finally, the yoga group could attend classes of four different yoga styles, each having a different emphasis. Although the relative composition of the yoga classes (postures/breathing/meditation) remained stable, there is still debate about which component of yoga causes the most substantial behavioral or physical benefits (7). Thus, a different ratio between the components could be necessary to detect stronger neuronal effects. Furthermore, these types of comprehensive changes may require longer time before macroscopic effects become evident.

In conclusion, we found that a yoga intervention of 12 weeks increases interoceptive awareness. However, we were not yet able to observe metabolic, synaptic density or volumetric correlates of this behavioral finding after this short intervention. Therefore, in line with previous results, longer interventions and/or higher frequency of yoga practice may be needed to objectivate cerebral metabolic and/or structural brain effects. Furthermore, indoor 12 weeks of cycling did significantly increase regional glucose metabolism in brain regions important for motor functioning and cognition, but did not result into interoceptive or measurable cognitive improvements.

DATA AVAILABILITY STATEMENT

The raw data supporting the conclusions of this article will be made available by the authors, without undue reservation.

ETHICS STATEMENT

The studies involving human participants were reviewed and approved by local University Ethics Committee of Leuven. The patients/participants provided their written informed consent to participate in this study.

AUTHOR CONTRIBUTIONS

JvA, KVL, and KD contributed to conception and design of the study. JvA, LJ, and KVL collected the data. JvA, LJ, JC, SS, MK, and KVL performed the (statistical) analysis. JvA wrote the first draft of the manuscript. JvA, LJ, JC, KD, SS, and KVL wrote sections of the manuscript. All authors contributed to manuscript revision, read, and approved the submitted version.

FUNDING

KVL is senior clinical research fellow for the Research Foundation-Flanders (FWO), JC is post-doctoral fellow for FWO.

ACKNOWLEDGMENTS

We acknowledge the skilled help of the local PET/MR technologists and radiopharmacy staff.

SUPPLEMENTARY MATERIAL

The Supplementary Material for this article can be found online at: https://www.frontiersin.org/articles/10.3389/fpsyt.2021.739356/full#supplementary-material

REFERENCES

1. Cramer H, Ward L, Steel A, Lauche R, Dobos G. Zhang Y. Prevalence, patterns, and predictors of yoga use: results of a us nationally representative survey. *Am J Prev Med.* (2016) 50:230–5. doi: 10.1016/j.amepre.2015.07.037
2. Riley KE, Park CL. How does yoga reduce stress? A systematic review of mechanisms of change and guide to future inquiry.

Health Psychol Rev. (2015) 7199:1–18. doi: 10.1080/17437199.2014.981778
3. Cartwright T, Mason H, Porter A, Pilkington K. Yoga practice in the UK: a cross-sectional survey of motivation, health benefits and behaviours. *BMJ Open.* (2020) 10:e031848. doi: 10.1136/bmjopen-2019-031848
4. van Aalst J, Ceccarini J, Demyttenaere K, Sunaert S, Van Laere K. What has neuroimaging taught us on the neurobiology of yoga? A review. *Front Integr Neurosci.* (2020) 14:34. doi: 10.3389/fnint.2020.00034
5. Critchley HD, Nicotra A, Chiesa PA, Nagai Y, Gray MA, Minati L, et al. Slow breathing and hypoxic challenge: cardiorespiratory consequences and their central neural substrates. *PLoS ONE.* (2015) 10:e0127082. doi: 10.1371/journal.pone.0127082
6. Streeter CC, Jensen JE, Perlmutter RM, Cabral HJ, Tian H, Terhune DB, et al. Yoga asana sessions increase brain GABA levels: a pilot study. *J Altern Complement Med.* (2007) 13:419–26. doi: 10.1089/acm.2007.6338
7. Villemure C, Ceko M, Cotton VA, Bushnell MC. Neuroprotective effects of yoga practice: age-, experience-, and frequency-dependent plasticity. *Front Hum Neurosci.* (2015) 9:281. doi: 10.3389/fnhum.2015.00281
8. Elías Hernández S, Suero J, Barros A, Luis González-Mora J, Rubia K. Increased grey matter associated with long-term sahaja yoga meditation: a voxel-based morphometry study. *PLoS ONE.* (2016) 11:e0150757. doi: 10.1371/journal.pone.0150757
9. Phillips C. Lifestyle modulators of neuroplasticity: how physical activity, mental engagement, and diet promote cognitive health during aging. *Neural Plast.* (2017) 2017:3589271. doi: 10.1155/2017/3589271
10. van Aalst J, Ceccarini J, Schramm G, Van Weehaeghe D, Rezaei A, Demyttenaere K, et al. Long-term Ashtanga yoga practice decreases medial temporal and brainstem glucose metabolism in relation to years of experience. *EJNMMI Res.* (2020) 10:50. doi: 10.1186/s13550-020-00636-y
11. Zimmer ER, Parent MJ, Souza DG, Leuzy A, Lecrux C, Kim HI, et al. [18F]FDG PET signal is driven by astroglial glutamate transport. *Nat Neurosci.* (2017) 20:393–5. doi: 10.1038/nn.4492
12. Finnema SJ, Nabulsi NB, Eid T, Detyniecki K, Lin SF, Chen MK, et al. Imaging synaptic density in the living human brain. *Sci Transl Med.* (2016) 8:1–10. doi: 10.1126/scitranslmed.aaf6667
13. Nabulsi NB, Mercier J, Holden D, Carre S, Najafzadeh S, Vandergeten M-C, et al. Synthesis and preclinical evaluation of 11C-UCB-J as a PET tracer for imaging the synaptic vesicle glycoprotein 2A in the brain. *J Nucl Med.* (2016) 57:777–84. doi: 10.2967/jnumed.115.168179
14. Holmes SE, Scheinost D, Finnema SJ, Naganawa M, Davis MT, DellaGioia N, et al. Lower synaptic density is associated with depression severity and network alterations. *Nat Commun.* (2019) 10:1–10. doi: 10.1038/s41467-019-09562-7
15. Chen M-K, Mecca AP, Naganawa M, Finnema SJ, Toyonaga T, Lin S, et al. Assessing synaptic density in alzheimer disease with synaptic vesicle glycoprotein 2A positron emission tomographic imaging. *JAMA Neurol.* (2018) 75:1215–24. doi: 10.1001/jamaneurol.2018.1836
16. Vanhaute H, Ceccarini J, Michiels L, Koole M, Sunaert S, Lemmens R, et al. *In vivo* synaptic density loss is related to tau deposition in amnestic mild cognitive impairment. *Neurology.* (2020) 95:e545–53. doi: 10.1212/wnl.0000000000009818
17. van Aalst J, Ceccarini J, Sunaert S, Dupont P, Koole M, Van Laere K. *In vivo* synaptic density relates to glucose metabolism at rest in healthy subjects, but is strongly modulated by regional differences. *J Cereb Blood Flow Metab.* (2021) 41:1978–87. doi: 10.1177/0271678X20981502
18. Park C, Groessl E, Maiya M, Sarkin A, Eisen S V, Riley K, et al. Comparison groups in yoga research: a systematic review and critical evaluation of the literature. *Complement Ther Med.* (2014) 22:920–9. doi: 10.1016/j.ctim.2014.08.008
19. Gilani SRM, Feizabad AK. The effects of aerobic exercise training on mental health and self-esteem of type 2 diabetes mellitus patients. *Heal Psychol Res.* (2019) 7:6576. doi: 10.4081/hpr.2019.6576
20. Beck AT, Steer RA, Carbin MG. Psychometric properties of the Beck Depression Inventory: twenty-five years of evaluation. *Clin Psychol Rev.* (1988) 8:77–100. doi: 10.1016/0272-7358(88)90050-5
21. Cramer H, Anheyer D, Lauche R, Dobos G. A systematic review of yoga for major depressive disorder. *J Affect Disord.* (2017) 213:70–7. doi: 10.1016/j.jad.2017.02.006
22. Hylander F, Johansson M, Daukantaite D, Ruggeri K. Yin yoga and mindfulness: a five week randomized controlled study evaluating the effects of the YOMI program on stress and worry. *Anxiety Stress Coping.* (2017) 30:365–78. doi: 10.1080/10615806.2017.1301189
23. Snaith N, Schultz T, Proeve M, Rasmussen P. Mindfulness, self-compassion, anxiety and depression measures in South Australian yoga participants: implications for designing a yoga intervention. *Complement Ther Clin Pract.* (2018) 32:92–9. doi: 10.1016/j.ctcp.2018.05.009
24. Gard T, Brach N, Hölzel BK, Noggle JJ, Conboy LA, Lazar SW. Effects of a yoga-based intervention for young adults on quality of life and perceived stress: the potential mediating roles of mindfulness and self-compassion. *J Posit Psychol.* (2012) 7:165–75. doi: 10.1080/17439760.2012.667144
25. Neukirch N, Reid S, Shires A. Yoga for PTSD and the role of interoceptive awareness: a preliminary mixed-methods case series study. *Eur J Trauma Dissociation.* (2019) 3:7–15. doi: 10.1016/j.ejtd.2018.10.003
26. Bornemann B, Herbert BM, Mehling WE, Singer T. Differential changes in self-reported aspects of interoceptive awareness through 3 months of contemplative training. *Front Psychol.* (2015) 5:1504. doi: 10.3389/fpsyg.2014.01504
27. Demyttenaere K, Mortier P, Kiekens G, Bruffaerts R. Is there enough "interest in and pleasure in" the concept of depression? The development of the Leuven Affect and Pleasure Scale (LAPS). *CNS Spectr.* (2019) 24:265–74. doi: 10.1017/s1092852917000578
28. Baer RA, Smith GT, Hopkins J, Krietemeyer J, Toney L. Using self-report assessment methods to explore facets of mindfulness. *Assessment.* (2006) 13:27–45. doi: 10.1177/1073191105283504
29. Cohen S, Kamarck T, Mermelstein R. A Global measure of perceived stress. *J Health Soc Behav.* (1983) 24:385–96. doi: 10.2307/2136404
30. Meyer TJ, Miller ML, Metzger RL, Borkovec TD. Development and validation of the penn state worry questionnaire. *Behav Res Ther.* (1990) 28:487–95. doi: 10.1016/0005-7967(90)90135-6
31. Neff KD, Kinney S, Kirkpatrick K, Schmitt LT, Hsieh Y-P, Chen W-C, et al. The development and validation of a scale to measure self-compassion. *Self Identity.* (2003) 2:223–50. doi: 10.1080/15298860390209035
32. Hunter GJ, Hamberg LM, Alpert NM, Choi NC. Fischman AJ. Simplified measurement of deoxyglucose utilization rate. *J Nucl Med.* (1996) 37:950–5.
33. Koole M, van Aalst J, Devrome M, Mertens N, Serdons K, Lacroix B, et al. Quantifying SV2A density and drug occupancy in the human brain using [11C]UCB-J PET imaging and subcortical white matter as reference tissue. *Eur J Nucl Med Mol Imaging.* (2018) 46:396–406. doi: 10.1007/s00259-018-4119-8
34. Rezaei A, Schramm G, Willekens SM, Delso G, Van Laere K, Nuyts J. A quantitative evaluation of joint activity and attenuation reconstruction in TOF-PET/MR brain imaging. *J Nucl Med.* (2019) 60:1649–55. doi: 10.2967/jnumed.118.220871
35. Schramm G, Koole M, Willekens SMA, Rezaei A, Van Weehaeghe D, Delso G, et al. Regional accuracy of ZTE-based attenuation correction in static and dynamic brain PET/MR. *Physics.* (2018) arXiv:1806.03481v1.
36. Rossano S, Toyonaga T, Finnema SJ, Naganawa M, Lu Y, Nabulsi N, et al. Assessment of a white matter reference region for 11C-UCB-J PET quantification. *J Cereb Blood Flow Metab.* (2019) 40:1890–901. doi: 10.1177/0271678X19879230
37. Wu HM, Bergsneider M, Glenn TC, Yeh E, Hovda DA, Phelps ME, et al. Measurement of the global lumped constant for 2-deoxy-2-[18F]fluoro-D-glucose in normal human brain using [15O]water and 2-deoxy-2-[18F]fluoro-D-glucose positron emission tomography imaging: a method with validation based on multiple methodologies. *Mol Imaging Biol.* (2003) 5:32–41. doi: 10.1016/S1536-1632(02)00122-1

38. Hammers A, Allom R, Koepp MJ, Free SL, Myers R, Lemieux L, et al. Three-dimensional maximum probability atlas of the human brain, with particular reference to the temporal lobe. *Hum Brain Mapp.* (2003) 19:224–47. doi: 10.1002/hbm.10123
39. Tzourio-Mazoyer N, Landeau B, Papathanassiou D, Crivello F, Etard O, Delcroix N, et al. Automated anatomical labeling of activations in SPM using a macroscopic anatomical parcellation of the MNI MRI single-subject brain. *Neuroimage.* (2002) 15:273–89. doi: 10.1006/nimg.2001.0978
40. Farokhian F, Beheshti I, Sone D, Matsuda H. Comparing CAT12 and VBM8 for detecting brain morphological abnormalities in temporal lobe epilepsy. *Front Neurol.* (2017) 8:428. doi: 10.3389/fneur.2017.00428
41. Michiels L, Delva A, van Aalst J, Ceccarini J, Vandenberghe W, Vandenbulcke M, et al. Synaptic density in healthy human aging is not influenced by age or sex: a 11C-UCB-J PET study. *Neuroimage.* (2021) 2021:117877. doi: 10.1016/j.neuroimage.2021.117877
42. DeCarli C, Massaro J, Harvey D, Hald J, Tullberg M, Au R, et al. Measures of brain morphology and infarction in the framingham heart study: establishing what is normal. *Neurobiol Aging.* (2005) 26:491–510. doi: 10.1016/j.neurobiolaging.2004.05.004
43. Walhovd KB, Westlye LT, Amlien I, Espeseth T, Reinvang I, Raz N, et al. Consistent neuroanatomical age-related volume differences across multiple samples. *Neurobiol Aging.* (2011) 32:916–32. doi: 10.1016/j.neurobiolaging.2009.05.013
44. Kakimoto A, Ito S, Okada H, Nishizawa S, Minoshima S, Ouchi Y. Age-related sex-specific changes in brain metabolism and morphology. *J Nucl Med.* (2016) 57:221–5. doi: 10.2967/jnumed.115.166439
45. Malpetti M, Ballarini T, Presotto L, Garibotto V, Tettamanti M, Perani D. Gender differences in healthy aging and Alzheimer's dementia: a 18 F-FDG-PET study of brain and cognitive reserve. *Hum Brain Mapp.* (2017) 38:4212–27. doi: 10.1002/hbm.23659
46. Hernández SE, Barros-Loscertales A, Xiao Y, González-Mora JL, Rubia K. Gray matter and functional connectivity in anterior cingulate cortex are associated with the state of mental silence during sahaja yoga meditation. *Neuroscience.* (2018) 371:395–406. doi: 10.1016/j.neuroscience.2017.12.017
47. de Jong M, Lazar SW, Hug K, Mehling WE, Hölzel BK, Sack AT, et al. Effects of mindfulness-based cognitive therapy on body awareness in patients with chronic pain and comorbid depression. *Front Psychol.* (2016) 7:967. doi: 10.3389/fpsyg.2016.00967
48. Wasson RS, Barratt C, O'Brien WH. Effects of mindfulness-based interventions on self-compassion in health care professionals: a meta-analysis. *Mindfulness (N Y).* (2020) 11:1914–34. doi: 10.1007/s12671-020-01342-5
49. Kinchen E, Loerzel V, Portoghese T. Yoga and perceived stress, self-compassion, and quality of life in undergraduate nursing students. *J Educ Health Promot.* (2020) 9:292. doi: 10.4103/jehp.jehp_463_20
50. Chong C, Tsunaka M, Tsang H, Chan E, Cheung W. Effects of yoga on stress management in healthy adults: a systematic review. *Altern Ther Health Med.* (2011) 17:32–8.
51. Aminoff EM, Kveraga K, Bar M. The role of the parahippocampal cortex in cognition. *Trends Cogn Sci.* (2013) 17:379–90. doi: 10.1016/j.tics.2013.06.009
52. Loprinzi PD. The effects of physical exercise on parahippocampal function. *Physiol Int.* (2019) 106:114–27. doi: 10.1556/2060.106.2019.10
53. Ruscheweyh R, Willemer C, Krüger K, Duning T, Warnecke T, Sommer J, et al. Physical activity and memory functions: an interventional study. *Neurobiol Aging.* (2011) 32:1304–19. doi: 10.1016/j.neurobiolaging.2009.08.001
54. Hötting K, Reich B, Holzschneider K, Kauschke K, Schmidt T, Reer R, et al. Differential cognitive effects of cycling versus stretching/coordination training in middle-aged adults. *Heal Psychol.* (2012) 31:145–55. doi: 10.1037/a0025371
55. Ferris LT, Williams JS, Shen CL. The effect of acute exercise on serum brain-derived neurotrophic factor levels and cognitive function. *Med Sci Sports Exerc.* (2007) 39:728–34. doi: 10.1249/mss.0b013e31802f04c7
56. Håkansson K, Ledreux A, Daffner K, Terjestam Y, Bergman P, Carlsson R, et al. Responses in healthy older persons to 35 minutes of physical exercise, cognitive training, and mindfulness: associations with working memory function. *J Alzheimer's Dis.* (2017) 55:645–57. doi: 10.3233/JAD-160593
57. Griffin ÉW, Mullally S, Foley C, Warmington SA, O'Mara SM, Kelly ÁM. Aerobic exercise improves hippocampal function and increases BDNF in the serum of young adult males. *Physiol Behav.* (2011) 104:934–41. doi: 10.1016/j.physbeh.2011.06.005
58. Cunha C, Brambilla R, Thomas KL. A simple role for BDNF in learning and memory? *Front Mol Neurosci.* (2010) 3:1. doi: 10.3389/neuro.02.001.2010
59. Vaynman S, Ying Z, Gomez-Pinilla F. Hippocampal BDNF mediates the efficacy of exercise on synaptic plasticity and cognition. *Eur J Neurosci.* (2004) 20:2580–90. doi: 10.1111/j.1460-9568.2004.03720.x
60. Liu PZ, Nusslock R. Exercise-mediated neurogenesis in the hippocampus via BDNF. *Front Neurosci.* (2018) 12:52. doi: 10.3389/fnins.2018.00052
61. Matthews DC, Davies M, Murray J, Williams S, Tsui WH Li Y, Andrews RD, et al. Physical activity, mediterranean diet and biomarkers-assessed risk of Alzheimer's: a multi-modality brain imaging study NIH public access. *Adv J Mol Imaging.* (2014) 4:43–57. doi: 10.4236/ami.2014.44006
62. Suwabe K, Byun K, Hyodo K, Reagh ZM, Roberts JM, Matsushita A, et al. Rapid stimulation of human dentate gyrus function with acute mild exercise. *Proc Natl Acad Sci USA.* (2018) 115:10487–92. doi: 10.1073/pnas.1805668115
63. Aguirre-Loaiza H, Arenas J, Arias I, Franco-Jímenez A, Barbosa-Granados S, Ramos-Bermúdez S, et al. Effect of acute physical exercise on executive functions and emotional recognition: analysis of moderate to high intensity in young adults. *Front Psychol.* (2019) 10:2774. doi: 10.3389/fpsyg.2019.02774
64. Talukdar T, Nikolaidis A, Zwilling CE, Paul EJ, Hillman CH, Cohen NJ, et al. Aerobic fitness explains individual differences in the functional brain connectome of healthy young adults. *Cereb Cortex.* (2018) 28:3600–9. doi: 10.1093/cercor/bhx232
65. Mainardi M, Fusco S, Grassi C. Modulation of hippocampal neural plasticity by glucose-related signaling. *Neural Plast.* (2015) 2015:657928. doi: 10.1155/2015/657928
66. Hölzel BK, Carmody J, Evans KC, Hoge EA, Dusek JA, Morgan L, et al. Stress reduction correlates with structural changes in the amygdala. *Soc Cogn Affect Neurosci.* (2009) 5:11–7. doi: 10.1093/scan/nsp034
67. Yang H, Leaver AM, Siddarth P, Paholpak P, Ercoli L, St. Cyr NM, et al. Neurochemical and neuroanatomical plasticity following memory training and yoga interventions in older adults with mild cognitive impairment *Front Aging Neurosci.* (2016) 8:277. doi: 10.3389/fnagi.2016.00277
68. Erickson KI, Voss MW, Prakash RS, Basak C, Szabo A, Chaddock L, et al. Exercise training increases size of hippocampus and improves memory. *Proc Natl Acad Sci USA.* (2011) 108:3017–22. doi: 10.1073/pnas.1015950108
69. Colcombe SJ, Erickson KI, Scalf PE, Kim JS, Prakash R, McAuley E, et al. Aerobic exercise training increases brain volume in aging humans. *J Gerontol A Biol Sci Med Sci.* (2006) 61:1166–70. doi: 10.1093/gerona/61.11.1166
70. Finnema SJ, Nabulsi NB, Mercier J, Lin S, Chen M-K, Matuskey D, et al. Kinetic evaluation and test–retest reproducibility of [11 C]UCB-J, a novel radioligand for positron emission tomography imaging of synaptic vesicle glycoprotein 2A in humans. *J Cereb Blood Flow Metab.* (2018) 38:2041–52. doi: 10.1177/0271678X17724947
71. Fattoretti P, Malatesta M, Cisterna B, Milanese C, Zancanaro C. Modulatory effect of aerobic physical activity on synaptic ultrastructure in the old mouse hippocampus. *Front Aging Neurosci.* (2018) 10:141. doi: 10.3389/fnagi.2018.00141
72. Li Y, Zhao L, Gu B, Cai J, Lv Y, Yu L. Aerobic exercise regulates Rho/cofilin pathways to rescue synaptic loss in aged rats. *PLoS ONE.* (2017) 12:e0171491. doi: 10.1371/journal.pone.0171491
73. Dodich A, Zollo M, Crespi C, Cappa SF, Laureiro Martinez D, Falini A, et al. Short-term Sahaja Yoga meditation training modulates brain structure and spontaneous activity in the executive control network. *Brain Behav.* (2019) 9:e01159. doi: 10.1002/brb3.1159
74. Eyre HA, Acevedo B, Yang H, Siddarth P, Van Dyk K, Ercoli L, et al. Changes in neural connectivity and memory following a yoga intervention

for older adults: a pilot study. *J Alzheimer's Dis.* (2016) 52:673–84. doi: 10.3233/JAD-150653
75. Streeter C, Gerbarg PL, Nielsen GH, Brown RP, Jensen JE, Silveri M, et al. Effects of yoga on thalamic gamma-aminobutyric acid, mood and depression: analysis of two randomized controlled trials. *Neuropsychiatry (London).* (2018) 8:1923–39. doi: 10.4172/Neuropsychiatry.1000535
76. Kwan BM, Dimidjian S, Rizvi SL. Treatment preference, engagement, and clinical improvement in pharmacotherapy versus psychotherapy for depression. *Behav Res Ther.* (2010) 48:799–804. doi: 10.1016/j.brat.2010.04.003

Conflict of Interest: The authors declare that the research was conducted in the absence of any commercial or financial relationships that could be construed as a potential conflict of interest.

Publisher's Note: All claims expressed in this article are solely those of the authors and do not necessarily represent those of their affiliated organizations, or those of the publisher, the editors and the reviewers. Any product that may be evaluated in this article, or claim that may be made by its manufacturer, is not guaranteed or endorsed by the publisher.

frontiers in Psychiatry

ORIGINAL RESEARCH
published: 11 November 2021
doi: 10.3389/fpsyt.2021.716707

EEG Signal Complexity Is Reduced During Resting-State in Fragile X Syndrome

Mélodie Proteau-Lemieux[1,2†], Inga Sophia Knoth[2†], Kristian Agbogba[2], Valérie Côté[2], Hazel Maridith Barlahan Biag[3], Angela John Thurman[3], Charles-Olivier Martin[2], Anne-Marie Bélanger[2], Cory Rosenfelt[4], Flora Tassone[3,5], Leonard J. Abbeduto[3,6], Sébastien Jacquemont[2,7], Randi Hagerman[3], François Bolduc[4], David Hessl[3,6], Andrea Schneider[3,8] and Sarah Lippé[1,2]*

[1] Department of Psychology, University of Montreal, Montreal, QC, Canada, [2] Research Center of the Sainte-Justine University Hospital, Montreal, QC, Canada, [3] University of California Davis Medical Investigation of Neurodevelopmental Disorders (MIND) Institute, Sacramento, CA, United States, [4] Department of Pediatric Neurology, University of Alberta, Edmonton, AB, Canada, [5] Department of Biochemistry and Molecular Medicine, University of California Davis School of Medicine, Sacramento, CA, United States, [6] Department of Psychiatry and Behavioral Sciences, University of California Davis School of Medicine, Sacramento, CA, United States, [7] Department of Pediatrics, University of Montreal, Montreal, QC, Canada, [8] California North State University, College of Psychology, Rancho Cordova, CA, United States

OPEN ACCESS

Edited by:
Wenbin Guo,
Central South University, China

Reviewed by:
Olga Mikhailovna Bazanova,
State Research Intstitute of Neuroscience and Medicine, Russia
Carlos M. Gómez,
Sevilla University, Spain

***Correspondence:**
Sarah Lippé
sarah.lippe@umontreal.ca

[†]These authors share first authorship

Specialty section:
This article was submitted to Neuroimaging and Stimulation, a section of the journal Frontiers in Psychiatry

Received: *23 June 2021*
Accepted: *06 October 2021*
Published: *11 November 2021*

Citation:
Proteau-Lemieux M, Knoth IS, Agbogba K, Côté V, Barlahan Biag HM, Thurman AJ, Martin C-O, Bélanger A-M, Rosenfelt C, Tassone F, Abbeduto LJ, Jacquemont S, Hagerman R, Bolduc F, Hessl D, Schneider A and Lippé S (2021) EEG Signal Complexity Is Reduced During Resting-State in Fragile X Syndrome. Front. Psychiatry 12:716707. doi: 10.3389/fpsyt.2021.716707

Introduction: Fragile X syndrome (FXS) is a genetic disorder caused by a mutation of the *fragile X mental retardation 1 gene* (*FMR1*). FXS is associated with neurophysiological abnormalities, including cortical hyperexcitability. Alterations in electroencephalogram (EEG) resting-state power spectral density (PSD) are well-defined in FXS and were found to be linked to neurodevelopmental delays. Whether non-linear dynamics of the brain signal are also altered remains to be studied.

Methods: In this study, resting-state EEG power, including alpha peak frequency (APF) and theta/beta ratio (TBR), as well as signal complexity using multi-scale entropy (MSE) were compared between 26 FXS participants (ages 5–28 years), and 77 neurotypical (NT) controls with a similar age distribution. Subsequently a replication study was carried out, comparing our cohort to 19 FXS participants independently recorded at a different site.

Results: PSD results confirmed the increased gamma, decreased alpha power and APF in FXS participants compared to NT controls. No alterations in TBR were found. Importantly, results revealed reduced signal complexity in FXS participants, specifically in higher scales, suggesting that altered signal complexity is sensitive to brain alterations in this population. The replication study mostly confirmed these results and suggested critical points of stagnation in the neurodevelopmental curve of FXS.

Conclusion: Signal complexity is a powerful feature that can be added to the electrophysiological biomarkers of brain maturation in FXS.

Keywords: fragile X syndrome, hyperexcitability, EEG resting-state, signal complexity, multiscale entropy, alpha peak frequency, neurodevelopmental disorders, development

INTRODUCTION

Fragile X syndrome (FXS) is an X-linked genetic disorder caused by dynamic mutations of the *fragile X mental retardation 1 gene* (*FMR1*), consequently leading to alterations, or to complete absence of the *fragile X mental retardation protein* (FMRP), its encoded protein. The main role of FMRP is to repress the translation of specific mRNAs during protein synthesis (1). Its absence leads to excessive protein synthesis (2), which is associated with impaired synaptic plasticity (3). FMRP is essential to brain development, as well as synaptic maturation and plasticity. FXS is the most common monogenetic cause of inherited intellectual disability (ID) and single gene cause of autism spectrum disorder (ASD). It is also associated with physical, behavioral, cognitive and emotional impairments. The clinical features of patients with FXS vary significantly from one individual to another, especially between men and women, due to the unaffected second X chromosome present in women.

Hyperexcitability is a core feature across FXS animal models and has been suggested to be a potential origin of various psychiatric and neurological symptoms observed in patients affected by the condition (4). Both overactivation of metabotropic glutamate receptors (mGluRs) leading to increased neuronal excitability (5, 6), as well as a compromised GABAergic system resulting in reduced inhibition (7), have been discussed as potential contributors to excitation/inhibition imbalance in FXS. Hence, the neurophysiological abnormalities found in humans support these notions of excitation/inhibition imbalance, including enhanced electrocortical responses and reduced intracortical inhibition, as measured by transcranial magnetic stimulation (8, 9). In addition, reduced levels of cAMP in FXS further interfere with neuronal connectivity and inhibitory responses (10). Alterations in cortical excitability may be linked to abnormal sensory processing in FXS patients. Studies investigating visual and auditory processing in FXS through event-related potentials (ERPs) with electroencephalogram (EEG) have shown important alterations in both modalities, characterized by increased amplitudes of sensory ERP components and reduced habituation to sensory stimuli (11–17).

Recent resting-state EEG studies have shown increased resting-state power in animal models of FXS, notably in delta and gamma frequency bands (18, 19). Studies with FXS adults (20), male adults (21) and young boys (22) obtained similar results. Gamma frequency bands are associated with high-level cognitive functions in healthy controls while performing cognitively demanding tasks (20, 23). However, perturbations in gamma oscillations during resting-state recordings have been reported in psychiatric disorders, as well as in neurodevelopmental conditions (20, 23–26). In fact, altered gamma power is thought to be associated with the cognitive deficits present in these populations, notably impaired social communication skills in FXS (20).

Resting-state EEG also showed evidence of increased theta power and decreased alpha power in FXS adults when compared to controls (20, 27). Alpha frequencies are the most dominant oscillations in adult resting-state EEG (20). Reduced alpha could be a marker of general brain dysfunction in FXS (27–29). Several alterations in resting-state EEG spectral domains have been identified in FXS, which could be reflected in specific EEG biomarkers of brain maturation and hyperexcitability. In particular, alpha peak frequency, theta/beta ratio, and signal complexity, a non-linear measure of brain dynamics, have been shown to be sensitive to atypical brain maturation and to the presence of neurodevelopmental disorders. This study aims at revealing whether these EEG biomarkers are affected in FXS.

First, alpha peak frequency (APF), namely the frequency at which maximum power occurs within the alpha band, shifts from theta to alpha during brain maturation. Importantly, it was found to be altered in many neurodevelopmental disorders, including attention deficit hyperactivity disorder (ADHD), ASD, and FXS (21, 28, 30).

Second, the theta/beta power ratio (TBR) of elevated slow theta waves and decreased fast beta waves is the most commonly known EEG biomarker for ADHD (31, 32). TBR could be affected in FXS since evidence of increased theta power has been shown (20, 27). However, how TBR is affected in FXS considering previous reports of elevated high beta/low gamma power in FXS is unclear.

Finally, complexity of the EEG signal is considered a marker of brain maturation and cognitive functioning (33), as it is known to increase with age. Moreover, its increase was found to be sensitive to specific sensory brain region maturation patterns (34). Although inconsistent, several studies with ADHD and ASD patients showed a general reduction in complexity, when compared to controls (35–37), while another study showed that people with ADHD have reduced complexity in the alpha frequency band (38). Multiscale entropy (MSE) is an ideal technique to quantitatively measure complexity, as it investigates temporal complexity of the signal at multiple time scales. Considering the presence of ADHD and ASD symptoms in FXS patients, it is expected that their signal complexity will also be reduced.

The present study aims to investigate, in a large sample of FXS patients, whether specific EEG markers of brain maturation, namely, APF, TBR, and complexity of the signal are affected in the condition. Here, we hypothesized that TBR of FXS patients would be elevated, and that alpha peak frequency would be reduced, compared to controls. We also predicted that FXS patients would show a reduction of EEG complexity. To our knowledge, this study is the first to explore TBR and EEG complexity in the FXS population. Furthermore, a replication study was carried out with an independently recorded additional FXS sample to ensure that EEG biomarkers can be replicated across different cohorts and study sites.

MATERIALS AND METHODS

Participants

Thirty nine participants with a genetic diagnosis of FXS were recruited for the study. The diagnosis was based on molecular genetic examinations (39), and FXS was diagnosed when 200 or more repetitions of CGG were present. Twenty-six participants were able to complete at least a partial resting-state recording. Analysis was conducted with a final sample of

TABLE 1 | Demographics of the study population.

	FXS	Controls
N	26	77
Males (*n*, %)	16 (61.54%)	40 (51.95%)
Females (*n*, %)	10 (38.46%)	37 (48.05%)
Age		
Mean ± SD	13.42 ± 6.7	11.55 ± 6.36
Range	5–28	5–30
Non-verbal IQ		
Mean ± SD	65.54 ± 22.84	110 ± 15.64
Range	36–123	44–113
ABC-C		
Composite score (mean ± SD)	33.35 ± 24.62	NA
Irritability subscale (mean ± SD)	9.73 ± 11.69	NA
Lethargy subscale (mean ± SD)	4.96 ± 4.22	NA
Stereotypy subscale (mean ± SD)	3.31 ± 2.87	NA
Hyperactivity subscale (mean ± SD)	9.31 ± 7.18	NA
Inappropriate speech subscale (mean ± SD)	3.73 ± 2.85	NA
Social avoidance subscale (mean ± SD)	2.31 ± 2.15	NA

ABC-C, Aberrant Behavior Checklist-Community; IQ, Intellectual quotient; SD, Standard deviation.

TABLE 2 | Comorbid diagnoses and medication in the FXS population.

	Male	Female
N	15	11
Comorbid diagnoses		
ASD	8	1
Epilepsy	1	0
Intellectual disability	9	3
Learning disability	3	2
Speech/language impairments	3	0
Medication		
Antipsychotics	0	0
Antidepressants	3	1
Anxiolytics	1 (GABA supp.)	0
Psychostimulants	6	1
Non-verbal IQ		
Mean ± SD	60.2 ± 23.62	72.82 ± 20.54
Range	36–123	44–113
T-test	$t_{(23)} = -1.48$, $p = 0.15$	
ABC-C		
Composite score (mean ± SD)	39.13 ± 18.88	25.45 ± 29.95
T-test	$t_{(24)} = 1.43$, $p = 0.167$	
Irritability subscale (mean ± SD)	10.13 ± 9.91	9.18 ± 14.28
T-test	$t_{(24)} = 0.2$, $p = 0.84$	
Lethargy subscale (mean ± SD)	5.27 ± 3.86	4.55 ± 4.82
T-test	$t_{(24)} = 0.42$, $p = 0.68$	
Stereotypy subscale (mean ± SD)	4.33 ± 2.61	1.91 ± 2.7
T-test	$t_{(24)} = 2.3$, $p = 0.03$*	
Hyperactivity subscale (mean ± SD)	11.13 ± 6.21	6.82 ± 7.95
T-test	$t_{(24)} = 1.56$ $p = 0.13$	
Inappropriate speech subscale (mean ± SD)	5.2 ± 2.57	1.73 ± 1.85
T-test	$t_{(24)} = 3.8$, $p = 0.001$*	
Social avoidance subscale (mean ± SD)	3.07 ± 2.31	1.27 ± 1.42
T-test	$t_{(24)} = 2.27$, $p = 0.03$*	

*ABC-C, Aberrant Behavior Checklist-Community; ASD, Autism spectrum disorder; SD, Standard deviation; *Statistically significant.*

26 FXS participants. Seventy-eight neurotypical controls (NT) with a similar age distribution were recruited for the study. All neurotypical controls completed the EEG resting-state recording, but one had to be excluded due to insufficient artifact-free data. Analysis was conducted with 77 neurotypical controls. **Table 1** provides demographic information on the final study population that was included for analysis. **Table 2** describes the FXS population in more detail.

FXS participants were recruited via the genetic clinics at the CHU Sainte-Justine Mother and Child University Hospital Center and at the University of Alberta, via parent associations and social media. NT controls were recruited via the NED lab's database of volunteers, posters and flyers in universities, colleges, and community centers, social media, and ads on classified websites. Exclusion criteria for the neurotypical group were histories of health-related problems potentially affecting development (e.g., complications during pregnancy and birth, brain trauma, epilepsy, neurodevelopmental disorders, psychopathology, etc.). The study protocol was reviewed and approved by the ethics committees at CHU Sainte-Justine and the University of Alberta and was carried out according to the declaration of Helsinki. Procedures were explained in detail prior to obtaining written informed consent from participants or legal caregivers and assent from participants.

Behavioral Measures

A short cognitive assessment was carried out using Leiter-R (40) or Leiter-3 (41) brief IQ for FXS and most of the NT participants. Few NT participants underwent WPPSI-IV (42) or WISC-V (43) (depending on age) evaluation instead of the Leiter. For these participants, the fluid reasoning scale was selected to ensure comparability with the non-verbal Leiter batteries. PIQ results are summarized in **Table 1**. The revised version of the Aberrant Behavior Checklist for Community [ABC-C; (44)], specifically developed for the FXS population, was used. In this version, social avoidance, which is highly associated with ASD and FXS, was added as a sixth subscale. The ABC-C was completed by the caregiver to assess autistic traits in the clinical populations.

Procedure

Pictograms and videos were used to prepare clinical and young NT participants for the EEG procedure. EEG net installation was adapted through storytelling and games to increase acceptance of the procedure. A movie was shown during net installation to increase collaboration in participants. For the resting-state recording, participants were told to relax as much as possible while moving as little as possible ("statues game") keeping their eyes open and directed toward the screen where a fixation cross was displayed. If necessary, to increase acceptance and reduce

movement artifacts, participants could watch a movie on the screen or favorite content on their tablet. As much as possible, resting EEG was recorded until a minimum of 2 min total of movement-free signals were obtained.

The EEG recording was carried out in soundproof experimental chambers in the CHU Sainte-Justine hospital and at the University of Alberta, using 128-electrode dense array EEG systems (Magstim EGI, Eugene, OR, USA). Signals were acquired and processed by G4 MacIntosh computers using NetStation Software (Version 4.5.4 at CHU Sainte-Justine and Version 2.0 at University of Alberta). EEG data were digitized and processed at a sampling rate of 1,000 Hz using the vertex electrode (Cz) as an online reference and an online bandpass filter of 0.1–500 Hz (Nyquist frequency) was applied. Impedances were verified prior to recording and kept below 40 kΩ (45).

Replication Study

An additional 20 EEG resting-state datasets recorded in FXS participants were provided by the University of California Davis MIND Institute with the goal of verifying if our results can be replicated in a different cohort of FXS participants. The study was approved by the Institutional Review Board at University of California, Davis. All participants and parents/caretakers of participants gave their written consent to participate in the study. Two min of open eyes resting-state were recorded analogous to the procedure in the Montreal/Edmonton cohort. In compliant participants, alternating blocks of eyes open and eyes closed resting-state were performed. For the purpose of the current paper, only open eyes resting-state was analyzed. One participant had to be excluded since not enough clean epochs were available. Thus, 19 datasets were submitted for analysis. EEG data were acquired using a Brain Products (Brain Products, Germany) Quickamp system with an Acticap 32-channel Ag+/Ag+Cl-active electrode array according to the 10–20 international channel location system and using Brain Recorder software. EEG was digitized and processed at a sampling rate of 1,000 Hz using FCz as an online reference and an online bandpass filter of 0.1–500 Hz. Impedances were maintained below 10kΩ.

EEG Signal Processing

Pre-processing

Offline analyses were carried out using MATLAB (version R2018b) and EEGLAB toolbox (v.14.1.2) (46, 47). Data were filtered with a 0.5 Hz high-pass filter, a 150 Hz low-pass filter, and a 60 Hz notch filter. For all participants recorded with the EGI 128-channel system, 28 electrodes around the face and neck were removed due to poorer signal quality in these areas. The remaining noisy electrodes were removed using a semi-automatic procedure: electrodes with a total standard deviation of >200 μV and <2 μV were automatically removed; electrodes with sporadic behavior were removed manually during subsequent visual inspection. Then, data were re-referenced to the average reference and blinks, saccades and cardiac activity were removed using independent component analysis (ICA). Continuous data was segmented into 2 s epochs using a 2-s sliding window in 1 s steps (50% overlap). This allowed us to increase the availability of clean data segments and it is also necessary for window corrections pre-PSD analyses. Artifact rejection was performed semi-automatically: epochs containing amplitudes >200 μV and <-200 μV were tagged and artifacted segments were manually removed during subsequent visual inspection, accounting for all remaining artifacts (movement etc.). Data analysis and quality metrics are presented in **Supplementary Table 1**. For data reduction purposes, eight regions of interest (ROI) were defined covering the following areas as closely matched as possible between EGI 128-channel and Brain Products 32-channels ActiCap locations (EGI and Brain Products): fronto-central (FCz, 5/3 electrodes for EGI/Brain Products system respectively), central (Cz, 5/3 electrodes), centro-occipital (Oz, 7/3 electrodes), /parieto-zentral (Pz, 6/4 electrodes), frontal-left (FL, 6/2 electrodes), frontal right (FR, 6/2 electrodes), temporal left (TL, 6/2 electrodes), temporal right (TR, 6/2 electrodes). Due to electrode removal during pre-processing, some participants missed some of the ROI. These were treated as missing data in subsequent analyses.

Power Spectral Density

Power spectral density (PSD) describes the signal distribution in terms of power per frequency using Fast Fourier Transformation (FFT). In order to reduce windowing effects, a hamming window was applied on the previously overlapped epochs before computing the FFT transform. The current method allowed us to analyze frequencies between 1 Hz and 100 Hz with a resolution of 0.5 Hz.

Multi-Scale Entropy

MSE was used to measure signal complexity in participants' EEG while at rest. MSE calculations were based on the algorithm proposed by (48) which generates multiple timescales through downsampling of the original EEG signal in a so-called coarse-graining procedure. The original timescale is divided into non-overlapping windows that are then averaged together. The time series shortens as window length increases. In the current study, the coarse-graining procedure was performed on all "clean" 2,000 ms epochs of resting-state data for every participant and ROI. SampEn estimates signal variability for every time series through the predictability of amplitude patterns within the time series (49). Pattern length was set to $m = 2$, meaning that the algorithm counts the number of matching sequences for two consecutive points in the signal. Tolerability was set to $r = 0.5$ indicating that amplitude points falling $\leq$50% of the time-series standard deviation equal were considered by the algorithm. Subsequently, the number of m + 1 sequences of data point matches is counted and SampEn is defined as the natural logarithm of the ratio of total m to $m + 1$ data point matches. Finally, MSE values for all epochs were averaged for each participant and ROI to obtain a final MSE score for every time scale from 1 to 40.

Statistical Analysis

Statistical analyses were performed using SPSS Statistics, version 23 (IBM Corp., Armonk, NY, USA). Data distribution was verified using histograms as well as skewness/kurtosis criteria (values within−1 and 1 were considered acceptable) and z-scores.

The significance level for statistical tests was set to 5% ($p = 0.05$) and Greenhouse-Geisser correction was applied to all mixed design ANOVAs. Significant interactions were investigated using follow-up ANOVAs and *post hoc* comparisons using Bonferroni correction. For PSD analysis, explorative *t*-tests between groups (FXS vs. controls) were performed for each frequency in 0.5Hz increments from 1 to 50 and 70 to 100Hz (50–70Hz were not included in the analysis due to the applied Notch filter) across all ROI in order to define frequency bands of interest. Subsequently, frequency bands of interest were averaged for each participant and ROI and compared between groups using a mixed-design ANOVA with age as covariable when appropriate. Alpha peak frequencies (APF) were defined as the frequency with maximum amplitude between 4.5 and 14 Hz for each participant and ROI. Mixed design ANOVA was carried out to compare APF between groups with age as covariable when appropriate. Theta-beta ratio (TBR) was calculated as the average of frequencies 4–8 Hz divided by the average of frequencies 14–30 Hz for each participant and ROI. TBR was compared between groups using mixed-design ANOVA with age as covariable when appropriate. For MSE, the complexity index was calculated as area-under-the-curve for scales 1–40 in order to obtain a general indication of signal complexity. Mixed design ANOVA was used to carry out group comparisons across ROIs for CI with age as covariable when appropriate. In a follow-up analysis, scales 1–20 and 21–40 were averaged in order to obtain a more fine-grained picture of differences in signal complexity between groups that were assessed in a subsequent mixed design ANOVA. Additionally, sex differences within the FXS group in APF, TBR, CI and averaged scales were assessed using mixed design ANOVA with age as covariable when appropriate. In order to assess the relationship between EEG measures and clinical outcomes, IQ and ABC-C composite score and subscales were correlated with APF, TBR, CI and averaged scales. Significance levels for correlations were corrected for multiple testing using Bonferroni's adjustment. Given that EEG measures correlated between ROI, Bonferroni's adjustment was corrected for correlated outcome variables (50). For the replication part of the study, all PSD and MSE measures were first compared between FXS cohorts using mixed design ANOVA. In subsequent exploratory analyses, the FXS replication cohort was compared to the control group to verify if results obtained in the original group comparison could be replicated. The same procedure of analyses will be followed as in the original FXS vs. controls comparison, but results will be reported with a focus on group effects to facilitate readability. Correlations between age and PSD/MSE measures were repeated in the UC Davis cohort.

RESULTS

We first analysed PSD in order to verify if we can replicate the results previously reported in the literature. We then analysed MSE in our cohort of FXS and control participants. Finally, we carried out a replication study with an independent sample of FXS participants to verify if our results can be replicated across cohorts and sites using different EEG systems.

PSD

Figure 1 shows group mean power spectra for FXS vs. controls in Cz. Explorative *t*-tests between groups (FXS vs. controls) across all ROIs revealed the following frequency bands of interest: 1–2.5 (delta) in Cz, FL, FR, FCz, TR, TL; 9.5–11 (alpha) and 25–49.5 (low gamma) in all ROI. A mixed design ANOVA controlled by age as some of the frequency bands correlated with age ($p < 0.02$), revealed significant main effects for ROI [$F_{(4.4,392.9)} = 43.65$, $p < 0.0001$, $\eta^2 = 0.33$] frequency bands [$F_{(1.5,135.7)} = 466.14$, $p < 0.0001$, $\eta^2 = 0.84$] and age [$F_{(1,89)} = 6044$, $p < 0.0001$, $\eta^2 = 0.4$] and significant interactions for ROI and age [$F_{(4.4,392.9)} = 5.88$, $p < 0.0001$, $\eta^2 = 0.06$], ROI and group [$F_{(4.4,392.9)} = 3.66$, $p = 0.005$, $\eta^2 = 0.04$], frequency band and age [$F_{(1.5,135.6)} = 87.7$, $p < 0.0001$, $\eta^2 = 0.5$], frequency band and group [$F_{(1.5,135.6)} = 12.57$, $p < 0.0001$, $\eta^2 = 0.12$], ROI and frequency band [$F_{(5.6,501.4)} = 41.19$, $p < 0.0001$, $\eta^2 = 0.32$], ROI and frequency band and age [$F_{(5.6,501.4)} = 12.61$, $p < 0.0001$, $\eta^2 = 0.12$], ROI and frequency band and group [$F_{(5.6,501.4)} = 4.6$, $p < 0.0001$, $\eta^2 = 0.049$]. In order to disentangle these interactions, follow-up ANOVAs per frequency band were carried out.

Delta (1-2.5)

In delta, significant main effects for group [$F_{(1,97)} = 8.14$, $p = 0.005$, $\eta^2 = 0.07$], ROI [$F_{(4.5,433.5)} = 53.55$, $p < 0.0001$, $\eta^2 = 0.35$] and age [$F_{(1,97)} = 100.78$, $p < 0.0001$, $\eta^2 = 0.5$] were observed as well as significant interactions between ROI and age [$F_{(4.7,433.5)} = 11.82$, $p < 0.0001$, $\eta^2 = 0.11$] and ROI and group [$F_{(4.5,433.5)} = 4.77$, $p = 0.001$, $\eta^2 = 0.047$]. *Post-hoc* comparisons using Bonferroni-correction revealed higher delta power in FXS ($p = 0.005$) and significant differences in delta power between almost all ROI. **Figure 2** shows a topographic representation of delta power in FXS (A) and controls (B).

Alpha (9.5-11)

In alpha, a significant main effect for group [$F_{(1,95)} = 10.67$, $p = 0.002$, $\eta^2 = 0.1$] and ROI [$F_{(3.4,320.4)} = 37.2$, $p < 0.0001$, $\eta^2 = 0.28$] was found as well as a significant interaction between ROI and group [$F_{(3.4,320.4)} = 3.36$, $p = 0.015$, $\eta^2 = 0.03$]. *Post-hoc* comparisons using Bonferroni-correction revealed lower alpha power in FXS ($p = 0.002$) and significant differences in alpha power mostly between Cz, Oz and all other ROIs. A topographic representation of alpha power in FXS and controls is shown in **Figure 3**.

Low Gamma (25-49.5)

Significant main effects for group [$F_{(1,95)} = 27.8$, $p < 0.0001$, $\eta^2 = 0.23$], ROI [$F_{(3.4,320.5)} = 41.79$, $p < 0.0001$, $\eta^2 = 0.31$] and age [$F_{(1,95)} = 12.8$, $p < 0.0001$, $\eta^2 = 0.12$) were observed as well as significant interactions between ROI and age [$F_{(3.4,320.5)} = 3.92$, $p = 0.007$, $\eta^2 = 0.04$] and ROI and group [$F_{(3.4,320.5)} = 3.37$, $p = 0.015$, $\eta^2 = 0.03$]. *Post-hoc* comparisons using Bonferroni-correction revealed higher gamma power in FXS ($p < 0.0001$) and significant differences in gamma power between almost all ROI ($p < 0.018$). Gamma power in FXS and controls is illustrated in **Figure 4**.

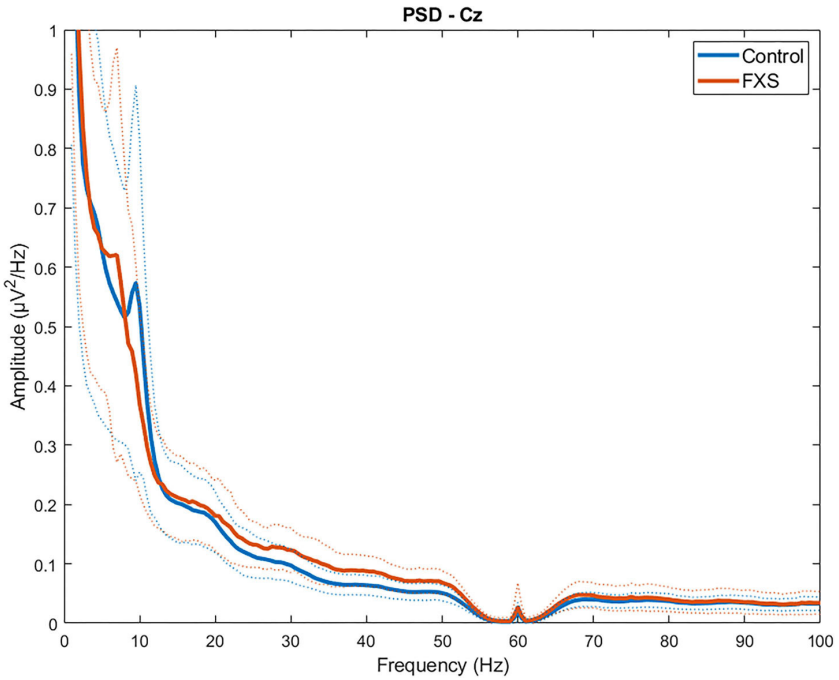

FIGURE 1 | Group average power spectra for FXS vs. controls in Cz region of interest. Dotted lines indicate SD for each group.

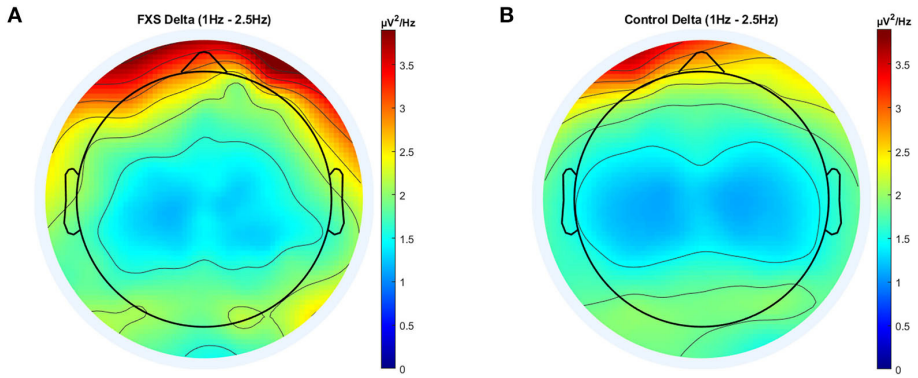

FIGURE 2 | Topographic representation of average power spectral density in the FXS **(A)** and control **(B)** group for the delta band (1–2.5 Hz).

Alpha Peak Frequency

Bonferroni's adjustment for eight correlations (one per ROI), corrected for the mean correlation between outcome variables ($r = 0.64$, $p < 0.0001$), determined a significance level of $p < 0.024$ for a correlation to be considered as significant. APF correlated positively with age in all ROI ($p < 0.03$), except Oz ($r = 0.22$, $p = 0.024$) and TR ($r = 0.33$, $p = 0.03$), confirming that APF increases with age. However, when correlations were carried out separately for FXS and controls, APF was still highly correlated with APF in controls across all ROI ($p < 0.009$); in FXS however, APF was only correlated with age in Cz ($r = 0.54$, $p = 0.005$) and FCz ($r = 0.44$, $p = 0.023$). To ensure that this effect is not simply due to the smaller sample size in the FXS group, this correlation will be repeated with the replication cohort. **Figure 5** shows an exemplary scatterplot for APF and age in Cz and Pz for FXS and controls. A mixed design ANOVA [ROI (8) X group (2)] controlled for age revealed a significant main effect for group [$F_{(1,97)} = 25.83$, $p < 0.0001$, $\eta^2 = 0.2$] and age [$F_{(1,97)} = 27.6$, $p < 0.001$, $\eta^2 = 0.22$], indicating lower APF in FXS when compared to controls ($p < 0.0001$). No significant interactions were found.

Theta-Beta Ratio

For correlations, a significance level of $p < 0.036$ was determined using Bonferroni-correction adjusted for mean correlation between outcome variables ($r = 0.85$, $p < 0.0001$). TBR

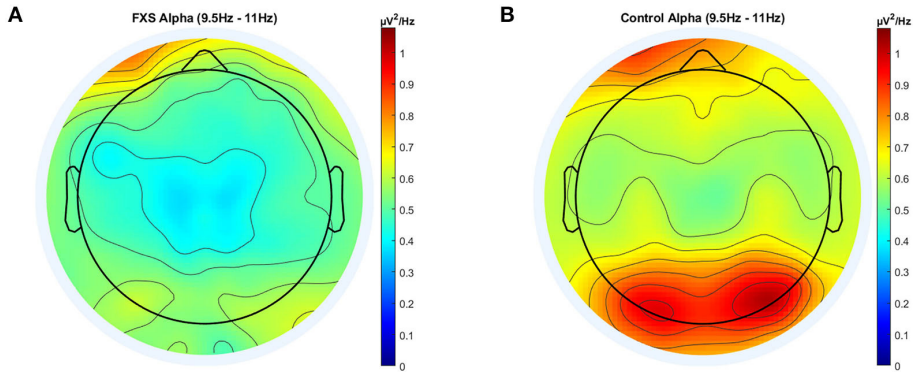

FIGURE 3 | Topographic representation of average power spectral density in the FXS **(A)** and control **(B)** group for the alpha band (9.5–11 Hz).

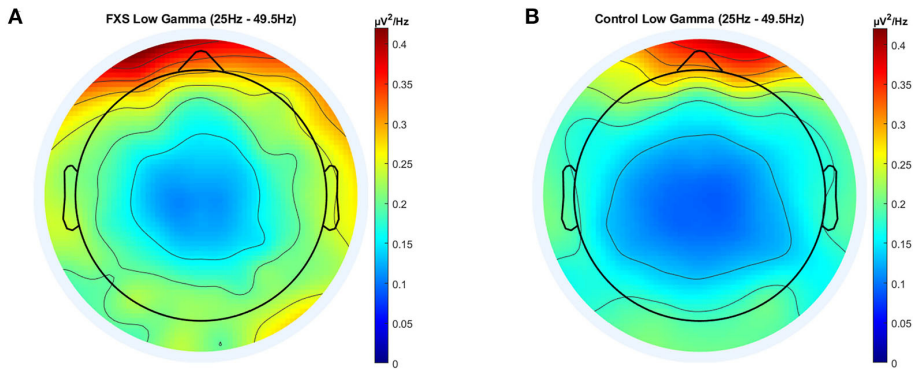

FIGURE 4 | Topographic representation of average power spectral density in the FXS **(A)** and control **(B)** group for the low gamma band (25–49.5 Hz).

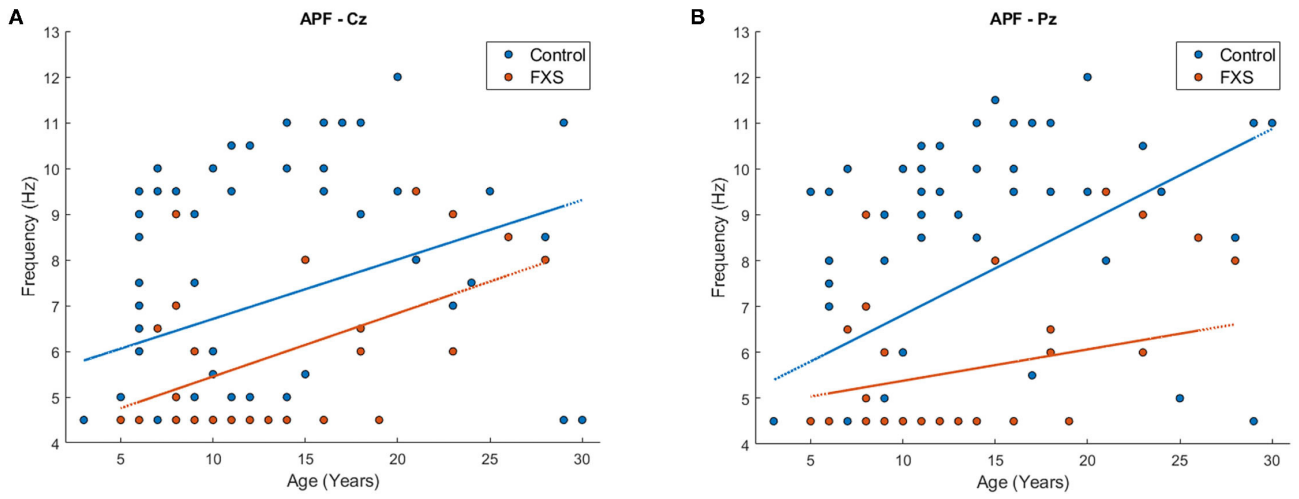

FIGURE 5 | Scatterplot for age and APF for FXS (red) and controls (blue) in region of interest Cz **(A)** and Pz **(B)**.

correlated negatively with age across all ROI in the whole sample ($p < 0.0001$) and within both groups (FXS; $p < 0.01$, controls: $p < 0.0001$). A mixed design ANOVA controlled by age revealed main effects for ROI [$F_{(4.9,439.2)} = 41.89$, $p < 0.0001$, $\eta^2 = 0.32$] and age [$F_{(1,89)} = 53.65$, $p < 0.0001$, $\eta^2 = 0.38$], and a significant interaction between age and ROI [$F_{(4.9,439.2)} = 10.31$, $p < 0.0001$, $\eta^2 = 0.1$] but no group effects or interactions.

MSE

Complexity Index

Significance level for correlations was corrected to $p < 0.031$ [Bonferroni-correction adjusted for mean correlation between outcome variables ($r = 0.77$, $p < 0.0001$)]. CI correlated highly with age across all ROI in the whole sample ($p < 0.006$). The same was found within the control group; strong positive correlations between CI and age across all ROI ($p < 0.0001$). In the FXS group however, the correlation between age and CI was less prominent and only found in central ($p < 0.023$) but not in lateral ROIs ($p > 0.4$). This correlation will be repeated in the replication study in order to verify the robustness of the result. A mixed design ANOVA controlled for age revealed main effects for ROI [$F_{(4.1,341.1)} = 16.1$, $p < 0.0001$, $\eta^2 = 0.16$], age [$F_{(1,84)} = 35.1$, $p < 0.0001$, $\eta^2 = 0.3$] and group [$F_{(1,84)} = 6.45$, $p = 0.013$, $\eta^2 = 0.07$], as well as interactions between ROI and age [$F_{(4.1,341.1)} = 8.17$, $p < 0.0001$, $\eta^2 = 0.09$] and ROI and group [$F_{(4,341.1)} = 2.64$, $p = 0.033$, $\eta^2 = 0.03$]. Bonferroni-corrected *post hoc* comparisons revealed lower CI in FXS as compared to controls and differences between most ROI. **Figure 6** shows a topographic representation of CI in FXS (A) and controls (B).

Averaged Time Scales S1–20, S21–40

Figure 7 illustrates MSE across time scales for FXS and control participants in Cz (A) and TL (B). Alpha level was corrected to $p < 0.016$ adjusted for mean correlation of output variables ($r = 0.60$, $p < 0.0001$). S1–20 correlated positively with age in all ROIs ($p < 0.0001$). In controls, age correlated with S1–20 in all ROI ($p < 0.014$) and with S21–40 in all ROI except TL ($p = 0.014$). In FXS, only S1–20 correlated with age for midline ROI (Cz: $r = 0.752$, $p < 0.0001$, FCz: $r = 0.67$, $p < 0.0001$, Oz: 0.77, $p < 0.0001$, Pz: 0.69, $p < 0.0001$), whereas S21–40 did not correlate with age in FXS. A mixed design ANOVA controlled for age revealed main effects for group [$F_{(1,84)} = 6.53$, $p = 0.012$, $\eta^2 = 0.072$], age [$F_{(1,84)} = 34.61$, $p = 0.0001$, $\eta^2 = 0.29$], averaged scales [$F_{(1,84)} = 335.78$, $p < 0.0001$, $\eta^2 = 0.8$] and ROI [$F_{(4.1,340.7)} = 15.96$, $p < 0.0001$, $\eta^2 = 0.16$], as well as interactions for ROI and age [$F_{(4.1,340.7)} = 8.07$, $p < 0.0001$, $\eta^2 = 0.09$], ROI and group [$F_{(4.1,340.7)} = 2.63$, $p = 0.034$, $\eta^2 = 0.03$], scales and age [$F_{(1,84)} = 6.83$, $p = 0.011$, $\eta^2 = 0.075$], scales and group [$F_{(1,84)} = 11.64$, $p = 0.001$, $\eta^2 = 0.12$], as well as ROI and scales [$F_{(4.7,393.5)} = 12.66$, $p < 0.0001$, $\eta^2 = 0.13$]. A follow-up mixed design ANOVA per averaged scale revealed a main effect for ROI [$F_{(4.5,376.2)} = 17.72$, $p < 0.0001$, $\eta^2 = 0.17$] and age [$F_{(1,84)} = 60.48$, $p < 0.0001$, $\eta^2 = 0.42$] but no main effects or interactions for group in the S1–20 scales. Conversely, a mixed design ANOVA for S21–40 revealed a main group effect [$F_{(1,84)} = 11.84$, $p = 0.001$, $\eta^2 = 0.12$] and a ROI and group interaction [$F_{(4.1,341.9)} = 2.64$, $p = 0.033$, $\eta^2 = 0.03$], as well as main effects for ROI [$F_{(4.1,341.9)} = 13.39$, $p < 0.0001$, $\eta^2 = 0.14$], age [$F_{(1,84)} = 10$, $p = 0.002$, $\eta^2 = 0.12$] and an ROI and age interaction [$F_{(4.1,341.9)} = 7.58$, $p < 0.0001$, $\eta^2 = 0.08$]. MSE was found to be lower in FXS compared to controls in higher time scales (S21–40), but not in lower time scales (S1–20). **Figure 8** shows a topographic representation of S1–20 and S21–40 in FXS (A, C) and controls (B, D).

EEG Measures and Clinical Outcomes

IQ

Using the Bonferroni-adjusted and for correlation between outcome variables adjusted alpha level of $p < 0.024$, APF correlated positively with IQ in the whole sample in Oz ($r = 0.23$, $p = 0.022$) and TL ($r = 0.24$, $p = 0.016$). Within groups, APF did not correlate with IQ in controls, but correlated negatively with IQ in FXS in Cz ($r = -0.49$, $p = 0.01$), FCz ($r = -0.45$, $p = 0.023$), TR ($r = -0.51$, $p = 0.012$) and TL ($r = -0.47$, $p = 0.017$). No correlations between TBR and IQ were found in the whole sample or within groups. CI, S1–20 and S20–40 were not found to be correlated with IQ for the whole sample or within groups.

ABC-C

Since the ABC-C is not an appropriate measurement tool for control populations, correlations were only carried out in the FXS group. APF at FL correlated positively with the inappropriate language subscale ($r = 0.463$, $p = 0.017$, note that alpha level for APF was corrected to $p < 0.024$), suggesting that FXS participants with a higher APF presented more inappropriate speech according to the ABC-C questionnaire. Further, APF in TR was found to be negatively correlated with the lethargy scale ($r = -0.48$, $p = 0.015$), suggesting less lethargy symptoms in FXS individuals with a higher APF. Expectedly, TBR correlated with the hyperactivity subscale in all frontal ROI (FL: $r = 0.55443$, $p = 0.0063$; FR: $r = 0.51$, $p = 0.01$; FCz: $r = 0.581$, $p = 0.003$; note that alpha level for TBR was corrected to $p < 0.036$), indicating that FXS participants with higher TBR presented more hyperactivity symptoms. CI correlated negatively with the ABC-C composite score at Pz ($r = -0.56$, $p = 0.007$, note that alpha level for CI was corrected to $p < 0.031$) and Cz ($r = -0.59$, $p = 0.002$); with the irritability subscale at Pz ($r = -0.55$, $p = 0.008$), TL ($r = -0.5$, $p = 0.012$) and Cz ($r = -0.66$, $p < 0.0001$); with the lethargy subscale at Pz ($r = -0.51$, $p = 0.016$); and with the hyperactivity subscale at Pz ($r = -0.57$, $p = 0.006$) and Cz ($r = -0.61$, $p = 0.001$). Similarly, S1–20 correlated negatively with the ABC composite score at Cz ($r = -0.49$, $p = 0.011$, note that alpha level for S1–20 and S21–40 was corrected to $p < 0.016$), FCz ($r = -0.53$, $p = 0.007$); with the irritability subscale at Cz ($r = -0.57$, $p = 0.002$) and FCz ($r = -0.54$, $p = 0.007$); with the hyperactivity scale at Cz ($r = -0.62$, $p = 0.001$), FCz ($r = -0.63$, $p = 0.001$) and Pz ($r = -0.57$, $p = 0.006$). Finally, S21-40 correlated negatively with the ABC-C composite score at Cz ($r = -0.57$, $p = 0.002$), FCz ($r = -0.54$, $p = 0.006$) and Pz ($r = -0.55$, $p = 0.009$); with the irritability scale at Cz ($r = -0.63$, $p = 0.001$); with the lethargy scale at FCz ($r = -0.5$, $p = 0.01$) and Pz ($r = -0.57$, $p = 0.006$); with the hyperactivity scale at Cz ($r = -0.5$, $p = 0.01$); and with the social avoidance scale at FCz ($r = -0.6$, $p = 0.001$). These correlations indicate that higher EEG signal complexity across measures predicts lower scores on the ABC-C questionnaire, specifically lower reported symptoms of irritability, lethargy, hyperactivity and social avoidance.

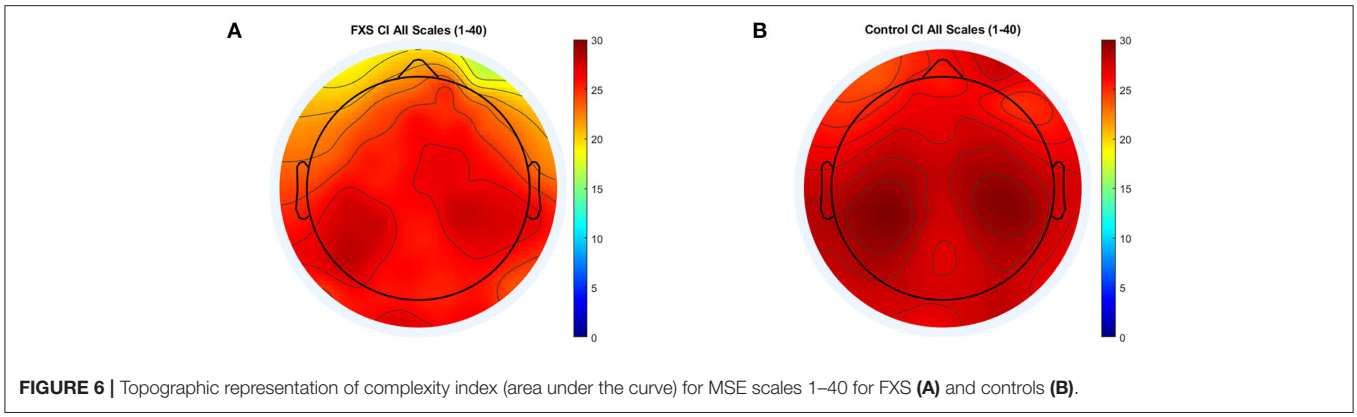

FIGURE 6 | Topographic representation of complexity index (area under the curve) for MSE scales 1–40 for FXS **(A)** and controls **(B)**.

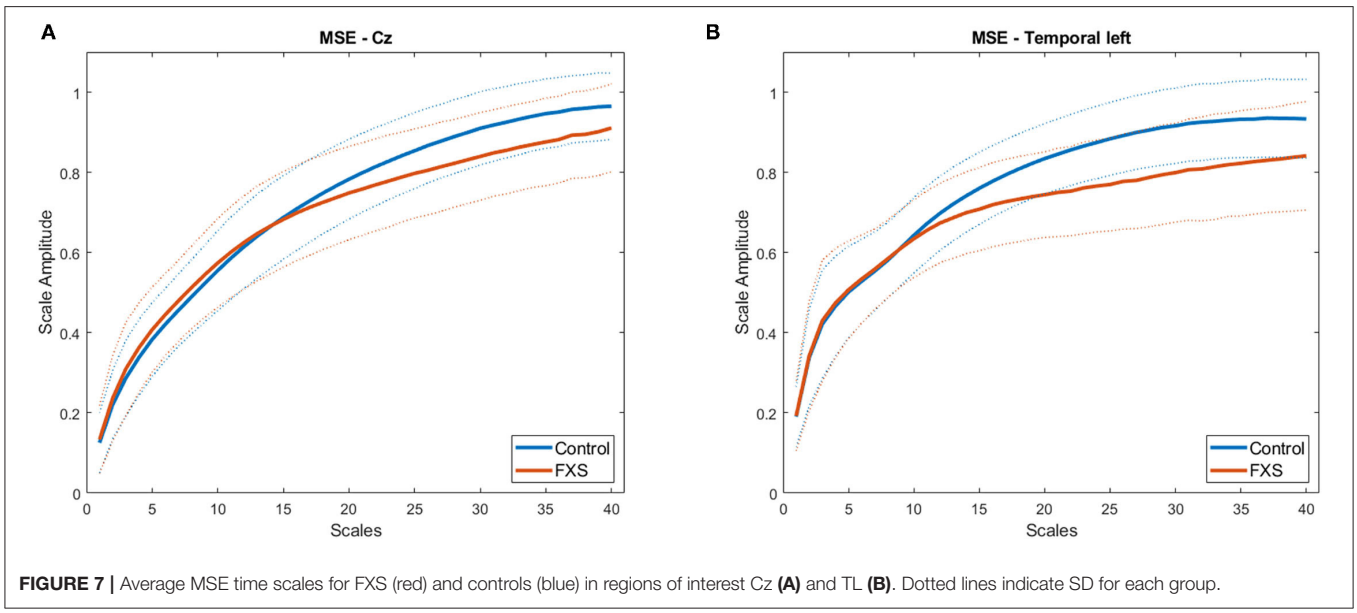

FIGURE 7 | Average MSE time scales for FXS (red) and controls (blue) in regions of interest Cz **(A)** and TL **(B)**. Dotted lines indicate SD for each group.

Sex Effects in the FXS Sample

Male and female FXS participants did not differ in IQ, but male participants scored significantly higher in the ABC-C composite score and some of the subscales (see **Table 2** for test statistics). No sex difference was found in APF [$F_{(1,22)} = 2.1$, $p = 0.16$, $\eta^2 = 0.09$] or TBR [$F_{(1,18)} = 1.8$, $p = 0.2$, $\eta^2 = 0.09$] across ROI. CI did not differ between male and female participants across ROIs [$F_{(1,18)} = 1.89$, $p = 0.19$, $\eta^2 = 0.09$]. A mixed design ANOVA revealed a weak interaction between sex, ROI and scales [$F_{(3.7,66.3)} = 2.59$, $p = 0.049$, $\eta^2 = 0.13$]. *Post hoc* comparisons revealed that MSE was higher for males in both averaged scales in TR only [$F_{(1,20)} = 6.5$, $p = 0.02$, $\eta^2 = 0.24$].

Replication Study

Cohort Description

Table 3 contains descriptive data of the UC Davis cohort. Age did not differ between cohorts [$t_{(42.5)} = 1.1$, $p = 0.27$] but age distribution is different with the Montreal / Edmonton cohort having a peak in younger participants. **Supplementary Figure 1** shows age distribution for both cohorts. Sex differed significantly between cohorts ($\chi 2 = 11$, $p = 0.001$) since the UC Davis cohort only included one female participant. Performance IQ differed between cohorts [$t_{(42.5)} = -2.93$, $p = 0.005$], with lower IQ in the UC Davis compared to the Montreal / Edmonton cohorts. For the ABC-C measures, FXS participants differed on the inappropriate speech subscale [$t_{(41)} = 3.29$, $p = 0.002$], but no group differences were found for the ABC-C composite score or any remaining subscales ($p > 0.51$).

PSD

APF did not correlate with age for any ROI in the UC Davis cohort ($p > 0.08$), whereas it was found to correlate positively with age in the Montreal/Edmonton cohort. TBR did not correlate with age after alpha level was Bonferroni-corrected and adjusted for the mean correlation of outcome variables ($r = 0.82$, $p < 0.0001$) to $p < 0.034$, whereas it had been found to correlate negatively with age in the Montreal/Edmonton cohort. Mixed design ANOVAs did not reveal any significant differences between cohorts in APF [$F_{(1,36)} = 2.75$, $p = 0.11$, $\eta^2 = 0.07$] or

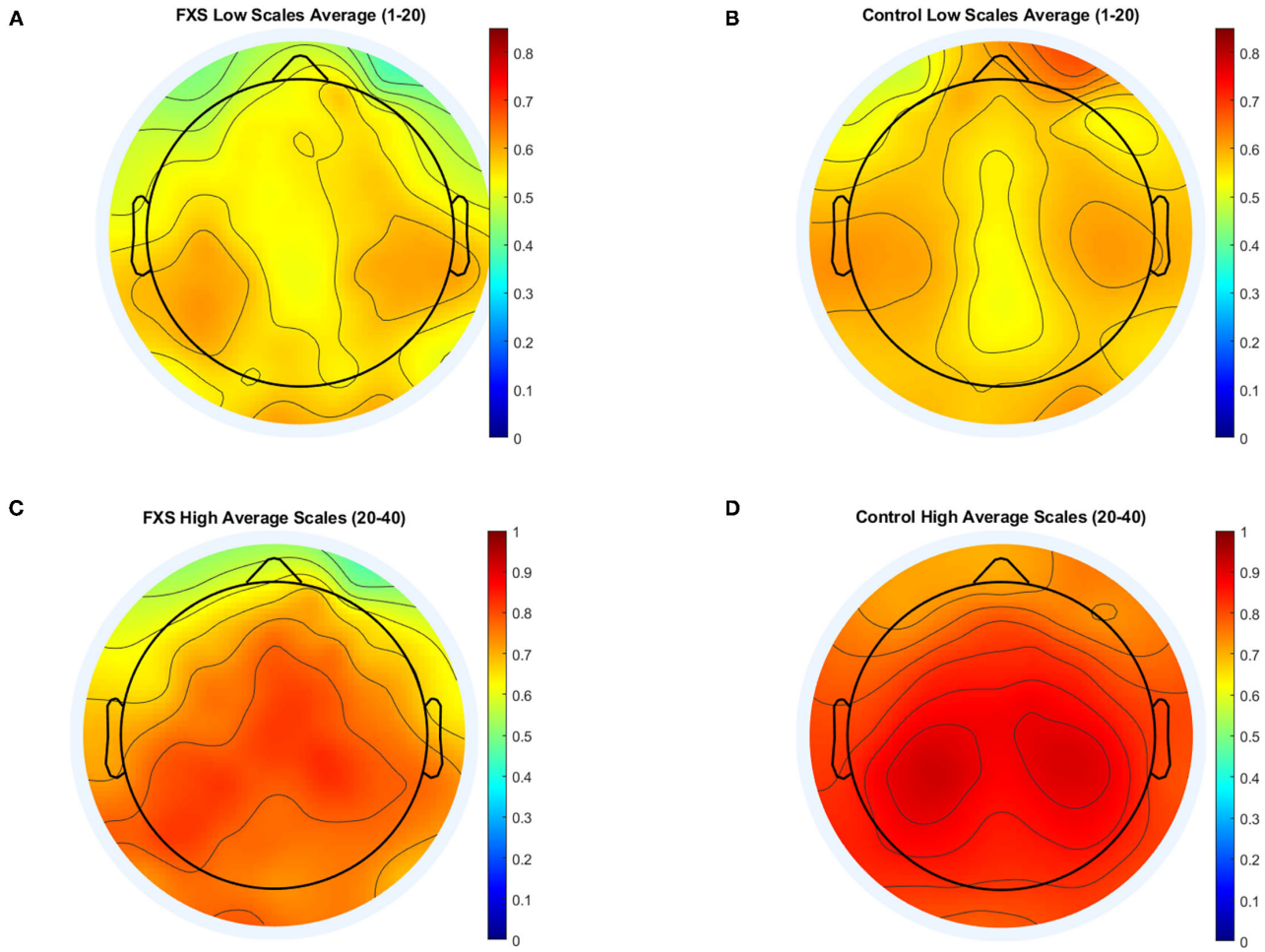

FIGURE 8 | Topographic representation of averaged time scales: lower time scales (1–20) for FXS **(A)** and controls **(B)** and higher time scales for FXS **(C)** and controls **(D)**.

TBR [$F_{(1,32)} = 0.53$, $p = 0.5$, $\eta^2 = 0.02$] nor significant ROI and cohort interactions {APF: [$F_{(4.7,169.34)} = 0.72$, $p = 0.6$, $\eta^2 = 0.02$], TBR: [$F_{(4.1,131.8)} = 1.52$, $p = 0.24$, $\eta^2 = 0.05$]} but a main effect for ROI {APF: [$F_{(4.7,169.3)} = 3.29$, $p = 0.009$, $\eta^2 = 0.08$], TBR: [$F_{(4.1,131.8)} = 20.53$, $p < 0.0001$, $\eta^2 = 0.4$]}. When compared to the control group, APF and TBR effects could be replicated in the replication cohort with significantly lower APF in FXS $F_{(1,85)} = 7.3$, $p = 0.008$, $\eta^2 = 0.08$) and no group effects or interactions for TBR $F_{(1,81)} = 2.98$, $p = 0.088$, $\eta^2 = 0.04$). A mixed design ANOVA revealed no FXS cohort effect for delta, alpha and low gamma [$F_{(1,33)} = 2.43$, $p = 0.13$, $\eta^2 = 0.07$], but a significant ROI, cohort and frequency band interaction [$F_{(4.1,135.8)} = 5.45$, $p = 0.0001$, $\eta^2 = 0.14$], as well as main effects for ROI [$F_{(4.6,150.3)} = 49.5$, $p < 0.001$, $\eta^2 = 0.6$], frequency bands [$F_{(1.2,38.5)} = 251.37$, $p < 0.0001$, $\eta^2 = 0.87$] and a ROI and frequency band interaction [$F_{(4.1,135.8)} = 25.38$, $p < 0.0001$, $\eta^2 = 0.44$]. Follow up ANOVAs by ROI revealed a cohort main effect [$F_{(1,38)} = 7.94$, $p = 0.008$, $\eta^2 = 0.17$] in Oz only. A significant interaction between frequency bands and groups [FXS replication cohort vs. controls: $F_{(1.7,132.5)} = 21.55$, $p < 0.0001$, $\eta^2 = 0.84$] in a mixed design age-controlled ANOVA covering delta, alpha and low gamma frequency bands led to follow-up analysis by frequency band. Compared to controls, the replication FXS cohort presented higher delta [$F_{(1,86)} = 27$, $p < 0.0001$, $\eta^2 = 0.24$] and gamma power $F_{(1,85)} = 95.8$, $p < 0.0001$, $\eta^2 = 0.53$), whereas no group effects were found in alpha power [$F_{(1,82)} = 0.007$, $p = 0.93$, $\eta^2 < 0.0001$].

MSE

CI, S1–20 and S21–40 did not correlate with age in any ROI for the UC Davis cohort ($p > 1.82$), whereas a slight correlation between CI and S1–20 and age was found in central ROI in the Montreal/Edmonton cohort. A mixed design ANOVA revealed no cohort main effect for CI [$F_{(1,31)} = 0.015$, $p = 0.9$, $\eta^2 = 0.0004$], or averaged MSE scales [$F_{(1,31)} = 0.017$, $p = 0.9$, $\eta^2 = 0.001$] nor any cohort and ROI interactions {CI: [$F_{(2.5,76.4)} = 2.47$, $p = 0.08$, $\eta^2 = 0.074$], averaged scales: [$F_{(2.5,76.4)} = 2.47$, $p = 0.08$, $\eta^2 = 0.074$]} or averaged scales and cohort interaction [$F_{(1,31)} = 0.79$, $p = 0.38$, $\eta^2 = 0.025$]. A ROI main effect was found for both CI [$F_{(2.5,76.4)} = 4.66$, $p = 0.008$, $\eta^2 = 0.13$] and averaged

TABLE 3 | Demographics of the "replication study cohort."

	FXS
N	19
Males (*n*, %)	18 (94.74%)
Females (*n*, %)	1 (5.26%)
Age	
Mean ± SD	15.26 ± 4.32
Range	8–22
Non-verbal IQ	
Mean ± SD	48.86 ± 14.76
ABC-C	
Composite score (mean ± SD)	51.27 ± 32.02
Irritability subscale (mean ± SD)	13.44 ± 13.01
Lethargy subscale (mean ± SD)	7.41 ± 6.88
Stereotypy subscale (mean ± SD)	6.32 ± 5.91
Hyperactivity subscale (mean ± SD)	9.56 ± 6.46
Inappropriate speech subscale (mean ± SD)	6.76 ± 3.11
Social avoidance subscale (mean ± SD)	3.68 ± 3.61

ABC-C, Aberrant Behavior Checklist-Community; FXS, Fragile X syndrome; SD, Standard deviation.

scales [$F_{(2.3,76.4)} = 4.6, p < 0.0001, \eta^2 = 0.13$]. When compared to controls, the FXS replication cohort presented a lower CI [$F_{(1,77)} = 5.8, p < 0.018, \eta^2 = 0.07$] as well as lower complexity in S21–40 [$F_{(1,77)} = 10.86, p = 0.001, \eta^2 = 0.12$], whereas no group differences were found in S1–20 [$F_{(1,77)} = 0.08, p < 0.78, \eta^2 = 0.001$].

Clinical Outcome Measures

IQ did not correlate with APF in the replication cohort, whereas negative correlations between IQ and APF in several ROI occurred in our original FXS sample. Further, no correlations were found between IQ and TBR, CI, S1–20 or S21–40 in our replication cohort, thus replicating the results of our original FXS sample. Analyses with the ABC-C scores were not performed in the replication cohort since missing data did not allow for a sufficient N to carry out correlations.

DISCUSSION

Several EEG markers were previously found relevant to brain maturation and hyperexcitability in the FXS population. The results of the present study replicated these findings. APF and alpha power were found to be decreased, and gamma power was increased in the FXS groups, compared to controls. Furthermore, this study was the first to show reduced signal complexity in higher time scales, as well as increased delta power in FXS participants. The main results of our study are summarized in **Table 4**.

MSE

EEG signal complexity was found to be significantly reduced in FXS participants, in both cohorts, compared to healthy controls. A decrease in signal complexity is concordant with alterations in brain maturation and developmental delay characterizing individuals with FXS. Diminished EEG signal complexity in FXS participants was found in all regions of interest investigated, suggesting it is a global phenomenon across resting-state signal generators.

Several studies found a general increase in brain signal complexity with age in neurotypical populations. Indeed, studies have found neurodevelopmental effects on signal complexity from infancy through adolescence (34, 51, 52). This developmental increase was clearly observed in our control group across all regions of interest. In FXS it is however a lot less evident, as CI only correlates with age in central and fronto-central regions and no age-related increase was found in the remaining regions of interest. This discrepancy could be explained by the smaller sample size of the FXS cohort. Moreover, in our FXS replication cohort, where the peak of the age distribution is found toward the end of the teenage years rather than in childhood, and that contains lower functioning individuals, the complexity index does not at all correlate with age. These results support the growing discrepancy with age found in FXS compared to neurotypical children, as a certain stagnation in CI development seems to take place during the teenage years. Our cohorts, ranging from 5 to 28 years old, allowed us to show this discrepancy. Our results suggest that early school years are when trajectories of signal complexity maturation differ across brain regions in FXS. However, whether EEG signal complexity differences are present before 5 years of age remains to be studied.

Some studies identified signal complexity as a relevant EEG marker of neurodevelopmental disorders. These studies also found a general reduction in EEG signal complexity in ADHD, ASD, and Tourette Syndrome (35–37, 53), as well as reduced complexity in the alpha frequency band (38). MSE could potentially be a useful biomarker in establishing the neurodevelopmental and neurobehavioral trajectories of patients with FXS. Augmented complexity was found to be correlated with lower ABC-C composite scores, as well as fewer symptoms on the irritability, lethargy, hyperactivity, and social avoidance subscales. A recent study investigating behavioral characteristics found in different clinical populations reported that patients with FXS scored higher on the irritability, lethargy and hyperactivity subscales than NT controls (54). These results are consistent with our observations and suggest that signal complexity might be reflecting the behavioral impairments associated with FXS. Since we have not excluded any comorbidities in our FXS population, those comorbidities could also have an impact on the reduced complexity found.

Reduced signal complexity in FXS was expected as several previous studies found unitary/simplified brain processes in this population. Topographically, Knoth et al. (14) found that a lower number of spatial principal components could explain FXS brain signals. Moreover, Côté et al. (11, 13), found low variability between trials of sensory responses, together with high amplitudes, suggesting a potential for synchronization of brain signals (55). Increased phase synchronization to sensory stimuli was indeed found in low-frequency bands (<20 Hz) in

TABLE 4 | Main results of the FXS cohorts.

	FXS vs. controls	FXS replication cohort vs. controls	FXS vs. FXS replication cohort
Power spectral density			
Delta	Higher delta power in FXS	Higher delta power in FXS	**Only in Oz**: slightly higher PSD in replication cohort, no other significant differences
Alpha	Lower alpha power in FXS	No significant difference	
Low gamma	Higher gamma power in FXS	Higher gamma power in FXS	
Alpha peak frequency	Lower alpha peak frequency in FXS	Lower alpha peak frequency in FXS	No significant difference
Theta-beta ratio	No significant difference	No significant difference	No significant difference
Multiscale entropy			
Complexity index	Lower CI in FXS	Lower CI in FXS	No significant difference
Average time scales (S1–20)	No significant difference	No significant difference	No significant difference
Average time scales (S21–40)	Lower MSE in FXS	Lower MSE in FXS	No significant difference

CI, Complexity index; FXS, Fragile X syndrome; MSE, Multiscale entropy.

FXS (56). Notably, the significant reduction in MSE values of FXS is found in the higher/coarser scales, potentially capturing lower frequency oscillations, while the finer-grained scales, where the increase in low gamma power observed in our FXS cohort could have introduced variability or noise, were not found significantly different.

PSD et TBR

The FXS group showed higher delta power, lower alpha power, and increased low gamma power. Results of the replication study cohort also showed higher delta power and increased low gamma power. These results were expected as they confirm previous studies, supporting a robust signature of FXS resting-state EEG (20–22, 27). Whereas, TBR was found to stabilize toward less discrepancies between theta and beta power with age, it did not differ between FXS and controls. In fact, 5–10 Hz frequency power is seemingly reduced, whereas high beta and low gamma powers are increased. Hence, although not significant, the TBR is potentially flattened by the modifications in spectral power found in FXS. Several medications, including the psychostimulant types, are known to modify beta power (57). Whether the absence of results is due to medication taken by the FXS participants remains to be studied. Despite the fact that TBR is considered an electrophysiological biomarker in the ADHD population, what TBR reflects is still a matter of debate (32, 58). Here, we found a positive relationship between TBR in the left frontal area of interest and the hyperactivity subscale of the ABC-C. Those results are consistent with the literature reporting an association between hyperactivity and higher TBR in ADHD children (59). A recent study found that resting-state TBR is not altered in ADHD but is positively correlated with the inattentive symptoms of the disorder (60). Since the ADHD-inattentive sub-type is prevalent in the FXS population (61), hypotheses of interaction between TBR and inattention will be worth exploring in future research.

Alpha peak frequency is a long-standing EEG marker of brain maturation (62). During development, APF migrates from the theta frequency range to the alpha frequency range. APF was indeed associated with age in our neurotypical control group. In the FXS group, correlations were found only in central but not lateral regions of interest—comparable to our results found for the relationship between CI and age in FXS. Again, no correlation between age and APF was found in our replication cohort that is characterized by a later peak in age distribution and lower functioning individuals. Considering that at an early age theta is particularly robust in central regions, these results are consistent with the growing discrepancies in brain function with age in FXS, and support the evidence showing a failure to shift the APF with age in children with ASD (63). Importantly, APF was significantly lower in both FXS cohorts, ranging in the theta frequency range, rather than the alpha frequency range. Although APF has not been widely investigated in FXS, reduced alpha power has been reported by several authors, in humans (20, 27, 64) and in rats (65). Our results are also consistent with studies of neurodevelopmental disorders showing reduced alpha power in children with ASD (30, 63) and ADHD (28), and decreased APF in children with ASD (62). Increased APF was also associated with higher scores on the inappropriate speech subscale. An association between APF and language acquisition has been reported in the literature (66), suggesting that FXS participants who scored higher on the inappropriate speech subscale might have better language abilities in general, though their speech may be unsuitable for certain situations. Notably, alpha power and APF were not found altered in female FXS patients in previous studies (21, 64). However, we did not find any sex differences in APF in our FXS sample. This discrepancy is potentially due to the fact that our FXS population is more diversified in terms of cognitive functioning, in both the male and female FXS participants.

Mechanisms Behind the Scenes

Hence, several EEG markers are seemingly characteristic of the FXS brain. They may be mechanistically divided into two categories of indices: delay of maturation, and hyperexcitability. Increase in delta power, reduced alpha peak frequency, and diminished EEG signal complexity are EEG markers that have been associated repeatedly with brain maturation (34, 62, 67–69). FXS individuals carrying the full mutation show a

flattened curve of cognitive neurodevelopment with a plateau around 6 years of age. Decades of research on the function of FMRP identified several mechanisms underlying FXS. Through the FMRP role in translational control, long-term synaptic and spine morphological plasticity, FXS is genuinely a neurodevelopmental disorder. FMRP is developmentally regulated, at least in mice, and implicated in the experience-dependent plasticity mechanisms of neurodevelopment, of which its dysregulation seemingly leads to permanent changes. Whether FMRP expression levels at specific moments during development are revealed by EEG markers most associated with brain maturation remains to be tested. Certainly, an increase in slow frequency band density, decrease in alpha power and alterations in signal complexity have been associated with several neurodevelopmental disorders affecting cognitive and behavioral neurodevelopment. In children with ASD, signal complexity was sensitive to the severity level of the symptoms (70). Notably, the significant differences changed topographically according to age from 4 to 8 years old. In our study, significant interactions between age and regions of interest were found in spectral power, complexity index and higher MSE time scales. Hence, the most group difference-sensitive EEG indices may vary during the course of development. Acquisition of data from younger FXS participants could enable the identification of specific critical moments during development where the neurodevelopmental trajectories diverge, thereby identifying ultimate periods to administer treatments for maximal gain.

On the other hand, increases in gamma power and reductions in alpha power have been associated with hyperexcitability in the FXS population. In a cognitive neuroscience framework, the alpha and gamma frequency bands have functional interactions, where alpha pulses are inhibited, reducing processing capacities in a given brain area. In this framework, alpha power is reduced by attention, and gamma oscillations are increased to process information (71). This inhibitory process, which happens through alpha activity (72), is thought to be driven by GABAergic interneurons (27). In the context of FXS, the impaired alpha activity could be generated by altered gamma power. Indeed, gamma activity is directly modulated by inhibitory GABAergic interneurons (65). The GABAergic system is known to be altered in FXS (7), consequently leading to hyperexcitability and increased gamma power. Furthermore, alpha oscillations reflect a neural mechanism aiming to gate the processing of external sensory information, altered in FXS (20, 27), as well as in other conditions such as pain (73).

From a neuroscience perspective, it has been established that local circuit glutamate-GABA interactions are part of the neural mechanisms underlying gamma activity (55), and that these interactions are altered in FXS. Indeed, overactivation of glutamatergic circuits and hypoactivation of GABAergic circuits have been documented (74). Furthermore, local circuit inhibitory interneurons are known to play an important role in regulating the flow of excitatory networks by providing inhibitory control (75). However, fast spiking inhibitory GABAergic interneurons, which are involved in high-frequency neural activity, are dysfunctional (12, 19, 56), leading to reduced local inhibition, and consequently resulting in neuronal hyperexcitability. Thus, our results support the gamma activity abnormalities and contribute to a better understanding of the cortical excitation/inhibition imbalance found in FXS (12, 65).

CONCLUSION

Our study confirms that several EEG markers characterizing brain maturation and hyperexcitability are altered in FXS. Moreover, the results obtained with our replication study cohort showed that results using different EEG systems are replicable, not only between FXS cohorts, but also between a FXS cohort and healthy controls. These results are encouraging and suggest the feasibility of multi-site studies. Future studies should consider pooling data using normalization techniques. Although further studies in younger participants are required, our results suggest critical points of stagnation in the neurodevelopmental curve that can be assessed particularly by signal complexity and alpha peak frequency, as they have been shown to be sensitive to both brain maturation and FXS phenotype. Hence, the significant findings obtained on MSE, APF, as well as delta, alpha, and gamma power suggest that several EEG atypicalities could be used as biomarkers for FXS. The next step is to determine if these markers are responsive to pharmacological treatments targeting specific mechanisms.

DATA AVAILABILITY STATEMENT

The original contributions presented in the study are included in the article/**Supplementary Material**, further inquiries can be directed to the corresponding author/s.

ETHICS STATEMENT

The studies involving human participants were reviewed and approved by Ethics Committees at CHU Sainte-Justine, the University of Alberta, and the University of California, Davis. Written informed consent to participate in this study was provided by the participants' legal guardian/next of kin.

AUTHOR CONTRIBUTIONS

MP-L and IK performed most of the analyses and wrote the manuscript. KA performed several analyses and created the figures. VC, HB, AT, C-OM, A-MB, and CR tested the participants and contributed to EEG signal analyses. Co-researchers FT, LA, SJ, RH, FB, DH, and AS contributed to the scientific conception of the study. SL is the senior scientist, she conceived the EEG project, and contributed to analyses, interpretation and writing. All authors contributed to the article and approved the submitted version.

FUNDING

This research was funded by the Azrieli Foundation, the Canadian Institutes of Health Research (CIHR) (grant number 142346) and the Natural Sciences and Engineering Research Council of Canada NSERC (grant number 386207).

ACKNOWLEDGMENTS

We would like to thank all participants and their families. We also want to acknowledge the financial support of our funding sources mentioned in the Funding section and all the professionals and students involved in this project, specifically Audrey-Ann Fauteux and Marguerite Nolin for their help with EEG pre-processing.

SUPPLEMENTARY MATERIAL

The Supplementary Material for this article can be found online at: https://www.frontiersin.org/articles/10.3389/fpsyt.2021.716707/full#supplementary-material

REFERENCES

1. Garber KB, Visootsak J, Warren ST. Fragile X syndrome. *Eur J Hum Genet.* (2008) 16:666–72. doi: 10.1038/ejhg.2008.61
2. Bolduc FV, Bell K, Cox H, Broadie KS, Tully T. Excess protein synthesis in Drosophila fragile X mutants impairs long-term memory. *Nat Neurosci.* (2008) 11:1143–5. doi: 10.1038/nn.2175
3. Bear MF, Dolen G, Osterweil E, Nagarajan N. Fragile X: translation in action. *Neuropsychopharmacology.* (2008) 33:84–7. doi: 10.1038/sj.npp.1301610
4. Contractor A, Klyachko VA, Portera-Cailliau C. Altered neuronal and circuit excitability in fragile X syndrome. *Neuron.* (2015) 87:699–715. doi: 10.1016/j.neuron.2015.06.017
5. Bassell GJ, Warren ST. Fragile X syndrome: loss of local mRNA regulation alters synaptic development and function. *Neuron.* (2008) 60:201–14. doi: 10.1016/j.neuron.2008.10.004
6. Bear MF, Huber KM, Warren ST. The mGluR theory of fragile X mental retardation. *Trends Neurosci.* (2004) 27:370–7. doi: 10.1016/j.tins.2004.04.009
7. D'Hulst C, Heulens I, Brouwer JR, Willemsen R, De Geest N, Reeve SP, et al. Expression of the GABAergic system in animal models for fragile X syndrome and fragile X associated tremor/ataxia syndrome (FXTAS). *Brain Res.* (2009) 1253:176–83. doi: 10.1016/j.brainres.2008.11.075
8. Morin-Parent F, Champigny C, Lacroix A, Corbin F, Lepage JF. Hyperexcitability and impaired intracortical inhibition in patients with fragile-X syndrome. *Transl Psychiatry.* (2019) 9:312. doi: 10.1038/s41398-019-0650-z
9. Proteau-Lemieux M, Lacroix A, Galarneau L, Corbin F, Lepage JF, Caku A. The safety and efficacy of metformin in fragile X syndrome: an open-label study. *Prog Neuropsychopharmacol Biol Psychiatry.* (2021) 110:110307. doi: 10.1016/j.pnpbp.2021.110307
10. Berry-Kravis E, Hicar M, Ciurlionis R. Reduced cyclic AMP production in fragile X syndrome: cytogenetic and molecular correlations. *Pediatric Res.* (1995) 38:638–43. doi: 10.1203/00006450-199511000-00002
11. Côté V, Lalancette E, Knoth IS, Côt,é L, Agbogba K, Vannasing P, et al. Distinct patterns of repetition suppression in fragile X syndrome, down syndrome, tuberous sclerosis complex and mutations in SYNGAP1. *Brain Res.* (2021) 1751:147205. doi: 10.1016/j.brainres.2020.147205
12. Ethridge LE, White SP, Mosconi MW, Wang J, Byerly MJ, Sweeney JA. Reduced habituation of auditory evoked potentials indicate cortical hyper-excitability in fragile X syndrome. *Transl Psychiatry.* (2016) 6:e787. doi: 10.1038/tp.2016.48
13. Knoth IS, Vannasing P, Major P, Michaud JL, Lippe S. Alterations of visual and auditory evoked potentials in fragile X syndrome. *Int J Dev Neurosci.* (2014) 36:90–7. doi: 10.1016/j.ijdevneu.2014.05.003
14. Knoth IS, Lajnef T, Rigoulot S, Lacourse K, Vannasing P, Michaud JL, et al. Auditory repetition suppression alterations in relation to cognitive functioning in fragile X syndrome: a combined EEG and machine learning approach. *J Neurodev Disord.* (2018) 10:4. doi: 10.1186/s11689-018-9223-3
15. Schneider A, Leigh MJ, Adams P, Nanakul R, Chechi T, Olichney J, et al. Electrocortical changes associated with minocycline treatment in fragile X syndrome. *J Psychopharmacol.* (2013) 27:956–63. doi: 10.1177/0269881113494105
16. Van der Molen MJ, Van der Molen MW, Ridderinkhof KR, Hamel BC, Curfs LM, Ramakers GJ. Auditory change detection in fragile X syndrome males: a brain potential study. *Clin Neurophysiol.* (2012) 123:1309–18. doi: 10.1016/j.clinph.2011.11.039
17. Van der Molen MJ, Van der Molen MW, Ridderinkhof KR, Hamel BC, Curfs LM, Ramakers GJ. Auditory and visual cortical activity during selective attention in fragile X syndrome: a cascade of processing deficiencies. *Clin Neurophysiol.* (2012) 123:720–9. doi: 10.1016/j.clinph.2011.08.023
18. Jonak CR, Lovelace JW, Ethell IM, Razak KA, Binder DK. Multielectrode array analysis of EEG biomarkers in a mouse model of fragile X syndrome. *Neurobiol Dis.* (2020) 138:104794. doi: 10.1016/j.nbd.2020.104794
19. Lovelace JW, Ethell IM, Binder DK, Razak KA. Translation-relevant EEG phenotypes in a mouse model of fragile X syndrome. *Neurobiol Dis.* (2018) 115:39–48. doi: 10.1016/j.nbd.2018.03.012
20. Wang J, Ethridge LE, Mosconi MW, White SP, Binder DK, Pedapati EV, et al. A resting EEG study of neocortical hyperexcitability and altered functional connectivity in fragile X syndrome. *J Neurodev Disord.* (2017) 9:11. doi: 10.1186/s11689-017-9191-z
21. Smith EG, Pedapati EV, Liu R, Schmitt LM, Dominick KC, Shaffer RC, et al. Sex differences in resting EEG power in fragile X syndrome. *J Psychiatr Res.* (2021) 138:89–95. doi: 10.1016/j.jpsychires.2021.03.057
22. Wilkinson CL, Nelson CA. Increased aperiodic gamma power in young boys with fragile X syndrome is associated with better language ability. *Mol Autism.* (2021) 12:17. doi: 10.1186/s13229-021-00425-x
23. White RS, Siegel SJ. Cellular and circuit models of increased resting-state network gamma activity in schizophrenia. *Neuroscience.* (2016) 321:66–76. doi: 10.1016/j.neuroscience.2015.11.011
24. Gokten ES, Tulay, EE., Beser B, Yuskel ME, Arikan K, et al. Predictive values of slow and fast EEG oscillations for methylphenidate response in ADHD. *Clin EEG Neurosci.* (2019) 50:332–8. doi: 10.1177/1550059419863206
25. Tikka SK, Nizamie SH, Das B, Katshu MZ, Goyal N. Increased spontaneous gamma power and synchrony in schizophrenia patients having higher minor physical anomalies. *Psychiatry Res.* (2013) 207:164–72. doi: 10.1016/j.psychres.2012.09.006
26. Wong H, Hooper AWM, Niibori Y, Lee SJ, Hategan LA, Zhang L, et al. Sexually dimorphic patterns in electroencephalography power spectrum and autism-related behaviors in a rat model of fragile X syndrome. *Neurobiol Dis.* (2020) 146:105118. doi: 10.1016/j.nbd.2020.105118
27. Van der Molen MJ, Van der Molen MW. Reduced alpha and exaggerated theta power during the resting-state EEG in fragile X syndrome. *Biol Psychol.* (2013) 92:216–9. doi: 10.1016/j.biopsycho.2012.11.013
28. Clarke AR, Barry RJ, Johnstone SJ, McCarthy R, Selikowitz M. EEG development in attention deficit hyperactivity disorder: from child to adult. *Clin Neurophysiol.* (2019) 130:1256–62. doi: 10.1016/j.clinph.2019.05.001
29. Edgar JC, Dipiero M, McBride E, Green HL, Berman J, Ku M, et al. Abnormal maturation of the resting-state peak alpha frequency in children with autism spectrum disorder. *Hum Brain Mapp.* (2019) 40:3288–98. doi: 10.1002/hbm.24598

30. Shephard E, Tye C, Ashwood KL, Azadi B, Asherson P, Bolton PF, et al. Resting-state neurophysiological activity patterns in young people with ASD, ADHD, and ASD + ADHD. *J Autism Dev Disord.* (2018) 48:110–22. doi: 10.1007/s10803-017-3300-4
31. Halawa IF, El Sayed BB, Amin OR, Meguid NA, Abdel Kader AA. Frontal theta/beta ratio changes during TOVA in Egyptian ADHD children. *Neurosciences.* (2017) 22:287–91. doi: 10.17712/nsj.2017.4.20170067
32. Lenartowicz A, Loo SK. Use of EEG to diagnose ADHD. *Curr Psychiatry Rep.* (2014) 16:498. doi: 10.1007/s11920-014-0498-0
33. Heisz JJ, Shedden JM, McIntosh AR. Relating brain signal variability to knowledge representation. *NeuroImage.* (2012) 63:1384–92. doi: 10.1016/j.neuroimage.2012.08.018
34. Lippe S, Kovacevic N, McIntosh AR. Differential maturation of brain signal complexity in the human auditory and visual system. *Front Hum Neurosci.* (2009) 3:48. doi: 10.3389/neuro.09.048.2009
35. Ghanbari Y, Bloy L, Christopher Edgar J, Blaskey L, Verma R, Roberts TP. Joint analysis of band-specific functional connectivity and signal complexity in autism. *J Autism Dev Disord.* (2015) 45:444–60. doi: 10.1007/s10803-013-1915-7
36. Liu T, Chen Y, Chen D, Li C, Qiu Y, Wang J. Altered electroencephalogram complexity in autistic children shown by the multiscale entropy approach. *Neuroreport.* (2017) 28:169–73. doi: 10.1097/WNR.0000000000000724
37. Misic B, Doesburg SM, Fatima Z, Vidal J, Vakorin VA, Taylor MJ, et al. Coordinated information generation and mental flexibility: large-scale network disruption in children with autism. *Cereb Cortex.* (2015) 25:2815–27. doi: 10.1093/cercor/bhu082
38. Chenxi L, Chen Y, Li Y, Wang J, Liu T. Complexity analysis of brain activity in attention-deficit/hyperactivity disorder: a multiscale entropy analysis. *Brain Res Bull.* (2016) 124:12–20. doi: 10.1016/j.brainresbull.2016.03.007
39. Tassone F. Advanced technologies for the molecular diagnosis of fragile X syndrome. *Expert Rev Mol Diag.* (2015) 15:1465–73. doi: 10.1586/14737159.2015.1101348
40. Roid GH, Miller LJ. Leiter international performance scale – revised: examiner's *Manual.* In: Roid GH, Miller LJ, Editors. *Leiter International Performance Scale – Revised*. Wood Dale, IL: Stoelting Co (1997).
41. Roid GH, Miller LJ, Pomplun M, Koch C. *Leiter International Performance Scale.* 3rd Ed. Wood Dale, IL: Stoelting Co (2013).
42. Wechsler D. *Wechsler Preschool and Primary Scale of Intelligence.* 4th Ed. Bloomington, MN: Psychological Corp (2012).
43. Weschler D. *Weschler Intelligence Scale for Children.* 5th Ed. Bloomington, MN: Psychological Corp (2014).
44. Sansone SM, Widaman KF, Hall SS, Reiss AL, Lightbody A, Kaufmann WE, et al. (2012). Psychometric study of the aberrant behavior checklist in fragile X syndrome and implications for targeted treatment. *J Autism Dev Disord.* 42:1377–92. doi: 10.1007/s10803-011-1370-2
45. Tucker DM. Spatial sampling of head electrical fields: the geodesic sensor net. *Electorencephalogr Clin Neurophysiol.* (1993) 87:154–63. doi: 10.1016/0013-4694(93)90121-B
46. Delorme A, Makeig S. EEGLAB: an open source toolbox for analysis of single-trial EEG dynamics including independent component analysis. *J Neurosci Methods.* (2004) 134:9–21. doi: 10.1016/j.jneumeth.2003.10.009
47. Makeig S, Debener S, Onton J, Delorme A. Mining event-related brain dynamics. *Trends Cogn Sci.* 8:204–10. doi: 10.1016/j.tics.2004.03.008
48. Costa M, Goldberger AL, Peng CK. Multiscale entropy analysis of biological signals. *Phys Rev E Stat Nonlin Soft Matter Phys.* (2005) 71(2 Pt 1):021906. doi: 10.1103/PhysRevE.71.021906
49. Richman JS, Moorman JR. Physiological time-series analysis using approximate entropy and sample entropy. *Am J Physiol Heart Circ Physiol.* (2000) 278:2039–49. doi: 10.1152/ajpheart.2000.278.6.H2039
50. Blakesley RE, Mazumdar S, Dew MA, Houck PR, Tang G, Reynolds, et al. Comparisons of methods for multiple hypothesis testing in neuropsychological research. *Neuropsychology.* (2009) 23:255–64. doi: 10.1037/a0012850
51. van Noordt S, Willoughby T. Cortical maturation from childhood to adolescence is reflected in resting state EEG signal complexity. *Dev Cogn Neurosci.* (2021) 48:100945. doi: 10.1016/j.dcn.2021.100945
52. Vakorin VA, Lippe S, McIntosh AR. Variability of brain signals processed locally transforms into higher connectivity with brain development. *J Neurosci.* (2011) 31:6405–13. doi: 10.1523/JNEUROSCI.3153-10.2011
53. Weng WC, Chang CF, Wong LC, Lin JH, Lee WT, Shieh JS. Altered resting-state EEG complexity in children with Tourette syndrome: a preliminary study. *Neuropsychology.* (2017) 31:395–402. doi: 10.1037/neu0000363
54. Côté V, Knoth IS, Lalancette È, Lavergne J-A, Côté L, et al. Behavioural characteristics related to adaptive functioning in young persons with tuberous sclerosis complex, down syndrome and fragile x syndrome. *J Dev Phys Disab.* (2020) 33:279–96. doi: 10.1007/s10882-020-09748-8
55. Ethridge L, Thaliath A, Kraff J, Nijhawan K, Berry-Kravis E. Development of neural response to novel sounds in fragile X syndrome: potential biomarkers. *Am J Intellect Dev Disabil.* (2020) 125:449–64. doi: 10.1352/1944-7558-125.6.449
56. Ethridge LE, White SP, Mosconi MW, Wang J, Pedapati EV, Erickson CA, et al. Neural synchronization deficits linked to cortical hyper-excitability and auditory hypersensitivity in fragile X syndrome. *Mol Autism.* (2017) 8:22. doi: 10.1186/s13229-017-0140-1
57. Chiarenza GA. Quantitative EEG in childhood attention deficit hyperactivity disorder and learning disabilities. *Clin EEG Neurosci.* (2021) 52:144–55. doi: 10.1177/1550059420962343
58. Clarke AR, Barry RJ, Karamacoska D, Johnstone SJ. The EEG theta/beta ratio: a marker of arousal or cognitive processing capacity? Appl Psychophysiol Biofeedback. (2019) 44:123–9. doi: 10.1007/s10484-018-09428-6
59. Clarke AR, Barry RJ, McCarthy R, Selikowitz M. Correlation between EEG activity and behavior in children with attention-deficit/hyperactivity disorder. *J of Neurother.* (2011) 15:193–9. doi: 10.1080/10874208.2011.595295
60. Zhang, D-W., Li H, Wu Z, Zhao Q, Song Y, et al. Electroencephalogramm theta/beta ratio and spectral power correlates of executive functions in children with AD/HD. *J Atten Disord.* (2019) 23:721–32. doi: 10.1177/1087054717718263
61. Deshpande PS, Coffey DB. Fragile X syndrome and attention-deficit/hyperactivity disorder symptoms. *J Child Adolesc Psychopharmacol.* (2011) 21:639–42. doi: 10.1089/cap.2011.2164
62. Dickinson A, DiStefano C, Senturk D, Jeste SS. Peak alpha frequency is a neural marker of cognitive function across the autism spectrum. *Eur J Neurosci.* (2018) 47:643–51. doi: 10.1111/ejn.13645
63. Edgar JC, Heiken K, Chen YH, Herrington JD, Chow V, Liu S, et al. Resting-state alpha in autism spectrum disorder and alpha associations with thalamic volume. *J Autism Dev Disord.* (2015) 45:795–804. doi: 10.1007/s10803-014-2236-1
64. Ethridge LE, De Stefano LA, Schmitt LM, Woodruff NE, Brown KL, Tran M, et al. Auditory EEG biomarkers in fragile X syndrome: clinical relevance. *Front Integr Neurosci.* (2019) 13:60. doi: 10.3389/fnint.2019.00060
65. Kozono N, Okamura A, Honda S, Matsumoto M, Mihara T. Gamma power abnormalities in a Fmr1-targeted transgenic rat model of fragile X syndrome. *Sci Rep.* (2020) 10:18799. doi: 10.1038/s41598-020-75893-x
66. Angelakis E, Lubar JF, Stathopoulou S. Electroencephalographic peak alpha frequency correlates of cognitive traits. *Neurosci Lett.* (2004) 371:60–63. doi: 10.1016/j.neulet.2004.08.041
67. Campbell IG, Feinberg I. Longitudinal trajectories of non-rapid eye movement delta and theta EEG as indicators of adolescent brain maturation. *Proc Natl Acad Sci USA.* (2009) 106:5177–80. doi: 10.1073/pnas.0812947106
68. Cragg L, Kovacevic N, McIntosh AR, Poulsen C, Martinu K, Leonard G, et al. Maturation of EEG power spectra in early adolescence: a longitudinal study. *Dev Sci.* (2011) 14:935–43. doi: 10.1111/j.1467-7687.2010.01031.x
69. Frohlich J, Miller MT, Bird LM, Garces P, Purtell H, Hoener MC, et al. Electrophysiological phenotype in angelman syndrome differs between genotypes. *Biol Psychiatry.* (2019) 85:752–9. doi: 10.1016/j.biopsych.2019.01.008
70. Hadoush H, Alafeef M, Abdulhay E. Brain complexity in children with mild and severe autism spectrum disorders: analysis of multiscale entropy in EEG. *Brain Topogr.* (2019) 32:914–21. doi: 10.1007/s10548-019-00711-1

71. Jensen O, Mazaheri A. Shaping functional architecture by oscillatory alpha activity: gating by inhibition. *Front Hum Neurosci.* (2010) 4:186. doi: 10.3389/fnhum.2010.00186
72. Kwok EYL, Cardy JO, Allman BL, Allen P, Herrmann B. Dynamics of spontaneous alpha activity correlate with language ability in young children. *Behav Brain Res.* (2019) 359:56–65. doi: 10.1016/j.bbr.2018.10.024
73. Simis M, Pacheco-Barrios K, Uygur-Kucukseymen E, Castelo-Branco L, Battistella LR, Fregni F. Specific electroencephalographic signatures for pain and descending pain inhibitory system in spinal cord injury. *Pain Med.* (2021). doi: 10.1093/pm/pnab124. [Epub ahead of print].
74. Gatto CL, Broadie K. Genetic controls balancing excitatory and inhibitory synaptogenesis in neurodevelopmental disorder models. *Front Synaptic Neurosci.* (2010) 2:1–19. doi: 10.3389/fnsyn.2010.00004
75. Cea-Del Rio CA, Huntsman MM. The contribution of inhibitory interneurons to circuit dysfunction in Fragile X Syndrome. *Front Cell Neurosci.* (2014) 8:245. doi: 10.3389/fncel.2014.00245

Conflict of Interest: The authors declare that the research was conducted in the absence of any commercial or financial relationships that could be construed as a potential conflict of interest.

frontiers in Psychiatry

CORRECTION
published: 24 February 2022
doi: 10.3389/fpsyt.2022.867000

Corrigendum: EEG Signal Complexity Is Reduced During Resting-State in Fragile X Syndrome

Mélodie Proteau-Lemieux[1,2†], Inga Sophia Knoth[2†], Kristian Agbogba[2], Valérie Côté[2], Hazel Maridith Barlahan Biag[3], Angela John Thurman[3], Charles-Olivier Martin[2], Anne-Marie Bélanger[2], Cory Rosenfelt[4], Flora Tassone[3,5], Leonard J. Abbeduto[3,6], Sébastien Jacquemont[2,7], Randi Hagerman[3], François Bolduc[4], David Hessl[3,6], Andrea Schneider[3,8] and Sarah Lippé[1,2]*

[1] Department of Psychology, University of Montreal, Montreal, QC, Canada, [2] Research Center of the Sainte-Justine University Hospital, Montreal, QC, Canada, [3] University of California Davis Medical Investigation of Neurodevelopmental Disorders (MIND) Institute, Sacramento, CA, United States, [4] Department of Pediatric Neurology, University of Alberta, Edmonton, AB, Canada, [5] Department of Biochemistry and Molecular Medicine, University of California Davis School of Medicine, Sacramento, CA, United States, [6] Department of Psychiatry and Behavioral Sciences, University of California Davis School of Medicine, Sacramento, CA, United States, [7] Department of Pediatrics, University of Montreal, Montreal, QC, Canada, [8] California North State University, College of Psychology, Rancho Cordova, CA, United States

Keywords: fragile X syndrome, hyperexcitability, EEG resting-state, signal complexity, multiscale entropy, alpha peak frequency, neurodevelopmental disorders, development

OPEN ACCESS

Edited and Reviewed by:
Wenbin Guo,
Central South University, China

***Correspondence:**
Sarah Lippé
sarah.lippe@umontreal.ca

†These authors share first authorship

Specialty section:
This article was submitted to Neuroimaging and Stimulation, a section of the journal Frontiers in Psychiatry

Received: *31 January 2022*
Accepted: *02 February 2022*
Published: *24 February 2022*

Citation:
Proteau-Lemieux M, Knoth IS, Agbogba K, Côté V, Barlahan Biag HM, Thurman AJ, Martin C-O, Bélanger A-M, Rosenfelt C, Tassone F, Abbeduto LJ, Jacquemont S, Hagerman R, Bolduc F, Hessl D, Schneider A and Lippé S (2022) Corrigendum: EEG Signal Complexity Is Reduced During Resting-State in Fragile X Syndrome. Front. Psychiatry 13:867000. doi: 10.3389/fpsyt.2022.867000

A Corrigendum on

EEG Signal Complexity Is Reduced During Resting-State in Fragile X Syndrome
by Proteau-Lemieux, M., Knoth, I. S., Agbogba, K., Côté, V., Barlahan Biag, H. M., Thurman, A. J., Martin, C-O., Bélanger, A-M., Rosenfelt, C., Tassone, F., Abbeduto, L. J., Jacquemont, S., Hagerman, R., Bolduc, F., Hessl, D., Schneider, A., and Lippé, S. (2021). Front. Psychiatry 12:716707. doi: 10.3389/fpsyt.2021.716707

In the original article, there was an error. The abstract states that we compared 26 FXS participants with 7 neurotypical controls. This is incorrect. As correctly stated in the methods and result sections, we compared 26 FXS participants to 77 neurotypical controls.

A correction has been made to **Methods** section of the **Abstract**.

Methods: In this study, resting-state EEG power, including alpha peak frequency (APF) and theta/beta ratio (TBR), as well as signal complexity using multi-scale entropy (MSE) were compared between 26 FXS participants (ages 5–28 years), and 77 neurotypical (NT) controls with a similar age distribution. Subsequently a replication study was carried out, comparing our cohort to 19 FXS participants independently recorded at a different site.

The authors apologize for this error and state that this does not change the scientific conclusions of the article in any way. The original article has been updated.

frontiers in Psychiatry

ORIGINAL RESEARCH
published: 18 March 2022
doi: 10.3389/fpsyt.2022.846201

Neurodevelopmental Trajectories in Children With Internalizing, Externalizing and Emotion Dysregulation Symptoms

Elisabet Blok[1,2†], *Eloy P. T. Geenjaar*[3,4†], *Eloïse A. W. Geenjaar*[1†], *Vince D. Calhoun*[3,4] *and Tonya White*[1,5*]

[1] Department of Child and Adolescent Psychiatry/Psychology, Erasmus MC Sophia Childrens Hospital, University Medical Center Rotterdam, Rotterdam, Netherlands, [2] The Generation R Study Group, Erasmus MC, University Medical Centre Rotterdam, Rotterdam, Netherlands, [3] School of Electrical and Computer Engineering, Georgia Institute of Technology, Atlanta, GA, United States, [4] Tri-institutional Center for Translational Research in Neuroimaging and Data Science (TReNDS), Atlanta, GA, United States, [5] Department of Radiology and Nuclear Medicine, Erasmus MC, University Medical Centre Rotterdam, Rotterdam, Netherlands

OPEN ACCESS

Edited by:
Martine Hoogman,
Radboud University Nijmegen Medical Centre, Netherlands

Reviewed by:
Jaroslav Rokicki,
Oslo University Hospital, Norway
Jakob Seidlitz,
University of Pennsylvania, United States

***Correspondence:**
Tonya White
t.white@erasmusmc.nl

[†] These authors share first authorship

Specialty section:
This article was submitted to Neuroimaging and Stimulation, a section of the journal Frontiers in Psychiatry

Received: 30 December 2021
Accepted: 03 February 2022
Published: 18 March 2022

Citation:
Blok E, Geenjaar EPT, Geenjaar EAW, Calhoun VD and White T (2022) Neurodevelopmental Trajectories in Children With Internalizing, Externalizing and Emotion Dysregulation Symptoms. Front. Psychiatry 13:846201. doi: 10.3389/fpsyt.2022.846201

Introduction: Childhood and adolescence are crucial periods for brain and behavioral development. However, it is not yet clear how and when deviations from typical brain development are related to broad domains of psychopathology.

Methods: Using three waves of neuroimaging data within the population-based Generation R Study sample, spanning a total age range of 6–16 years, we applied normative modeling to establish typical development curves for (sub-)cortical volume in 37 brain regions, and cortical thickness in 32 brain regions. Z-scores representing deviations from typical development were extracted and related to internalizing, externalizing and dysregulation profile (DP) symptoms.

Results: Normative modeling showed regional differences in developmental trajectories. Psychopathology symptoms were related to negative deviations from typical development for cortical volume in widespread regions of the cortex and subcortex, and to positive deviations from typical development for cortical thickness in the orbitofrontal, frontal pole, pericalcarine and posterior cingulate regions of the cortex.

Discussion: Taken together, this study charts developmental curves across the cerebrum for (sub-)cortical volume and cortical thickness. Our findings show that psychopathology symptoms, are associated with widespread differences in brain development, in which those with DP symptoms are most heavily affected.

Keywords: neurodevelopment, normative modeling, childhood, adolescence, psychopathology

1. INTRODUCTION

Over the course of childhood and adolescence, both the brain and behavior undergo tremendous development. Regarding the relationship between the developing brain and atypical behavior, a body of evidence has associated differences in brain morphology to multiple domains of psychopathology (1–5). These studies have assessed multiple measures of brain morphology, including cortical volume and cortical thickness. However, the brain regions that have been

identified are widespread and vary substantially across studies (5, 6). Additionally, the direction of effect also differs across studies, meaning that some studies find positive relationships between cortical thickness/volume and psychopathology, whereas others find negative associations (1, 7–10).

The age at which children are assessed may potentially be a crucial factor to unravel why effects across studies differ in both location and direction. Non-linear patterns in brain development across age may partially underlie differences in the direction of observed effects. Total brain volume, for example, increases until adolescence, where it reaches a plateau and starts to decline (11), whereas gray matter volume reaches this peak in early childhood (12). Additionally, evidence suggests that distinct brain lobes and regions within lobes, develop at their own pace (11, 13). The asynchronous development of regions and lobes may be an explanation for the effect differences observed in the brain regions involved in these studies. Recent work has therefore used data-driven normative modeling, a technique that can be used to derive typical development curves for brain morphology (14–16). Emerging evidence suggests that deviations from typical brain development, estimated using these normative models, improves prediction of psychopathology over predictions based on raw brain morphology measures (17).

Two broad domains of psychopathology, that have been widely studied in children, in relation to brain morphology include the internalizing domain (e.g., anxiety, depression) and the externalizing domain (e.g., aggressive behavior). A third domain is emotion dysregulation, which includes symptoms of both the internalizing and externalizing domain. Regions that were reported most consistently across studies for the internalizing domain include the orbitofrontal cortex (OFC) (1, 6, 8, 9, 18, 19), rostral middle frontal cortex (2, 3, 20), anterior cingulate cortex (ACC) (2, 3, 6, 19), amygdala (2, 3, 7, 20, 21) and hippocampus (2, 6, 18, 20). Regions that have shown to be associated with externalizing symptoms partially overlap with those reported for internalizing symptoms. These include the OFC (22), ACC (23–25), amygdala (4, 5, 26–28), hippocampus (24, 27, 29) and striatum (10, 23, 26). Research on emotion dysregulation is relatively scarce. However, Shaw et al. proposed that the OFC, amygdala and striatum, brain regions involved in the bottom-up response to emotional cues, are mainly associated with symptoms of emotion dysregulation (30).

The direction of the effect in earlier work on internalizing symptoms, seems to be dependent on the age range that is used in studies. Namely, studies including younger age ranges generally observed positive associations (1, 7, 19), whereas in older age ranges negative associations are observed (8, 9). In contrast, for externalizing symptoms, the majority of studies, including a meta-analysis for cortical and subcortical gray matter volume, point toward lower volume and thickness in children with externalizing disorders (5, 10, 22, 24–29), while a few report higher cortical volume or thickness (10, 31) and one reports a non-linear relationship (23).

The aims of this study were (i) to establish normative development curves for cortical thickness and (sub-)cortical volumes, covering the gray matter of the cerebrum, and (ii) to study to what extent deviations from typical development are related to psychopathology symptoms in a large population-based cohort of children and adolescents. We hypothesized that all three domains of psychopathology would be related to deviations from normative development of brain morphology. Specifically, we hypothesized that for internalizing symptoms, alterations would be most prominent in the rostral middle frontal cortex, OFC, amygdala and hippocampus; for externalizing in the ACC, OFC, amygdala, hippocampus and striatum; and for DP symptoms in the OFC, amygdala and striatum. Further, we hypothesized that the direction of these deviations varies with age for internalizing symptoms, with positive deviations at younger and negative deviations at older ages. For the externalizing domain we hypothesized that, in line with most prior work, higher symptoms are related to negative deviations from normative development at all ages.

2. MATERIALS AND METHODS

2.1. Participants

This study is embedded in the neuroimaging component of the Generation R Study, a large, longitudinal, population-based cohort with an observational design. The recruitment strategy has been described elsewhere (32–34). In brief, women living within specific zip codes of Rotterdam with a delivery date between April 2002 and January 2006 were invited to participate. The families are still being followed. When children were 6–10 years old (T1), 8–12 years old (T2), and 13 to 16 years old (T3), neuroimaging and behavioral data were collected. Children were included in the current study if they had good quality neuroimaging and behavioral data available in at least one wave of data collection. Neuroimaging data were excluded if any of the following conditions were present: dental braces, incidental findings that significantly alter brain morphology, or poor image quality. At T1, a total of 842 children were included, at T2, 2,708 children were included and at T3, 1,904 were included, resulting in a total sample of 5,454 scans from 4,415 children. A flowchart of the study sample is provided in **Figure 1**. The Generation R Study was approved by the medical ethics committee at the Erasmus MC and conducted according to the Declaration of Helsinki. Written informed consent, and when applicable assent, was obtained from the caregivers and their children.

2.2. Measures

2.2.1. Behavioral Assessment

Child behavior was assessed using the Child Behavior Checklist (CBCL). At T1, the CBCL version for children aged 1.5–5 years was used (35), and at T2 and T3, the CBCL version for children aged 6–18 years was used (36). Both versions are reliable and valid questionnaires to assess child behavior (35, 36). The CBCL v1.5-5 has 99 items, and v6-18 has 112 items that are scored on a three-point Likert scale (0 = not true, 1 = somewhat true, 2 = very true). From the CBCL v1.5-5, seven empirically derived syndrome scales were calculated. From the CBCL v6-18, eight syndrome scales were obtained. These syndrome scales were summed into three broad domains of psychopathology [internalizing, externalizing and dysregulation profile (DP) symptoms]. In the CBCL v1.5-5, the internalizing scale includes the emotionally

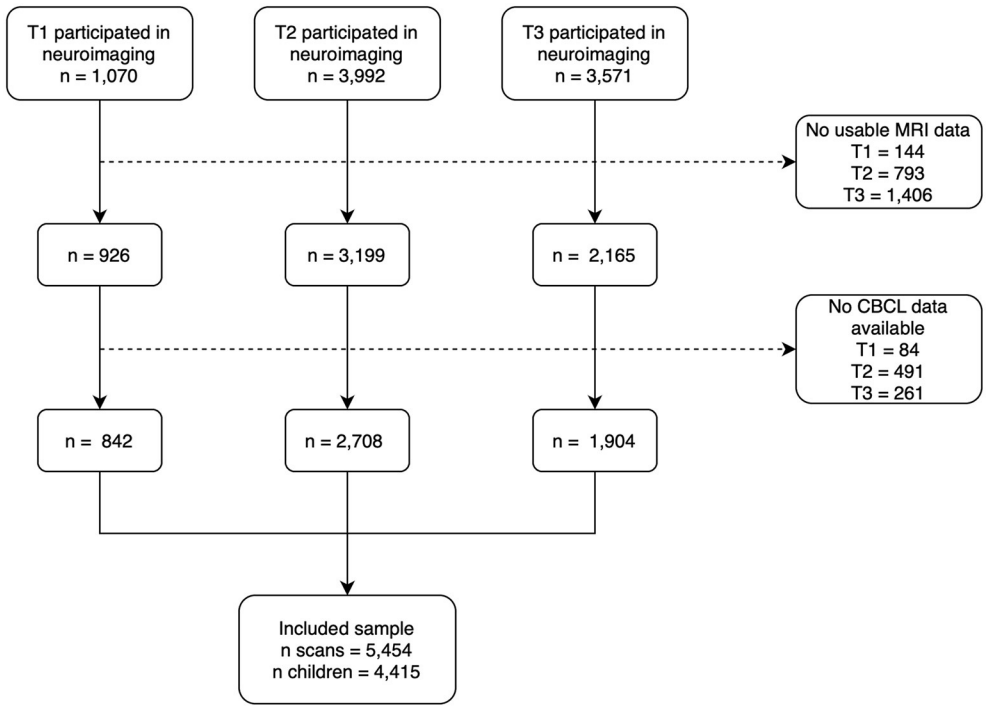

FIGURE 1 | Flowchart of the study sample.

reactive, anxious/depressed, withdrawn and somatic complaints syndrome scales, and in the CBCL v6-18 it is a sum-score of the anxious/depressed, withdrawn/depressed and somatic complaints syndrome scales. Externalizing symptoms were assessed with the attention problems and aggressive behavior syndrome scales in CBCL v1.5-5, and with the rule-breaking behavior and aggressive behavior syndrome scales in v6-18. Lastly, the DP is a comorbid profile, which is the summed score of the anxious/depressed, attention problems and aggressive behavior syndrome scales in both CBCL versions (35, 36).

2.2.2. MRI Acquisition

Neuroimaging data were collected on two scanners. At T1, structural MRI scans were acquired on a 3.0 Tesla GE Discovery MR750 MRI System (General Electric, Milwaukee, WI, USA). At T2 and T3, structural MRI scans were collected using a 3.0 Tesla GE Discovery MR750w MRI System (General Electric, Milwaukee, WI, USA). In all waves, we used an 8-channel receive only head coil. At T1, images were acquired using an inversion recovery fast spoiled gradient recalled (IR-FSPGR) sequence (sequence parameters: TE: 4.2 ms, TR: 10.3 ms, TI: 350 ms, flip angle: 16°, acquisition time: 5 min 40 s, FOV: 230.4 x 230.4, in-plane resolution: 0.9 mm^3, coverage: whole-brain) (33). At T2 and T3, images were acquired using a 3D coronal inversion recovery fast spoiled gradient recalled (IR-FSPGR, BRAVO) sequence (sequence parameters: TE: 3.4 ms, TR: 8.77 ms, TI: 600 ms, flip angle: 10°, acquisition time: 5 min 20 s, FOV: 220 x 220, in-plane resolution: 1.0 mm^3, phase encoding: R/L, fat suppression: yes, coverage: whole-brain) (34).

2.2.3. MRI Processing

Image processing for data from T1 to T3 was performed using FreeSurfer analysis suite v6.0.0 (http://surfer.nmr.mgh.harvard.edu/). All images were processed individually using FreeSurfer. FreeSurfer processing steps have been described in detail previously (37). Briefly, the analysis stream includes converting raw DICOM data to "MGZ-files," skull stripping, intensity normalization, and voxel segmentation of gray matter, white matter and cerebrospinal fluid. Labeling of the gray matter regions was performed using the Desikan-Killiany atlas (38).

2.2.4. MRI Quality Assurance

MRI quality assurance has been described previously (33, 34, 39). To summarize, FreeSurfer image reconstructions were visually inspected by at least one rater. Based on how well FreeSurfer delineated the gray-white matter and the outer gray matter boundaries, each scan was rated on a Likert scale. Raters included master students, PhD students and postdoctoral researchers, who were all trained extensively, which was completed after correctly rating 30 scans of which quality was determined previously. At T1 and T2, scans were rated on a five point Likert scale (unusable, poor, sufficient, good, excellent). At T3, scans were rated on a three point Likert scale (poor, questionable, good). All scans that were unusable or of poor quality were excluded from the analyses. Quality assessment based on visual inspection was also compared to an automated quality assessment, which has been described previously for T1 and T2 data (40). Visual ratings were also

TABLE 1 | Demographic characteristics.

	T1		T2		T3	
	n		*n*		*n*	
Age MRI (Mean, SD)	842	7.96 (1)	2,708	10.1 (0.57)	1,904	14 (0.6)
Age CBCL (Mean, SD)	842	6.06 (0.45)	2,708	9.7 (0.28)	1,904	13.52 (0.36)
Measures in %						
Child national origin						
Dutch	596	70.78%	1,771	65.4%	1,199	62.97%
Non Dutch	246	29.22%	937	34.6%	705	37.03%
Maternal education						
Low	30	3.56%	47	1.74%	57	2.99%
Middle	335	39.79%	986	36.41%	708	37.18%
High	477	56.65%	1675	61.85%	1139	59.82%
Household income						
<€2,000.- per month	196	23.28%	528	19.5%	404	21.22%
>€2,000.- per month	646	76.72%	2,180	80.5%	1,500	78.78%
Measures in median, IQR						
Handedness	842	0.82 (0.64–0.92)	2708	0.83 (0.67–1)	1,904	0.83 (0.67–1)
Child psychopathology						
Internalizing	842	6 (2–11)	2,708	3 (1–7)	1,904	4 (1–8)
Externalizing	842	8 (3–15)	2,708	2 (0–5)	1,904	2 (0–6)
Dysregulation Profile	842	10 (4–18)	2,708	6 (3–11)	1,904	6 (3-12)

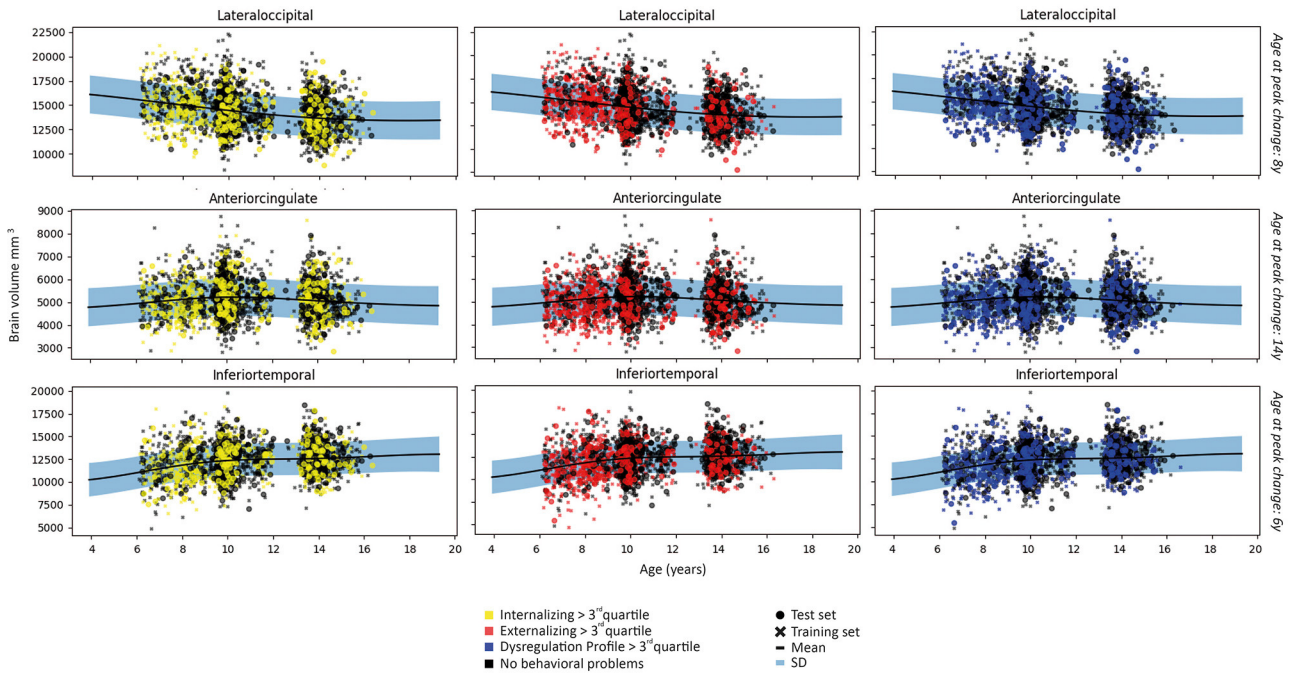

FIGURE 2 | Examples of patterns of (sub-)cortical volume for each subject in the first fold and the fit of the normative model to the (sub-)cortical volume in the training set. A wider prediction range outside of data distribution is used for visualization purposes. For illustrative purposes, measures are rescaled to the original means and standard deviations.

compared to this automated quality assessment at T3, as well as to the Euler number which can be extracted after FreeSurfer reconstruction (41), this comparison is depicted in **Supplementary Figure S1**.

2.2.5. Covariates

Multiple covariates were included in the analyses. Sex was derived from medical records at birth. Handedness was measured at each data collection wave, with the Edinburgh Handedness

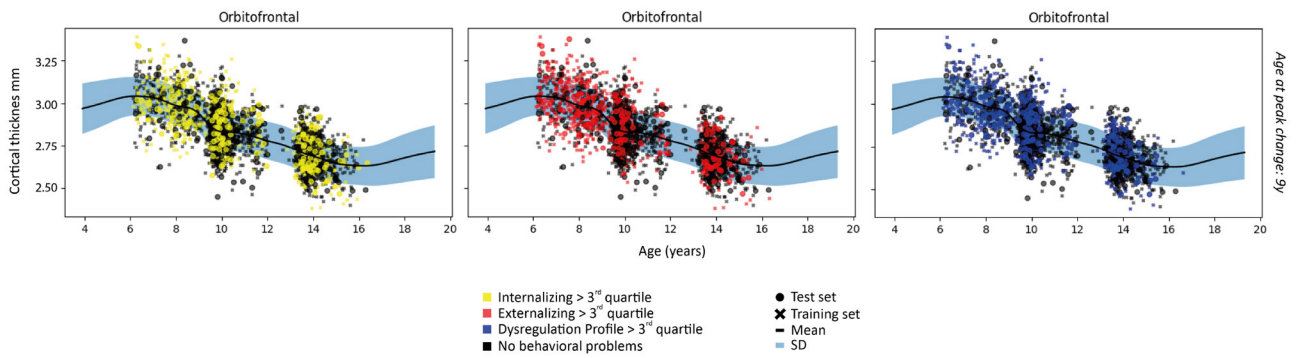

FIGURE 3 | Examples of patterns of cortical thickness for each subject in the first fold and the fit of the normative model to the cortical thickness in the training set. A wider prediction range outside of data distribution is used for visualization purposes. For illustrative purposes, measures are rescaled to the original means and standard deviations.

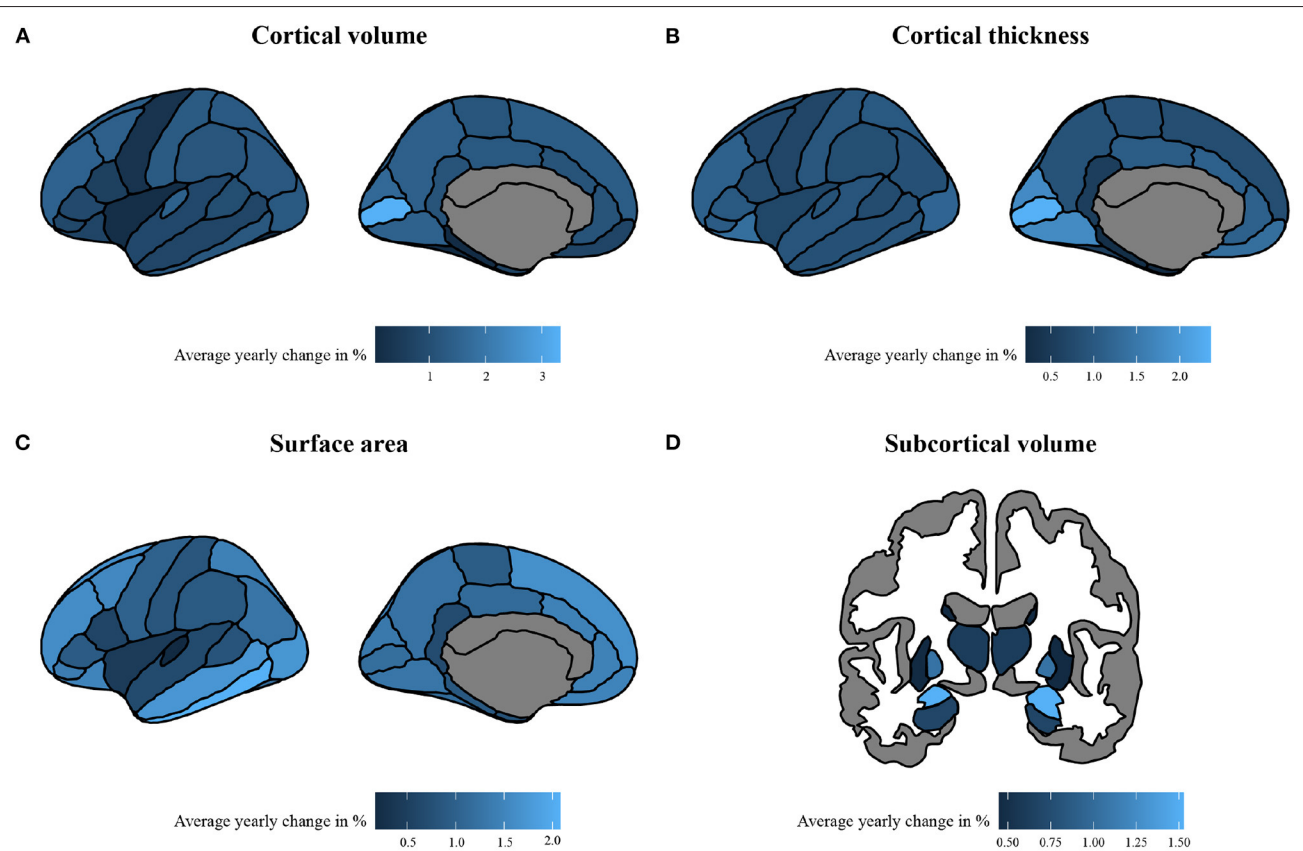

FIGURE 4 | The absolute average percentage change per year of morphological measures. The change is calculated with absolute percentages of change per year, calculated across a span of 6–16 years in **(A)** cortical volume, **(B)** cortical thickness, **(C)** surface area, and **(D)** subcortical volume. To enhance interpretability, absolute average change was calculated using brain measures that were rescaled to their original means and standard deviations.

Inventory (EHI) (42), from which a laterality quotient was obtained ranging from –1 (fully left-handed) to +1 (fully right-handed). Maternal education, household income and child national origin were assessed using a questionnaire. Maternal education and household income were assessed at T1 and used as proxies for socioeconomic status (SES). Maternal education was divided into three categories: low (no education/primary school), middle (high school/vocational training), and high (higher vocational training/university) and household income into two categories: below €2000,- per month and above €2000,- per month. Child national origin was assessed at baseline, based on the birth country of the parents, it was categorized as

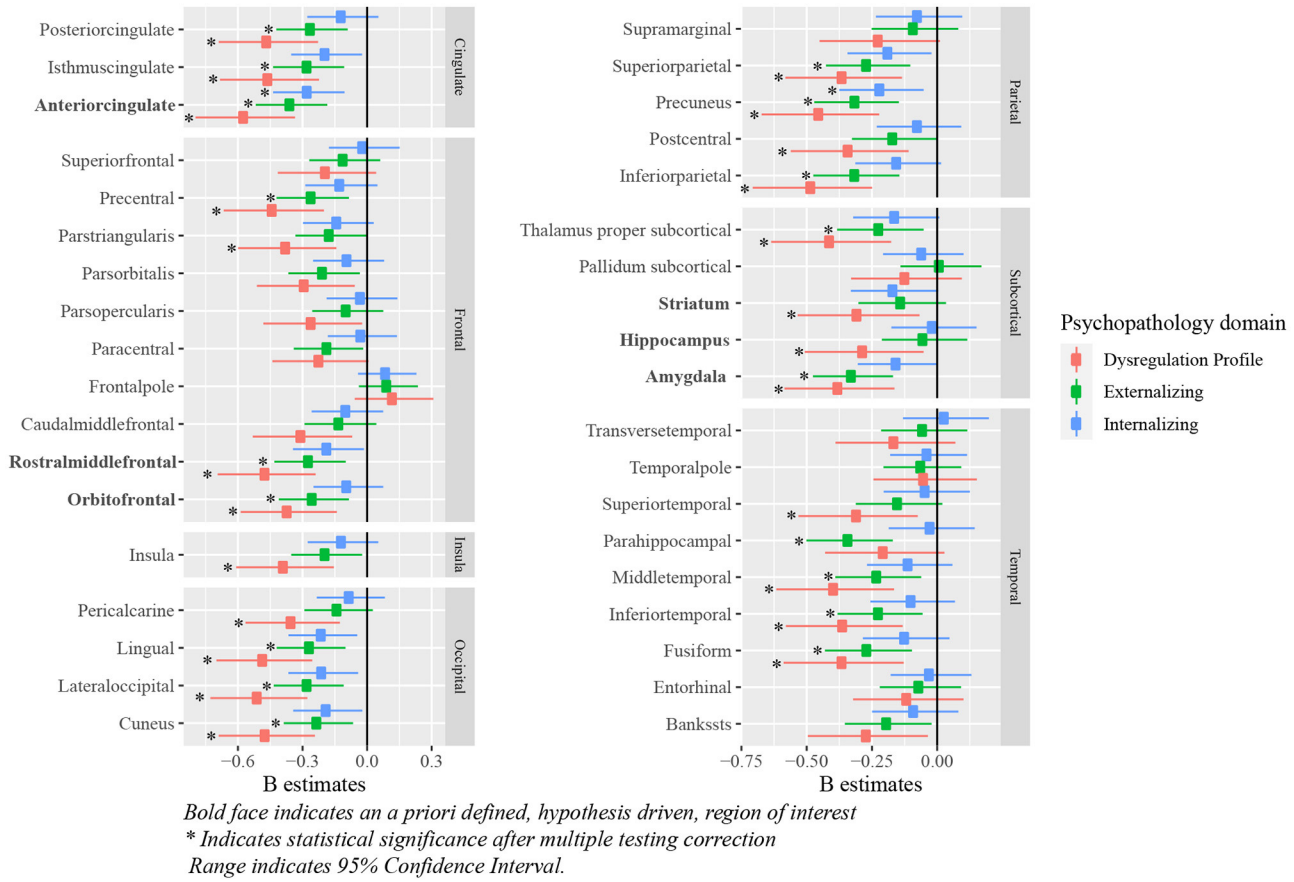

FIGURE 5 | Standardized B estimates of the relationship between z-scores (representing deviations of typical development in (sub-)cortical volume) and psychopathology symptoms. Bold face indicates an a priori defined, hypothesis driven, region of interest *indicates statistical significance after multiple testing correction range indicates 95% confidence interval.

Dutch and non-Dutch (African, American western, American non-western, Asian western, Asian non-western, Cape Verdean, Dutch Antilles, European, Indonesian, Moroccan, Oceania, Surinamese and Turkish).

2.3. Statistical Analyses

Our primary analyses assessed the relationship between deviations from typical development in cortical and subcortical regions of interest (ROIs) and multiple domains of psychopathology, using normative modeling. Specifically we included the following ROIs: the ACC (sum of rostral and caudal ACC), OFC (sum of lateral and medial OFC), rostral middle frontal cortex, the amygdala, hippocampus and the striatum (sum of putamen, caudate and nucleus accumbens). For cortical ROIs, we included measures of cortical thickness as well as cortical gray matter volume, for subcortical ROIs, gray matter volumes were included. In our secondary analyses, we explored the remaining (sub-)cortical regions labeled within FreeSurfer (38, 43), following the same procedure as for our primary analyses. To reduce the total number of tests, brain measures were averaged across both hemispheres.

The analyses consisted of five steps. First, we residualized brain morphology measures for possible covariate effects using two different models. In model 1 the effects of sex and handedness were regressed out of brain and CBCL measures, in model 2 the effects of SES and child national origin were additionally regressed out. Second, these residualized brain morphology measures were used to fit our normative model. A common way to fit a normative model is to use Gaussian process regression with age, and have the model predict the brain measure from those inputs. Generally, the subjects used in these analyses are considered to have typical development and the model is then validated using a held out subset of typically developing subjects (14–16). The Generation R study, however, is a population-based sample that is not enriched for children with psychopathology. Thus, we fit the model on all participants, which has been described as a viable option previously (15). Importantly, the current sample did not merely include cross-sectional data, but also longitudinal data for many of the participants. We leveraged the longitudinal data by bootstrapping multiple unique combinations of subsets of scans as training sets. In the individual training sets, all

participants were only included once, to prevent overfitting on a single person's development. To reach an approximately even distribution of participants across ages in each training set, approximately 50% of the scans acquired at T2 and T3 were not included in each individual training set. In each test set, 10% of the participants from T1, T2, and T3 were included.

We used Gaussian process regression (GPR) to fit (non)-linear normative trajectories to each brain measure across age. GPRs fit a Gaussian process to the given data points, such that any age, along a continuum (x-axis), is associated with a normal distribution for each brain region (y-axis). This approach is especially well-suited for normally distributed data. Given that we used a population sample, we assume that points for each brain region are normally distributed. Each brain measure was thus fit using a separate Gaussian process with GPytorch's (44) exact Gaussian processes module. The Gaussian process is continuous and can interpolate and extrapolate from the age range of a given set of points. An added benefit of associating a normal distribution with each brain measure given a certain age is that we can use the standard deviation of the distribution to calculate how confident the Gaussian process is in its prediction. It also allows us to interpret the distributions over time as each brain measure's normative trajectory. An important hyperparameter for Gaussian process regression is its kernel, which determines the shape of the line that the normal distributions are centered on. We empirically evaluate a variety of typical kernels for each brain region to limit assumptions about their normative trajectory. Before fitting the GPR, all brain measures were standardized to a mean of 0 and a standard deviation of 1, to accommodate direct comparisons of effect-size estimates across brain regions and measures. The age was rescaled between 0 and 1 based on the minimum and maximum age in the dataset. To assure we obtain the best fit for the trajectory of a given region, we evaluated multiple types of kernels on an unseen validation set. This validation set was a small (10% of each wave in the training fold) subsample of the training set. The kernels we used included a linear, Matern, radial basis function (RBF), and a rational quadratic kernel. We averaged the performance of each kernel over the validation sets to select the best kernel. The best kernel and complete training set, including the validation set, were used to train the final model. The final models for each training set were then used to predict the mean and standard deviance at each age in the test fold.

Third, the difference between these predicted mean and standard deviations for each morphological value and the true morphological values were used to calculate the z-scores for each participant. The formula for this calculation is shown in Equation 1.

$$\mathbf{z} = \frac{\mathbf{y} - \hat{\mathbf{y}}}{\hat{\sigma}} \quad (1)$$

Where, $\mathbf{y}$ are the true values for the brain measures at each age, $\hat{\mathbf{y}}$ are the mean predicted brain measures at each age, and $\hat{\sigma}$ are the predicted variances at each age. Note that because the normative model predicts a normal distribution at each age, average predicted brain measure at each age is the most likely value of that brain measure. Fourth, the association between the deviations of each individual from normative development and psychopathology was tested, using separate linear mixed model analyses. Internalizing, externalizing and DP symptoms were entered as dependent variables, z-scores for all brain measures were entered as independent variables, and a random effect was applied for participant ID. Finally, these analyses were repeated with an interaction term for age, to assess whether differences in the slope of deviations from typical development were age-dependent.

To assess the robustness of the findings, two sensitivity analyses were performed. First, normative development curves for (sub-)cortical volume in each region were fit with the effect of total intracranial volume (ICV) regressed out of individual volumes. Z-scores obtained from this model were subsequently related to psychopathology symptoms, to assess whether the effects observed were global or specific to regions. Second, we assessed whether deviations from typical development are specific to psychopathology domains. Therefore, analyses were repeated for brain regions that showed a significant relationship with two or more individual psychopathology domains, in which all significant psychopathology domains were entered in the model simultaneously.

Lastly, as *post-hoc* analyses, both normative developmental trajectories and deviations due to psychopathology

TABLE 2 | Hypothesis driven (sub-)cortical volume model 2.

Brain region	Psychopathology symptoms	B	S.E.	*p*-value
Anterior cingulate	Internalizing	–0.271	0.085	1.39e-03*
	Externalizing	–0.351	0.085	3.61e-05*
	Dysregulation Profile	–0.566	0.118	1.71e-06*
Orbitofrontal	Internalizing	–0.087	0.083	2.92e-01
	Externalizing	-0.248	0.083	2.91e-03*
	Dysregulation Profile	–0.364	0.114	1.42e-03*
Rostral middle frontal	Internalizing	–0.18	0.084	3.28e-02
	Externalizing	–0.265	0.084	1.73e-03*
	Dysregulation Profile	–0.467	0.116	6.03e-05*
Amygdala	Internalizing	–0.152	0.078	5.19e-02
	Externalizing	–0.323	0.078	3.92e-05*
	Dysregulation Profile	–0.374	0.107	5.05e-04*
Hippocampus	Internalizing	–0.012	0.083	8.81e-01
	Externalizing	–0.048	0.084	5.62e-01
	Dysregulation Profile	–0.28	0.116	1.6e-02*
Striatum	Internalizing	–0.163	0.085	5.57e-02
	Externalizing	–0.134	0.086	1.18e-01
	Dysregulation Profile	–0.301	0.119	1.16e-02*

**Indicates significance after correction for multiple testing using FDR-BH at a q-value of 0.05.*

were established for surface area in all hypothesis-driven and exploratory regions of interest, after which deviations from typical development were related to all psychopathology domains.

Bootstrapping and regression analyses were performed in R version 3.6.3 (45), normative modeling was performed in Python version 3.9.0 (46). Missing data in the covariates were imputed 30 times with 30 iterations using multiple imputation through chained equations with the mice package (47). The false discovery rate (FDR) was controlled using the Benjamini Hochberg procedure (48). Primary analyses were corrected for a total of 27 tests, at q-value = 0.05. Exploratory analyses were separately corrected for a total of 180 tests (q-value = 0.05). Analyses using an interaction term were corrected for multiple testing following the same procedure for a total of 207 tests. Hypotheses and analyses for this project were publicly preregistered, a time-stamped version of this preregistration is available via: www.osf.io/aqc4s. Slight deviations from our initial preregistration are described in the **Supplementary Material**. Analysis scripts are publicly available via https://github.com/eloygeenjaar/normative-smri-psychopathology.

3. RESULTS

3.1. Sample Characteristics

Sample characteristics are described in **Table 1**. At all time points the majority of the children included were of Dutch national origin (T1 = 70.8%, T2 = 65.4%, T3 = 63.0%), had mothers with high educational levels (T1 = 56.7%, T2 = 61.9%, T3 = 59.8%) and came from households with an income >€2,000.- per month (T1 = 76.7%, T2 = 80.5%, T3 = 78.8%).

3.2. Normative Development of Brain Morphology

The linear and/or non-linear development curves were fit for each residualized region (model 1 and model 2) included in the Desikan-Killiany atlas (38). Examples of the most common patterns that we observed are depicted in **Figures 2**, **3**. Full results from the normative model are shown in **Supplementary Figures S2, S3**. The average change in (sub-)cortical volume and cortical thickness across 6–16 years of age is provided in **Figure 4**.

3.2.1. Cortical and Subcortical Volume

Normative development curves between age 6–16 revealed an increasing slope for (sub-)cortical volume in the entorhinal, inferior temporal, middle temporal, temporal pole, hippocampus, pallidum and thalamic regions; a decreasing slope for the cuneus, frontal pole, isthmus cingulate, lateral occipital, lingual, paracentral, pars opercularis, pars triangularis, pericalcarine, precuneus, post central, supramarginal and transverse temporal regions; and an inverted U-shaped curve for the anterior cingulate, banks of superior temporal sulcus, caudal middle frontal, inferior parietal, orbitofrontal, pars orbitalis, precentral, posterior cingulate, rostral middle frontal, superior frontal, superior parietal, superior temporal, amygdala and striatal regions. Flat trajectories were observed in the fusiform, insula and parahippocampal regions. These patterns were consistent across model 1 and 2. Given that normative development curves were fit on 12 bootstrapped folds of the dataset, the optimal fit differed slightly between individual folds, however, patterns described were consistent across all folds.

3.2.2. Cortical Thickness

The normative models fit on cortical thickness data showed a decreasing slope from early to later neurodevelopment in the majority of regions (see **Supplementary Figure S1**). The steepest slope was primarily seen between 6 and 12 years of age. Noteworthy exceptions with a fairly flat slope across neurodevelopment were the entorhinal and temporal pole regions. These patterns were consistent across models and folds.

3.3. Deviations From Normative Development and Psychopathology

3.3.1. Hypothesis Driven Analyses

3.3.1.1. Cortical and Subcortical Volume

All a priori selected, hypothesis driven, regions of interest for cortical and subcortical volume showed a negative relationship with some psychopathology domains, meaning that psychopathology symptoms were related to negative deviations from typical brain development. After correction for multiple testing, negative deviations from typical development in the ACC were related to all psychopathology domains; negative deviations in the OFC, the rostral middle frontal cortex, and the amygdala were related to externalizing and DP symptoms. Lastly, negative deviations from typical development in hippocampal and striatal volume were related to DP symptoms. Full results are shown in **Figure 5** (model 2), **Table 2** and **Supplementary Table S1** (model 1).

3.3.1.2. Cortical Thickness

Positive associations were observed between deviations from typical cortical thickness development in the OFC, and externalizing and DP symptoms after correction for multiple testing. No associations were observed between deviations from normative development in the ACC and rostral middle frontal cortex, and each of the psychopathology domains. Full results are shown in **Figure 6** (model 2), **Table 3** and **Supplementary Table S2** (model 1).

3.3.2. Exploratory Analyses

3.3.2.1. Cortical and Subcortical Volume

Exploratory analyses revealed significant negative associations between deviations from typical development in several (sub-)cortical volume regions and psychopathology domains. After correction for multiple testing, all psychopathology domains were related to negative deviations from typical development in the precuneus. Negative deviations from typical development in the cuneus, fusiform, inferior parietal, inferior temporal, isthmus cingulate, lateral occipital, lingual, middle temporal, posterior cingulate, precentral, superior parietal and thalamus were observed for externalizing and DP symptoms. Lastly, negative deviations in the parahippocampal region were

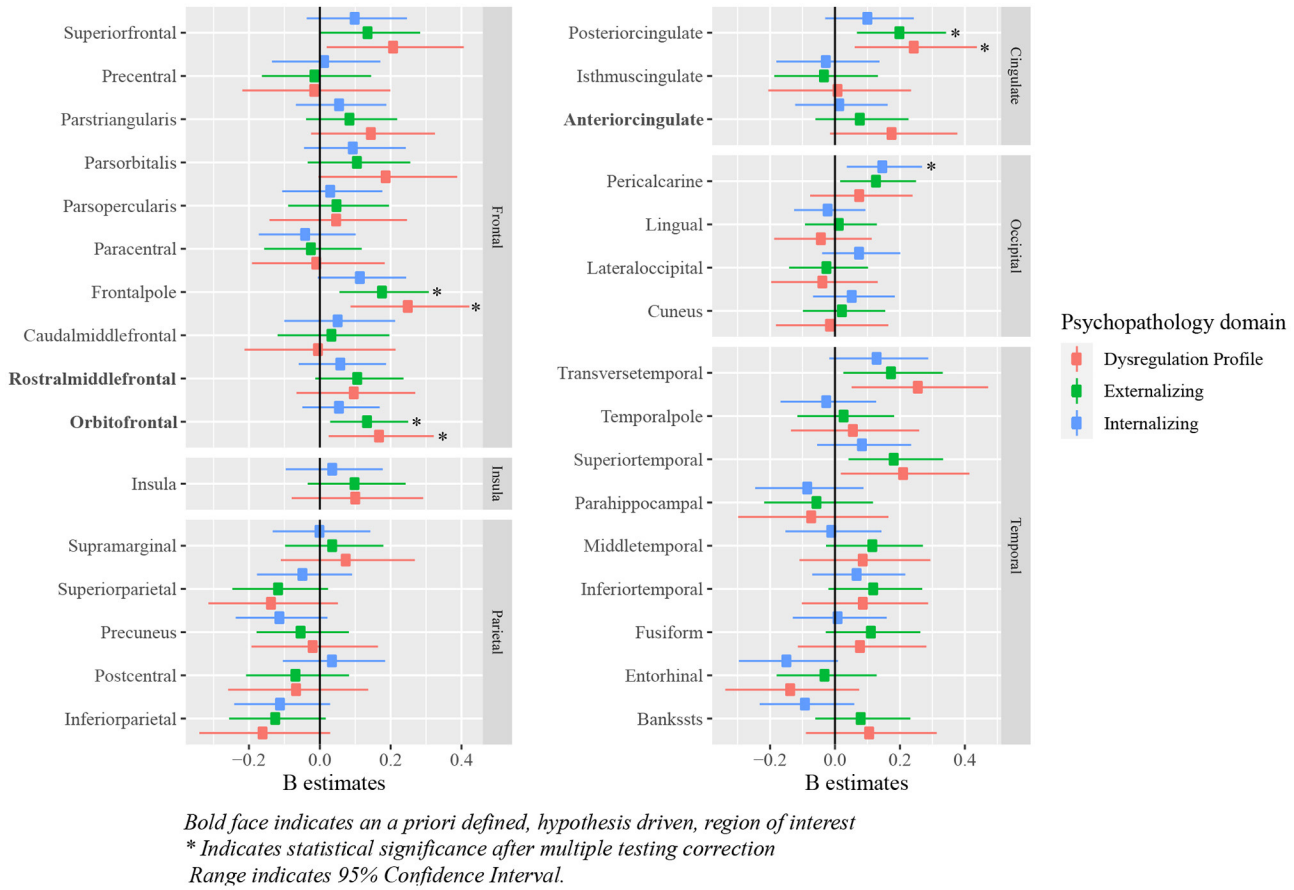

FIGURE 6 | Standardized B estimates of the relationship between z-scores (representing deviations of typical development in cortical thickness) and psychopathology symptoms. Bold face indicates an a priori defined, hypothesis driven, region of interest *indicates statistical significance after multiple testing correction range indicates 95% confidence interval.

specific to externalizing symptoms and negative deviations in the insula, pars triangularis, pericalcarine, postcentral and superior temporal region were specific to DP symptoms. Full results are shown in **Figure 5** (model 2), **Table 4** and **Supplementary Table S3** (model 1).

3.3.2.2. Cortical Thickness

Positive deviations were observed in the pericalcarine region in relation to internalizing symptoms. Additionally, positive deviations from typical development in the frontal pole and the posterior cingulate region were related to higher externalizing and DP symptoms. Deviations from typical development in cortical thickness for most regions were not related to psychopathology symptoms. Full results are shown in **Figure 6** (model 2), **Table 5** and **Supplementary Table S4** (model 1).

3.3.3. Interaction Effect Age

After correction for multiple testing, a significant positive interaction effect between age and the deviations from typical development in cortical volume was observed in the fusiform and parahippocampal region in relation to externalizing symptoms. This indicates that with increasing age, deviations from typical development become larger in those with externalizing symptoms. Full results are shown in **Supplementary Tables S5–S8**.

3.3.4. Sensitivity Analyses

In the first sensitivity analysis we repeated our analyses on cortical and subcortical volume while correcting for ICV, to assess whether the observed relationships were global or region specific. While the relationships attenuated in many regions, some region specific deviations were identified. In our hypothesis driven regions, the relationship between the ACC development and all psychopathology domains, as well as the relationship between the amygdala and externalizing symptoms remained statistically significant after adjustment for ICV. Additionally, exploratory analyses indicated a significant relationship between the lingual region and all psychopathology domains; between the cuneus, inferior parietal, lateral occipital and precuneus, and externalizing and DP symptoms; and between the isthmus cingulate, pars triangularis, pericalcarine and posterior cingulate, and DP symptoms. Full results are shown in **Supplementary Tables S9, S10**.

In the second sensitivity analysis we assessed whether, for those regions that showed a significant relationship with multiple

TABLE 3 | Hypothesis driven cortical thickness model 2.

Brain region	Psychopathology symptoms	B	S.E.	*p*-value
Anterior cingulate	Internalizing	0.02	0.073	7.86e-01
	Externalizing	0.083	0.073	2.56e-01
	Dysregulation Profile	0.181	0.1	7.11e-02
Orbitofrontal	Internalizing	0.06	0.056	2.83e-01
	Externalizing	0.139	0.056	1.33e-02*
	Dysregulation Profile	0.173	0.076	2.22e-02*
Rostral middle frontal	Internalizing	0.064	0.063	3.11e-01
	Externalizing	0.112	0.064	7.89e-02
	Dysregulation Profile	0.102	0.086	2.34e-01

**Indicates significance after correction for multiple testing using FDR-BH at a q-value of 0.05.*

psychopathology domains, certain psychopathology domains were associated to deviations from typical development above and beyond other psychopathology symptoms. Regarding cortical volume, our findings indicated that internalizing and externalizing symptoms are not related to deviations from typical development when controlling for other psychopathology domains. DP symptoms, however, were related to deviations from typical development in the ACC and the precuneus, when adjusting for internalizing and externalizing symptoms. Additionally, DP symptoms were related to deviations in the rostral middle frontal, cuneus, inferior parietal, isthmus cingulate, lateral occipital, middle temporal, posterior cingulate, precentral and thalamic region after adjustment for externalizing symptoms. For cortical thickness, none of the psychopathology symptoms were related when controlling for other psychopathology domains. Full results are shown in **Supplementary Tables S11, S12**.

3.3.5. *Post-hoc* Analyses

As *post-hoc* analyses, normative trajectories were established for cortical surface area. Normative trajectories showed an inverted U-shaped relationship for the majority of regions. Notable exceptions were positive trajectories in the anterior cingulate, entorhinal, fusiform, inferior temporal, insula, middle temporal, orbitofrontal, parahippocampal, pars opercularis, pars orbitalis, pars triangularis and temporal pole; and a negative trajectory for the transverse temporal region. Examples of the most common patterns are shown in **Figure 7** and full results from the normative model are shown in **Supplementary Figure S4**.

Relationships between deviations from typical development of surface area and psychopathology largely mirrored the associations between cortical volume and psychopathology, in which most regions showed negative deviations from typical development. Full results are presented in **Figure 8** and **Tables 6**, **7**.

4. DISCUSSION

This study aimed to assess the relationship between deviations from typical brain development and psychopathology symptoms using three waves of neuroimaging and behavioral data from a large population-based cohort. We applied normative modeling to derive typical development curves, which showed regional differences in the development of subcortical and cortical volume, as well as cortical thickness and surface area. Psychopathology symptoms were related to deviations from typical development in subcortical volumes, and widespread regions across the cortex for cortical volume and surface area, and some regions for cortical thickness.

Our hypothesis driven and exploratory analyses together revealed that deviations from normative development related to psychopathology symptoms are not restricted to the a priori defined regions of interest, but rather that these deviations were present in regions across the entire cortex, as well as subcortical gray matter volumes. This raises the idea that the observed associations might not be region specific, but rather represent a global effect on brain development. Indeed, the majority of these findings did not remain after additional correction for ICV, indicating that the effects obtained are mostly global. Some areas, however, show a significant relationship on top of this global effect. Taken together, the observed pattern suggests that, while some regions may be particularly important for the emergence of psychopathology symptoms or affected by downstream effects of psychopathology (39), associations between cortical volume and psychopathology are not necessarily restricted to these regions. Given that emotion and behavior require integration of information that involves many brain regions, these small, but widespread differences may together lead to differences in psychopathology symptoms. Thus, our findings bolster the importance of analyzing the entire cortex and subcortex when assessing the relationship between brain morphology and psychopathology in youth, as opposed to restricting analyses to a priori defined regions of interest.

In line with our hypotheses, children with externalizing symptoms deviated from typical development for (sub-)cortical volumes in the ACC, OFC and amygdala, and children with DP symptoms deviated from typical development in the OFC, amygdala and striatum. As opposed to our initial hypothesis, we did not find evidence for a relationship between internalizing symptoms and the hypothesized regions of interest. Additionally, the relationship between deviations from typical development in the hippocampus and the striatum, and externalizing symptoms did not reach statistical significance. In line with the widespread alterations in development of subcortical and cortical volume, we additionally observed associations between the development of the ACC, and internalizing and DP symptoms, the rostral middle frontal cortex and externalizing and DP symptoms, and the hippocampus and DP symptoms. Earlier research on brain morphology and DP symptoms is relatively scarce, which is likely to explain why fewer regions had been reported to be related to DP symptoms previously. Our findings showed that associations between brain morphology and the DP were even more widespread than those for internalizing and externalizing symptoms. After correction for ICV, our results indicated region specific deviations from typical development for cortical volume in the ACC in relation to all psychopathology domains. Indeed, the ventral part of the ACC has been shown to have an important role in emotion regulation,

TABLE 4 | Exploratory (sub-)cortical volume model 2.

	Internalizing			Externalizing			Dysregulation profile		
Brain region	**B**	**S.E.**	***p*-value**	**B**	**S.E.**	***p*-value**	**B**	**S.E.**	***p*-value**
Banks of the superior temporal sulcus	–0.084	0.084	3.19e-01	–0.188	0.085	2.7e-02	–0.266	0.117	2.37e-02
Caudal middle frontal	–0.092	0.085	2.8e-01	–0.124	0.085	1.45e-01	–0.3	0.118	1.09e-02
Cuneus	–0.183	0.082	2.58e-02	–0.226	0.082	5.96e-03*	-0.466	0.114	4.63e-05*
Entorhinal	–0.024	0.079	7.65e-01	–0.064	0.08	4.2e-01	–0.111	0.108	3.06e-01
Frontal pole	0.093	0.069	1.77e-01	0.099	0.07	1.58e-01	0.125	0.093	1.8e-01
Fusiform	–0.119	0.085	1.61e-01	–0.263	0.085	1.99e-03*	-0.358	0.117	2.28e-03*
Inferior parietal	–0.149	0.084	7.57e-02	–0.31	0.084	2.39e-04*	–0.478	0.117	4.35e-05*
Inferior temporal	–0.094	0.083	2.57e-01	–0.219	0.083	8.56e-03*	–0.356	0.114	1.85e-0*
Insula	–0.112	0.084	1.81e-01	–0.188	0.084	2.55e-02	-0.381	0.116	9.99e-04*
Isthmus cingulate	–0.188	0.084	2.52e-02	–0.272	0.084	1.27e-03*	–0.454	0.117	1.15e-04*
Lateral occipital	–0.204	0.083	1.38e-02	–0.271	0.083	1.08e-03*	–0.503	0.115	1.3e-05*
Lingual	–0.206	0.081	1.17e-02	–0.26	0.082	1.46e-03*	–0.478	0.114	2.74e-05*
Middle temporal	–0.105	0.084	2.08e-01	–0.226	0.084	7.23e-03*	–0.391	0.115	6.96e-04*
Paracentral	–0.022	0.082	7.9e-01	–0.179	0.082	2.96e-02	–0.217	0.114	5.74e-02
Parahippocampal	–0.021	0.084	8.02e-01	–0.336	0.084	7.29e-05*	–0.201	0.117	8.56e-02
Pars opercularis	–0.024	0.084	7.77e-01	–0.09	0.084	2.86e-01	–0.253	0.117	3.11e-02
Pars orbitalis	–0.086	0.084	3.07e-01	–0.2	0.085	1.84e-02	-0.285	0.116	1.42e-02
Pars triangularis	-0.134	0.084	1.11e-01	-0.168	0.084	4.51e-02	–0.371	0.116	1.47e-03*
Pericalcarine	–0.076	0.081	3.48e-01	–0.132	0.081	1.03e-01	–0.346	0.112	2.02e-03*
Posterior cingulate	–0.113	0.084	1.81e-01	–0.256	0.085	2.48e-03*	–0.459	0.118	1.01e-04*
Postcentral	–0.07	0.083	4e-01	–0.164	0.083	4.79e-02	–0.335	0.115	3.67e-03*
Precentral	–0.12	0.085	1.62e-01	–0.253	0.086	3.24e-03*	–0.433	0.119	2.71e-04*
Precuneus	–0.214	0.082	9.7e-03*	–0.309	0.083	1.92e-04*	–0.448	0.115	1.02e-04*
Superior frontal	–0.013	0.084	8.76e-01	–0.104	0.084	2.17e-01	–0.186	0.117	1.1e-01
Superior parietal	–0.183	0.082	2.61e-02	–0.265	0.082	1.36e-03*	–0.358	0.114	1.69e-03*
Superior temporal	–0.04	0.084	6.35e-01	–0.146	0.085	8.47e-02	–0.303	0.117	9.43e-03*
Supramarginal	–0.069	0.084	4.11e-01	–0.085	0.085	3.14e-01	–0.22	0.118	6.2e-02
Temporal pole	–0.033	0.075	6.62e-01	–0.057	0.076	4.56e-01	–0.046	0.101	6.49e-01
Transverse temporal	0.033	0.084	6.91e-01	–0.05	0.084	5.54e-01	–0.16	0.117	1.73e-01
Pallidum	–0.053	0.079	5e-01	0.014	0.079	8.55e-01	–0.118	0.108	2.77e-01
Thalamus	–0.157	0.084	6.31e-02	–0.218	0.085	1.01e-02*	–0.406	0.117	5.43e-04*

**Indicates significance after correction for multiple testing using FDR-BH at a q-value of 0.05.*

including contextual fear generalization and the top-down regulation of aggressive impulses (49–52), and the dorsal ACC is crucial for cognitive control (53). Altered development of amygdala volume was only associated to externalizing and DP symptoms in this study, which is surprising given the role of the amygdala in processing of emotional cues that are important for all psychopathology domains (54). We had predicted that deviations in amygdala volume would also be associated with internalizing symptoms, although an earlier meta-analysis indicated that results on amygdala volume are somewhat inconsistent across studies, resulting in an absence of an effect in this meta-analysis (6). Regarding cortical thickness, deviations from typical development in the OFC were related to externalizing and DP symptoms, which is in line with the results obtained for cortical volume. However, in contrast with the findings for cortical volume, no associations between deviations from typical development in the ACC and any type of psychopathology were observed. Lastly, we hypothesized deviations from typical development in cortical thickness in the rostral middle frontal cortex to be related to internalizing symptoms, however, we did not find evidence for the presence of this relationship.

Deviations from typical development in surface area in children with symptoms of psychopathology showed remarkably similar results as those obtained for cortical volume. The overlap is likely partially explained by the high correlations between cortical volume and surface area, which in our sample ranged between 0.26 and 0.94. Given the low correlation between cortical thickness and surface area, these findings point toward surface area as an important brain morphology measure to study in relation to psychopathology. Although surface area is studied less extensively than cortical volume and cortical thickness in relation to psychopathology, recent work also showed similar results between psychopathology, and both cortical volume and

TABLE 5 | Exploratory cortical thickness model 2.

	Internalizing			Externalizing			Dysregulation profile		
Brain region	**B**	**S.E.**	***p*-value**	**B**	**S.E.**	***p*-value**	**B**	**S.E.**	***p*-value**
Banks of the superior temporal sulcus	–0.086	0.074	2.46e-01	0.086	0.075	2.51e-01	0.112	0.103	2.77e-01
Caudal middle frontal	0.056	0.08	4.81e-01	0.039	0.081	6.31e-01	0.001	0.109	9.95e-01
Cuneus	0.058	0.064	3.65e-01	0.028	0.065	6.66e-01	–0.009	0.088	9.2e-01
Entorhinal	–0.143	0.078	6.58e-02	–0.026	0.079	7.44e-01	–0.132	0.105	2.11e-01
Frontal pole	0.119	0.064	6.18e-02	0.182	0.064	4.83e-03*	0.254	0.086	2.99e-03*
Fusiform	0.015	0.074	8.43e-01	0.117	0.074	1.15e-01	0.083	0.101	4.09e-01
Inferior parietal	–0.106	0.069	1.24e-01	–0.12	0.07	8.54e-02	–0.156	0.094	9.9e-02
Inferior temporal	0.073	0.073	3.17e-01	0.124	0.074	9.22e-02	0.092	0.099	3.52e-01
Insula	0.041	0.07	5.58e-01	0.104	0.071	1.4e-01	0.106	0.095	2.63e-01
Isthmus cingulate	–0.022	0.081	7.88e-01	–0.028	0.081	7.36e-01	0.014	0.112	8.98e-01
Lateral occipital	0.081	0.061	1.9e-01	–0.02	0.062	7.49e-01	–0.032	0.084	6.99e-01
Lingual	–0.016	0.056	7.73e-01	0.018	0.056	7.48e-01	–0.037	0.077	6.29e-01
Middle temporal	–0.005	0.076	9.5e-01	0.121	0.076	1.11e-01	0.092	0.103	3.71e-01
Paracentral	–0.035	0.07	6.11e-01	–0.019	0.07	7.84e-01	–0.004	0.096	9.67e-01
Parahippocampal	–0.079	0.085	3.53e-01	–0.051	0.085	5.54e-01	–0.067	0.118	5.72e-01
Pars opercularis	0.035	0.072	6.26e-01	0.053	0.073	4.65e-01	0.052	0.099	5.99e-01
Pars orbitalis	0.099	0.073	1.77e-01	0.111	0.074	1.34e-01	0.192	0.1	5.48e-02
Pars triangularis	0.06	0.065	3.55e-01	0.09	0.066	1.72e-01	0.15	0.089	9.26e-02
Pericalcarine	0.152	0.059	1.01e-02*	0.133	0.06	2.6e-02	0.081	0.08	3.13e-01
Posterior cingulate	0.106	0.07	1.27e-01	0.205	0.07	3.48e-03*	0.249	0.096	9.56e-03*
Postcentral	0.04	0.074	5.86e-01	–0.063	0.074	3.97e-01	–0.061	0.101	5.45e-01
Precentral	0.018	0.078	8.17e-01	–0.009	0.079	9.07e-01	–0.01	0.107	9.27e-01
Precuneus	–0.108	0.066	1.02e-01	–0.048	0.066	4.68e-01	–0.014	0.091	8.76e-01
Superior frontal	0.104	0.072	1.48e-01	0.141	0.073	5.32e-02	0.213	0.099	3.13e-02
Superior parietal	–0.043	0.068	5.29e-01	–0.112	0.069	1.05e-01	–0.132	0.093	1.58e-01
Superior temporal	0.09	0.074	2.25e-01	0.187	0.074	1.18e-02	0.216	0.101	3.25e-02
Supramarginal	0.005	0.07	9.44e-01	0.041	0.071	5.64e-01	0.079	0.097	4.13e-01
Temporal pole	–0.02	0.075	7.86e-01	0.033	0.076	6.63e-01	0.062	0.101	5.4e-01
Transverse temporal	0.135	0.078	8.31e-02	0.179	0.078	2.21e-02	0.261	0.107	1.48e-02

**Indicates significance after correction for multiple testing using FDR-BH at a q-value of 0.05.*

surface area, but no relationship with cortical thickness (55). Contrary to these findings and the current findings, other work has observed alterations in cortical thickness in relation to multiple domains of psychopathology, whereas alterations in surface area were specific to externalizing disorders (56). A critical difference is, however, that the latter study evaluated the association between childhood psychopathology and brain morphology in mid-adulthood, and thus may not generalize to developmental populations. It will be important for future work to extend the current findings by assessing the relationship between brain morphology and psychopathology at multiple ages across the lifespan.

In both our hypothesis driven and exploratory analyses we showed that deviations from normative development were associated with psychopathology. Although the overlap in confidence intervals in the majority of regions do not suggest significant differences in effect sizes between psychopathology domains, a consistent pattern is observed with the largest effect sizes for DP symptoms and the smallest effect sizes for internalizing symptoms. This pattern was also observed in earlier work using the first and third wave of the current sample, for the relationship between cognitive performance, and internalizing, externalizing and DP symptoms (57, 58). These findings align closely with recent evidence that some alterations in brain structure and function are shared across many psychiatric disorders (59, 60). It is likely that the overlap in involved brain regions can partially be attributed to the high correlation among psychopathology domains. For example, internalizing and externalizing symptoms generally correlate with a coefficient of around 0.5 (61). Achenbach et al. (61) recommended adjustment for externalizing symptoms when internalizing symptoms are assessed and vice versa. Following this recommendation we performed sensitivity analyses for those regions in which deviations from typical development were related to multiple psychopathology domains. Our findings indicated that only DP symptoms were related to regional deviations from typical development above and beyond internalizing and externalizing symptoms. Thus, our findings add to the current knowledge

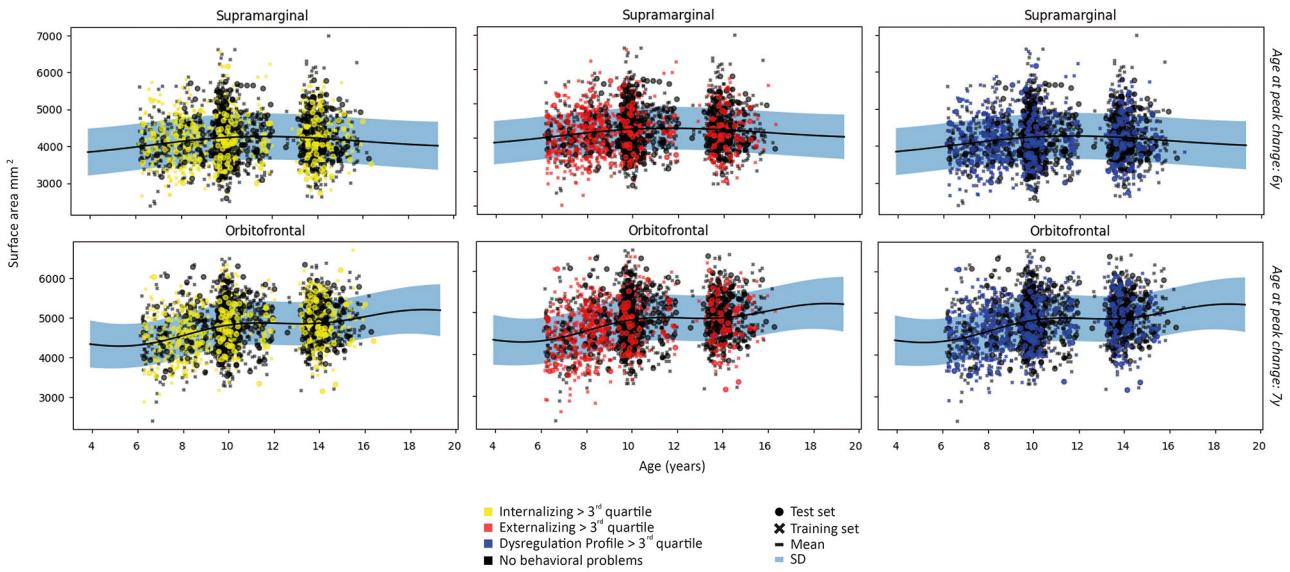

FIGURE 7 | Examples of patterns of surface area for each subject in the first fold and the fit of the normative model to the surface area in the training set. A wider prediction range outside of data distribution is used for visualization purposes. For illustrative purposes, measures are rescaled to the original means and standard deviations.

that those with DP symptoms are most heavily affected in terms of symptomatology (62) and cognitive performance (57, 58), that they are also most heavily affected in terms of deviations from brain development. A promising line of research that has emerged in recent years, aims to unpack the shared variance between individual dimensions of psychopathology into a general psychopathology factor (63, 64). The variance in symptomatology that remains after extraction of the general psychopathology factor can then be viewed as more specific internalizing and externalizing symptoms. Indeed, recent work has used a similar approach to normative modeling as used in the current study, and showed that general psychopathology was associated with deviations from typical development for gray matter volume in widespread regions across the cortex, and additionally identified regions that associated with specific psychopathology dimensions (17). This study focused on gray matter volume and used clinical cases to assess associations with psychopathology. Thus, a promising extension of our study would be to assess whether deviations from typical development in relation to the general psychopathology factor are also more pronounced in cortical volume than cortical thickness.

Regarding the direction of effect, negative deviations from typical development were observed for cortical volume and surface area, and psychopathology, whereas positive deviations were observed in the relationship between cortical thickness and psychopathology. These directions were consistent across all psychopathology domains, in which very few interaction effects for age were observed. The absence of this interaction effect suggests that the direction of effect between psychopathology symptoms and deviations from typical development were largely stable between 6 and 16 years of age. Thus, while we had hypothesized an age-dependent effect on the deviations of typical development related to internalizing symptoms, we only provide evidence for age related effects in the development of the fusiform and parahippocampal volume in relation to externalizing symptoms. To provide more context to the direction of effect, both in cortical volume and thickness, it would be beneficial to not only establish typical development curves using cross-sectional data, but also using longitudinal MRI data. Indeed, some evidence suggests that longitudinal trajectories of cortical development are different in those with internalizing (1, 8) and externalizing symptoms (24). Extending findings of the current study, by studying temporal changes in the deviations from typical development in relation to temporal changes in psychopathology, could provide unique insights in the bidirectional relationship between behavioral and brain development.

Findings from our normative model are in line with contemporary work that finds the average growth trajectory for gray matter volume to peak at 6–10 years of age, after which it declines (12, 65–67). This pattern is also observed for total brain volume, although earlier work did not model a decline in total brain volume after this peak (68) . The parietal and occipital lobe mirror this inverted U-shaped pattern in our normative model. Regional differences in developmental trajectories have been reported previously (11, 13, 69) and indeed we extend prior knowledge by showing that, similar to the earlier work (69), across a span of 6–16 years of age, many regions in the frontal and temporal lobe reach their peak volume after 6 years of age. Thus, our findings indicate that each brain region develops at its own pace, with brain regions located in the same lobe showing similar developmental trajectories. We also observed almost identical patterns in subcortical gray matter volume as previous work (12, 66), which showed inverted

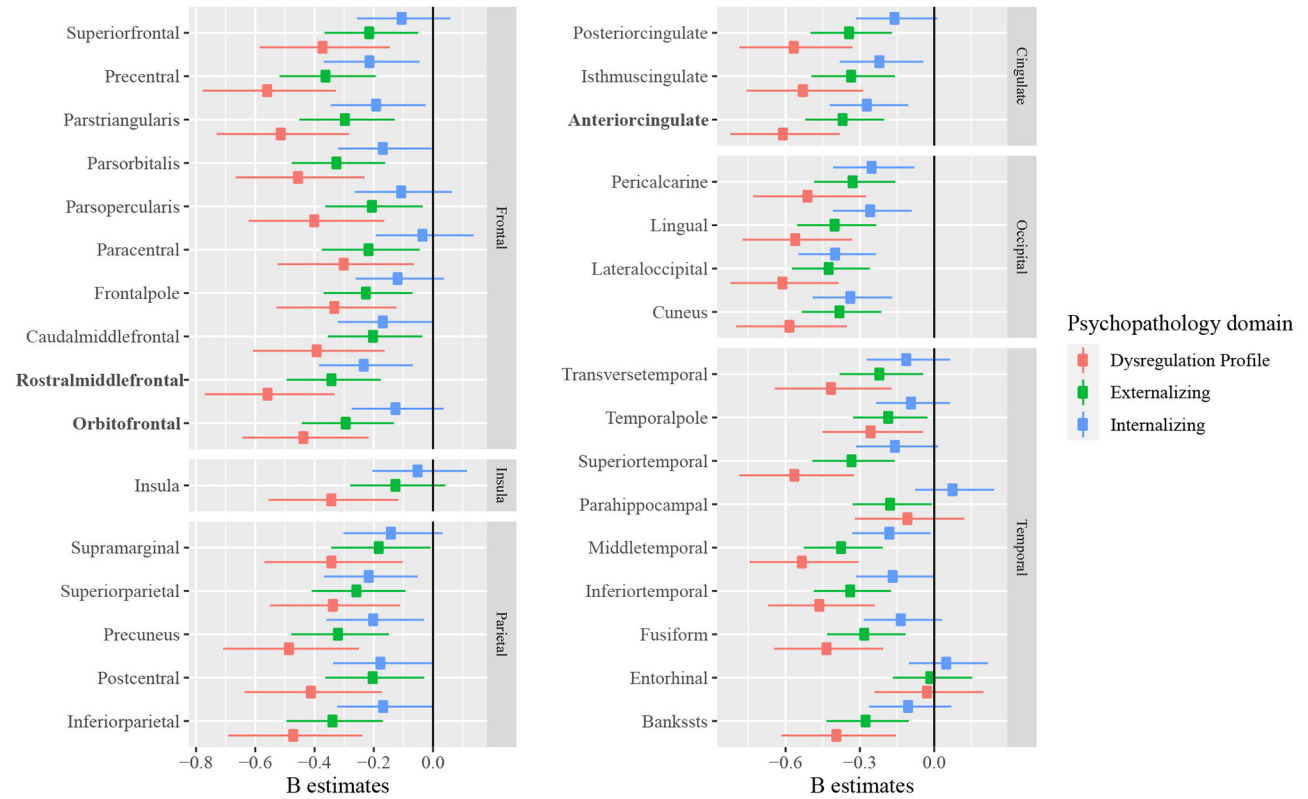

FIGURE 8 | Standardized B estimates of the relationship between z-scores (representing deviations of typical development in surface area) and psychopathology symptoms. Bold face indicates an a priori defined, hypothesis driven, region of interest range indicates 95% confidence interval.

U-shaped trajectories that reached a peak around 15 years of age. Our findings indicate either an inverted U-shaped or positive developmental trajectory for individual subcortical regions. Further, our model showed that cortical thickness has a negative developmental curve for the vast majority of regions, with only some regions showing a fairly flat trajectory. This is consistent with earlier findings showing a decrease in cortical thickness across this age range (70) and largely consistent with other work, although the peak of cortical thickness was either reached at earlier (66) ages for average cortical thickness or later ages for average as well as regional cortical thickness (65, 71). Further, our findings showed that the rate of change differs across brain regions. For example, regions in the occipital lobe have a steep decline in cortical thickness between 6 and 12 years of age, after which they reach a plateau, whereas regions in the parietal and cingulate cortex have a more linear decline over time, of which most do not yet reach a plateau at 16 years of age. Regarding surface area, earlier work indicated that across the entire cortex, development follows an inverted U-shaped trajectory across childhood and adolescence (65, 66). In line with these findings, our results indicate similar trajectories for most regions. However, our findings also indicate that for regions mostly in the frontal and temporal lobe, surface area continues to increase until after 10–12 years of age, mirroring the regional differences in development observed for cortical volume and thickness.

TABLE 6 | Hypothesis driven surface area model 2.

Brain region	Psychopathology symptoms	B	S.E.	*p*-value
Anterior cingulate	Internalizing	–0.263	0.081	1.17e-03
	Externalizing	–0.361	0.081	9.13e-06
	Dysregulation Profile	–0.602	0.113	1e-07
Orbitofrontal	Internalizing	–0.119	0.079	1.31e-01
	Externalizing	–0.288	0.079	3e-04
	Dysregulation Profile	–0.43	0.109	7.68e-05
Rostral middle frontal	Internalizing	–0.227	0.081	5.09e-03
	Externalizing	–0.336	0.081	3.62e-05
	Dysregulation Profile	–0.551	0.112	9.35e-07

Our study has several strengths and limitations. First, a key strength of the current study is that we used normative modeling to establish z-scores representing deviations from

TABLE 7 | Exploratory surface area model 2.

Brain region	B	S.E.	*p*-value	B	S.E.	*p*-value	B	S.E.	*p*-value
Banks of the superior temporal sulcus	–0.097	0.085	2.52e-01	–0.268	0.085	1.6e-03	–0.386	0.118	1.06e-03
Caudal middle frontal	–0.162	0.081	4.63e-02	–0.196	0.082	1.66e-02	–0.386	0.113	6.88e-04
Cuneus	–0.33	0.082	5.72e-05	–0.374	0.082	5.63e-06	–0.576	0.114	4.77e-07
Entorhinal	0.057	0.081	4.84e-01	–0.007	0.082	9.3e-01	–0.021	0.112	8.53e-01
Frontal pole	–0.112	0.076	1.4e-01	–0.219	0.077	4.26e-03	–0.326	0.103	1.64e-03
Fusiform	–0.127	0.081	1.16e-01	–0.274	0.081	7.17e-04	–0.426	0.112	1.5e-04
Inferior parietal	–0.161	0.083	5.2e-02	–0.332	0.083	6.5e-05	–0.465	0.115	5.86e-05
Inferior temporal	–0.159	0.079	4.5e-02	–0.33	0.08	3.45e-05	–0.455	0.11	3.62e-05
Insula	–0.045	0.082	5.81e-01	–0.12	0.082	1.45e-01	–0.336	0.112	2.68e-03
Isthmus cingulate	–0.213	0.086	1.35e-02	–0.327	0.086	1.54e-04	–0.522	0.12	1.47e-05
Lateral occipital	–0.391	0.08	1.06e-06	–0.417	0.08	2.15e-07	–0.604	0.111	6.54e-08
Lingual	–0.25	0.081	2.09e-03	–0.394	0.081	1.42e-06	–0.552	0.113	1.11e-06
Middle temporal	–0.172	0.081	3.32e-02	–0.367	0.081	6.35e-06	–0.526	0.112	3.05e-06
Paracentral	–0.028	0.084	7.36e-01	–0.211	0.084	1.27e-02	–0.294	0.117	1.22e-02
Parahippocampal	0.082	0.081	3.11e-01	–0.17	0.082	3.75e-02	–0.1	0.113	3.77e-01
Pars opercularis	–0.1	0.084	2.31e-01	–0.199	0.084	1.78e-02	–0.394	0.117	7.65e-04
Pars orbitalis	–0.162	0.08	4.36e-02	–0.319	0.081	8.05e-05	–0.449	0.111	5.65e-05
Pars triangularis	–0.185	0.082	2.41e-02	–0.29	0.082	4.24e-04	–0.507	0.114	9.36e-06
Pericalcarine	–0.244	0.083	3.5e-03	–0.321	0.084	1.33e-04	–0.503	0.116	1.59e-05
Posterior cingulate	–0.152	0.084	6.98e-02	–0.335	0.084	6.64e-05	–0.558	0.117	1.84e-06
Postcentral	–0.171	0.085	4.5e-02	–0.196	0.085	2.14e-02	–0.405	0.118	6.33e-04
Precentral	–0.207	0.083	1.21e-02	–0.356	0.083	1.79e-05	–0.553	0.115	1.61e-06
Precuneus	–0.195	0.084	2.03e-02	–0.314	0.084	2e-04	–0.479	0.117	4.42e-05
Superior frontal	–0.099	0.081	2.2e-01	–0.208	0.081	1.01e-02	–0.366	0.112	1.13e-03
Superior parietal	–0.21	0.081	9.34e-03	–0.251	0.081	1.91e-03	–0.331	0.112	3.23e-03
Superior temporal	–0.15	0.085	7.67e-02	–0.325	0.085	1.33e-04	–0.556	0.118	2.65e-06
Supramarginal	–0.135	0.085	1.14e-01	–0.176	0.086	3.99e-02	–0.336	0.119	4.93e-03
Temporal pole	–0.085	0.076	2.63e-01	–0.177	0.077	2.08e-02	–0.248	0.103	1.64e-02
Transverse temporal	–0.104	0.086	2.25e-01	–0.213	0.086	1.36e-02	–0.408	0.12	6.9e-04

normative development, which were subsequently related to psychopathology symptoms. Earlier work has shown that these regional deviations form typical development provide a greater prediction accuracy for psychopathology symptoms than using raw measures of brain morphology (17). Second, this study included a large age range, spanning early childhood to mid-adolescence, which allowed us to extend contemporary findings (12, 70) in an age range that has not been studied extensively. Third, we were able to adjust our analyses for many potentially confounding factors. Although we interpreted the second model, some associations observed in model 1, corrected for biological sex and handedness, attenuated upon adjustment for SES and child national origin. These differences in the results obtained from the first and second model indicate the importance of adjustment for potentially confounding factors. Fourth, the population-based setting of the current study is both a strength and limitation. To derive typical developmental trajectories of brain morphology, a population-based sample is ideal. However, the majority of participants in this study exhibit relatively low levels of psychopathology, limiting the power to detect associations that might exist in those with clinical psychopathology levels. Fifth, while the current sample covers a large and important age range for developmental studies, the data acquired was not equally distributed across all ages. This can potentially influence the results around ages where fewer data was available. Sixth, although the current findings were derived from one of the largest population-based samples covering childhood and adolescence, our findings warrant replication in other comparable cohorts. Seventh, the data at T1 was obtained on a different MRI scanner than the data at T2 and T3, which may have influenced the results. Finally, a limitation of the current study is the amount of inter-individual variability in brain morphology measures and subsequently in the obtained z-scores. This results in small effect sizes in the associations we observed. However, small effect sizes are consistently reported for studies on brain morphology and psychopathology, and in those that have obtained large effect sizes, the effect size is often inflated by the small sample size (72).

In summary, this study charted regional typical development of subcortical and cortical volume, surface area and cortical thickness. Findings showed that deviations from this typical development curve were related to psychopathology symptoms in widespread regions of the cerebral (sub-)cortex. DP symptoms were related to regional deviations from typical brain

development above and beyond internalizing and externalizing symptoms in cortical volume. Our findings underline the evidence that assessing deviations from typical development in terms of (sub-)cortical volume and thickness can provide insights in the coupling between brain and behavioral development.

DATA AVAILABILITY STATEMENT

The datasets presented in this article are not readily available because Generation R data is available to researchers upon reasonable request. Requests should be directed to the management team of the Generation R Study. Individual level data are not publicly available for privacy and ethical restrictions. Requests to access the datasets should be directed to generationr@erasmusmc.

ETHICS STATEMENT

The studies involving human participants were reviewed and approved by METC Erasmus MC. Written informed consent to participate in this study was provided by the participants' legal guardian/next of kin.

AUTHOR CONTRIBUTIONS

EAWG: methodology, writing–original draft, and writing–review and editing. EB: conceptualization, data curation, formal analysis, methodology, visualization, writing–original draft, and writing–review and editing. EPTG: formal analysis, codebase maintenance, methodology, visualization, writing–original draft, and writing–review and editing. TW: conceptualization, funding acquisition, methodology, project administration, resources, supervision, and writing–review and editing. VC: methodology, resources, and writing–review and editing. All authors contributed to the article and approved the submitted version.

FUNDING

This work was supported by the Sophia Children's Hospital Research Foundation (SSWO) Project #S18-68, #S20-48 and the Netherlands Organization for Health Research and Development (ZonMw) TOP Project Number 91211021. The general design of the Generation R Study is made possible by financial support from the Erasmus Medical Center, Rotterdam, ZonMw, the Netherlands Organization for Scientific Research (NWO), and the Ministry of Health, Welfare and Sport, and is conducted by the Erasmus Medical Center in close collaboration with the Faculty of Social Sciences of the Erasmus University Rotterdam, and the Stichting Trombosedienst & Artsenlaboratorium Rijnmond (STAR-MDC), Rotterdam.

ACKNOWLEDGMENTS

The authors thank all participants and parents, students, practitioners, hospitals, midwives, and pharmacies involved in the Generation R Study.

SUPPLEMENTARY MATERIAL

The Supplementary Material for this article can be found online at: https://www.frontiersin.org/articles/10.3389/fpsyt.2022.846201/full#supplementary-material

REFERENCES

1. Whittle S, Vijayakumar N, Simmons JG, Allen NB. Internalizing and externalizing symptoms are associated with different trajectories of cortical development during late childhood. *J Am Acad Child Adolescent Psychiatry*. (2020) 59:177–85. doi: 10.1016/j.jaac.2019.04.006
2. Duval ER, Javanbakht A, Liberzon I. Neural circuits in anxiety and stress disorders: a focused review. *Ther Clin Risk Manag*. (2015) 11:115. doi: 10.2147/TCRM.S48528
3. Bora E, Fornito A, Pantelis C, Yücel M. Gray matter abnormalities in major depressive disorder: a meta-analysis of voxel based morphometry studies. *J Affect Disord*. (2012) 138:9–18. doi: 10.1016/j.jad.2011.03.049
4. Rubia K. "Cool" inferior frontostriatal dysfunction in attention-deficit/hyperactivity disorder versus "hot" ventromedial orbitofrontal-limbic dysfunction in conduct disorder: a review. *Biol Psychiatry*. (2011). 69:e69–87. doi: 10.1016/j.biopsych.2010.09.023
5. Rogers JC, De Brito SA. Cortical and subcortical gray matter volume in youths with conduct problems: a meta-analysis. *JAMA Psychiatry*. (2016) 73:64–72. doi: 10.1001/jamapsychiatry.2015.2423
6. Koolschijn PCM, van Haren NE, Lensvelt-Mulders GJ, Hulshoff Pol HE, Kahn RS. Brain volume abnormalities in major depressive disorder: a meta-analysis of magnetic resonance imaging studies. *Hum Brain Mapp*. (2009) 30:3719–35. doi: 10.1002/hbm.20801
7. Albaugh MD, Nguyen TV, Ducharme S, Collins DL, Botteron KN, D'Alberto N, et al. Age-related volumetric change of limbic structures and subclinical anxious/depressed symptomatology in typically developing children and adolescents. *Biol Psychol*. (2017) 124:133–40. doi: 10.1016/j.biopsycho.2017.02.002
8. Bos MG, Peters S, van de Kamp FC, Crone EA, Tamnes CK. Emerging depression in adolescence coincides with accelerated frontal cortical thinning. *J Child Psychol Psychiatry*. (2018) 59:994–1002. doi: 10.1111/jcpp.12895
9. Newman E, Thompson WK, Bartsch H, Hagler DJ, Chen CH, Brown TT, et al. Anxiety is related to indices of cortical maturation in typically developing children and adolescents. *Brain Struct Funct*. (2016) 221:3013–25. doi: 10.1007/s00429-015-1085-9
10. Fairchild G, Hagan CC, Walsh ND, Passamonti L, Calder AJ, Goodyer IM. Brain structure abnormalities in adolescent girls with conduct disorder. *J Child Psychol Psychiatry*. (2013) 54:86–95. doi: 10.1111/j.1469-7610.2012.02617.x
11. Giedd JN, Blumenthal J, Jeffries NO, Castellanos FX, Liu H, Zijdenbos A, et al. Brain development during childhood and adolescence: a longitudinal MRI study. *Nat Neurosci*. (1999) 2:861–3. doi: 10.1038/13158
12. Bethlehem RA, Seidlitz J, White SR, Vogel JW, Anderson KM, Adamson C, et al. Brain charts for the human lifespan. *bioRxiv*. (2021).
13. Nordt M, Gomez J, Natu VS, Rezai AA, Finzi D, Kular H, et al. Cortical recycling in high-level visual cortex during childhood development. *Nat Hum Behav*. (2021) 5:1686–97. doi: 10.1101/2020.07.18.209783

14. Marquand AF, Rezek I, Buitelaar J, Beckmann CF. Understanding heterogeneity in clinical cohorts using normative models: beyond case-control studies. *Biol Psychiatry*. (2016) 80:552–61. doi: 10.1016/j.biopsych.2015.12.023
15. Marquand AF, Kia SM, Zabihi M, Wolfers T, Buitelaar JK, Beckmann CF. Conceptualizing mental disorders as deviations from normative functioning. *Mol Psychiatry*. (2019) 24:1415–24. doi: 10.1038/s41380-019-0441-1
16. Ziegler G, Ridgway GR, Dahnke R, Gaser C, Initiative ADN, et al. Individualized Gaussian process-based prediction and detection of local and global gray matter abnormalities in elderly subjects. *Neuroimage*. (2014) 97:333–48. doi: 10.1016/j.neuroimage.2014.04.018
17. Parkes L, Moore TM, Calkins ME, Cook PA, Cieslak M, Roalf DR, et al. Transdiagnostic dimensions of psychopathology explain individuals' unique deviations from normative neurodevelopment in brain structure. *Transl Psychiatry*. (2021) 11:1–13. doi: 10.1038/s41398-021-01342-6
18. Merz EC, He X, Noble KG, et al. Anxiety, depression, impulsivity, and brain structure in children and adolescents. *Neuroimage Clin*. (2018) 20:243–51. doi: 10.1016/j.nicl.2018.07.020
19. Ducharme S, Albaugh MD, Hudziak JJ, Botteron KN, Nguyen TV, Truong C, et al. Anxious/depressed symptoms are linked to right ventromedial prefrontal cortical thickness maturation in healthy children and young adults. *Cereb Cortex*. (2014) 24:2941–50. doi: 10.1093/cercor/bht151
20. Whittle S, Lichter R, Dennison M, Vijayakumar N, Schwartz O, Byrne ML, et al. Structural brain development and depression onset during adolescence: a prospective longitudinal study. *Am J Psychiatry*. (2014) 171:564–71. doi: 10.1176/appi.ajp.2013.13070920
21. Strawn JR, Wehry AM, DelBello MP, Rynn MA, Strakowski S. Establishing the neurobiologic basis of treatment in children and adolescents with generalized anxiety disorder. *Depress Anxiety*. (2012) 29:328–39. doi: 10.1002/da.21913
22. Ameis SH, Ducharme S, Albaugh MD, Hudziak JJ, Botteron KN, Lepage C, et al. Cortical thickness, cortico-amygdalar networks, and externalizing behaviors in healthy children. *Biol Psychiatry*. (2014) 75:65–72. doi: 10.1016/j.biopsych.2013.06.008
23. Ducharme S, Hudziak JJ, Botteron KN, Ganjavi H, Lepage C, Collins DL, et al. Right anterior cingulate cortical thickness and bilateral striatal volume correlate with child behavior checklist aggressive behavior scores in healthy children. *Biol Psychiatry*. (2011) 70:283–90. doi: 10.1016/j.biopsych.2011.03.015
24. Oostermeijer S, Whittle S, Suo C, Allen N, Simmons J, Vijayakumar N, et al. Trajectories of adolescent conduct problems in relation to cortical thickness development: a longitudinal MRI study. *Transl Psychiatry*. (2016) 6:e841. doi: 10.1038/tp.2016.111
25. Vijayakumar N, Whittle S, Dennison M, Yücel M, Simmons J, Allen NB. Development of temperamental effortful control mediates the relationship between maturation of the prefrontal cortex and psychopathology during adolescence: a 4-year longitudinal study. *Dev Cogn Neurosci*. (2014) 9:30–43. doi: 10.1016/j.dcn.2013.12.002
26. Fairchild G, Passamonti L, Hurford G, Hagan CC, von dem Hagen EA, van Goozen SH, et al. Brain structure abnormalities in early-onset and adolescent-onset conduct disorder. *Am J Psychiatry*. (2011) 168:624–33. doi: 10.1176/appi.ajp.2010.10081184
27. Huebner T, Vloet TD, Marx I, Konrad K, Fink GR, Herpertz SC, et al. Morphometric brain abnormalities in boys with conduct disorder. *J Am Acad Child Adolescent Psychiatry*. (2008) 47:540–7. doi: 10.1097/CHI.0b013e3181676545
28. Sterzer P, Stadler C, Poustka F, Kleinschmidt A. A structural neural deficit in adolescents with conduct disorder and its association with lack of empathy. *Neuroimage*. (2007) 37:335–42. doi: 10.1016/j.neuroimage.2007.04.043
29. Bos MG, Wierenga LM, Blankenstein NE, Schreuders E, Tamnes CK, Crone EA. Longitudinal structural brain development and externalizing behavior in adolescence. *J Child Psychol Psychiatry*. (2018) 59:1061–72. doi: 10.1111/jcpp.12972
30. Shaw P, Stringaris A, Nigg J, Leibenluft E. Emotion dysregulation in attention deficit hyperactivity disorder. *Am J Psychiatry*. (2014) 171:276–93. doi: 10.1176/appi.ajp.2013.13070966
31. Vetter NC, Backhausen LL, Buse J, Roessner V, Smolka MN. Altered brain morphology in boys with attention deficit hyperactivity disorder with and without comorbid conduct disorder/oppositional defiant disorder. *Hum Brain Mapp*. (2020) 41:973–83. doi: 10.1002/hbm.24853
32. Jaddoe VW, van Duijn CM, Franco OH, van der Heijden AJ, van IIzendoorn MH, de Jongste JC, et al. The Generation R Study: design and cohort update 2012. *Eur J Epidemiol*. (2012) 27:739–56. doi: 10.1007/s10654-012-9735-1
33. White T, El Marroun H, Nijs I, Schmidt M, van der Lugt A, Wielopolki PA, et al. Pediatric population-based neuroimaging and the Generation R Study: the intersection of developmental neuroscience and epidemiology. *Eur J Epidemiol*. (2013) 28:99–111. doi: 10.1007/s10654-013-9768-0
34. White T, Muetzel RL, El Marroun H, Blanken LM, Jansen P, Bolhuis K, et al. Paediatric population neuroimaging and the Generation R Study: the second wave. *Eur J Epidemiol*. (2018) 33:99–125. doi: 10.1007/s10654-017-0319-y
35. Achenbach TM, Rescorla LA. *Manual for the ASEBA Preschool Forms and Profiles, Vol. 30*. Burlington, VT: University of Vermont, Research Center for Children, Youth (2000).
36. Achenbach T, Rescorla L. *Manual for the ASEBA school-Age Forms & Profiles: An Integrated System of Multi-Informant Assessment*. Burlington, VT: University of Vermont; Research Center for Children, Youth, & Families (2001).
37. Fischl B. FreeSurfer. *Neuroimage*. (2012) 62:774–81. doi: 10.1016/j.neuroimage.2012.01.021
38. Desikan RS, Ségonne F, Fischl B, Quinn BT, Dickerson BC, Blacker D, et al. An automated labeling system for subdividing the human cerebral cortex on MRI scans into gyral based regions of interest. *Neuroimage*. (2006) 31:968–80. doi: 10.1016/j.neuroimage.2006.01.021
39. Muetzel RL, Blanken LM, van der Ende J, El Marroun H, Shaw P, Sudre G, et al. Tracking brain development and dimensional psychiatric symptoms in children: a longitudinal population-based neuroimaging study. *Am J Psychiatry*. (2018) 175:54–62. doi: 10.1176/appi.ajp.2017.16070813
40. White T, Jansen PR, Muetzel RL, Sudre G, El Marroun H, Tiemeier H, et al. Automated quality assessment of structural magnetic resonance images in children: comparison with visual inspection and surface-based reconstruction. *Hum Brain Mapp*. (2018) 39:1218–31. doi: 10.1002/hbm.23911
41. Rosen AF, Roalf DR, Ruparel K, Blake J, Seelaus K, Villa LP, et al. Quantitative assessment of structural image quality. *Neuroimage*. (2018) 169:407–18. doi: 10.1016/j.neuroimage.2017.12.059
42. Oldfield RC. The assessment and analysis of handedness: the Edinburgh inventory. *Neuropsychologia*. (1971) 9:97–113. doi: 10.1016/0028-3932(71)90067-4
43. Fischl B, Salat DH, Busa E, Albert M, Dieterich M, Haselgrove C, et al. Whole brain segmentation: automated labeling of neuroanatomical structures in the human brain. *Neuron*. (2002) 33:341–55. doi: 10.1016/S0896-6273(02)00569-X
44. Gardner JR, Pleiss G, Bindel D, Weinberger KQ, Wilson AG. Gpytorch: blackbox matrix-matrix gaussian process inference with gpu acceleration. *arXiv preprint* arXiv:180911165. (2018).
45. R Core Team. *R: A Language and Environment for Statistical Computing*. Vienna (2017). Available online at: https://www.R-project.org/.
46. Van Rossum G, et al. Python programming language. In: *USENIX Annual Technical Conference, Vol. 41* (Santa Clara, CA). (2007). p. 36.
47. van Buuren S, Groothuis-Oudshoorn K, Robitzsch A, Vink G, Doove L, Jolani S. Package 'mice'. *Computer Software*. (2015).
48. Benjamini Y, Hochberg Y. Controlling the false discovery rate: a practical and powerful approach to multiple testing. *J R Stat Soc B*. (1995) 57:289–300. doi: 10.1111/j.2517-6161.1995.tb02031.x
49. Allman JM, Hakeem A, Erwin JM, Nimchinsky E, Hof P. The anterior cingulate cortex: the evolution of an interface between emotion and cognition. *Ann N Y Acad Sci*. (2001) 935:107–17. doi: 10.1111/j.1749-6632.2001.tb03476.x
50. Siever LJ. Neurobiology of aggression and violence. *Am J Psychiatry*. (2008) 165:429–42. doi: 10.1176/appi.ajp.2008.07111774
51. Sterzer P, Stadler C. Neuroimaging of aggressive and violent behaviour in children and adolescents. *Front Behav Neurosci*. (2009) 3:35. doi: 10.3389/neuro.08.035.2009
52. Bian XL, Qin C, Cai CY, Zhou Y, Tao Y, Lin YH, et al. Anterior cingulate cortex to ventral hippocampus circuit mediates contextual fear generalization. *J Neurosci*. (2019) 39:5728–39. doi: 10.1523/JNEUROSCI.2739-18.2019

53. Shenhav A, Botvinick MM, Cohen JD. The expected value of control: an integrative theory of anterior cingulate cortex function. *Neuron*. (2013) 79:217–40. doi: 10.1016/j.neuron.2013.07.007
54. Blair RJR. Responding to the emotions of others: dissociating forms of empathy through the study of typical and psychiatric populations. *Conscious Cogn*. (2005) 14:698–718. doi: 10.1016/j.concog.2005.06.004
55. Mewton L, Lees B, Squeglia L, Forbes MK, Sunderland M, Krueger R, et al. The relationship between brain structure and general psychopathology in preadolescents. *J Child Psychol Psychiatry*. (2020). doi: 10.31234/osf.io/r4pxy
56. Romer AL, Elliott ML, Knodt AR, Sison ML, Ireland D, Houts R, et al. Pervasively thinner neocortex as a transdiagnostic feature of general psychopathology. *Am J Psychiatry*. (2021) 178:174–82. doi: 10.1176/appi.ajp.2020.19090934
57. Basten M, van der Ende J, Tiemeier H, Althoff RR, Rijlaarsdam J, Jaddoe VW, et al. Nonverbal intelligence in young children with dysregulation: the Generation R Study. *Eur Child Adolescent Psychiatry*. (2014) 23:1061–70. doi: 10.1007/s00787-014-0551-x
58. Blok E, Schuurmans IK, Tijburg AJ, Hillegers M, Koopman-Verhoeff ME, Muetzel RL, et al. Cognitive performance in children and adolescents with psychopathology traits: a cross-sectional multicohort study in the general population. *Development and Psychopathology*. (2022) 1–15. doi: 10.1017/S0954579422000165
59. Barch DM. The neural correlates of transdiagnostic dimensions of psychopathology. *Am J Psychiatry*. (2017) 174:613–5. doi: 10.1176/appi.ajp.2017.17030289
60. Sprooten E, Rasgon A, Goodman M, Carlin A, Leibu E, Lee WH, et al. Addressing reverse inference in psychiatric neuroimaging: meta-analyses of task-related brain activation in common mental disorders. *Hum Brain Mapp*. (2017) 38:1846–64. doi: 10.1002/hbm.23486
61. Achenbach TM, Ivanova MY, Rescorla LA, Turner LV, Althoff RR. Internalizing/externalizing problems: review and recommendations for clinical and research applications. *J Am Acad Child Adolescent Psychiatry*. (2016) 55:647–56. doi: 10.1016/j.jaac.2016.05.012
62. Carlson GA. Presidential address: emotion dysregulation in children and adolescents. *J Am Acad Child Adolescent Psychiatry*. (2020) 59:15–9. doi: 10.1016/j.jaac.2019.11.004
63. Lahey BB, Applegate B, Hakes JK, Zald DH, Hariri AR, Rathouz PJ. Is there a general factor of prevalent psychopathology during adulthood? *J Abnorm Psychol*. (2012) 121:971. doi: 10.1037/a0028355
64. Caspi A, Houts RM, Belsky DW, Goldman-Mellor SJ, Harrington H, Israel S, et al. The p factor: one general psychopathology factor in the structure of psychiatric disorders? *Clin Psychol Sci*. (2014) 2:119–37. doi: 10.1177/2167702613497473
65. Raznahan A, Shaw P, Lalonde F, Stockman M, Wallace GL, Greenstein D, et al. How does your cortex grow? *J Neurosci*. (2011) 31:7174–7. doi: 10.1523/JNEUROSCI.0054-11.2011
66. Liu S, Wang YS, Zhang Q, Zhou Q, Cao LZ, Jiang C, et al. Chinese color nest project: an accelerated longitudinal brain-mind cohort. *Dev Cogn Neurosci*. (2021) 52:101020. doi: 10.1016/j.dcn.2021.101020
67. Mills KL, Goddings AL, Herting MM, Meuwese R, Blakemore SJ, Crone EA, et al. Structural brain development between childhood and adulthood: Convergence across four longitudinal samples. *Neuroimage*. (2016) 141:273–81. doi: 10.1016/j.neuroimage.2016.07.044
68. Peterson M, Warf BC, Schiff SJ. Normative human brain volume growth. *J Neurosurg*. (2018) 21:478–85. doi: 10.3171/2017.10.PEDS17141
69. Tamnes CK, Herting MM, Goddings AL, Meuwese R, Blakemore SJ, Dahl RE, et al. Development of the cerebral cortex across adolescence: a multisample study of inter-related longitudinal changes in cortical volume, surface area, and thickness. *J Neurosci*. (2017) 37:3402–12. doi: 10.1523/JNEUROSCI.3302-16.2017
70. Bethlehem RA, Seidlitz J, Romero-Garcia R, Trakoshis S, Dumas G, Lombardo MV. A normative modelling approach reveals age-atypical cortical thickness in a subgroup of males with autism spectrum disorder. *Commun Biol*. (2020) 3:1–10. doi: 10.1038/s42003-020-01212-9
71. Shaw P, Kabani NJ, Lerch JP, Eckstrand K, Lenroot R, Gogtay N, et al. Neurodevelopmental trajectories of the human cerebral cortex. *J Neurosci*. (2008) 28:3586–94. doi: 10.1523/JNEUROSCI.5309-07.2008
72. Feng C, Thompson WK, Paulus MP. Effect sizes of associations between neuroimaging measures and affective symptoms: a meta-analysis. *Depress Anxiety*. (2021) 39:19–25. doi: 10.1002/da.23215

Conflict of Interest: The authors declare that the research was conducted in the absence of any commercial or financial relationships that could be construed as a potential conflict of interest.

Publisher's Note: All claims expressed in this article are solely those of the authors and do not necessarily represent those of their affiliated organizations, or those of the publisher, the editors and the reviewers. Any product that may be evaluated in this article, or claim that may be made by its manufacturer, is not guaranteed or endorsed by the publisher.

frontiers | Frontiers in Psychiatry

ORIGINAL RESEARCH
published: 19 May 2022
doi: 10.3389/fpsyt.2022.840095

Neural Correlates of Reactive Aggression in Adult Attention-Deficit/Hyperactivity Disorder

*Babette Jakobi[1,2], Alejandro Arias-Vasquez[1,3], Erno Hermans[2,4], Priscilla Vlaming[1], Jan Buitelaar[2,4], Barbara Franke[1,3], Martine Hoogman[1,3] and Daan van Rooij[2]**

[1] Department of Human Genetics, Donders Institute for Brain, Cognition and Behavior, Radboud University Nijmegen Medical Center, Nijmegen, Netherlands, [2] Centre for Cognitive Neuroimaging, Donders Institute for Brain Cognition and Behavior, Nijmegen, Netherlands, [3] Department of Psychiatry, Donders Institute for Brain, Cognition and Behavior, Radboud University Nijmegen Medical Center, Nijmegen, Netherlands, [4] Department of Cognitive Neuroscience, Donders Institute for Brain, Cognition and Behavior, Radboud University Nijmegen Medical Center, Nijmegen, Netherlands

OPEN ACCESS

Edited by:
Ali Saffet Gonul, Ege University, Turkey

Reviewed by:
Nicola Großheinrich, Catholic University of Applied Sciences of North Rhine – Westphalia, Germany
Nelly Alia-Klein, Icahn School of Medicine at Mount Sinai, United States

***Correspondence:**
Daan van Rooij
d.vanrooij@donders.ru.nl

Specialty section:
This article was submitted to Neuroimaging and Stimulation, a section of the journal Frontiers in Psychiatry

Received: *20 December 2021*
Accepted: *27 April 2022*
Published: *19 May 2022*

Citation:
Jakobi B, Arias-Vasquez A, Hermans E, Vlaming P, Buitelaar J, Franke B, Hoogman M and van Rooij D (2022) Neural Correlates of Reactive Aggression in Adult Attention-Deficit/Hyperactivity Disorder. Front. Psychiatry 13:840095. doi: 10.3389/fpsyt.2022.840095

Despite not being part of the core diagnostic criteria for attention-deficit/hyperactivity disorder (ADHD), emotion dysregulation is a highly prevalent and clinically important component of (adult) ADHD. Emotionally dysregulated behaviors such as reactive aggression have a significant impact on the functional outcome in ADHD. However, little is known about the mechanisms underlying reactive aggression in ADHD. In this study, we aimed to identify the neural correlates of reactive aggression as a measure of emotionally dysregulated behavior in adults with persistent ADHD during implicit emotion regulation processes. We analyzed associations of magnetic resonance imaging-based whole-brain activity during a dynamic facial expression task with levels of reactive aggression in 78 adults with and 78 adults without ADHD, and also investigated relationships of reactive aggression with symptoms and impairments. While participants with ADHD had higher reactive aggression scores than controls, the neural activation patterns of both groups to processing of emotional faces were similar. However, investigating the brain activities associated with reactive aggression in individuals with and without ADHD showed an interaction of diagnosis and reactive aggression scores. We found high levels of activity in the right insula, the hippocampus, and middle and superior frontal areas to be particularly associated with high reactive aggression scores within the ADHD group. Furthermore, the limbic activity was associated with more hyperactivity/impulsivity symptoms. These results suggest a partly differential mechanism associated with reactive aggression in ADHD as compared to controls. Emotional hyper-reactivity in the salience network as well as more effortful top–down regulation from the self-regulation network might contribute to emotionally dysregulated behavior as measured by reactive aggression.

Keywords: adult ADHD, emotion dysregulation, dynamic facial expressions, reactive aggression, task-based fMRI

INTRODUCTION

Attention-deficit/hyperactivity disorder (ADHD) is a highly prevalent neurodevelopmental disorder (1), characterized by core symptoms of inattention and/or hyperactivity and impulsivity (2). Symptoms of ADHD persist into adulthood in up to 66% of affected individuals (1) and are commonly accompanied by emotion regulation problems (3). Even though symptoms of emotion dysregulation (ED) are prevalent in people with ADHD (with 24–50% in children and up to 70% in adults) and are an important predictor of ADHD symptoms (4), they have long been disregarded in diagnostic and therapeutic context (3).

An important expression of severe ED in ADHD is reactive aggression (5–9). Not only is aggressive behavior a frequent catalyst for diagnostic consultation (6), recent research reports that reactive aggression in ADHD remains significantly elevated after correction for comorbidities such as conduct disorder and oppositional defiant disorder (8, 10). Literature often distinguishes two types of aggressive behaviors. While proactive aggression links to instrumentalized and controlled aggressive behaviors, reactive aggression is a mirror of a dysregulated emotional response, e.g., to fear or anger (11). Reactive aggression can have a large impact on multiple dimensions of life. People with ADHD and co-occurring aggression show the most maladaptive strategies in emotion regulation and social decision making (12), often resulting in unstable dysfunctional relationships and families, peer rejection and victimization, functional impairments in school and later occupation, as well as an elevated risk of contact with criminality (6, 9, 10, 13). Reactive aggression has also consistently been linked to suicidal behaviors and attempts (9, 14). Abel et al. (9) reported that this elevated risk of suicidal behavior in reactive aggression is modulated by hyperactivity and impulsivity symptoms, irrespective of comorbidities such as depression.

Altered structural or functional maturation of several brain areas might point toward a neurodevelopmental link of ADHD with reactive aggression. Among small morphological differences in several areas, the structural alterations implicated in ADHD involve reduced volumes within the limbic system, e.g., the amygdala and the hippocampus (15), as well as differential cortical thickness in frontal and parietotemporal brain regions (16). Besides structural implications in ADHD, these regions also exhibit altered functional connectivity and altered activity profiles in ADHD [as reviewed by Rubia (17)]; they have been linked to altered emotional reactivity and memory [limbic system, orbito, and ventromedial frontal cortex (18, 19)] as well as executive functioning and attentional frontal and parietotemporal networks (20).

Emotional subprocesses are relevant for the emergence of reactive aggression and are frequently assessed using functional magnetic resonance imaging (fMRI) paradigms inducing an implicit or explicit emotional reaction to emotionally salient stimuli, e.g., the implicit processing of facial emotional expressions. FMRI studies in children and adolescents with ADHD have revealed patterns of elevated bottom-up emotional reactivity, reflected in altered activity in the amygdala, insula, ventral striatum, and the orbitofrontal cortex (OFC; 17, 21–24). Additionally, differences in the top–down modulation of emotional responses were found in tasks involving active emotion regulation. Differential activation of the amygdala or insula and hypo-connectivity of those structures to prefrontal structures, such as the ventrolateral PFC, the anterior cingulate cortex (ACC), and the temporoparietal junction (TPJ) have been observed in ADHD (25–27). Only few fMRI studies on face emotion processing were carried out in adults with ADHD, covering only small, remitted, or partially remitted samples and focusing on response inhibition and attention. The authors reported (subthreshold) activity- and connectivity differences in limbic and prefrontal circuit in an emotional go/no-go task (28) or hyperactivity in face-processing areas and differential connectivity to regions linked to attention in remitted adults in a dynamic facial expression task (29).

The above-mentioned brain regions altered in people with ADHD are overlapping broadly with the neural correlates of reactive aggression. While reactive aggressive behavior appears to be facilitated by activity of the limbic system and hypothalamus, prefrontal activity seems to indicate inhibition of such behaviors (30). Alia-Klein et al. (31) summarize the emergence of anger as a basis of reactive aggression to (1) reactivity of the salience network (dACC, Insula and limbic structures), influenced by (2) social cognition and self-referential processes in the mentalizing network (TPJ, SFG, posteriorCC, and dorsolateralPFC) and downregulated by (3) the self-regulation network (PFC, ACC, and IFG).

Hence, reactive aggression is associated with an imbalance of cognitive control (implemented in prefrontal areas) and hyper-reactivity to emotional stimuli of the limbic system and insula (8, 32, 33).

Despite the high impact on the quality of life, our understanding of the co-occurrence of ADHD with and reactive aggression and of the underlying mechanisms is limited. Neural circuits engaged in reactive aggression -as a severe form of ED- overlap with structurally and functionally implicated brain regions in ADHD and are linked together in functional neuroimaging studies on children and adolescents. However, research on the neural circuits or alterations during emotion processing underlying reactive aggression in adults with persistent ADHD is clearly underrepresented, does not cover implicit facial emotion processing nor integrate behavioral impairments such as ratings of reactive aggression.

This study aimed to identify the neural correlates of reactive aggression in adults with persistent ADHD during implicit emotion regulation processes. We acquired fMRI during a dynamic facial expression task (34, 35). We investigated the neural correlates of reactive aggression in adults with and without ADHD and analyzed the covariance of whole-brain activity with levels of reactive aggression scores from a questionnaire. We expected reactive aggression to be associated with altered neural activation within the emotion regulation network. Moreover, we aimed to identify subprocesses relevant for reactive aggression. We hypothesized more emotional reactivity, as reflected in hyperactivity of the limbic system and anterior insula, and/or more effortful or less cognitive control processes, as reflected in differential prefrontal activity to be relevant for the occurrence

of higher reactive aggression in ADHD. We also explored the association of ADHD diagnosis and clinically relevant variables with the reactive aggression scores and *post hoc* correlations with the neural activity in areas implicated in reactive aggression in the fMRI analysis [insula, hippocampus, precentral gyrus, superior and middle frontal gyrus, middle temporal gyrus (MTG), and lingual gyrus].

MATERIALS AND METHODS

Participants and Experimental Procedure

A total number of 83 adults with a confirmed diagnosis of ADHD and 79 healthy control subjects participated in this fMRI experiment. Participants were recruited *via* newspaper advertisements, patient organizations, and local sports clubs in and around Nijmegen, Netherlands. All of the participants provided written informed consent before participating in the study and received monetary compensation for their participation. The study was approved by the local medical ethical committee.

Participants were included in the ADHD group if they had been diagnosed with ADHD by a clinician. To confirm the diagnosis and assess previous and current symptoms in all participants, we conducted the Diagnostic Interview for Adult ADHD [DIVA 2.0; (36)]. The DIVA includes nine subscales for the symptoms of inattentiveness and hyperactivity/impulsivity and further assesses subjective impairment over life domains such as occupation, family and relationships, social contacts, hobbies and self-image in childhood as well as adulthood. Participants were included in the control group when the following criteria were met: absence of previous diagnoses of ADHD, of current neurological or psychiatric disorders and of first-degree family members with ADHD. Exclusion criteria for all participants comprised (1) an age younger than 18 or older than 60 years, (2) neurological disorders, (3) psychosis or substance abuse in the last 6 months, (4) current major depression, (5) psycho-pharmaceutical therapy other than stimulants, (6) impairments of hearing, seeing and sensorimotor abilities as well as (7) problems with understanding Dutch (to ensure that all of the participants understood the study protocol and the task instructions). The 40 participants with ADHD that received regular pharmacological treatment with stimulants, were asked to pause their medication intake 24 h prior to participation. Missing data of the reactive proactive aggression questionnaire of five participants from the ADHD and failed fMRI data preprocessing of one control subject resulted in a total sample of 78 participants with and 78 participants without ADHD. Both groups had comparable distributions of age, sex, IQ, and educational background (see **Table 1** for a demographic description of the sample including the relevant questionnaire data).

Participation was structured in two parts. The first part included the diagnostic screening for ADHD using the DIVA (36) and a short screening for comorbid psychiatric disorders following the Structured Clinical Interview for DSM, SCID-5. Demographic information was collected and IQ testing was performed using block-design and vocabulary subtests of the Wechsler Adult Intelligence Scale (37). In the second part, structural and functional magnetic resonance imaging (MRI) scans were acquired. After the visit, participants were asked to fill in questionnaires *via* an online platform, among others the Reactive-Proactive Aggression Questionnaire [RPQ; (11)]. The RPQ is a 23-item self-report questionnaire inquiring 11 example sentences of reactive and 12 of proactive aggression that are scored by the participant in a scale of never, sometimes and often. As reactive, but not proactive aggression is implicated in ED as well as ADHD, only the reactive subscale was used in the subsequent analyses. In the **Supplementary Section** "Analysis of Proactive Aggression," **Supplementary Table 2**, we attached a linear regression on proactive aggression and ADHD.

To investigate implicit emotion processing during MRI, an adapted dynamic facial expression task was applied, showing faces morphing from a neutral face to an angry, fearful or happy facial expression in short clips of four frames. This task has proven to elicit activity in structures reflecting emotion processing, such as the amygdala (38). The stimuli were taken from a standardized set and consisted of 10 gray-scale clips per emotion, each represented by a different actor of male and female gender in equal distribution. During the experimental session, we presented 6 blocks per emotion with a duration of 22.5 s,

TABLE 1 | Demographic description of the sample.

Measure	Control group, *n* = 78	ADHD group, *n* = 78	Difference, *p*-value
Sex, percentage male participants	48.7%	43.6%	*0.596*
Age in years (SD)	34.2 (13.1)	34.1 (10.54)	*0.656*
Education (SD)	4.6 (1.6)	4.1 (1.6)	*0.019*
IQ (SD)	106.1 (13.6)*	108.7 (13.8)	*0.479*
DIVA, mean number of symptoms			
Attention symptoms in Adulthood (or current; SD)	0.79 (1.27)	7.32 (1.99)	$p < 0.001$***
Attention symptoms in childhood (SD)	0.49 (0.84)	7.23 (1.83)	$p < 0.001$***
Hyperactivity/Impulsivity adult (SD)	0.83 (1.37)	5.59 (2.24)	$p < 0.001$***
Hyperactivity/Impulsivity child (SD)	0.83 (1.36)	5.57 (2.65)	$p < 0.001$***
DIVA, percentage of adults reporting impairment			
Occupation	0%	74.3%	$p < 0.001$***
Relationship and family	0%	65.4%	$p < 0.001$***
Social contacts	0%	39.7%	$p < 0.001$***
Hobby	1.2%	53.8%	$p < 0.001$***
Self-image	0%	64.1%	$p < 0.001$***
RPQ, mean score			
Reactive aggression score (SD)	5.57 (3.31)	8.17 (4.05)	$p < 0.001$***
Proactive aggression score (SD)	1.42 (2.43)	1.90 (2.61)	0.242

*Mean scores and standard deviations of age, highest achieved educational degree (measured on a scale of 1 to 8 in the Dutch education system), BMI, IQ score, number of present symptoms of inattention and hyperactivity/impulsivity in childhood and adulthood and the percentage of subjects reporting impairments in occupation, relationship and family, social contacts, hobbies, and self-image from the DIVA. The bottom of the table shows the mean scores and standard deviation of the results from the RPQ, proactive aggression is excluded from further analysis. *The IQ estimate of one control subject was missing. Statistical testing was performed using the Mann–Whitney test as well as the Chi-squared test for distribution free comparisons of independent samples with a significance level of p = 0.001, marked by ***.*

which consisted of 50 trials, 5 repetitions for each of the 10 actors. The blocks were presented in counterbalanced order interleaved with 9 blocks showing a fixation cross. In one random trial of each block, a red dot was displayed on the forehead of the actor (see **Supplementary Figure 1** in the section **Supplementary Material**). Participants were asked to press the button on a response box fixated on their leg as soon as the red dot appeared on the actor's face, to sustain their attention while preserving passive processing of the emotional faces. The scanning time for this task was approximately 10 min.

Image Acquisition

Magnetic resonance imaging scans were conducted using a 32-channel coil and a 3 Tesla Siemens Magnetom Prisma scanner (Siemens Trio, Erlangen, Germany). A T1-weighted MPRAGE sequence (TI = 1,100 ms, flip angle = 8°, TE = 3.03 ms, TR = 2300.0 ms, bandwidth = 130 Hz/Px) with 192 sagittal slices (slice thickness = 1.0 mm) was used for the structural scanning, providing whole-brain coverage. Functional blood oxygen level-dependent (BOLD) images were collected using a T2*-weighted echo-planar imaging (EPI) sequence (TR = 1,000 ms, TE = 34.0, flip angle = 60°, FOV = 210 mm, voxel size = 2 mm × 2 mm × 2 mm, 66 slices, interleaved acquisition, slice thickness = 2.00 mm). Preprocessing was performed in FSL FEAT. The first 5 images were discarded from further analysis. Mean framewise displacement of all participants was below the cutoff of 0.5 mm for 10% of the frames. After grand mean scaling and boundary based registration to the structural image and realignment as motion correction, a Gaussian filter of 5 mm kernel was applied to the images. Motion correction was performed using a dedicated independent component analysis based selection algorithm (39). Additionally, the average signal of white-matter and corticospinal fluid were subtracted from the data. For analyses on the group level, we normalized individual scans to Montreal Neurological Institute 152 standard space, 2 mm resolution.

Analysis

Functional Magnetic Resonance Imaging Task Activation

Single subject fMRI analysis were performed in FSL FEAT (version 6.0.3) using a general linear model (GLM) with three regressors of interest modeling the onsets of happy, angry and fearful face blocks with a duration of 22.5 s as well two regressors of no interest modeling the trials where the red dot indicated the attention control task and the timing of the response as event markers with a duration of 0 s. As the task distracted from emotion processing, related BOLD activity and behavioral results of the task were excluded. Results were corrected for age and sex. All events were convolved with the canonical hemodynamic response function.

Three group level contrasts were defined by contrasting each emotional condition against the implicit baseline of the fixation blocks resulting in Happy > Fixation, Angry > Fixation, and Fear > Fixation images. We included the factors diagnosis in two groups and emotion in the three levels angry, fear and happy in a mixed factorial model and investigated the group effects for each emotion separately as well as for all conditions together (Emotion > Fixation). Results are reported at a cluster-level corrected significance threshold of $p < 0.05$.

We further investigated effects of sex on the brain activity during emotion processing.

Analysis of Functional Magnetic Resonance Imaging Task Activation and Reactive Aggression

To analyze the relationship between reactive aggressive scores with implicit emotion regulation and emotional reactivity, we included the contrast of all emotions versus the implicit baseline (Emotion > Fixation) as one summary measure per subject as well as the individual reactive aggression scores as a mean centered continuous covariate in the second level GLM. We were interested in the group specific correlates of reactive aggressive behavior, more specifically which brain regions would be relevant for higher reactive aggression scores in ADHD. Therefore we first investigated the interaction of diagnosis with reactive aggression, to see if there were group differences dependent on reactive aggression scores. Based on this interaction, we further looked at the effect in each group individually to find clusters associated with the co-occurance of higher reactive aggression within the ADHD group. To correct for multiple comparisons in this exploratory analysis, we applied a Monte-Carlo-simulation of 1,000 iterations for cluster extent correction on the uncorrected *t*-maps at $p = 0.001$ [(40, 41), this method is publicly accessible at https://drive.google.com/file/d/16HVUD-PZaEpwHoZE99YXDxhcuLawjW7O/] resulting in a cluster extent of 11 resampled voxels at a cluster extent threshold of $p = 0.05$ assuming a type 1 error of 0.01.

Post hoc Associations of Clinical Measures

To investigate the association between ADHD and the reactive aggression score of the RPQ, we used a linear regression analysis, modeling the Reactive Aggression scores by the binomial factor "diagnosis" (1 = ADHD group, 0 = control group). We included age and sex as covariates in the model. The analysis was conducted in R version 3.6.1.

To investigate the association of clinical outcome with aggression, we introduced DIVA subscales of adult symptoms (Hyperactivity/Impulsivity, Inattention) and impairments (Occupation, Relationships and family, Social contacts, Hobbies, and Self-image) as compounds to a linear model of reactive aggression scores. To assess clinical implications of our results, we analyzed the relationship of ADHD specific neural correlates of reactive aggression with the clinical expression of ADHD. We therefore analyzed correlations between symptoms and the activity in the right limbic system, the right precentral, inferior middle temporal and lingual gyri as well as the middle and superior frontal clusters showing positive covariance with elevated reactive aggression. Results are reported as Spearman's ρ and Bonferroni-corrected for multiple correlations.

We additionally performed a sensitivity analysis to investigate potential influences of medication on reactive aggression, the number of hyperactivity and impulsivity symptoms and impairments measured with the DIVA as well as the brain activity

associated with reactive aggression in the ADHD group, see the section **Supplementary Analysis**.

RESULTS

Functional Magnetic Resonance Imaging Task Activation

For the whole-brain analysis of viewing all emotions compared to the implicit baseline, ADHD cases and controls did not show any differential activation patterns. Both diagnostic groups showed BOLD responses to emotional faces in broad clusters spanning several areas. These regions included temporoparietal, inferior, and superior frontal cortical areas as well as several subcortical areas including parts of the limbic system, see **Supplementary Table 1** and **Supplementary Figure 2**. No significant differences were found either when analyzing the emotions separately. Comparisons were made at the FWE-corrected threshold of $p = 0.05$.

We furthermore found two clusters in the left superior frontal as well as left OFC associated with sex differences during emotion processing, see **Supplementary Table 3**.

Neural Correlates of Reactive Aggression

Interaction of Reactive Aggression and Diagnostic Group

We found a significant interaction between ADHD diagnosis and reactive aggression scores in the activation of clusters assigned to the right precentral and postcentral gyri, superior parietal, middle temporal areas, lingual gyrus, and the caudate nucleus at a significance level of $p = 0.05$. Activity was higher for high reactive aggression scores in the ADHD group and lower for low reactive aggression scores in healthy controls. **Figure 1** shows the cluster of significant interaction, for further information see **Table 2**. There were no clusters showing an inverse effect.

TABLE 2 | Interaction of diagnosis and reactive aggression.

Cluster label	Voxels	*P*	Z-MAX	*X* (mm)	*Y* (mm)	*Z* (mm)
R Precentral gyrus	127	<0.05	4.97	30	−10	52
R Lingual gyrus	63	<0.05	3.68	16	−54	−6
R Superior parietal lobe	39	<0.05	3.84	30	−56	58
R Inferior/middle temporal gyrus	24	<0.05	3.64	58	−36	−16
R Postcentral gyrus	22	<0.05	3.86	18	−42	58
R Occipital Pole	11	<0.05	3.34	4	−86	32
L Caudate	11	<0.05	3.54	−6	8	10

Results of the whole-brain analysis for the interaction of reactive aggression with diagnosis, cluster extent correction of 11 voxel for p = 00.05.

Reactive Aggression in the Attention-Deficit/Hyperactivity Disorder Group

The analysis of reactive aggression within the ADHD group showed significantly elevated activation levels of clusters including the precentral gyrus, cortical frontal and temporal areas, as well as subcortical structures such as the hippocampus. Furthermore two clusters within the right Amygdala [$p_{unc.} < 0.001$, $xyz = (22, -8, -8)$ and $p_{unc.} < 0.001$ $xyz = (28, -10, -1)$] were activated, but did not exceed the threshold of 11 voxels each. The activity in all clusters was positively associated with higher reactive aggression scores. There was no significant effect of low reactive aggression, see **Figure 2** and **Table 3** for more information on the significant clusters.

Reactive Aggression in the Control Group

No positive relationship of reactive aggression with brain activity was found in the control group. However, we additionally investigated a potential inverse effect, e.g., negative associations of reactive aggression scores with the brain activity of healthy controls. We found a negative relationship of reactive aggression with the activity in a cluster in the left MTG, right superior parietal lobule as well as the right precentral and lingual gyri (**Figure 3** and **Table 3**).

Post hoc Associations of Clinical Measures

The linear regression analysis of reactive aggression modeled by diagnostic group revealed a significant association of the factor diagnosis with reactive aggression scores ($t = 4.50$; $p < 0.001$, $r_{standardized} = 0.34$). Age was not associated with reactive aggression, but male gender was ($t = -3.72$; $p = 0.004$,

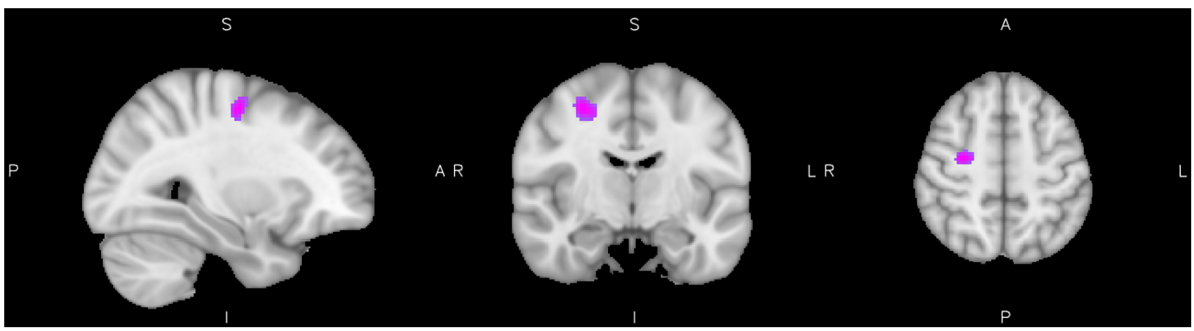

FIGURE 1 | Interaction of diagnosis with reactive aggression. Results from the interaction of reactive aggression and diagnosis at the maximum of the cluster in the precentral gyrus (slices $x = 30$ left, $y = -10$ middle, and $z = 52$ right), cluster extent corrected for $p = 0.05$.

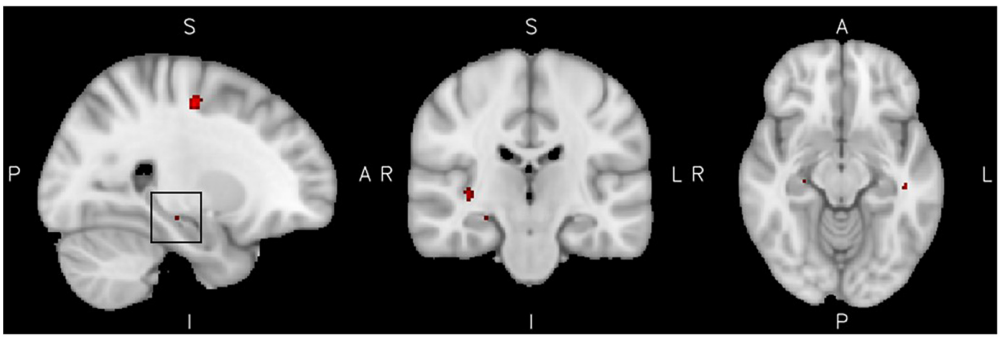

FIGURE 2 | High reactive aggression in ADHD. Results from the reactive aggression analysis in the ADHD group at the maximum of the cluster of 14 voxel in the hippocampus, highlighted by a black square in the left figure (slices $x = 26$ left, $y = -22$ middle, and $z = -12$ right), at a cluster extent correction of $p = 0.05$.

$r_{standardized} = -0.28$). **Table 4** summarizes the results of the regression analysis.

We furthermore found associations between reactive aggression scores and the number of hyperactivity/impulsivity symptoms as well as self-reported impairment in the domains of "relationships and families" as well as "self-image" in adulthood from the DIVA in the regression analysis of the DIVA subscales, see **Table 5**.

Additionally, the number of hyperactivity/impulsivity symptoms was correlated positively with the activity in two clusters associated with reactive aggression in the ADHD group; the more hyperactivity symptoms the adults with ADHD had, the more activation was seen in the right hippocampus (Spearman's $\rho = 0.29$, $p = 0.046$) and the lingual gyrus (Spearman's $\rho = 0.31$, $p = 0.041$). No correlations with neural activation in areas linked to reactive aggression were observed for inattention symptoms, see **Figure 4**.

The sensitivity analysis of medication effects yielded no significant medication effects, see the section **Supplementary Analysis**.

TABLE 3 | Neural correlates of reactive aggression.

Cluster label	Voxels	*P*	Z-MAX	*X* (mm)	*Y* (mm)	*Z* (mm)
ADHD						
R Precentral gyrus	83	<0.05	5.45	24	−12	50
L Middle frontal gyrus	42	<0.05	3.74	32	18	56
R Superior frontal gyrus	33	<0.05	3.78	6	32	62
R Inferior/middle temporal gyrus	33	<0.05	4.99	64	−32	−18
R Insula	20	<0.05	4.38	36	−22	2
R Lingual gyrus	18	<0.05	3.5	16	−70	−6
Not assigned	16	<0.05	4.27	−44	−26	−12
Not assigned	14	<0.05	3.82	30	2	28
R Hippocampus	14	<0.05	3.43	26	−22	−12
Controls						
L Midde/inferior temporal gyrus	240	<0.05	4.37	−62	−60	−4
R Superior parietal lobule	88	<0.05	3.82	28	−56	58
R Lingual gyrus	60	<0.05	3.77	18	−52	−4
R Precentral gyrus	24	<0.05	3.78	32	−10	56
R Superior Parietal Lobule	13	<0.05	3.62	28	−42	58

Results of the whole-brain analysis for the analysis of reactive aggression within the ADHD group (top) and the control group (bottom) separately, cluster extent correction of 11 voxel for p = 0.05.

DISCUSSION

In this study, we aimed to identify neural correlates of reactive aggression, in adults with ADHD. To our knowledge, this is the first study to use a behavioral measure of reactive aggression as a marker of ED during implicit emotion regulation in adults with ADHD. We found areas of differential brain activity during emotion processing in the ADHD group in covariance with high reactive aggression to be localized in the limbic system and insula as well as in middle and superior frontal areas.

Reactive Aggression

In line with previous literature on reactive aggression in ADHD, our analysis of reactive aggression indicated significantly elevated levels of reactive aggression in adults with ADHD compared to the control group (32). Higher scores of reactive aggression were also associated with male sex, in congruence with literature on male reactive aggression and externalizing behavior (5, 10). Previous literature shows that increased reactive aggression often correlates with, or has predictive value for ADHD symptom severity (9), with closer developmental coupling with hyperactivity/impulsivity symptoms (42). Indeed, the association of reactive aggression with the subscales of the DIVA diagnostic instrument used in our study confirmed that symptoms of hyperactivity/impulsivity, but not inattention, were associated with reactive aggression. Interestingly, individuals reporting problems in relationships and/or family or with their self-image showed higher levels of reactive aggression, implying that impairments in the social life-domains could be particularly frequent in people with ADHD and high reactive aggression traits. This finding is in line with the literature on ED being an important predictor for the social, functional, and occupational outcome of ADHD (43, 44). Especially for the persistent phenotype of ADHD, ED such as

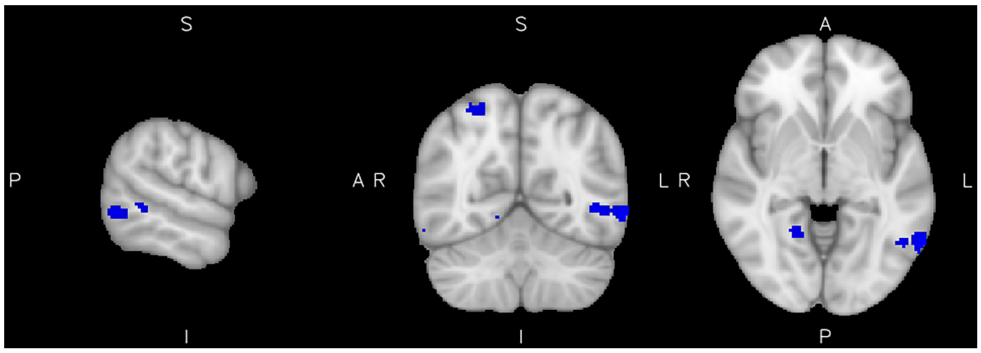

FIGURE 3 | Low reactive aggression in the control group. Results from the reactive aggression analysis of the control group at the maximum of the cluster in the left middle temporal gyrus (slices $x = -62$ left, $y = -60$ middle, and $z = -4$ right), at a cluster extent correction of $p = 0.05$.

reactive aggression is considered a constitutional component (45), showing most pronounced expression and associated impairments in adulthood (46). This clinical subgroup might thus be more vulnerable to social impairments and is particularly important to investigate further.

TABLE 4 | Regression of reactive aggression.

Regressors	Estimate	Standard error	*t*-value	*p*-value
ADHD diagnosis (y/n)	0.33	0.57	4.50	<0.001***
Age	0.03	0.02	0.40	0.69
Sex	−0.28	0.57	−3.72	<0.001***

*Summary of regression analysis of reactive aggressive behavior, showing regression coefficients, standard errors, t- and p-values as well as levels of significance in codes from 0.001 as "***," from 0.01 as "**," or from 0.05 as "*" to the model.*

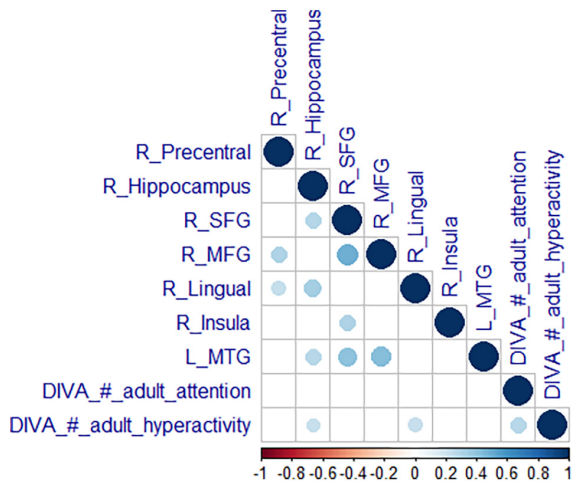

FIGURE 4 | Correlation of neural activity with symptoms. Correlation matrix of mean estimates in the significant clusters from the reactive aggression whole-brain analysis with expressions of the core symptoms (attention and hyperactivity). We are reporting Spearman's correlation coefficient *p* (bottom scale) with a blue color for a positive and a red color for a negative correlation. Results were Bonferroni corrected.

Functional Magnetic Resonance Imaging Task Activation

The fMRI whole-brain analysis of emotional faces revealed activation in the limbic system (associated with emotion processing and memory), the fusiform gyrus (associated with face processing), broad temporoparietal and frontal networks. These findings are in line with the original paradigm (38), which used this task to investigate manipulations of amygdala responsiveness, as well as a meta-analysis of implicit facial emotion processing (47). Notably, the attention distraction task withdrew attention from the emotional stimulus toward the red dot, to measure implicit ED. This might skew the findings toward the study of emotion hyperreactivity and underrepresent the contribution of impaired executive functioning to the production of emotionally dysregulated behavior in ADHD. Studies on explicit emotion regulation, report more commonly associated areas such as the anterior cingulate and dorsal and ventromedial prefrontal cortex (27), which might be more relevant for tasks without distraction from the emotional stimulus. However, we find evidence, that even in this implicit emotion regulation scenario, middle and superior frontal areas are engaged, suggesting that executive functioning plays a role for implicit emotion regulation as well.

We found no neural activation differences between adults with and without ADHD, irrespective of emotional valence, suggesting

TABLE 5 | Associations of clinical measures with reactive aggression.

Regressors	Estimate	Standard error	*t*-value	*p*-value
Hyperactivity/Impulsivity	0.28	0.17	2.11	0.036*
Inattention	0.09	0.14	0.71	0.479
Occupation	0.34	0.93	0.11	0.917
Relationship and family	6.41	0.89	2.07	0.041*
Social contacts	2.03	0.81	0.71	0.479
Hobby	−2.17	0.79	−0.78	0.436
Self-image	−6.59	0.93	−2.02	0.045*

*Summary of regression analysis of reactive aggressive behavior, showing regression coefficients, standard errors, t- and p-values as well as levels of significance in codes from 0.001 as "***," from 0.01 as "**," or from 0.05 as "*" to the model.*

that implicit emotional reactivity is not altered in people with ADHD. While several fMRI studies in children with ADHD reported group differences in the activity and connectivity of the amygdala, the ventral striatum, and the OFC, these effects were often moderated by medical treatment and were not replicated in adult populations [for a review see Rubia (17)]. In the current study, *post hoc* analyses of medication effects on reactive aggression, symptoms, impairments and the neural correlates of reactive aggression revealed no significant associations (see section **Supplementary Analyses**).

However, sex seemed to influence emotion processing in the left orbitofrontral and superior frontal cortex. These areas are implicated in cognitive control processes, relevant for downregulation of emotional responses and might play a role for general sex differences in emotional reactions or aggression.

Neural Correlates of Reactive Aggression

While the neurocognitive architecture of emotion processing does not seem to be altered over the whole ADHD group compared to the controls, we expected the neurocognitive architecture to differ in adults with ADHD and co-occurring reactive aggression. Therefore, we investigated the association of reactive aggression with whole-brain activity in both diagnostic groups. We found a significant interaction between ADHD diagnosis and reactive aggression in areas such as the lingual gyrus, caudate, superior parietal, middle temporal, and premotor areas during processing of emotional faces, pointing toward differential neural correlates in adults with ADHD and reactive aggression compared to control subjects with reactive aggression.

When focusing the analysis on the ADHD group, activity in the right precentral, right lingual and left middle temporal gyri was particularly increased in people with ADHD if they had higher reactive aggression scores. Furthermore, small clusters within the right insula, the right limbic system (hippocampus and subthreshold parts of the amygdala) and middle and superior frontal areas were implicated in emotion processing in the ADHD group with high reactive aggression only.

The insula as well as the hippocampus and amygdala are associated with the reactivity and assignment of salience during emotion processing in ADHD (31, 48). Emotional reactivity in the amygdala might be influenced by the hippocampus, which controls emotional memory recalling and regulation, especially in positive contexts (49), and the insula, engaged in down-regulation and maintaining homeostasis during the experience of negative emotions (48, 50). Knowing that measures of structure and volume of the brain in these areas show alterations in children with ADHD, one could hypothesize that an altered neurodevelopment of these structures could influence the vulnerability of individuals with ADHD to develop reactive aggressive behavior: differential maturation might lead to higher liability to develop a hyperreactivity of the limbic system, which might suggest a more intense emotional sensation and higher sensitivity to emotional stimuli in subjects with ADHD.

Our results on altered activity of limbic structures and the insula during emotion processing are in line with previous findings in medication-naive individuals with ADHD (22, 51). These authors discuss medication might drive a normalization effect of differential amygdala response. Interestingly, in our sample medication was not associated with reactive aggression, brain activity or ADHD symptoms in adulthood, which suggests that for the persistent phenotype of ADHD in our sample, stimulant medication seemed to be inefficient to further improve symptoms significantly.

Interestingly, we observed higher activity in middle and superior frontal clusters in patients with high reactive aggression scores. This activation is associated with stronger cognitive control and might suggest more effortful top–down emotion regulation, a process frequently disturbed in ADHD (52), implying both subprocesses, emotional reactivity as well as top–down regulation are implied in reactive aggression in adult ADHD.

The activation of the left MTG as well as premotor areas was observed specifically in the ADHD group. The left MTG or temporo-parietal junction is often implicated in theory of mind abilities (53). This ability to understand other people's beliefs and intentions might represent a protective mechanism for ED. The activity in the MTG could reflect higher efforts to retrieve intentions from the facial expressions in the ADHD group. Higher premotor activity could be related to more allocation of attention. Both could be cause or consequence of higher estimation of salience in the ADHD group with higher reactive aggression scores (e.g., hippocampus), which could trigger a deeper processing of the seemingly important emotional stimuli.

The healthy control group did not show any clusters associated with high reactive aggression, in coherence with the notably low levels of reactive aggression in this group. Interestingly, decreased activity in people in the control group with particularly low reactive aggression scores in some clusters that are implicated in the ADHD group as well suggest a protective function of these areas to develop reactive aggression (in particular the left MTG, precentral, and lingual gyri).

Associations of Clinical Measures

We found positive correlations between the expression of hyperactivity/impulsivity symptoms and the activity related to reactive aggression in the hippocampus as well as the lingual gyrus in individuals with ADHD. The more hyperactivity/impulsivity symptoms adults with ADHD showed, the more these areas were engaged during emotion processing in association with reactive aggression. This association of ADHD symptoms with brain activity related to reactive aggression could be an example of a deviant neurocognitive mechanism behind ED in ADHD where the brain mediates both, ED as well as ADHD symptoms. Inattentive symptoms or impairments were not significantly correlated with neural activities. These findings point toward a specific susceptibility of the hyperactive type of ADHD to exhibit ED such as reactive aggression, in line with findings on the close developmental coupling of hyperactive/impulsive symptoms with reactive aggression (42) and general association of the hyperactive subtype with ED and aggression (54).

Strengths and Weaknesses

All results need to be viewed in the context of the strengths and limitations of this study. Our sample sizes exceed most previous fMRI studies related to this topic in ADHD and is demographically well balanced.

However, task activation maps across all subjects did not show some areas classically associated with emotion regulation, such as the anterior cingulate, OFC, dlPFC, and vmPFC, or the amygdala (55), the latter only showing up as small subthreshold clusters. This was likely due to the implicit nature of our task. While emotion regulation paradigms mostly direct the participant's attention toward the processing of an emotion or even ask for explicit emotion regulation (55), we employed an implicit paradigm in which the participant's attention was not focused on the processing of emotional content and they were not asked to regulate their emotions, potentially affecting effect sizes and activity in areas relevant for top–down control. Notably, the clustersize of the reported results of the covariance of reactive aggression with ADHD is overall small, all described results should be carefully discussed as true findings. The small clustersizes might be related to the small effect sizes elicited from implicit emotion processing task in combination with an indirect measure of trait-reactive aggression as well as the vast heterogeneity in the ADHD population. Future studies with sufficient statistical power to address for expected small effect sizes that investigate subgroups within the spectrum of ADHD could elucidate this matter further. Furthermore, contrasting the emotional conditions to a fixation cross (implicit baseline) instead of neutral faces, as we did here, expectedly captured not only emotion processing but also general social cognition processes. For the investigation of adult ADHD and the association to ED, broader social processes, e.g., general face processing difficulties, might play a role as well. Notably, we included reactive aggression as a trait-behavioral measure of ED. The applied task is measuring emotion processing closer to everyday-life situations compared to explicit emotion regulation tasks. Importantly, the integration of trait behavioral reactive aggression as a reflection of very relevant real-life ED together with the activity during emotion processing is suitable to reveal which areas are relevant for emotionally dysregulated behavior and potentially highlight social cognition and emotional (sub)processes that are implicated in ED. However, the implementation of a task to elicit an emotional response, without attention distraction during fMRI could result in bigger effect sizes and a more precise delineation of the network of ED in ADHD. We furthermore recommend the implementation of a longitudinal design to study relevant brain networks for ED in ADHD, due to the close coupling of developmental trajectory of hyperactivity/impulsivity with the expression of ED.

CONCLUSION

In conclusion, these findings convey evidence for a differential emotion processing mechanism in subjects with ADHD and reactive aggression, with a specific liability of individuals with hyperactivity/impulsivity symptoms to experience these alterations. The brain regions related to this mechanism suggest difficulties with both emotional hyper-reactivity (as reflected in the insula and amygdala), and more effortful regulation of emotional responses (implicated by hippocampus and frontal activity) in the ADHD group with higher reactive aggression. This differential mechanism appears to be related to an altered neurocognitive brain architecture of ADHD and supports the diagnostic and clinical view of emotionally dysregulated ADHD as a subgroup in the spectrum of the disorder, as discussed by Shaw P et al. (3). In the light of these findings, future research may evaluate more targeted intervention for the emotionally dysregulated group, such as behavioral emotion regulation interventions and their effect on reactive aggressive behavior (56).

DATA AVAILABILITY STATEMENT

The raw data supporting the conclusions of this article will be made available by the authors upon motivated request with the intention to investigate ADHD.

ETHICS STATEMENT

The studies involving human participants were reviewed and approved by CCMO. The patients/participants provided their written informed consent to participate in this study.

AUTHOR CONTRIBUTIONS

MH, BF, and AA-V contributed to study conception and supervision, obtained the funding. PV and BJ provided the samples and data. BJ and DR conducted the analyses and data interpretation. BJ, DR, MH, and AA-V contributed to writing group. All authors contributed to manuscript revision, read and approved the submitted version.

ACKNOWLEDGMENTS

We acknowledge funding from Netherlands Organization for Scientific Research (NWO), i.e., from the Veni Innovation Program (grant 016-196-115 to MH) and the Dutch National Science Agenda NeurolabNL project (grant 400-17-602). The work was also supported by funding from the European Community's Horizon 2020 Programme (H2020/2014 – 2020) under grant agreements n° 728018 (Eat2beNICE) and n° 667302 (CoCA), and by the European College of Neuropsychopharmacology (ECNP) Network "ADHD Across the Lifespan."

SUPPLEMENTARY MATERIAL

The Supplementary Material for this article can be found online at: https://www.frontiersin.org/articles/10.3389/fpsyt.2022.840095/full#supplementary-material

REFERENCES

1. Faraone SV, Asherson P, Banaschewski T, Biederman J, Buitelaar JK, Ramos-Quiroga JA, et al. ADHD. *Nat Rev Dis Primers*. (2015) 1:15020.
2. American Psychiatric Association. *Diagnostic and Statistical Manual of Mental Disorders*. Wahington, DC: American Psychiatric Association (2013).
3. Shaw P, Stringaris A, Nigg J, Leibenluft E. Emotion dysregulation in attention deficit hyperactivity disorder. *Am J Psychiatry*. (2014) 171:276–93. doi: 10.1176/appi.ajp.2013.13070966
4. Christiansen H, Hirsch O, Albrecht B, Chavanon M-L. Attention-deficit/hyperactivity disorder (ADHD) and emotion regulation over the life span. *Curr Psychiatry Rep*. (2019) 21:1–11. doi: 10.1007/s11920-019-1003-6
5. Connor DF, Chartier KG, Preen EC, Kaplan RF. Impulsive aggression in attention-deficit/hyperactivity disorder: symptom severity, co-morbidity, and attention-deficit/hyperactivity disorder subtype. *J Child Adolesc Psychopharmacol*. (2010) 20:119–26. doi: 10.1089/cap.2009.0076
6. King S, Waschbusch DA. Aggression in children with attention-deficit/hyperactivity disorder. *Expert Rev Neurotherap*. (2010) 10:1581–94.
7. Saylor KE, Amann BH. Impulsive aggression as a comorbidity of attention-deficit/hyperactivity disorder in children and adolescents. *J Child Adolesc Psychopharmacol*. (2016) 26:19–25. doi: 10.1089/cap.2015.0126
8. Lickley RA, Sebastian CL. The neural basis of reactive aggression and its development in adolescence. *Psychol Crime Law*. (2018) 24:313–33. doi: 10.1016/j.bpsc.2019.05.003
9. Abel MR, Poquiz JL, Fite PJ, Doyle RL. Reactive aggression and suicidal behaviors in children receiving outpatient psychological services: the moderating role of hyperactivity and inattention. *Child Psychiatry Hum Dev*. (2020) 51:2–12. doi: 10.1007/s10578-019-00905-5
10. Slaughter KE, Leaberry KD, Fogleman ND, Rosen PJ. Reactive and proactive aggression in children with and without ADHD and negative emotional lability. *Soc Dev*. (2020) 29:320–38. doi: 10.1111/sode.12402
11. Raine A, Dodge K, Loeber R, Gatzke-Kopp L,. Lynam D, Reynolds C, et al. The reactive-proactive aggression questionnaire: differential correlates of reactive and proactive aggression in adolescent boys. *Aggress Behav*. (2006) 32:159–71.
12. Martel MM. Research review: a new perspective on attention-deficit/hyperactivity disorder: emotion dysregulation and trait models. *J Child Psychol Psychiatry*. (2009) 50:1042–51. doi: 10.1111/j.1469-7610.2009.02105.x
13. Evans SC, Fite PJ, Hendrickson ML, Rubens SL, Mages AK. The role of reactive aggression in the link between hyperactive–impulsive behaviors and peer rejection in adolescents. *Child Psychiatry Hum Dev*. (2015) 46:903–12. doi: 10.1007/s10578-014-0530-y
14. Bridge JA, Reynolds B, McBee-Strayer SM, Sheftall AH, Ackerman J, Stevens J, et al. Impulsive aggression, delay discounting, and adolescent suicide attempts: effects of current psychotropic medication use and family history of suicidal behavior. *J Child Adolesc Psychopharmacol*. (2015) 25:114–23. doi: 10.1089/cap.2014.0042
15. Hoogman M, Bralten J, Hibar DP, Mennes M, Zwiers MP, Schweren LS, et al. Subcortical brain volume differences in participants with attention deficit hyperactivity disorder in children and adults: a cross-sectional mega-analysis. *Lancet Psychiatry*. (2017) 4:310–9.
16. Hoogman M, Muetzel R, Guimaraes JP, Shumskaya E, Mennes M, Zwiers MP, et al. Brain imaging of the cortex in ADHD: a coordinated analysis of large-scale clinical and population-based samples. *Am J Psychiatry*. (2019) 176:531–42. doi: 10.1176/appi.ajp.2019.18091033
17. Rubia K. Cognitive neuroscience of attention deficit hyperactivity disorder (ADHD) and its clinical translation. *Front Hum Neurosci*. (2018) 12:100. doi: 10.3389/fnhum.2018.00100
18. Phelps EA. Human emotion and memory: interactions of the amygdala and hippocampal complex. *Curr Opin Neurobiol*. (2004) 14:198–202. doi: 10.1016/j.conb.2004.03.015
19. Sarkheil P, Klasen M, Schneider F, Goebel R, Mathiak K. Amygdala response and functional connectivity during cognitive emotion regulation of aversive image sequences. *Eur Arch Psychiatry Clin Neurosci*. (2019) 269:803–11. doi: 10.1007/s00406-018-0920-4
20. Makris N, Biederman J, Valera EM, Bush G, Kaiser J, Kennedy DN, et al. Cortical thinning of the attention and executive function networks in adults with attention-deficit/hyperactivity disorder. *Cereb Cortex*. (2007) 17:1364–75. doi: 10.1093/cercor/bhl047
21. Brotman MA, Rich BA, Guyer AE, Lunsford JR, Horsey SE, Reising MM, et al. Amygdala activation during emotion processing of neutral faces in children with severe mood dysregulation versus ADHD or bipolar disorder. *Am J Psychiatry*. (2010) 167:61–9. doi: 10.1176/appi.ajp.2009.09010043
22. Posner J, Nagel BJ, Maia TV, Mechling A, Oh M, Wang Z, et al. Abnormal amygdalar activation and connectivity in adolescents with attention-deficit/hyperactivity disorder. *J Am Acad Child Adolesc Psychiatry*. (2011) 50:828–37.e823. doi: 10.1016/j.jaac.2011.05.010
23. Hwang S, White SF, Nolan ZT, Williams WC, Sinclair S, Blair R. Executive attention control and emotional responding in attention-deficit/hyperactivity disorder—a functional MRI study. *Neuroimage*. (2015) 9:545–54. doi: 10.1016/j.nicl.2015.10.005
24. Vetter NC, Buse J, Backhausen LL, Rubia K, Smolka MN, Roessner V. Anterior insula hyperactivation in ADHD when faced with distracting negative stimuli. *Hum Brain Mapp*. (2018) 39:2972–86. doi: 10.1002/hbm.24053
25. Passarotti AM, Sweeney JA, Pavuluri MN. Emotion processing influences working memory circuits in pediatric bipolar disorder and attention-deficit/hyperactivity disorder. *J Am Acad Child Adolesc Psychiatry*. (2010) 49:1064–80. doi: 10.1016/j.jaac.2010.07.009
26. Posner J, Maia TV, Fair D, Peterson BS, Sonuga-Barke EJ, Nagel BJ. The attenuation of dysfunctional emotional processing with stimulant medication: an fMRI study of adolescents with ADHD. *Psychiatry Res*. (2011) 193:151–60. doi: 10.1016/j.pscychresns.2011.02.005
27. Materna L, Wiesner CD, Shushakova A, Trieloff J, Weber N, Engell A, et al. Adult patients with ADHD differ from healthy controls in implicit, but not explicit, emotion regulation. *J Psychiatry Neurosci*. (2019) 44:340. doi: 10.1503/jpn.180139
28. Schulz KP, Bédard A-CV, Fan J, Clerkin SM, Dima D, Newcorn JH, et al. Emotional bias of cognitive control in adults with childhood attention-deficit/hyperactivity disorder. *Neuroimage*. (2014) 5:1–9. doi: 10.1016/j.nicl.2014.05.016
29. Lindholm P, Lieslehto J, Nikkinen J, Moilanen I, Hurtig T, Veijola J, et al. Brain response to facial expressions in adults with adolescent ADHD. *Psychiatry Res*. (2019) 292:54–61. doi: 10.1016/j.pscychresns.2019.09.003
30. Nelson RJ, Trainor BC. Neural mechanisms of aggression. *Nat Rev Neurosci*. (2007) 8:536–46.
31. Alia-Klein N, Gan G, Gilam G, Bezek J, Bruno A, Denson TF, et al. The feeling of anger: from brain networks to linguistic expressions. *Neurosci Biobehav Rev*. (2020) 108:480–97. doi: 10.1016/j.neubiorev.2019.12.002
32. Bubenzer-Busch S, Herpertz-Dahlmann B, Kuzmanovic B, Gaber TJ, Helmbold K, Ullisch MG, et al. Neural correlates of reactive aggression in children with attention-deficit/hyperactivity disorder and comorbid disruptive behaviour disorders. *Acta Psychiatr Scand*. (2016) 133:310–23. doi: 10.1111/acps.12475
33. Puiu AA, Wudarczyk O, Goerlich KS, Votinov M, Herpertz-Dahlmann B, Turetsky B, et al. Impulsive aggression and response inhibition in attention-deficit/hyperactivity disorder and disruptive behavioral disorders: findings from a systematic review. *Neurosci Biobehav Rev*. (2018) 90:231–46. doi: 10.1016/j.neubiorev.2018.04.016
34. Sato W, Yoshikawa S, Kochiyama T, Matsumura M. The amygdala processes the emotional significance of facial expressions: an fMRI investigation using the interaction between expression and face direction. *Neuroimage*. (2004) 22:1006–13. doi: 10.1016/j.neuroimage.2004.02.030
35. Hermans EJ, Putman P, Van Honk J. Testosterone administration reduces empathetic behavior: a facial mimicry study. *Psychoneuroendocrinology*. (2006) 31:859–66. doi: 10.1016/j.psyneuen.2006.04.002
36. Kooij JJS, Francken MH. *DIVA 2.0. Diagnostic Interview Voor ADHD in Adults Bij Volwassenen [DIVA 2 0 Diagnostic Interview ADHD in Adults]*. The Hague: DIVA Foundation (2010).
37. Wechsler D. *Wechsler Adult Intelligence Scale – Archives of Clinical Neuropsychology*. New York, NY: Psychological Corporation (1955).
38. Van Marle HJ, Hermans EJ, Qin S, Fernández G. From specificity to sensitivity: how acute stress affects amygdala processing of biologically

salient stimuli. *Biol Psychiatry*. (2009) 66:649–55. doi: 10.1016/j.biopsych.2009.05.014
39. Pruim RH, Mennes M, van Rooij D, Llera A, Buitelaar JK, Beckmann CF. ICA-AROMA: a robust ICA-based strategy for removing motion artifacts from fMRI data. *Neuroimage*. (2015) 112:267–77.
40. Slotnick SD, Moo LR, Segal JB, Hart J Jr. Distinct prefrontal cortex activity associated with item memory and source memory for visual shapes. *Cogn Brain Res.* (2003) 17:75–82. doi: 10.1016/s0926-6410(03)00082-x
41. Slotnick SD. Cluster success: fMRI inferences for spatial extent have acceptable false-positive rates. *Cogn Neurosci*. (2017) 8:150–5.
42. Murray AL, Obsuth I, Zirk-Sadowski J, Ribeaud D, Eisner M. Developmental relations between ADHD symptoms and reactive versus proactive aggression across childhood and adolescence. *J Attent Disord*. (2020) 24:1701–10.
43. Bunford N, Evans SW, Langberg JM. Emotion dysregulation is associated with social impairment among young adolescents with ADHD. *J Attent Disord.* (2018) 22:66–82. doi: 10.1177/1087054714527793
44. Bodalski EA, Knouse LE, Kovalev D. Adult ADHD, emotion dysregulation, and functional outcomes: examining the role of emotion regulation strategies. *J Psychopathol Behav Assess.* (2019) 41:81–92. doi: 10.1007/s10862-018-9695-1
45. Beheshti A, Chavanon M-L, Christiansen H. Emotion dysregulation in adults with attention deficit hyperactivity disorder: a meta-analysis. *BMC Psychiatry.* (2020) 20:120. doi: 10.1186/s12888-020-2442-7
46. Skirrow C, Asherson P. Emotional lability, comorbidity and impairment in adults with attention-deficit hyperactivity disorder. *J Affect Disord.* (2013) 147:80–6. doi: 10.1016/j.jad.2012.10.011
47. Shi H, Wang X, Yao S. Comparison of activation patterns between masking and inattention tasks: a coordinate-based meta-analysis of implicit emotional face processing. *Front Hum Neurosci*. (2013) 7:459. doi: 10.3389/fnhum.2013.00459
48. Zhu Y, Gao H, Tong L, Li Z, Wang L, Zhang C, et al. Emotion regulation of hippocampus using real-time fMRI neurofeedback in healthy human. *Front Hum Neurosci*. (2019) 13:242. doi: 10.3389/fnhum.2019.00242
49. Schumacher A, Villaruel FR, Ussling A, Riaz S, Lee AC, Ito R. Ventral hippocampal CA1 and CA3 differentially mediate learned approach-avoidance conflict processing. *Curr Biol*. (2018) 28:1318–24.
50. Steward T, Pico-Perez M, Mata F, Martinez-Zalacain I, Cano M, Contreras-Rodriguez O, et al. Emotion regulation and excess weight: impaired affective processing characterized by dysfunctional insula activation and connectivity. *PLoS One*. (2016) 11:e0152150. doi: 10.1371/journal.pone.0152150
51. Hulvershorn LA, Mennes M, Castellanos FX, Di Martino A, Milham MP, Hummer TA, et al. Abnormal amygdala functional connectivity associated with emotional lability in children with attention-deficit/hyperactivity disorder. *J Am Acad Child Adolesc Psychiatry*. (2014) 53:351-61.
52. Craig F, Margari F, Legrottaglie AR, Palumbi R, De Giambattista C, Margari L. A review of executive function deficits in autism spectrum disorder and attention-deficit/hyperactivity disorder. *Neuropsychiatr Dis Treat*. (2016) 12:1191–202.
53. Samson D, Apperly IA, Chiavarino C, Humphreys GW. Left temporoparietal junction is necessary for representing someone else's belief. *Nat Neurosci*. (2004) 7(5):499–500.
54. Wheeler Maedgen J, Carlson CL. Social functioning and emotional regulation in the attention deficit hyperactivity disorder subtypes. *J Clin Child Psychol*. (2000) 29:30–42.
55. Ochsner KN, Silvers JA, Buhle JT. Functional imaging studies of emotion regulation: a synthetic review and evolving model of the cognitive control of emotion. *Ann N Y Acad Sci.* (2012) 1251:E1. doi: 10.1111/j.1749-6632.2012.06751.x
56. Sánchez M, Lavigne R, Romero JF, Elósegui E. Emotion regulation in participants diagnosed with attention deficit hyperactivity disorder, before and after an emotion regulation intervention. *Front Psychol*. (2019) 10:1092. doi: 10.3389/fpsyg.2019.0109

Conflict of Interest: The authors declare that the research was conducted in the absence of any commercial or financial relationships that could be construed as a potential conflict of interest.

Publisher's Note: All claims expressed in this article are solely those of the authors and do not necessarily represent those of their affiliated organizations, or those of the publisher, the editors and the reviewers. Any product that may be evaluated in this article, or claim that may be made by its manufacturer, is not guaranteed or endorsed by the publisher.

frontiers | Frontiers in Psychiatry

TYPE Review
PUBLISHED 01 August 2022
DOI 10.3389/fpsyt.2022.866926

OPEN ACCESS

EDITED BY
Neeltje E. M. Van Haren,
Sophia Children's Hospital, Netherlands

REVIEWED BY
Elisabet Blok,
Sophia Children's Hospital, Netherlands
Luke Norman,
King's College London, United Kingdom

*CORRESPONDENCE
Ana Cubillo
ana.cubillo@econ.uzh.ch;
ana.cubillo@upk.ch

SPECIALTY SECTION
This article was submitted to Neuroimaging and Stimulation, a section of the journal Frontiers in Psychiatry

RECEIVED 31 January 2022
ACCEPTED 12 July 2022
PUBLISHED 01 August 2022

CITATION
Cubillo A (2022) Neurobiological correlates of the social and emotional impact of peer victimization: A review. *Front. Psychiatry* 13:866926. doi: 10.3389/fpsyt.2022.866926

Neurobiological correlates of the social and emotional impact of peer victimization: A review

Ana Cubillo[1,2]*

[1]Jacobs Center for Productive Youth Development, Zurich Center for Neuroeconomics, University of Zürich, Zurich, Switzerland, [2]Department of Child and Adolescent Psychiatry, University Psychiatric Clinic Basel, Basel, Switzerland

Peer victimization is very common during late childhood and adolescence. Despite the relatively reduced number of studies, the neurobiological underpinnings of the negative impact of peer victimization experiences have received increasing attention in recent years. The present selective review summarizes the most recent available evidence and provides a general overview of the impact of peer victimization experiences on social processing and decision-making at the neurobiological level, highlighting the most pressing areas requiring further research. Three key cognitive areas show a clear negative impact of peer victimization and bullying experiences: social valuation processing, reward and reinforcement learning and self-regulation processes. Victims show enhanced activation in key regions of the limbic system including the amygdala, rostral and dorsal anterior cingulate cortices, suggestive of enhanced sensitivity to social stimuli. They also show enhanced recruitment of lateral prefrontal regions crucially involved in cognitive and emotional regulation processes, and abnormal reward-related striatal function. The presence of psychopathology is a complex factor, increased as a consequence of peer victimization, but that also constitutes vulnerability to such experiences.

KEYWORDS

peer victimization, social processing, adolescents, neurobiology, reward

Introduction

For better and worse, social interactions play a large role in human development and well-being. Humans are social organisms by nature, requiring social contact for survival and reproduction. Human offspring rely on parental or other adult's care for survival for an extended period of time because their physical and cognitive development extends over decades. This allows the human species to develop complex behavior and thinking patterns, but also makes them highly dependent on the positive or negative influences of relevant others during key sensitive and vulnerable periods. Social interactions during early childhood are focused primarily on parents or caregivers, slowly shifting through late childhood and adolescence toward peers. This shift is accompanied by progressive

maturation in neural systems supporting social processing (1, 2). Any adverse social experiences during these early phases of life can have cascade effects and substantially influence subsequent development. While the role of early adverse events such as parental abuse or neglect on neural development has been widely investigated for decades, the effects of acute and chronic peer victimization or bullying have more recently received much-needed attention as well (1) (Figure 1). Given the high prevalence and the pervasive, long-lasting impact, it is still surprising the relatively reduced number of publications focused on the neurobiological mechanisms of early experiences of peer victimization. However, the neural mechanisms of peer victimization experiences have received increasing attention in the last few years. It is therefore necessary to review what we now know and highlight the areas where more research is urgently needed. This article reviews the most recent evidence on the impact of peer victimization on brain function during social learning and decision-making and highlight the most pressing aspects for future research studies.

Peer victimization can take the form of relational victimization (social exclusion, rumor spreading) and/or physical victimization (bullying, punching). These two forms of victimization have been shown to be highly correlated, with polyvictimization, conceptualized as the simultaneous exposure to different types of abuse, being highly common (3). Peer victimization and bullying are frequent in late childhood and adolescence, with prevalence estimates between 35 and 49% (4, 5). Such high frequency does not imply it should be treated as a "harmless rite of passage". On the contrary, similar to the negative and long-lasting impact of early experiences of neglect or abuse on life outcomes (6–10), there is now compelling evidence for pervasive adverse short- and long-term effects of peer victimization on physical and somatic symptoms, psychological health (increase rates of anxiety, depression

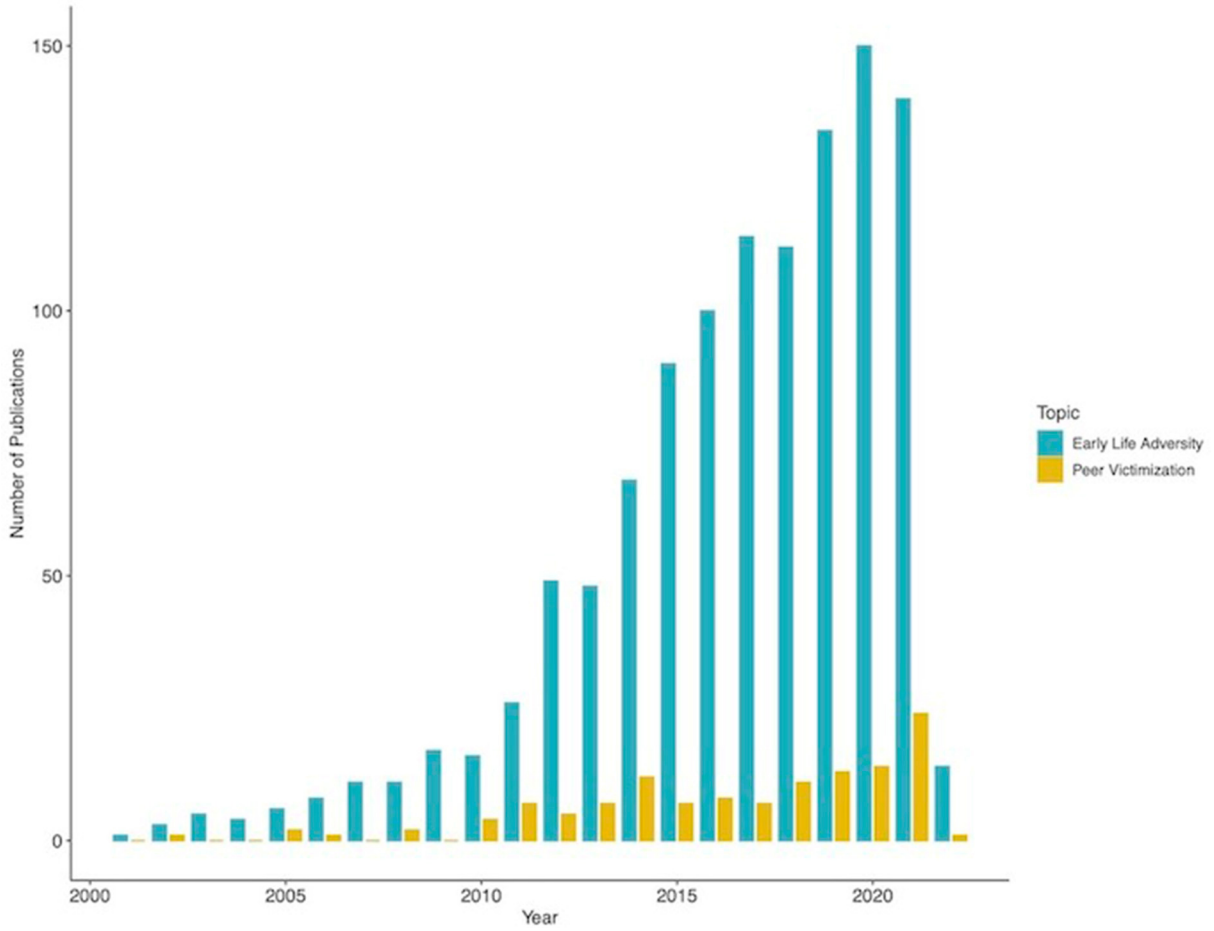

FIGURE 1
Comparison of the number of publications on neural mechanisms of peer victimization. The figure shows the number of publications displayed in a search in pubmed with the words "Peer victimization" and "brain" relative to the number of publications on "Early Life Adversity" and "Brain". Search data: 25 January 2022.

and suicidality), inflammation markers, stress response, social relationships, academic and occupational achievements or cognitive function (11–19).

Recent studies have started to shed light on the neurobiological correlates of peer victimization experiences, showing that experiences of social rejection, exclusion or bullying may trigger enhanced activation on or connectivity in regions supporting valuation and salience processes. The most recent evidence suggests peer victimization enhances individual's sensitivity to social stimuli (20–25), which together with altered reward and reinforcement learning processing (20, 26–28) and the difficulties in emotion and behavioral regulation lead to the increased need to engage regulatory circuits in order to implement behavioral, cognitive and emotional adaptations (29–31), not always successfully. Given the key role of peer interactions in socio-emotional development during childhood and adolescence, this selective review focuses on the associations between early experiences of peer victimization and bullying and altered neurobiological function during social valuation, and social decision-making, summarizing the most recent findings. A summary of the main results of the above studies, which are reviewed here, can be seen in Table 1.

Peer victimization is associated with enhanced sensitivity to social stimuli

Social interactions become crucial during late childhood and adolescence, evidenced by the sharp increase in the relevance and the time they spend with peers (41). Many studies have shown the significant influence of social agents during adolescence on decision-making or risk-taking tasks, both negative (increasing the likelihood of risky decisions) but also positive (they can also reduce the proportion of risky decisions made), which is applicable not only to peers (42–45) but also to relevant adults with whom adolescents maintain significant affective relationships (46, 47). At the neural developmental level, the enhanced sensitivity to social stimuli might be determined by the imbalanced development of the limbic system supporting emotion and incentive processing, relative to that of prefrontal regions supporting regulatory processes. Thus, neural maturation processes of the key regions supporting cognitive control, reward and social processing show a protracted trajectory starting in early childhood and continuing well into adulthood (48–56). The early development of the limbic system relative to the prefrontal cortex facilitates an enhanced individual sensitivity to incentives and emotional contexts (57, 58), thus increasing the risk of severe and long-lasting consequences when an insult occurs during crucial sensitive periods (59–61). Adolescence constitutes indeed the time when the imbalance on the neurodevelopmental trajectories of limbic systems involved in incentive and emotion processing, and prefrontal cognitive control systems is maximal (62–65). Furthermore, hormonal changes including those in crucial stress response systems, Hypothalamus-Pituitary-Adrenal axis (HPA axis) and the Hypothalamus-Pituitary-Gonadal axis (HPG axis), have their peak during this developmental stage (66), thus contributing to the onset or exacerbation of many psychopathological disorders (67). Hence, adolescence is a developmental period where individuals are highly sensitive to social stimuli. This enhanced sensitivity to social stimuli from peers may however play an adaptive role, facilitating the progressive independence of biologically mature individuals from protective parental environments (62), increasing their environmental exploration. It is therefore expected that social stimuli engage brain regions involved in processing of saliency.

The key regions processing salience include both the prefrontal cortex and limbic brain regions. The medial prefrontal cortex (mPFC) plays a key role as part of the neural networks supporting the modulation of amygdala responses to emotional stimuli, thus contributing to emotion regulation processes (68). The key sensitive period for the development of the structure and functional connectivity between amygdala and mPFC lays between late childhood and early adolescence (69, 70). Therefore, disturbances on this developmental phase might result in persistent disruption of emotion regulation skills or emotional reactivity to events. Together with the increased stress-reactivity observed during this phase (71), it would significantly impair their ability to successfully cope with peer victimization situations. Increased stress-induced HPA response in the adolescent brain might affect regions known to be stress-sensitive and that are still under development, in particular amygdala, prefrontal cortex or hippocampus, making the adolescent brain highly sensitive to these stressful situations (72). In support of this suggestion, recent evidence has shown that cortisol response in adolescents mediated the association between cyberbullying and perceived stress (73), as well as the association between early victimization experiences, subsequent abnormal cortisol response and reduced area in prefrontal cortex (74).

Indeed, because of this already heightened sensitivity, experiences of peer victimization and bullying may lead to pervasive, deleterious consequences. Theories like the Sociometer Theory (75) or the Need to Belong (76) postulate the existence of internal monitoring systems that interpret environmental signals of acceptance or rejection during social interactions with peers. These signals provide the individual a sense of belonging and the relational value with respect to the group. This need to belong is already present in very young children (77), with emotional, cognitive and behavioral detrimental effects (such as emotional distress; symptoms of depression, anxiety or irritability; hypervigilance for social cues or persistence/tolerance of abusive behaviors) when not fulfilled (76). Individuals would therefore be innately inclined to establish a number of interpersonal relationships that would

TABLE 1 Summary of main findings of studies on peer victimization combining brain imaging techniques and behavioral paradigms on social, emotional and cognitive control processes.

Reference	Population	Ages	Design	Methods	Key results
Asscheman et al. (32)	Children ($N = 55$, 0F); low preferred by peers $N = 27$, high preferred by peers $N = 28$	8-12	Longitudinal peer preference assessment, Cross-sectional imaging WB + ROI	Cyberball	**a) Behavior:** low preferred boys less satisfaction after inclusion **b) Imaging** Exclusion: Low preferred > high preferred dlPFC, SMG • No differences in ROI dACC analysis
Cara et al. (29)	Children typically developing ($N = 37$, 12F)	9–14	Cross-sectional WB	Change task (modified Go/NoGo)	**a) Behavior** • No association exposure to violence and performance **B) Imaging** • Exposure to lifetime violence associated with reduced activation in dACC, L IFC, R SFG, bilateral precentral cortex, L insula • Exposure to last year violence associated with reduced activation in dACC, precentral gryus, bilat SFG, bilat MFG, L SPL • Negative association between dACC, Insula, SPL activation and progressive task performance deterioration
Cisler et al. (20)	Assault victims ($N = 30$, all F), and typically developing ($N = 30$, all F)	11–17	Cross-sectional ROI	Social and non-social Reinforcement Learning (three-arm bandit) tasks Emotion processing task	**a) Behavior** • No differences in social vs. non-social; no differences between groups **b) Imaging** • Salience network (dACC, Insula) identified at ICA analysis weaker encoding of negative PE in victims vs. TD in both tasks. ***This association varied as a function of trauma.*** • Increased activation dACC, Insula during fear faces in high victimized group
Ethridge et al. (26)	Young adults exposed to victimization ($N = 61$, 54F)	18–25	Cross-sectional	Doors task EEG study	• Past-year relational but not physical victimization was associated with smaller neural response to gain, indicative of blunted reward response
Fowler et al. (33)	Study 1: healthy adolescents ($N = 33$, 20F) Study 2: Adolescents ($N = 26$, all F) with ($N = 17$) and without ($N = 9$) past exposure to peer victimization	11–16 14–16	Cross-sectional	Relational Value task	**Study 1 a) Behavior** • Higher proportion of trials classified as indicative of low relational value associated with increased levels of peer victimization **b) Imaging** • Negative association between levels of peer victimization and functional connectivity between VS-bilat IFC, VS-mPFC, VS- right Put Low> High peer victimization • Positive association between levels of peer victimization and functional connectivity between VS- Left inferior occipital cortex **Study 2 a) Behavior** • Higher proportion of trials classified as indicative of low relational value associated with increased levels of peer victimization

(Continued)

TABLE 1 Continued

Reference	Population	Ages	Design	Methods	Key results
					b) Imaging • Negative association between levels of peer victimization and functional connectivity between VS-bilat IFC in Low> High peer victimization (small volume correction)
Jarcho et al. (34)	Adolescents $N = 47$ (Low Victimized $N =$ 20, 10F; High Victimized $N = 27$, 13F)	10–12	Longitudinal wariness and victimization assessment, cross-sectional imaging ROI	fMRI virtual school paradigm	**Receipt of social evaluation:** High victimized: wariness between ages 2 and 7 was associated with activation in right amygdala during unpredicted positive peer evaluation, associated with higher social anxiety symptoms
Kiefer et al. (35)	Adolescents ($N = 24$, 14F)	12–15	Cross-sectional	Cyberball Perfusion MRI study	• Perfusion changes during social exclusion (exclusion vs. inclusion contrast) in the left IFC and sgACC were positively associated with the extent of previous experiences of bullying • Perfusion changes during social exclusion (exclusion vs. inclusion contrast) in the left IFC were positively associated with reported feelings of rejection after task performance
Lee et al. (30)	Adolescents $N = 23$ (all male); High peer verbal abuse $N = 11$, low peer verbal abuse $N = 12$	15–17	Cross-sectional WB+ ROI	fMRI emotional stroop—variation with swear words	**a) Behavior:** No sign differences between groups **b) Imaging:** • Swear words > neutral: high > low verbal abuse L vlPFC, insula • Increased funct connectivity L vlPFC-L hippocampus during swear condition in high>low verbal abuse groups
Lenow et al. (27)	Adolescents ($N = 32$, all F); Victims interpersonal violence $N = 15$, non-victims $N = 17$	12–16	Cross-sectional	Trust game (behavioral only)	• Interaction between Learning Rate and Preference stochasticity (PS): at high PS, learning rate was positively associated with assault frequency
McIver et al. (36)	Adolescents (N45, 36F), from which a) peer victimized ($N = 15$); b) defenders ($N = 15$); c) controls ($N = 15$)	17–19	Cross-sectional ROI	Cyberball	• No significant differences in experienced distress between groups • Exclusion> Inclusion: increased functional connectivity L amyg-ACC and L amyg-R Insula controls > Victimized; defenders had different pattern of functional connectivity with more connectivity in ACC-mPFC during inclusion than exclusion, opposite to what was described for the control and victimized groups • Functional connectivity mPFC-lAmyg in victimized individuals moderates association between victimization and depressive symptoms—these only present when connectivity is positive
Oppenheimer et al. (37)	Adolescents with diagnosis of anxiety disorder ($N = 36$, 19F).	11–16	Cross-sectional ROI	Chatroom Interact Task	• Increased peer victimization mediated the association between right anterior insula activation during social rejection and suicidal ideation (controlling for depressive symptoms)
Perino et al. (38)	Adolescents with conduct problems ($N =$ 24, 12F)	13–18	Cross-sectional WB	Cyberball (observer role)	• Bullying scores associated with activation in bilateral amygdala, vStr, Insula, mPFC, PCC during exclusion>Inclusion

(Continued)

TABLE 1 Continued

Reference	Population	Ages	Design	Methods	Key results
Rappaport et al. (28)	Adolescents/Young adults $N = 56$ (26 F), 16 Major Depressive Disorder, 13 MDD NOS	16–20	Longitudinal assessment of victimization symptoms, ERP cross-sectional	Island getaway Doors task ERP study	• Early but not recent peer victimization associated with blunted reward response to social acceptance
Rudolph et al. (22)	Adolescents $N = 47$ (23 non-victimized, 24 victimized, all F)	14–17	Longitudinal peer victimization and symptoms assessment, cross-sectional imaging WB + ROI	Cyberball	• Exclusion> inclusion: Victimized > TD in dACC, amygdala, inferior fusiform gyrus • dACC, sgACC, Insula activation positively associated with higher internalizing symptoms • Association between activation in dACC/sgACC/Insula and internalizing symptoms was partially explaned by a link between activation in these regions and avoidance motivation for victims but not for non-victims
Rudolph et al. (39)	Adolescents $N = 43$ (all F)	14–16	Longitudinal assessment victimization, cross-sectional MRI	Emotion regulation task	• Victimization positively correlated with Amyg-R vlPFC functional connectivity in context negative emotion and negatively correlated with labeling accuracy during negative emotions • Victimization predicted amyg- R vlPFC connectivity in girls with high but not low rejection sensitivity—during ER task • Victimization predicted labeling accuracy in girls with high rejection sensitivity (but not low)
Schriber et al. (23)	Community based sample ($N = 166$, 90F)	16–18	Longitudinal (hostile school environment and familiar support assessment, MRI is cross-sectional and ROI)	Cyberball	• Hostile school environment directly associated with increased social deviance, mediated by activation in sgACC during exclusion contrast in Cyberball task • Activation in sgACC during social exclusion in task was associate with depressive symptoms, deviant behavior and hostile school environment • Family connectedness moderate the mediation model
Swartz et al. (40)	Adolescents from community sample ($N = 49$, 24F)	12–15	Cross-sectional WB + ROI	Emotional face matching task Bullying and victimization are self-report in Qualtrics	• Relational bullying predicted by enhanced activation amygdala during angry faces and reduced during fearful faces, as well as lower activation in rostral ACC to fearful faces • Relational peer victimization associated with lower amygdala to angry faces and fearful faces
Telzer et al. (31)	Adolescents ($N = 46$, all F); Chronically victimized $N = 25$, non-victimized $N = 21$	14–18	Longitudinal victimization and symptomatic assessment, cross-sectional imaging WB	Stoplight Task (twice, pre and post exclusion experiences at Cyberball, only second time inside scanner)	**a) Behavior:** No between-group behavioral differences (risky choices) before exclusion experiences, Vict>nonVict risky choices after exclusion **b) Imaging** • Risky decisions: Vict>nonVict: bilat amyg, vStr, OFC, mPFC, TPJ; Vic<NonVict SMA • Safe decisions: Vict>nonVict mPFC, dlPFC, vlPFC, dmPFC • pass outcomes: Vict>NonVict Striatum; Vict<NonVictbilat Insula **c) Association neural reactivity and antisocial behaviors:** • Risky decisions: bilat amyg, OFC, mPFC, dmPFC, pSTS • Safe decisions: mPFC, dmPFC, TPJ, pSTS, vlPFC, dlPFC

(Continued)

TABLE 1 Continued

Reference	Population	Ages	Design	Methods	Key results
					• Pass outcomes: reduced act in TPJ, STS, mPFC, dmPFC
Telzer et al. (24)	Adolescents ($N = 38$, all F) Chronically victimized $N = 21$, non-victimized $N = 17$	14–16	Longitudinal victimization and symptomatic assessment, cross-sectional imaging WB+ROI	Social evaluation task	**a) Behavior:** Peer victimization score associated with response time (in-group>out-group) and memory biases Vict>nonVict **b) Imaging:** • positive association between peer victimization scores and increased activation in-group vs. out-group peers in amygdala, vStr, fusiform gyrus, TPJ • This activation was associated with lower social self-esteem and increased internalizing and externalizing symptoms at 9-months follow-up • in-group>out-group activation in vStr, TPJ and amyg is positively associated with in-group memory bias, activation in fusiform negatively with in-group RT bias
de Water et al. (21)	Typically developing ($N = 52$, 17F), subgroup with peer ratings ($N = 31$, 17F)	12–16	Cross-sectional WB	Cyberball Popularity and acceptance rated by classroom peers	**Exclusion > Inclusion: Ball** • vlPFC **Inclusion:no ball> Inclusion: ball** • vlPFC **Exclusion> Inclusion: no Ball** • dACC **Effect own peer status (Exclusion > Inclusion: Ball)** • dACC More> Less accepted **Effect virtual player popularity** • rACC condition popularity interaction, increased activation by inclusion average popular& exclusion high popular players **Effect peer x virtual player popularity** • Exclusion by popular> exclusion by average enhanced VStr and mPFC in high vs. average popular participants
Will et al. (89)	Chronically rejected ($N = 18$, 6F) and highly accepted adolescents ($N = 25$, 12F)	12–15	Behavioral longitudinal assessments, imaging cross-sectional WB	Cyberball Dictator game	**a) Behavior:** no between group differences **b) Imaging** (equal treatment excludes>equal treatment includers) • Vict>non-Vict: R lateral PFC, R Caudate • Positive Association with perspective taking—dmPFC, across all participants • Positive Association with regulation problems—L Anterior Insula, pre-SMA/dACC, across all participants
Will et al. (25)	Chronically rejected ($N = 19$, 7F) and highly accepted adolescents ($N = 27$, 13F)	12–15	Behavioral longitudinal assessments, imaging cross-sectional WB	Cyberball	**a) Behavior** • Comparable distress after exclusion in Need Satisfaction questionnaire **b) Imaging** **Exclusion > Inclusion: ball** • Rejected > Accepted dACC **Incidental exclusion (Inclusion: no ball> Inclusion: ball)** • Rejected > Accepted preSMA, dACC, anterior PFC

WB, Whole Brain analysis; ROI, Region of Interest analysis; F, Female; Vict, victimized; TD, typically developing; PE, prediction error; R, right; L, left; ICA, Independent Component Analysis; PFC, prefrontal cortex; OFC, orbitofrontal cortex; dlPFC, dorsolateral prefrontal cortex; vlPFC, ventrolateral prefrontal cortex; dmPFC, dorsomedial prefrontal cortex; mPFC, medial prefrontal cortex; SMG, supramarginal gyrus; rACC, rostral ACC; dACC, dorsal anterior cingulate cortex; sgACC, subgenual anterior cingulate cortex; PCC, posterior cingulate cortex; IFC, inferior frontal cortex; SFG, superior frontal gyrus; MFG, medial frontal gyrus; vStr, ventral Striatum; SPL, superior parietal lobe; TPJ, temporo-pareital junction; STS, superior temporal sulcus; RT, reaction time; SMA, supplementary motor area; amyg, amygdala.

need to have a positive, stable and significant character. Consequently, social deprivation becomes a punishment and positive social contact a reinforcer (76). Experiences of peer victimization and bullying during adolescence can trigger the need to belong to a group, which is not satisfied and enhances the social monitoring system (including regions typically processing social salience, mentalization or affective processing) (24). This might suggest increased sensitivity and hypermonitoring of social signals, with the goal to identify potential avenues to recover the homeostatic state where those needs are met, increasing behavior that has the potential outcome of being accepted by the group.

Preliminary evidence supporting this suggestion comes from a recent study using a minimal group approach (24). In this case, participants were included in a group and shown pictures that could be (1) pictures of other members of the same group (in-group), (2) pictures from participants who are in a separate group (out-group) or (3) pictures of participants who have not been assigned to any group (neutral). After establishing the minimal group, female adolescents (aged 14–16) who suffered severe long-term victimization performed a social evaluation task inside the scanner, where they were asked to indicate to each of the facial stimuli simply whether they liked them or not. Afterwards, they were presented with images of new faces together with faces used in the establishment of the minimal group, and they had to indicate whether they had already seen that face or not. Victimized girls showed enhanced activation in regions supporting social monitoring processes including the amygdala, ventral striatum (vStr), fusiform gyrus and temporo-parietal junction (TPJ) during assessments of in-group vs. out-group pictures. The higher social sensitivity is suggested by the association between imaging and behavioral results, as activation in amygdala and vStr was associated with implicit behavior bias toward the in-group, with increased reaction time (RT) and memory to in-group pictures. These results would support hypothesis of enhanced sensitivity to social stimuli after experiences of peer victimization, results that are further strengthened by reported increases of cortical thickness in the fusiform gyrus of victims of bullying relative to non-victims (78). Thus, the structural and functional abnormalities in this key area might indicate enhanced sensitivity to facial expressions.

Other studies have utilized paradigms assessing facial emotion processing to investigate a potential enhanced sensitization to social stimuli after experiences of victimization. Such a task was used to investigate brain function in female adolescents victims of interpersonal abuse (aged 11–17), where participants were presented with neutral or fearful faces and they had to press for the gender of the face (20). The study found increased activation in the dorsal anterior cingulate gyrus (dACC) and the anterior insula during processing of fearful expressions in those participants who had a high exposure to victimization relative to those with low or no exposure to victimization experiences (20).

One of the most commonly used tasks to assess neural and behavioral responses to social exclusion is the Cyberball task (79). In that task, participants are typically induced to play an interactive ball-tossing game with 2 other players (real or pre-programmed). They usually play two rounds, one where they are included in the game and receive the ball about 1/3 of the trials, and a second round where they are ostensibly left out of the game by the other two players. By contrasting the inclusion vs. exclusion blocks the paradigm aims to investigate social exclusion.

Several recent studies have investigated the neural correlates of social rejection in victimized adolescents. Thus, victimized adolescents (14–17 years of age) whose status had been assessed longitudinally over the previous 7 years showed enhanced activation compared to non-victimized peers in the dACC, amygdala, and fusiform gyrus in the exclusion > inclusion comparison (22). In another study in a slightly younger sample (aged 12–15) participants had been assessed once a year on their social status in the classroom between the ages of 6 and 12 (25). The version of the task used allows for the comparison not only of exclusion vs. inclusion rounds, but also investigated the incidental exclusion events (inclusion: no ball vs. inclusion: receive ball). Despite their comparable levels of stress reported after social exclusion, participants who had experienced chronic rejection showed enhanced activation relative to those without such experiences in dACC during exclusion relative to inclusion rounds, as well as increased activation in dACC and anterior prefrontal cortex (PFC) during incidental exclusions (25).

Another cross-sectional study used the Cyberball task to investigate behavioral and neural responses to social exclusion as a function of the popularity and acceptance status of both participant and interacting partner (21). The authors differentiate between individuals who are accepted (i.e., whether they were liked or not in the classroom, rated by classroom peers) and popular (i.e., popularity rates, not necessarily the most liked in the classroom group). Thus, typically developing adolescents (12–16 years old) played a version of Cyberball in which both themselves and the opponents could be high or average accepted and high or average popular. Most prominently, exclusion enhanced activation relative to inclusion conditions in the dACC and the ventrolateral prefrontal cortex (vlPFC). Participants who were themselves more accepted showed enhanced activation in the dACC during exclusion (vs inclusion:no ball) condition. Participants' own popularity was positively associated with increased activation in vStr and medial prefrontal cortex (mPFC) when they were excluded by highly popular but not by average-popular virtual players (21). This contrasts with the results from the Will et al. study (25), where the enhanced activation in dACC during exclusion trials was observed in chronically rejected adolescents rather than in those without relevant rejection experiences. However, these studies differ in two key elements. One is that while Will et al. include chronically rejected adolescents, participants in the de Water

et al. study included a community sample of students who were high or average accepted/popular. In addition, this study required the knowledge about the social status of the opponent to be integrated in relation to one's own. In the case of highly accepted participants, this might have led to conflict detection, to be potentially resolved by the increased engagement of the dACC. Finally, it must be noted the difference in the contrast used, as Will et al. used the Exclusion>Inclusion Ball contrast whereas De Water et al. used the Exclusion > Inclusion No Ball contrast. This is an important differentiation that they include given that participants who are highly popular may show some antisocial behaviors.

The impact of experiences of bullying and peer victimization on neural responses to social rejection has also been investigated combining perfusion brain imaging methods and the Cyberball paradigm (35). Previous experiences of bullying were associated with increased perfusion in key regions for social pain processing including the subgenual anterior cingulate cortex (sgACC) and left inferior frontal cortex (IFC). Furthermore, the authors observed a positive association between perfusion in the left IFC and self-reported feelings of rejection. Thus, the evidence from this study provides further support to the hypothesis that experiences of bullying and peer victimization enhance sensitivity of social pain/social processing systems, potentially related to increased mentalizing and rumination processes that increase individual sensitivity to signals of social exclusion (35).

Not only altered regional activation has been described, but also abnormal functional connectivity. Thus, recent studies have shown that adolescent girls (14–16 years of age) exposed to high peer victimization had to either passively observe emotional faces, or choose one of the two words to label the emotion shown by the facial stimulus. The victimized group had stronger positive connectivity between right vlPFC and amygdala (indicative of worse emotion regulation abilities) in those cases with high sensitivity to social rejection (39). Similarly, altered functional connectivity was recently reported in a study using the Cyberball (across all exclusion and inclusion conditions) (36). Reduced connectivity between left amygdala and right insula as well as between left amygdala and ACC was observed in peer victimized adolescents relative to non-victimized peers (36). This raises the possibility that peer victimization may have disrupted the maturational process by which the mPFC downregulates amygdala activation when facing emotional stimuli (80–82).

The evidence also suggests that altered brain function is not only present in victims but also in those perpetrating bullying behaviors. In a recent study, a community sample of boys (aged 12–15) performed a face matching task inside the scanner and provided additional self-report measures on bullying and victimization behaviors (40). While high self-reported victimization was associated with high amygdala activation to both angry and fearful faces, bullying behaviors were associated with heightened amygdala response to angry faces and reduced response to fearful faces. In addition, increased activation in the genual ACC to fearful faces was associated with less bullying behaviors.

Similarly, Perino et al. (38) conducted a study in which adolescents with conduct problems (aged 13–18) watched a passive version of the Cyberball where others were excluded (bullied) or included during the game. Self-rated bullying behaviors were positively correlated with differences in activation in the mPFC, insula, vStr and amygdala when watching exclusion relative to inclusion rounds. While the authors interpreted these results as indicating that bullying is associated with neural activation during situations where social hierarchy cues are salient, these results could also be indicative of enhanced salience of emotionally relevant stimuli. In line with this, another study showed that enhanced activation during social exclusion blocks in the Cyberball task is associated with the presence of subsequent problematic behaviors (23). Thus, increased activation in the sgACC during exclusion compared to inclusion blocks was shown to mediate the association between past experiences of hostile school environment (experienced between 1 and 3 years before the scanning session) and subsequent social deviant behavior, measured 6 months after scanning session and defined as the presence of externalizing behaviors and affiliation with deviant peers (23). However, it is important to note that the presence of relevant family support modulated this effect, mitigating the impact of the hostile school environment (23).

In summary, the most recent evidence suggests that individuals who had been exposed to peer victimization or bullying might show hypervigilance or enhanced sensitivity to social stimuli and social valuation. This could be related to their need to belong to social groups, and enhance activation in salience networks including the sgACC, dACC, anterior insula, dorsomedial prefrontal cortex or amygdala, triggering potentially distressing emotional responses and increasing their risk to psychopathology.

Altered reinforcement learning and reward processing

An additional potential mechanism linked to the behavioral consequences of peer victimization is altered reinforcement learning and reward responses. The study from Cisler et al. (20) using reinforcement learning models provides interesting evidence supporting this hypothesis. They used an interpersonal trust game and a non-social three-armed bandit control task to investigate brain function in female adolescents victims of interpersonal abuse and how brain activity patterns might be associated with the persistence of PTSD symptoms (20). Participants (aged 11–17) had to choose one out of three people in whom to invest 10$, and they would receive either 20$ or

0$ in return from the investee. The non-social version of the game used pictures of three houses instead of human faces, and winning 20$ vs. 0$ was dependent on whether the door would open or not. This study found that compared to non-victimized adolescents, increased exposure to victimization was associated with increased activation in the dACC, insula as well as with reduced activation during those trials where the expected reward was not delivered (negative prediction errors) (20). This effect was observed both for social and non-social incentives, albeit with slightly stronger effect in the social context (20). Thus, victimized adolescents showed increased activation in key regions processing salience including the dACC, insula and amygdala during facial emotion processing, whereas during negative prediction errors these areas showed underactivation compared to healthy control individuals (20).

Similarly, using event related potentials (ERP), it has been shown that peer victimization in late adolescents (aged 16–20) was associated to blunted reward responses to monetary reward, but even more so to social rewards (28). Moreover, a recent EEG study in healthy young adults (18–25 years of age) showed the association between blunted reward response during feedback in a forced-choice task that was associated with self-reported relational victimization but not with physical victimization (26). Although not including brain imaging, it is worth mentioning the study from Lenow et al. (27). The authors used computational modeling analysis and a modified version of a trust game. In their study, female adolescents (12–16 years old) victim of early life interpersonal violence had to decide which of the 3 potential faces was most trustworthy (27). Not only did victimized girls had a lower learning rate than those in the control group, but learning rate was shown to interact with preference stochasticity, by which girls with higher learning rate also had higher stochasticity rates. Thus, victimized individuals might update the assigned reward value based in the most recent history, ignoring previous potentially contradictory evidence which might lead to situations where they are highly vulnerable. In addition, these results indicate random changes in their trustworthiness preferences which, while adaptive in highly volatile environments, might be suboptimal in more realistic, stable environments (27). These results are in line with recent evidence on adolescents with a history of maltreatment during an associative learning task (83), with initial beliefs of reward being more volatile and random, and reduced ability to learn about the reward pattern and to use the information about rewards adequately (83). While such reward beliefs could be adaptive in households with high volatility, they might in turn lead to behavioral difficulties. This study furthermore showed that problems in associative learning might partially account for the link between early adversity and behavioral problems.

Thus, victimized adolescents might show abnormal reward and punishment processing which might interfere with their ability to make decisions, both in the presence of monetary incentives but also on social contexts. Individuals subject to victimization and bullying experiences might therefore show reduced ability to learn from feedback, being less able to anticipate the consequences of their actions (for example, rewards or losses in a lab-based paradigm). In addition, they might experience stronger emotional reaction to losses/rewards, even at the time of the cue, leading to suboptimal decisions. Taken together, these results have interesting implications that might also provide some preliminary insight on the mechanisms by which victimization occurs and perpetuates. Their difficulties to learn from the previous reward history (27), and their blunted neural response in anticipation or response to reward (26, 28) or to the absence of reward when this is expected (20) might lead to behavioral adaptations increasing the individual vulnerability to internalizing symptoms like depression or anxiety, or perpetuating abusive or toxic relationships.

Peer victimization is associated with an increased need to recruit regulatory systems

The influence of emotions on social decision making processes is well established (84, 85). The enhanced sensitivity to social stimuli observed in adolescents who have experienced peer victimization might interfere with the implementation of self-regulation, controlled processes required when facing relevant social situations.

Studies investigating differences in impulsive and risky behavior have provided some support to this respect. Telzer et al. (31) investigated the association between previous experiences of victimization in female adolescents and subsequent impulsive, risky behavior. Participants (aged 14–18) performed a simulation driving task, where at the road crossings they saw a yellow traffic light and could make a risky decision and try to cross before the light went red or make a safe decision and stop. They played the task before and after a classic Cyberball game, the second time inside the scanner. While the two groups did not differ in their initial task performance, the group of chronically victimized girls showed higher proportion of risky decisions after the exclusion experience in the Cyberball. Furthermore, they had higher activation of cognitive control regions during "safe" choices (vlPFC and dorsolateral prefrontal cortex - dlPFC-) interpreted as a result of the need to make stronger effort to implement control over their behavior. During risky decisions on the other hand there was increased recruitment of affective sensitivity (amygdala, vStr and orbitofrontal cortex) and social cognition (superior temporal sulcus -STS- and TPJ) regions, which in addition were associated with aggressive behaviors in everyday life. The authors suggest that would be interpreted as taking risk behaviors to satisfy the need to belong, as a way to get peers acceptance. A recent study investigated the association between exposure to violence in adolescence (lifetime and in

the last year) and brain activation and performance during a modified version of a basic motor response inhibition task, the Go/NoGo task (29). Adolescents (9–14 years old) showed that increased exposure to violence (both types) was associated with reduced activation in key regions of inhibitory function network, including the dACC or the mPFC, which in the case of violence during last year also included superior parietal regions. Furthermore, the reduced activation in the dACC and posterior parietal areas was associated with progressive performance deterioration, with latency increasing with time on task. Hence, the authors suggest that exposure to violence affects basic self-regulation function. Similarly, a study in adolescents (15–17 years old) exposed to peer and parental verbal abuse showed that during the performance of an emotional Stroop task that included swearing words, there was enhanced activation during their swearing>neutral condition in the left vlPFC and enhanced functional connectivity between left vlPFC-hippocampus, which might be interpreted as a need to implement higher cognitive control due to the enhanced sensitivity to the aversive stimuli (30).

Some recent evidence suggests that the enhanced sensitivity to social stimuli may trigger the additional recruitment of key regulatory regions, such as the dlPFC to implement self-regulation processes. Different studies have shown that activation in this region varies in children and adolescents during social exclusion situations as a function of their previous experiences with school peers. Thus, a longitudinal study assessed whether primary school children (aged 8–12) were high- or low-preferred over 3 years prior to performing the Cyberball task in the scanner. Despite the lack of between-group differences in their reported distress after exclusion experiences, boys who were low relative to highly preferred showed increased activation in bilateral dlPFC and right supramarginal gyrus during exclusion (relative to inclusion:others) contrast (32). The authors suggest their finding of enhanced activation in the supramarginal gyrus could be associated with the reported involvement in this region in internal blame attribution (86). This would link with the idea that adolescents lack the adult cognitive biases to protect their self-esteem after experiences of social rejection, thus blaming themselves after such exclusion processes. Such interpretation is also consistent with the suggestion of enhanced recruitment of dlPFC regions being required to implement emotion or behavioral regulation processes. This is also in line with evidence from typically developing populations showing the role of the dlPFC to regulate emotions and aggressive responses after socio-emotional feedback (87, 88). Indeed, longitudinal increases in activation of the dlPFC have been associated with a reduction in aggressive behaviors especially after receiving negative social feedback (87, 88). Therefore, recent available evidence supports the role of the dlPFC as key to self-regulate responses after social exclusion experiences both in typically developing (87, 88) and vulnerable children (32).

A recent study used the Social Evaluation Paradigm (33), where adolescents were presented with pictures of same-aged peers and had to indicate (a) how they liked each of them and (b) how they anticipated each of those peers would rate (i.e., like) the participant back. Neural responses to the subset of pictures rated positively (i.e., liked) by the participants in (a) and where a positive evaluation was anticipated (i.e., the participant anticipated that peer would also like him/her back, high relational value), were compared to those that were positively rated in (a) but negatively in part (b) that is, the participant liked the peer but anticipated that peer would not like him back (low relational value) (33). There was a significant positive association between the number of trials with low perceived relational value and levels of self-reported experiences of peer victimization, as well as an association between peer victimization experiences and reduced functional connectivity in the contrast of low>high relational value between the VStr-bilateral IFC, mPFC and right putamen, together with increased functional connectivity between VStr-left inferior occipital cortex (33). Comparable effects were observed in a smaller sample of females with higher levels of peer victimization. As suggested by the authors, the altered connectivity patterns might be signaling an increased need to implement self-regulation processes, given the role of the IFC to downregulate striatal responses to appetitive/salient stimuli (33).

Another study provides further evidence on the additional recruitment of self-regulation regions required in chronically victimized adolescents (89). Participants (12–15 years old) experienced first the exclusion and inclusion phases of the Cyberball, to next perform a Dictator game, where they have to decide how to split some monetary units with those individuals who had previously accepted or rejected them during the Cyberball. This provided participants with the opportunity to retaliate and punish those who previously rejected them. Behaviorally, victimized and non-victimized participants did not differ on their unequal choice distribution for excluders. They also did not differ on brain regions engaged during punishment of excluders. However, during trials where they chose not to punish those who previously excluded them (compared to choices not to punish those who included them), chronically rejected individuals show enhanced recruitment of the lateral PFC and caudate, which highlights the need to recruit additional control regions to successfully implement self-regulation. In addition, positive associations between activation in this contrast in the anterior insula and dACC and parent-reported behavioral regulation problems were observed across all participants.

To sum up, individuals exposed to victimization experiences may need to engage behavioral and emotional self-regulation networks to a larger extent than non-victimized individuals in order to reduce the emotional distress or the aggressive reactions triggered by the increased sensitivity to social stimuli. However, whether this can be considered as part of a potential

resilience mechanism would need further research. It could be that those individuals who are not able to additionally engage self-regulation regions cannot refrain aggressive behaviors, thus becoming bully-victims. Given the scarce evidence on the topic and the instability in the trajectories of individuals in a bully-victim role (90), only longitudinal brain imaging studies can clarify this aspect.

Association with psychopathology: Vulnerability and modulating factors

The increased risk for internalizing and externalizing disorders subsequent to experiences of peer victimization has long been highlighted (3, 91–93). While both relational and physical victimization have been associated with increased externalizing problems, individuals subject to physical victimization typically show increased aggressive behaviors, whereas victims of relational victimization more often develop internalizing problems (3). Despite the idea that physical victimization might lead to more aggression [according to the "cycle of violence" theory (94)] and that relational or emotional victimization is more strongly associated with internalizing symptoms, a recent study shows this is not the case, with every type of victimization being similarly associated with general psychopathology and invariant of gender (95).

Recent studies have provided evidence on how changes in brain morphology may mediate the association between peer victimization and psychopathology. Thus, experiences of peer victimization have been associated with reduced volumes in the medial orbitofrontal cortex both in adolescents at high risk of psychosis and healthy participants (96), with structural abnormalities in the striatum which mediated the presence of generalized anxiety symptoms (97) and with volumetric changes in the nucleus accumbens mediating the increase in symptoms of depression during adolescence (98). Similarly, adults with symptoms of depression and history of bullying between 13 and 17 years of age showed altered white matter integrity, with increased fractional anisotropy measures in the superior corona radiata, which are hypothesized to be subsequent to hyperactivation in the fear network (99).

Some of the studies reviewed provide further evidence to help improve our knowledge of the mechanisms underlying such mediating role and report associations between altered function in key brain regions and psychopathological symptoms, internalizing in most of the cases. Thus, enhanced activation in salience and social processing regions in victimized adolescents (vs. non-victimized peers) during exclusion (vs. inclusion) conditions in the Cyberball task (dACC, sgACC and anterior insula) was significantly associated with increased internalizing symptoms (across all participants) (22). During a social valuation task, victimized girls showed enhanced activation in social monitoring networks including the amygdala, vStr, fusiform gyrus and TPJ during assessments of in-group vs. out-group pictures, activation that was inversely associated to self-esteem across schools years, and positively associated with internalizing and externalizing symptoms 9 months later (24). Thus, higher social sensitivity and need to belong increased vulnerability to subsequent psychopathology. In addition to alterations in local activity, positive functional connectivity between mPFC and amygdala was significantly associated with depressive symptoms (36). However, the authors report a reduced functional connectivity across both inclusion and exclusion blocks of the Cyberball task was observed between the left amygdala and the ACC. This raises the possibility that peer victimization may have disrupted the maturational process by which the mPFC downregulates amygdala activation when facing emotional stimuli (80–82). On the other hand, in the study from Lee et al. (30) the increased recruitment of vlPFC and enhanced vlPFC-hippocampus connectivity was associated with less severe anxiety and depression symptomatology, which they interpreted as a reduced impact at the psychopathological level in those able to implement stronger self-regulatory processes. However, there is also evidence of a lack of association between differences in brain activation and psychopathology, as it is the case of the study from Cisler et al. (20). In addition, the experience of peer victimization has been shown to mediate the association between enhanced activation in the anterior amygdala and suicidal ideation in adolescents with depression symptoms (37). Thus, peer victimization might not only be linked to negative mental health outcomes but also worse their severity or adverse consequences for individuals with mental health symptomatology.

It is important to note here the key mediator role that the coping strategies implemented by victimized adolescents might play. Thus, the association between activation in the dACC and sgACC and internalizing symptoms were partially mediated by avoidance strategies in victimized youth, whereas the association between insula activation and symptoms was significant overall and did not differ between the two groups (22). These findings are indeed in line with recent evidence on children who experienced early adverse threatening events, whose increased internalizing symptoms observed at adolescence were mediated by the use of avoidance strategies (100). Hence, these adverse, threatening social experiences might have sensitized neural systems processing social signals and increased the risk for internalizing psychopathology in those individuals who use maladaptive coping strategies.

While studies have mostly focused on the association between experiences of peer victimization and subsequent depression or anxiety symptoms, it is important to note that pre-existent psychopathology or symptoms might lead to increased risk for further victimization (91, 93). Similarly, the most recent studies show how other aspects such as increased sensitivity to social rejection or wariness that have also been typically associated as consequences of peer victimization experiences

can indeed constitute significant vulnerability factors. A recent study used the virtual school paradigm to investigate wariness as a potential vulnerability factor by which exposure to peer victimization might contribute to abnormal neural function (34). In this paradigm, participants receive positive, negative or neutral feedback from a virtual peer with a reputation of being "mean", "nice" or "unpredictable". The results show that in highly victimized children, wariness rated by the parents between ages 2 and 7 was associated with higher amygdala activation during unpredictable positive peer evaluation when they were 11 years old, which was associated with concurrent social anxiety (34). Thus, wariness in early childhood might constitute a vulnerability factor to subsequent social anxiety when faced with social stress situations. Similarly, adolescents girls exposed to high peer victimization showed stronger positive connectivity between right vlPFC and amygdala (indicative of worse emotion regulation abilities) only in those cases with high sensitivity to social rejection (contrast: facial emotion labeling vs. passive watching) (39). While the mediating role of high rejection sensitivity was detrimental in those cases who were exposed to high peer victimization, exposure high rejection sensitivity was associated to better emotion regulation (increased negative functional connectivity between amygdala and rVLPFC) in cases with low peer victimization. These results would suggest that individual differences might be protective or risk factors as a function of the environmental experiences of the individual.

Not only the presence of previous psychopathology has been shown as an additional factor of vulnerability to victimization (34, 91, 101). A similar role has been proposed for cognitive function. Thus, it has been recently suggested that the presence of cognitive deficits could be conceptualized as potential pre-existent risk factors, which could in addition complicate intervention response (102). Also deficits in response inhibition have been hypothesized as a potential vulnerability factor by which children who suffer peer victimization might display later bullying behaviors (103), and executive function measures have been suggested to moderate the association between early victimization and subsequent aggressive behaviors (104). Therefore, community studies would be helpful in order to clarify when and how this enhanced sensitivity to social stimuli and social rejection appear, as well as the altered reinforcement learning. We would be able to detect vulnerable individuals early in time, which might help to provide them with the potential support or tools to better navigate their social environments at a sensitive developmental phase. School based intervention programs on social skills could be feasible cost-effective possibilities to address this.

On the other hand, the previous experience with supportive others (family, friends) might serve a protective function, mitigating the deleterious impact of peer victimization experiences (23, 105–107). Recent evidence has also shown that the association between cyberbullying and well-being in adolescence might be influenced by the level of social connectedness (108). One potential hypothesis is that previous experiences with supportive social networks might provide some sense of belonging, fulfilling this need to some extent. It might also serve as scaffolding for the development of potential defensive cognitive biases, similar to those observed in adults. Thus, the discrepancy between the negative information received by the peer rejection and the image of the self is resolved in adults by cognitive biases such as externalizing the negative feedback received or updating their opinions of the peers after their rejection (109–111). These strategies allow them to protect their self-view after experiences of peer rejection, helping reduce or minimize their negative impact, severity or duration. Such strategies are not yet in place in children and adolescents, as they show a tendency to internalize the ground for peer rejection when that happens and to maintain their views of peers after these have rejected them (110). Some preliminary evidence suggests the right supramarginal gyrus as enhanced in adolescents who experience social rejection (32), region that has been suggested to be involved in internal blame attribution. Intriguingly, recent evidence using social networks analyses in combination with structural brain imaging has shown a higher degree of similarity in brain morphology of adolescents who are close friends than in unrelated distant friends (112). Thus, studies investigating the potential role of peer support in the mitigation of the adverse impact of experiences of peer victimization at the neural level would be needed.

There are some potentially relevant factors that are however typically not reported and should be considered in light of recent available evidence, such as race or cultural background of the community, which may influence the neurodevelopment of the social monitoring system and in turn contribute to the increased vulnerability to negative peer interactions. An interesting study has shown that persistent experiences of social discrimination also have long term consequences that affect social behaviors differently depending on race (113). White and Black South Africans who had experienced the Apartheid were exposed to clips depicting victims (forgiving/unforgiving) and perpetrators (apologetic/unapologetic) of apartheid crimes. While previous experiences of social adversity were associated with reduced compassion across participants, social discrimination had differential effects on neural activation, potentially due to the fact of different types of social discrimination experienced. Thus, Black participants experienced social discrimination due to race reasons and this was associated with increased activation in social saliency and pain processing networks, whereas White participants who experienced social discrimination mostly due to income level, weight or gender reasons showed undifferentiated amygdala activation. This suggests that not only race but also the structural and cultural differences of the societies leave their imprint at the neural level, at least partially shaping the processing of social stimuli and therefore determining socio-emotional development. While

these structural differences at societal level are difficult to tackle, increased awareness of their impact should help improve our understanding on how the social context of the individual determines his socio-emotional development, potentially increasing their vulnerability to peer victimization or bullying experiences.

Conclusions

The most recent evidence on the neurobiological correlates of the social and emotional impact of peer victimization and bullying experiences suggests that these experiences increase an already sharpened individual sensitivity to social exclusion or rejection, enhancing neural responses to social stimuli and social valuation processes. This enhanced neural response to social stimuli might require the additional recruitment of self-regulation networks in order to successfully implement controlled responses to emotions and behaviors, which might in turn contribute to the development of deviant behavioral adaptations and psychopathology. In addition, altered reward and reinforcement learning processes may contribute to the unsuccessful behavioral adaptation and perpetuate the display of inadequate behaviors.

The studies reviewed here provide some insights on the potential mechanisms by which peer victimization negatively impact socio-emotional development. While the presence of some factors like familiar or peer support might mitigate these negative effects, the presence of risk factors such as pre-existent psychopathology or enhanced sensitivity to rejection may increase their vulnerability to further abuse or victimization. However, the role of other factors such as age, gender, frequency and intensity of the peer victimization event(s), previous positive and negative social experiences or the presence of potential school support which are likely to moderate the consequences of victimization has yet to be investigated.

One key aspect to consider is the cross-sectional character of the brain imaging data here reported. While a significant strength of some of the studies reviewed includes some longitudinal report on victimization levels, with varied sources of information and not restricted to self-informant (22–25, 28, 31, 32, 34, 39, 89), the imaging data has typically a cross-sectional nature. It is therefore not possible neither to unequivocally disentangle the factors driving the association between experiences of peer victimization and the reported altered brain structure, function or connectivity, nor to exclude that just as it happens with psychopathology, the pre-existence of abnormal brain structure or function might constitute a potential risk factor that increases the likelihood of becoming subject to peer victimization. Studies where negative peer experiences are assessed retrospectively have the associated risk of potential recall bias in terms of the timing, frequency and severity of the recalled event, and therefore may not accurately identify the potential impact at different stages of brain development, where sensitive periods might confer differential risks. However, it is only by collecting brain imaging data in parallel that we may identify the relative contribution of these experiences and the identification of factors that may contribute to individual's vulnerability and resilience. Only by conducting longitudinal, population-based studies can we improve our knowledge on these areas.

Particularly interesting are the findings on impaired reinforcement learning and reward processing. Conducting further research in this area has the potential to improve our understanding on the mechanisms by which these negative early experiences can increase the risk for psychopathology, especially internalizing symptoms, and to perpetuate behaviors that expose the individuals to further victimization. Thus, future studies should better delineate the extend and variability of these difficulties and the potential benefits of different interventions. These could focus on generating alternative behavioral patterns and identifying potential cognitive distortions, using behavioral management or problem-solving techniques.

The specific characteristics of the experience may also differentially impact on brain systems. Models investigating the impact of early experiences on development have taken different approaches. While some have considered that adverse experiences might have a cumulative effect (114), such consideration would assume a comparable impact of the different events due to similar dysregulation on the stress-response system. Other models have suggested that the type of event experienced would influence the individual's stress response leading to different behavioral and clinical presentations (115). Dimensional models propose the differential impact of early adverse events as a function of the type of experience, differentiating between neglect/deprivation and abuse/threat (10, 116, 117). While it might wise to assume that these models could also be applicable to experiences of peer victimization, the reviewed evidence is not unequivocal in this respect and further research is required to test whether and how such models would apply depending on the type of experience.

Two areas of research are promising fields that might help to improve our understanding on the neural mechanisms of peer victimization in adolescence. The first one is the use of connectomics. This method uses graph theory to help quantify, visualize and improve our understanding of brain network organization, especially in terms of the whole-brain integration of structural and functional connectivity at the system level (118). It conceives of the brain as a network [the 'connectome', (119)], composed by a set of nodes (brain regions) linked by edges (axonal projections) (120, 121). The term "developmental miswiring" has been coined to refer to the disruption of normative development, which might increase individual vulnerability to neuropsychiatric disorders (122). While there is some preliminary evidence on how network reconfiguration might modulate resilience

or susceptibility to psychopathology (123), studies specifically addressing the impact of peer victimization on neural networks might significant contribute to improve our understanding on vulnerability and resilience processes. In addition, the use of graph theory methods constitutes a promising avenue to implement social network analyses (112). Such studies have the potential to improve our understanding on the mechanisms by which social, family or peer support might contribute to protect or mitigate the adverse effects of peer victimization experiences. However, the available evidece to date has a cross-sectional nature and therefore further evidence including longitudinal studies is currently required.

It is finally important to mention that assessing the impact of victimization, bullying or social exclusion/rejection processes in adolescence in the scanner necessarily implies a virtual interaction. Although this might on one hand reduce the generalization of the findings into real life situations, we have to consider how much media use, and especially in situations like the current COVID pandemic might influence the way adolescents relate and present to others using social media (124). An increased online contact, which is difficult to control together with the developmental need of high social contact with peers increases the risk of been cyberbullied. Thus, it is important to highlight the need to further investigate cyberbullying and the mechanisms underlying it adverse consequences (125). It therefore constitutes a relevant aspect to be further studied, given that social media use involves key processes that are still under development during childhood and adolescence including reward and emotion-based processing, emotion regulation or mentalizing. Improved knowledge of the medium and long-term impact on these processes might be crucial to investigate well-being and to identify vulnerable individuals and provide measures to protect them from the potential negative consequences (124).

This selective review has focused on the neural and cognitive mechanisms by which social interactions and socio-emotional development may be affected after peer victimization and bullying experiences. However, it cannot be overlooked that other consequences are also commonly observed such as altered inflammatory and immune responses or somatic symptoms, to mention some. In conclusion, the most recent evidence on experiences of victimization and bullying during adolescence suggest that, just as the impact of early adverse events, they have severe and long-lasting consequences on socio-emotional development, interfering with typical neural development. The consequences might however differ depending on a number of factors including the age and gender of the participant at the time, or the type, intensity, duration or circumstances of the adverse event. Finally, individual differences in vulnerability and resilience should be considered. An improved understanding of the neurobiological consequences of exposure to such situations might help identify individualized intervention targets.

Author contributions

AC: conceptualization, literature search, and manuscript writing.

Funding

The author was supported by funding from the Jacobs Center for Productive Youth Development to the Department of Economics, University of Zurich, for a separate project.

Conflict of interest

The author declares that the research was conducted in the absence of any commercial or financial relationships that could be construed as a potential conflict of interest.

Publisher's note

References

1. Guyer AE, Jarcho JM (2018). Neuroscience and peer relations. In: *Handbook of Peer Interactions, Relationships, and Groups, 2nd ed*. New York, NY: The Guilford Press. p. 177–199

2. Nelson EE, Jarcho JM, Guyer AE. Social re-orientation and brain development: An expanded and updated view. *Dev Cogn Neurosci.* (2016) 17:118–27. doi: 10.1016/j.dcn.2015.12.008

3. Casper DM, Card NA. Overt and relational victimization: a meta-analytic review of their overlap and associations with social-psychological adjustment. *Child Dev.* (2017) 88:466–83. doi: 10.1111/cdev.12621

4. Bradshaw CP, Sawyer AL, O'Brennan LM. Bullying and peer victimization at school: perceptual differences between students and school staff. *School Psych Rev.* (2007) 36:361–82. doi: 10.1080/02796015.2007.12087929

5. Modecki KL, Minchin J, Harbaugh AG, Guerra NG, Runions KC. Bullying prevalence across contexts: a meta-analysis measuring cyber and traditional bullying. *J Adolesc Health.* (2014) 55:602–11. doi: 10.1016/j.jadohealth.2014.06.007

6. Gur RE, Moore TM, Rosen AFG, Barzilay R, Roalf DR, Calkins ME, et al. Burden of environmental adversity associated with psychopathology, maturation, and brain behavior parameters in youths. *JAMA Psychiatry.* (2019) 76:966. doi: 10.1001/jamapsychiatry.2019.0943

7. Lansford JE, Godwin J, McMahon RJ, Crowley M, Pettit GS, Bates JE, et al. Early physical abuse and adult outcomes. *Pediatrics.* (2021) 147:e20200873. doi: 10.1542/peds.2020-0873

8. McLaughlin KA, Greif Green J, Gruber MJ, Sampson NA, Zaslavsky AM, Kessler RC, et al. Childhood adversities and first onset of psychiatric disorders in a national sample of US adolescents. *Arch Gen Psychiatry.* (2012) 69:1151. doi: 10.1001/archgenpsychiatry.2011.2277

9. Nusslock R, Miller GE. Early-life adversity and physical and emotional health across the lifespan: a neuroimmune network hypothesis. *Biol Psychiatry.* (2016) 80:23–32. doi: 10.1016/j.biopsych.2015.05.017

10. Teicher MH, Samson JA, Anderson CM, Ohashi K. The effects of childhood maltreatment on brain structure, function and connectivity. *Nat Rev Neurosci.* (2016) 17:652–66. doi: 10.1038/nrn.2016.111

11. Brunstein Klomek A, Marrocco F, Kleinman M, Schonfeld IS, Gould MS. Bullying, depression, and suicidality in adolescents. *J Am Acad Child Adolesc Psychiatry.* (2007) 46:40–9. doi: 10.1097/01.chi.0000242237.84925.18

12. Copeland WE, Wolke D, Angold A, Costello EJ. Adult psychiatric outcomes of bullying and being bullied by peers in childhood and adolescence. *JAMA Psychiatry.* (2013) 70:419. doi: 10.1001/jamapsychiatry.2013.504

13. Espejo-Siles R, Zych I, Llorent VJ. Empathy, social and emotional competencies, bullying perpetration and victimization as longitudinal predictors of somatic symptoms in adolescence. *J Affect Disord.* (2020) 271:145–51. doi: 10.1016/j.jad.2020.03.071

14. Giletta M, Slavich GM, Rudolph KD, Hastings PD, Nock MK, Prinstein MJ, et al. Peer victimization predicts heightened inflammatory reactivity to social stress in cognitively vulnerable adolescents. *J Child Psychol Psychiatry.* (2018) 59:129–39. doi: 10.1111/jcpp.12804

15. McDougall P, Vaillancourt T. Long-term adult outcomes of peer victimization in childhood and adolescence: Pathways to adjustment and maladjustment. *Am Psychol.* (2015) 70:300–10. doi: 10.1037/a0039174

16. Schacter HL. Effects of peer victimization on child and adolescent physical health. *Pediatrics.* (2021) 147:e2020003434. doi: 10.1542/peds.2020-003434

17. Takizawa R, Maughan B, Arseneault L. Adult health outcomes of childhood bullying victimization: Evidence from a five-decade longitudinal British birth cohort. *Am J Psychiatry.* (2014) 171:777–84. doi: 10.1176/appi.ajp.2014.13101401

18. Wolke D, Copeland WE, Angold A, Costello EJ. Impact of bullying in childhood on adult health, wealth, crime, and social outcomes. *Psychol Sci.* (2013) 24:1958–70. doi: 10.1177/0956797613481608

19. Wolke D, Lereya ST. Long-term effects of bullying. *Arch Dis Child.* (2015) 100:879–85. doi: 10.1136/archdischild-2014-306667

20. Cisler JM, Esbensen K, Sellnow K, Ross M, Weaver S, Sartin-Tarm A, et al. Differential roles of the salience network during prediction error encoding and facial emotion processing among female adolescent assault victims. *Biol Psychiatry Cogn Neurosci Neuroimag.* (2019) 4:371–80. doi: 10.1016/j.bpsc.2018.08.014

21. de Water E, Mies GW, Ma I, Mennes M, Cillessen AHN, Scheres A. Neural responses to social exclusion in adolescents: effects of peer status. *Cortex.* (2017) 92:32–43. doi: 10.1016/j.cortex.2017.02.018

22. Rudolph KD, Miernicki ME, Troop-Gordon W, Davis MM, Telzer EH. Adding insult to injury: Neural sensitivity to social exclusion is associated with internalizing symptoms in chronically peer-victimized girls. *Soc Cogn Affect Neurosci.* (2016) 11:829–42. doi: 10.1093/scan/nsw021

23. Schriber RA, Rogers CR, Ferrer E, Conger RD, Robins RW, Hastings PD, et al. Do hostile school environments promote social deviance by shaping neural responses to social exclusion? *J Res Adolesc.* (2018) 28:103–20. doi: 10.1111/jora.12340

24. Telzer EH, Fowler CH, Davis MM, Rudolph KD. Hungry for inclusion: Exposure to peer victimization and heightened social monitoring in adolescent girls. *Dev Psychopathol.* (2019) 1–14. doi: 10.1017/S0954579419001433

25. Will, G-. J, van Lier, P. A. C, Crone, E. A, and Güroglu, B. (2016). Chronic childhood peer rejection is associated with heightened neural responses to social exclusion during adolescence. *J Abnormal Child Psychol.* 44, 43–55. doi: 10.1007/s10802-015-9983-0

26. Ethridge P, Sandre A, Dirks MA, Weinberg A. Past-year relational victimization is associated with a blunted neural response to rewards in emerging adults. *Soc Cogn Affect Neurosci.* (2018) 13:1259–67. doi: 10.1093/scan/nsy091

27. Lenow J, Cisler J, Bush K. Altered trust learning mechanisms among female adolescent victims of interpersonal violence. *J Interpers Violence.* (2018) 33:159–79. doi: 10.1177/0886260515604411

28. Rappaport BI, Hennefield L, Kujawa A, Arfer KB, Kelly D, Kappenman ES, et al. Peer Victimization and dysfunctional reward processing: erp and behavioral responses to social and monetary rewards. *Front Behav Neurosci.* (2019) 13:120. doi: 10.3389/fnbeh.2019.00120

29. Cará VM, Esper NB, de Azeredo LA, Iochpe V, Dalfovo NP, Santos RC, et al. An fMRI study of inhibitory control and the effects of exposure to violence in Latin-American early adolescents: Alterations in frontoparietal activation and performance. *Soc Cogn Affect Neurosci.* (2019) 14:1097–107. doi: 10.1093/scan/nsz092

30. Lee SW, Choi J, Lee JS, Yoo JH, Kim KW, Kim D, et al. Altered function of ventrolateral prefrontal cortex in adolescents with peer verbal abuse history. *Psychiatry Invest.* (2017) 14, 441. doi: 10.4306/pi.2017.14.4.441

31. Telzer EH, Miernicki ME, Rudolph KD. Chronic peer victimization heightens neural sensitivity to risk taking. *Dev Psychopathol.* (2018) 30:13–26. doi: 10.1017/S0954579417000438

32. Asscheman JS, Koot S, Ma I, Buil JM, Krabbendam L, Cillessen AHN, et al. Heightened neural sensitivity to social exclusion in boys with a history of low peer preference during primary school. *Dev Cogn Neurosci.* (2019) 38:100673. doi: 10.1016/j.dcn.2019.100673

33. Fowler CH, Lin LC, Rudolph KD, Telzer EH. Like me back: neural correlates of low perceived relational value in peer victimized youth. *J Res Adolesc.* (2021) 31:435–50. doi: 10.1111/jora.12615

34. Jarcho JM, Grossman HY, Guyer AE, Quarmley M, Smith AR, Fox NA, et al. Connecting childhood wariness to adolescent social anxiety through the brain and peer experiences. *J Abnorm Child Psychol.* (2019) 47:1153–64. doi: 10.1007/s10802-019-00543-4

35. Kiefer M, Sim EJ, Heil S, Brown R, Herrnberger B, Spitzer M, et al. Neural signatures of bullying experience and social rejection in teenagers. *PLOS ONE.* (2021) 16, e0255681. doi: 10.1371/journal.pone.0255681

36. McIver TA, Bosma RL, Goegan S, Sandre A, Klassen J, Chiarella J, et al. Functional connectivity across social inclusion and exclusion is related to peer victimization and depressive symptoms in young adults. *J Affect Disord.* (2019) 253:366–75. doi: 10.1016/j.jad.2019.04.085

37. Oppenheimer CW, Silk JS, Lee KH, Dahl RE, Forbes E, Ryan N, et al. Suicidal ideation among anxious youth: a preliminary investigation of the role of neural processing of social rejection in interaction with real world negative social experiences. *Child Psychiatry Hum Dev.* (2020) 51:163–73. doi: 10.1007/s10578-019-00920-6

38. Perino MT, Guassi Moreira JF, Telzer EH. Links between adolescent bullying and neural activation to viewing social exclusion. *Cogn Affect Behav NeuroSci.* (2019) 19:1467–78. doi: 10.3758/s13415-019-00739-7

39. Rudolph KD, Skymba HV, Modi HH, Davis MM, Yan Sze W, Rosswurm CP, et al. How does peer adversity "Get inside the Brain?" Adolescent girls' differential susceptibility to neural dysregulation of emotion following victimization. *Dev Psychobiol.* (2021) 63:481–495. doi: 10.1002/dev.22022

40. Swartz JR, Carranza AF, Knodt AR. Amygdala activity to angry and fearful faces relates to bullying and victimization in adolescents. *Soc Cogn Affect Neurosci.* (2019) 14:1027–35. doi: 10.1093/scan/nsz084

41. Lam CB, McHale SM, Crouter AC. Time with peers from middle childhood to late adolescence: developmental course and adjustment correlates. *Child Dev.* (2014) 85:1677–93. doi: 10.1111/cdev.12235

42. Bouhours L, Camarda A, Ernst M, Osmont A, Borst G, Cassotti M, et al. How does social evaluation influence hot and cool inhibitory control in adolescence? *PLoS ONE.* (2021) 16:e0257753. doi: 10.1371/journal.pone.0257753

43. Chein J, Albert D, O'Brien L, Uckert K, Steinberg L. Peers increase adolescent risk taking by enhancing activity in the brain's reward circuitry. *Dev Sci.* (2011) 14:F1–10. doi: 10.1111/j.1467-7687.2010.01035.x

44. Gardner M, Steinberg L. Peer influence on risk taking, risk preference, and risky decision making in adolescence and adulthood: an experimental study. *Dev Psychol.* (2005) 41:625–35. doi: 10.1037/0012-1649.41.4.625

45. Güroglu B. Adolescent brain in a social world: unravelling the positive power of peers from a neurobehavioral perspective. *Eur J Dev Psychol.* (2021) 18:471–93. doi: 10.1080/17405629.2020.1813101

46. Guassi Moreira JF, Telzer EH. Mother still knows best: Maternal influence uniquely modulates adolescent reward sensitivity during risk taking. *Dev Sci.* (2018) 21:e12484. doi: 10.1111/desc.12484

47. Telzer EH, Ichien NT, Qu Y. Mothers know best: Redirecting adolescent reward sensitivity toward safe behavior during risk taking. *Soc Cogn Affect Neurosci.* (2015) 10:1383–91. doi: 10.1093/scan/nsv026

48. Blakemore SJ, Burnett S, Dahl RE. The role of puberty in the developing adolescent brain. *Hum Brain Mapp.* (2010) 31:926–33. doi: 10.1002/hbm.21052

49. Casey BJ, Galvan A, Hare TA. Changes in cerebral functional organization during cognitive development. *Curr Opin Neurobiol.* (2005) 15:239–44. doi: 10.1016/j.conb.2005.03.012

50. Casey BJ, Jones RM, Hare TA. The adolescent brain. *Ann N Y Acad Sci.* (2008) 1124:111–26. doi: 10.1196/annals.1440.010

51. Geier C, Luna B. The maturation of incentive processing and cognitive control. *Pharmacol Biochem Behav.* (2009) 93:212–21. doi: 10.1016/j.pbb.2009.01.021

52. Ladouceur CD, Kerestes R, Schlund MW, Shirtcliff EA, Lee Y, Dahl RE, et al. Neural systems underlying reward cue processing in early adolescence: The role of puberty and pubertal hormones. *Psychoneuroendocrinology.* (2019) 102:281–91. doi: 10.1016/j.psyneuen.2018.12.016

53. Luna B. Developmental changes in cognitive control through adolescence. *Adv Child Dev Behav.* (2009) 37:233–78. doi: 10.1016/S0065-2407(09)03706-9

54. Shaw P, Kabani NJ, Lerch JP, Eckstrand K, Lenroot R, Gogtay N, et al. Neurodevelopmental trajectories of the human cerebral cortex. *J NeuroSci.* (2008) 28:3586–94. doi: 10.1523/JNEUROSCI.5309-07.2008

55. Somerville LH, Casey BJ. Developmental neurobiology of cognitive control and motivational systems. *Curr Opin Neurobiol.* (2010) 20:236–41. doi: 10.1016/j.conb.2010.01.006

56. Sowell ER. Longitudinal mapping of cortical thickness and brain growth in normal children. *J NeuroSci.* (2004) 24:8223–31. doi: 10.1523/JNEUROSCI.1798-04.2004

57. Christakou A. Present simple and continuous: Emergence of self-regulation and contextual sophistication in adolescent decision-making. *Neuropsychologia.* (2014) 65:302–12. doi: 10.1016/j.neuropsychologia.2014.09.008

58. Crone EA, Dahl RE. Understanding adolescence as a period of social-affective engagement and goal flexibility. *Nat Rev Neurosci.* (2012) 13:636–50. doi: 10.1038/nrn3313

59. Callaghan BL, Tottenham N. The neuro-environmental loop of plasticity: a cross-species analysis of parental effects on emotion circuitry development following typical and adverse caregiving. *Neuropsychopharmacology.* (2016) 41:163–76. doi: 10.1038/npp.2015.204

60. Luby JL, Baram TZ, Rogers CE, Barch DM. Neurodevelopmental optimization after early-life adversity: cross-species studies to elucidate sensitive periods and brain mechanisms to inform early intervention. *Trends NeuroScis.* (2020) 43:744–51. doi: 10.1016/j.tins.2020.08.001

61. Mackes NK, Golm D, Sarkar S, Kumsta R, Rutter M, Fairchild G, et al. Early childhood deprivation is associated with alterations in adult brain structure despite subsequent environmental enrichment. *Proc Natl Acad Sci.* (2020) 117:641–649. doi: 10.1073/pnas.1911264116

62. Casey BJ, Getz S, Galvan A. The adolescent brain. *Dev Rev.* (2008) 28:62–77. doi: 10.1016/j.dr.2007.08.003

63. Galvan A, Hare TA, Parra CE, Penn J, Voss H, Glover G, et al. Earlier development of the accumbens relative to orbitofrontal cortex might underlie risk-taking behavior in adolescents. *J Neurosci.* (2006) 26:6885–92. doi: 10.1523/JNEUROSCI.1062-06.2006

64. Qu Y, Galvan A, Fuligni AJ, Lieberman MD, Telzer EH. Longitudinal changes in prefrontal cortex activation underlie declines in adolescent risk taking. *J NeuroSci.* (2015) 35:11308–14. doi: 10.1523/JNEUROSCI.1553-15.2015

65. Steinberg L. A dual systems model of adolescent risk-taking. *Dev Psychobiol.* (2010) 52:216–24. doi: 10.1002/dev.20445

66. Roberts AG, Lopez-Duran NL. Developmental influences on stress response systems: Implications for psychopathology vulnerability in adolescence. *Compr Psychiatry.* (2019) 88:9–21. doi: 10.1016/j.comppsych.2018.10.008

67. Merikangas KR, He J, Burstein M, Swanson SA, Avenevoli S, Cui L, et al. Lifetime Prevalence of Mental Disorders in U.S. Adolescents: Results from the National Comorbidity Survey Replication–Adolescent Supplement (NCS-A). *J Am Acad Child Adolesc Psychiatry*. (2010) 49:980–89. doi: 10.1016/j.jaac.2010.05.017

68. Ochsner KN, Gross JJ. The cognitive control of emotion. *Trends Cogn Sci.* (2005) 9:242–9. doi: 10.1016/j.tics.2005.03.010

69. Gabard-Durnam LJ, Flannery J, Goff B, Gee DG, Humphreys KL, Telzer E, et al. The development of human amygdala functional connectivity at rest from 4 to 23years: a cross-sectional study. *Neuroimage.* (2014) 95:193–207. doi: 10.1016/j.neuroimage.2014.03.038

70. Gee DG, Humphreys KL, Flannery J, Goff B, Telzer EH, Shapiro M, et al. A Developmental shift from positive to negative connectivity in human amygdala-prefrontal circuitry. *J NeuroSci.* (2013) 33:4584–93. doi: 10.1523/JNEUROSCI.3446-12.2013

71. Spear LP. Heightened stress responsivity and emotional reactivity during pubertal maturation: Implications for psychopathology. *Dev Psychopathol.* (2009) 21:87–97. doi: 10.1017/S0954579409000066

72. Romeo RD. The teenage brain: the stress response and the adolescent brain. *Curr Dir Psychol Sci.* (2013) 22:140–5. doi: 10.1177/0963721413475445

73. González-Cabrera J, Calvete E, León-Mejía A, Pérez-Sancho C, Peinado JM. Relationship between cyberbullying roles, cortisol secretion and psychological stress. *Comput Human Behav.* (2017) 70:153–60. doi: 10.1016/j.chb.2016.12.054

74. du Plessis MR, Smeekens S, Cillessen AHN, Whittle S, Güroglu B. Bullying the brain? Longitudinal links between childhood peer victimization, cortisol, and adolescent brain structure. *Front Psychol.* (2019) 9:2706. doi: 10.3389/fpsyg.2018.02706

75. Leary MR, Baumeister RF. The nature and function of self-esteem: sociometer theory. *Adv Exp Soc Psychol.* (2000) 32:1–62. doi: 10.1016/S0065-2601(00)80003-9

76. Baumeister RF, Leary MR. The need to belong: desire for interpersonal attachments as a fundamental human motivation. *Psychol Bull.* (1995) 117:497–529. doi: 10.1037/0033-2909.117.3.497

77. Over H. The origins of belonging: social motivation in infants and young children. *Philos Transac Royal Soc B Biol Sci.* (2016) 371:20150072. doi: 10.1098/rstb.2015.0072

78. Muetzel RL, Mulder RH, Lamballais S, Cortes Hidalgo AP, Jansen P, Güroglu B, et al. Frequent bullying involvement and brain morphology in children. *Front Psychiatry.* (2019) 10:696. doi: 10.3389/fpsyt.2019.00696

79. Williams KD, Jarvis B. Cyberball: A program for use in research on interpersonal ostracism and acceptance. *Behav Res Methods.* (2006) 38:174–80. doi: 10.3758/BF03192765

80. Callaghan BL, Gee DG, Gabard-Durnam L, Telzer EH, Humphreys KL, Goff B, et al. Decreased amygdala reactivity to parent cues protects against anxiety following early adversity: an examination across 3 years. *Biol Psychiatry Cogn NeuroSci Neuroimag.* (2019) 4:664–71. doi: 10.1016/j.bpsc.2019.02.001

81. Gee DG, Gabard-Durnam L, Telzer EH, Humphreys KL, Goff B, Shapiro M, et al. Maternal buffering of human amygdala-prefrontal circuitry during childhood but not during adolescence. *Psychol Sci.* (2014) 25:2067–78. doi: 10.1177/0956797614550878

82. Gee DG, Gabard-Durnam LJ, Flannery J, Goff B, Humphreys KL, Telzer EH, et al. Early developmental emergence of human amygdala-prefrontal connectivity after maternal deprivation. *Proc Nat Acad Sci.* (2013) 110:15638–43. doi: 10.1073/pnas.1307893110

83. Hanson JL, van den Bos W, Roeber BJ, Rudolph KD, Davidson RJ, Pollak SD, et al. Early adversity and learning: Implications for typical and atypical behavioral development. *J Child Psychol Psychiatry.* (2017) 58:770–8. doi: 10.1111/jcpp.12694

84. Collins AGE, Shenhav A. Advances in modeling learning and decision-making in neuroscience. *Neuropsychopharmacology.* (2022) 47:104–18. doi: 10.1038/s41386-021-01126-y

85. Lerner JS, Li Y, Valdesolo P, Kassam KS. Emotion and Decision Making. *Annu Rev Psychol.* (2015) 66:799–823. doi: 10.1146/annurev-psych-010213-115043

86. Seidel EM, Eickhoff SB, Kellermann T, Schneider F, Gur RC, Habel U, et al. Who is to blame? Neural correlates of causal attribution in social situations. *Social NeuroSci.* (2010) 5, 335–50. doi: 10.1080/17470911003615997

87. Achterberg M, van Duijvenvoorde ACK, van der Meulen M, Bakermans-Kranenburg MJ, Crone EA. Heritability of aggression following social evaluation in middle childhood: an fMRI study. *Hum Brain Mapp.* (2018) 39:2828–41. doi: 10.1002/hbm.24043

88. Achterberg M, van Duijvenvoorde ACK, van IJzendoorn MH, Bakermans-Kranenburg MJ, Crone EA. Longitudinal changes in DLPFC activation during childhood are related to decreased aggression following social rejection. *Proc Natl Acad Sci.* (2020) 117, 8602–10. doi: 10.1073/pnas.1915124117

89. Will GJ, Crone EA, van Lier PAC, Güroglu B. Neural correlates of retaliatory and prosocial reactions to social exclusion: associations with chronic peer rejection. *Dev Cogn NeuroSci.* (2016) 19:288–97. doi: 10.1016/j.dcn.2016.05.004

90. Zych I, Ttofi MM, Llorent VJ, Farrington DP, Ribeaud D, Eisner MP, et al. A longitudinal study on stability and transitions among bullying roles. *Child Dev.* (2020) 91:527–45. doi: 10.1111/cdev.13195

91. Forbes MK, Fitzpatrick S, Magson NR, Rapee RM. Depression, anxiety, and peer victimization: bidirectional relationships and associated outcomes

transitioning from childhood to adolescence. *J Youth Adolesc.* (2019) 48:692–702. doi: 10.1007/s10964-018-0922-6

92. Kamper-DeMarco KE, Ostrov JM. Prospective associations between peer victimization and social-psychological adjustment problems in early childhood. *Aggress Behav.* (2017) 43:471–82. doi: 10.1002/ab.21705

93. Reijntjes A, Kamphuis JH, Prinzie P, Telch MJ. Peer victimization and internalizing problems in children: a meta-analysis of longitudinal studies. *Child Abuse Neglect.* (2010) 34:244–52. doi: 10.1016/j.chiabu.2009.07.009

94. Widom C. The cycle of violence. *Science.* (1989) 244:160–6. doi: 10.1126/science.2704995

95. Forbes MK, Magson NR, Rapee RM. Evidence that different types of peer victimization have equivalent associations with transdiagnostic psychopathology in adolescence. *J Youth Adolesc.* (2020) 49:590–604. doi: 10.1007/s10964-020-01202-4

96. Vargas T, Damme KSF, Mittal VA. Bullying victimization in typically developing and clinical high risk (CHR) adolescents: a multimodal imaging study. *Schizophr Res.* (2019) 213:40–7. doi: 10.1016/j.schres.2018.11.017

97. Quinlan EB, Barker ED, Luo Q, Banaschewski T, Bokde ALW, Bromberg U, et al. Peer victimization and its impact on adolescent brain development and psychopathology. *Mol Psychiatry.* (2018) 1–11. doi: 10.1038/s41380-018-0297-9

98. Lee KH, Yoo JH, Lee J, Kim SH, Han JY, Hong SB, et al. The indirect effect of peer problems on adolescent depression through nucleus accumbens volume alteration. *Sci Rep.* (2020) 10, 12870. doi: 10.1038/s41598-020-69769-3

99. Graziano RC, Bruce SE, Paul RH, Korgaonkar MS, Williams LM. The effects of bullying in depression on white matter integrity. *Behav Brain Res.* (2019) 363:149–54. doi: 10.1016/j.bbr.2019.01.054

100. Milojevich HM, Norwalk KE, Sheridan MA. Deprivation and threat, emotion dysregulation, and psychopathology: concurrent and longitudinal associations. *Dev Psychopathol.* (2019) 31:847–57. doi: 10.1017/S0954579419000294

101. Morabito DM, Burani K, Hajcak G. Depressive symptoms prospectively predict peer victimization: a longitudinal study among adolescent females. *Child Psychiatry Hum Dev.* (2021). doi: 10.1007/s10578-020-01100-7

102. Danese A, Moffitt TE, Arseneault L, Bleiberg BA, Dinardo PB, Gandelman SB, et al. The origins of cognitive deficits in victimized children: implications for neuroscientists and clinicians. *Am J Psychiatry.* (2017) 174:349–61. doi: 10.1176/appi.ajp.2016.16030333

103. Edalati H, Afzali MH, Conrod PJ. Poor response inhibition and peer victimization: a neurocognitive ecophenotype of risk for adolescent interpersonal aggression. *J Abnorm Psychol.* (2018) 127:830–9. doi: 10.1037/abn0000380

104. McQuade JD. Peer victimization and changes in physical and relational aggression: the moderating role of executive functioning abilities. *Aggress Behav.* (2017) 43:503–12. doi: 10.1002/ab.21708

105. Kochel KP, Bagwell CL, Ladd GW, Rudolph KD. Do positive peer relations mitigate transactions between depressive symptoms and peer victimization in adolescence? *J Appl Dev Psychol.* (2017) 51:44–54. doi: 10.1016/j.appdev.2017.04.003

106. Masten CL, Telzer EH, Fuligni AJ, Lieberman MD, Eisenberger NI. Time spent with friends in adolescence relates to less neural sensitivity to later peer rejection. *Soc Cogn Affect Neurosci.* (2012) 7:106–14. doi: 10.1093/scan/nsq098

107. Rudolph KD, Monti JD, Modi H, Sze WY, Troop-Gordon W. Protecting youth against the adverse effects of peer victimization: why do parents matter? *J Abnorm Child Psychol.* (2020) 48:163–76. doi: 10.1007/s10802-019-00576-9

108. McLoughlin LT, Simcock G, Schwenn P, Beaudequin D, Boyes A, Parker M, et al. Social connectedness, cyberbullying, and well-being: preliminary findings from the longitudinal adolescent brain study. *CyberPsychol Behav Soc Netw.* (2022) 25:301–9. doi: 10.1089/cyber.2020.0539

109. Hughes BL, Beer JS. Protecting the Self: The effect of social-evaluative threat on neural representations of self. *J Cogn Neurosci.* (2013) 25:613–22. doi: 10.1162/jocn_a_00343

110. Rodman AM, Powers KE, Somerville LH. Development of self-protective biases in response to social evaluative feedback. *Proc Nat Acad Sci.* (2017) 114:13158–63. doi: 10.1073/pnas.1712398114

111. vanDellen MR, Campbell WK, Hoyle RH, Bradfield EK. Compensating, resisting, and breaking: a meta-analytic examination of reactions to self-esteem threat. *Pers Soc Psychol Rev.* (2011) 15:51–74. doi: 10.1177/1088868310372950

112. D'Onofrio P, Norman LJ, Sudre G, White T, Shaw P. The anatomy of friendship: neuroanatomic homophily of the social brain among classroom friends. *Cerebral Cortex.* (2021) bhab398:1–10. doi: 10.1093/cercor/bhab398

113. Fourie MM, Stein DJ, Solms M, Gobodo-Madikizela P, Decety J. Effects of early adversity and social discrimination on empathy for complex mental states: an fMRI investigation. *Sci Rep.* (2019) 9:12959. doi: 10.1038/s41598-019-49298-4

114. Evans GW, Li D, Whipple SS. Cumulative risk and child development. *Psychol Bull.* (2013) 139:1342–96. doi: 10.1037/a0031808

115. Ellis BJ, Oldehinkel AJ, Nederhof E. The adaptive calibration model of stress responsivity: an empirical test in the tracking adolescents' individual lives survey study. *Dev Psychopathol.* (2017) 29:1001–21. doi: 10.1017/S0954579416000985

116. McCrory EJ, Gerin MI, Viding E. Annual research review: childhood maltreatment, latent vulnerability and the shift to preventative psychiatry—the contribution of functional brain imaging. *J Child Psychol and Psychiatry.* (2017) 58:338–57. doi: 10.1111/jcpp.12713

117. McLaughlin KA, Sheridan MA. Beyond cumulative risk: a dimensional approach to childhood adversity. *Curr Dir Psychol Sci.* (2016) 25:239–45. doi: 10.1177/0963721416655883

118. Fornito A, Zalesky A, Breakspear M. The connectomics of brain disorders. *Nat Revs NeuroSci.* (2015) 16:159–72. doi: 10.1038/nrn3901

119. Sporns O, Tononi G, Kötter R. The human connectome: a structural description of the human brain. *PLoS Comput Biol.* (2005) 1:e42. doi: 10.1371/journal.pcbi.0010042

120. Bassett DS, Xia CH, Satterthwaite TD. Understanding the emergence of neuropsychiatric disorders with network neuroscience. *Biol Psychiatry Cogn NeuroSci Neuroimag.* (2018) 3:742–53. doi: 10.1016/j.bpsc.2018.03.015

121. Bullmore E, Sporns O. Complex brain networks: graph theoretical analysis of structural and functional systems. *Nature Revs NeuroSci.* (2009) 10:186–98. doi: 10.1038/nrn2575

122. Di Martino A, Fair DA, Kelly C, Satterthwaite TD, Castellanos FX, Thomason ME, et al. Unraveling the miswired connectome: a developmental perspective. *Neuron.* (2014) 83:1335–53. doi: 10.1016/j.neuron.2014.08.050

123. Ohashi K, Anderson CM, Bolger EA, Khan A, McGreenery CE, Teicher MH, et al. Susceptibility or resilience to maltreatment can be explained by specific differences in brain network architecture. *Biol Psychiatry.* (2019) 85:690–702. doi: 10.1016/j.biopsych.2018.10.016

124. Crone EA, Konijn EA. Media use and brain development during adolescence. *Nat Commun.* (2018) 9:588. doi: 10.1038/s41467-018-03126-x

125. McLoughlin LT, Lagopoulos J, Hermens DF. Cyberbullying and adolescent neurobiology. *Front Psychol.* (2020) 11:1511. doi: 10.3389/fpsyg.2020.01511

Frontiers in Psychiatry

Explores and communicates innovation in the field of psychiatry to improve patient outcomes

The third most-cited journal in its field, using translational approaches to improve therapeutic options for mental illness, communicate progress to clinicians and researchers, and consequently to improve patient treatment outcomes.

Discover the latest Research Topics

See more →

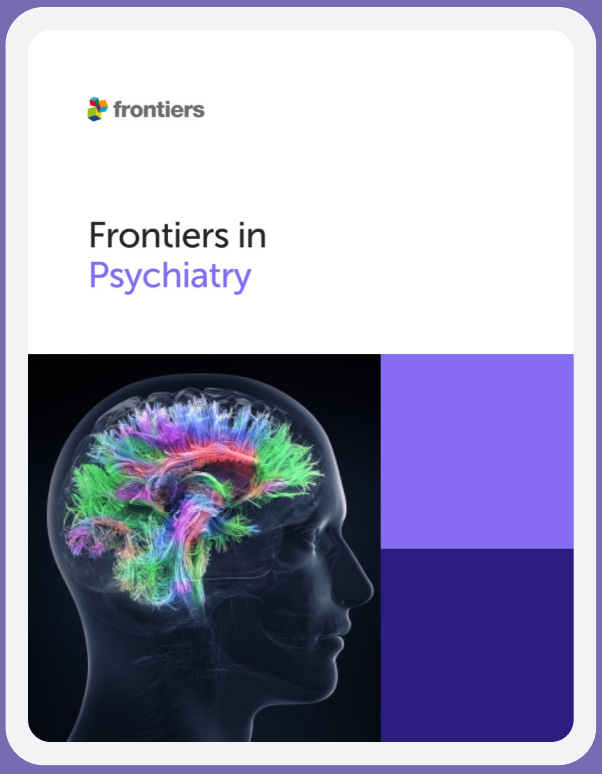

Frontiers

Avenue du Tribunal-Fédéral 34
1005 Lausanne, Switzerland
frontiersin.org

Contact us

+41 (0)21 510 17 00
frontiersin.org/about/contact